

University of Montana

## ScholarWorks at University of Montana

---

Graduate Student Theses, Dissertations, &  
Professional Papers

Graduate School

---

2002

### Factors controlling the formation of mineral precipitates lining the channel in Rabbit Creek Yellowstone National Park Wyoming

Matthew V. Vitale

*The University of Montana*

Follow this and additional works at: <https://scholarworks.umt.edu/etd>

**Let us know how access to this document benefits you.**

---

#### Recommended Citation

Vitale, Matthew V., "Factors controlling the formation of mineral precipitates lining the channel in Rabbit Creek Yellowstone National Park Wyoming" (2002). *Graduate Student Theses, Dissertations, & Professional Papers*. 7742.

<https://scholarworks.umt.edu/etd/7742>

This Thesis is brought to you for free and open access by the Graduate School at ScholarWorks at University of Montana. It has been accepted for inclusion in Graduate Student Theses, Dissertations, & Professional Papers by an authorized administrator of ScholarWorks at University of Montana. For more information, please contact [scholarworks@mso.umt.edu](mailto:scholarworks@mso.umt.edu).



**Maureen and Mike  
MANSFIELD LIBRARY**

The University of  
**Montana**

---

Permission is granted by the author to reproduce this material in its entirety,  
provided that this material is used for scholarly purposes and is properly cited in  
published works and reports.

**\*\*Please check "Yes" or "No" and provide signature\*\***

Yes, I grant permission

\_\_\_\_\_

No, I do not grant permission

\_\_\_\_\_

Author's Signature: Maureen Mansfield

Date: 12-20-02

Any copying for commercial purposes or financial gain may be undertaken only with  
the author's explicit consent.

---





**Factors controlling the formation of mineral precipitates lining the channel in  
Rabbit Creek, Yellowstone National Park, Wyoming**

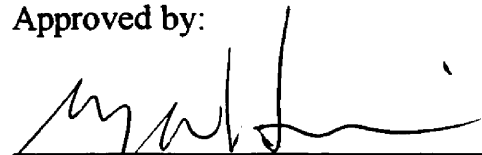
**Matthew V. Vitale**

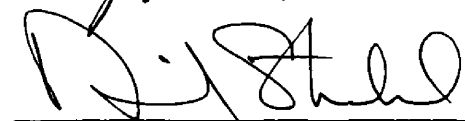
**B.A. University of Maine, 1998**

**Presented in partial fulfillment of the requirements  
for the degree of Master of Science  
The University of Montana**

**2002**

Approved by:

  
\_\_\_\_\_  
Dr. Nancy Hinman, Chair

  
\_\_\_\_\_  
Dean, Graduate School

12-30-02  
\_\_\_\_\_  
Date

UMI Number: EP38543

All rights reserved

INFORMATION TO ALL USERS

The quality of this reproduction is dependent upon the quality of the copy submitted.

In the unlikely event that the author did not send a complete manuscript and there are missing pages, these will be noted. Also, if material had to be removed, a note will indicate the deletion.



UMI EP38543

Published by ProQuest LLC (2013). Copyright in the Dissertation held by the Author.

Microform Edition © ProQuest LLC.

All rights reserved. This work is protected against unauthorized copying under Title 17, United States Code



ProQuest LLC.  
789 East Eisenhower Parkway  
P.O. Box 1346  
Ann Arbor, MI 48106 - 1346

Matthew V. Vitale, M.S., December 2002  
Geology

**Factors controlling the formation of mineral precipitates lining the channel in Rabbit Creek, Yellowstone National Park, Wyoming**

Director: Nancy W. Hinman



Surface water and groundwater exchange chemicals through the biologically rich hyporheic zone. Hydrothermally fed creeks are unique because mineral-rich thermal water precipitates minerals in outflow channels inhibiting surface water and groundwater exchange. Rabbit Creek, in Yellowstone National Park, is fed mostly by a siliceous hot spring and is extensively armored. The creek has both single and anastomosing type reaches that flow through a flat basin. The purpose of this study was to examine the factors controlling mineral precipitation in the channel of Rabbit Creek. Standard hydrogeological and hydrogeochemical techniques and mineral characterization methods were used.

Losing and gaining creek reaches were identified. Groundwater discharged in single channel reaches through the soil zone since the armoring is mostly impermeable. Amorphous silica precipitates in anastomosing reaches where the creek is either losing or no interaction occurs with groundwater.

Geochemistry controls the details of mineral deposition. The shallow groundwater becomes reduced in winter so metals become soluble. When groundwater is discharged to the creek, rapid metal oxidation and subsequent deposition in the creek occurs. The alkaline creek pH promotes silica polymerization. As water travels downstream, temperature decreases result in decreasing silica solubility. Silica is more likely to precipitate in anastomosing creek reaches where the water is spread over a larger surface area and thus cools more quickly.

Cyanobacterial mats provide a substrate for silica deposition. Silica settled out of solution and deposited when trapped in the cyanobacterial mats. Mats were thicker and covered a larger spatial area during the winter likely due to a decrease in the thermal regime that produced optimal growing conditions.

Silica concentration and saturation in the creek were highest in winter due to hydrothermal dynamics and creek water cooling. This, combined with the influx of metals from groundwater, induced mineral deposition more effectively than at other times of the year. The implication is creek channel mineral deposition occurs mostly in winter.

## Acknowledgments

Thank you to my committee members: Nancy Hinman, Bill Woessner, and Scott Woods.

Several people helped with field work: Virginia Rodriguez, Aaron Tenesch, David Woessner, Adam Johnson, Danielle Hughes, Toby Hewitt, Kevin Loustaunau, and Vite Vitale.

Johnnie Moore, Heiko Langner, and the techs of the Murdoch Biogeochemistry Laboratory aided in lab analyses. Mike Hofmann instructed on the use of XRD. Annilivia Harris at the Montana Crime Lab provided support for SEM analyses. Employees of Yellowstone National Park answered questions and aided in fieldwork logistics. Patricia Colberg and colleagues at the University of Wyoming helped to sustain me during this project. Thanks to all others who helped at some point.

Research funding for the project was provided by the National Science Foundation (Biocomplexity Research Grant), NASA-EPSCoR, and the NASA Astrobiology Institute Johnson Space Center Team. Research was conducted under Yellowstone National Park Permit YELL-2001-SCI-0134 and YELL-2002-SCI-0134.

I am grateful to past management practices of the Greater Yellowstone Ecosystem for inhibiting urban sprawl and continuing to be the wildest lands in the country.

And no acknowledgements page would be complete without a thoughtful quote:

*“Water is the lifeblood of the wilderness.”*

From the Homestake Wilderness in Colorado  
(author not found yet)

## Table of Contents

<b>Abstract</b>	ii
<b>Acknowledgements</b>	iii
<b>Table of Contents</b>	iv
<b>List of Tables</b>	vi
<b>List of Figures</b>	vii
<b>1.0 Introduction</b>	1
1.1 Purpose of Research	2
1.2 Silica and Mineral Deposition in Hydrothermal Environments	3
1.3 Previous Research	7
<b>2.0 Description of Study Site</b>	9
2.1 Rabbit Creek Basin Geology	9
2.2 Rabbit Creek	13
<b>3.0 Methods</b>	16
3.1 Surface Hydrology	17
3.2 Hydrogeology	18
3.3 Geochemistry	21
3.4 Collection of Mineral Precipitates	23
3.5 Mineral Identification	25
3.6 Geomorphology	29
3.7 Photographic Documentation	30
<b>4.0 Results and Interpretation</b>	31
4.1 Surface Hydrology	31
4.2 Hydrogeology	35
4.3 Geochemistry	42
4.4 Collection of Mineral Precipitates	63
4.5 Mineral Identification	70
4.6 Geomorphology	80
4.7 Photographic Documentation	84

<b>5.0</b>	<b>Discussion</b>	<b>87</b>
5.1	Hydrologic Controls on Mineral Precipitation	87
5.2	Chemical Controls on Mineral Precipitation	89
5.3	Microbial Influences on Precipitation	94
5.4	Seasonal Timing of Mineral Precipitate Formation	95
5.5	Conceptual Model of Rabbit Creek and the Rabbit Creek Basin	95
<b>6.0</b>	<b>Conclusions</b>	<b>98</b>
	<b>References Cited</b>	<b>100</b>
	<b>Glossary</b>	<b>110</b>
	<b>Appendix A: An extensive review of silica and iron geochemistry</b>	<b>112</b>
	<b>Appendix B: Measured hydrological data</b>	<b>128</b>
	<b>Appendix C: Cumulative water chemistry and quality</b>	<b>139</b>
	<b>Appendix D: Rabbit Creek basin archived chemistry</b>	<b>168</b>
	<b>Appendix E: X-ray diffraction scans</b>	<b>170</b>
	<b>Appendix F: Creek channel cross-sectional measurements</b>	<b>171</b>
	<b>Appendix G: Creek channel reconnaissance mapping</b>	<b>173</b>

## List of Tables

Table 1	Descriptions of rock samples and collection locations.	26
Table 2	Major cations (Al, Ca, Fe, K, Mg, Na, and Si).	45
Table 3	Chloride concentrations in piezometers <i>ura</i> and <i>urb</i> .	55
Table 4	Iron concentration (ferrous and total iron ) from January to July, 2002 using the ferrozine method.	58
Table 5	X-ray diffraction reference angles and d-spaces (angstroms) with measured d-spaces for comparison for sample <i>rll</i> .	74
Table 6	Sample locations where thin section rock samples were collected in the field.	77
Table 7	Porosity statistics for thin sections samples.	79
Table 8	Mineral precipitate porosity $\rho$ -values.	80



## List of Figures

Figure 1	Quartz and cristobalite solubility plotted with amorphous silica.	5
Figure 2	Speciation diagram for amorphous silica and quartz species.	6
Figure 3a	Location map of Rabbit Creek in Yellowstone National Park.	10
Figure 3b	Location of the study site in the Rabbit Creek Basin	10
Figure 4	Landform map of the Rabbit Creek basin.	11
Figure 5	Rabbit Creek Basin Y-5 well log from research drilling in July and August, 1967.	12
Figure 6a	Cyanobacteria mat in the creek near the hot spring source of Rabbit Creek.	14
Figure 6b	Typical creek channel where mineral deposits line the channel.	14
Figure 7a	Creek channel mineral lining.	15
Figure 7b	Close-scale photograph of mineral lining.	15
Figure 8	Piezometer and staff gauge locations in Rabbit Creek.	20
Figure 9	Surface water sample locations.	21
Figure 10a	Schematic design of long bead tubes placed in the deeper creek sections.	25
Figure 10b	Bead tube after two months in the single channel section of the study site.	25
Figure 11	Flo-Dar hydrograph from August 19 – 31, 2001.	32
Figure 12	Bobber test creek hydrograph measured in the study site.	33
Figure 13a	Discharge comparison between the Flo-Dar surface water velocity meter and a USGS bobber test as a 1:1 scatter plot.	34
Figure 13b	Discharge comparison between the Flo-Dar surface water velocity meter and a USGS bobber test as a function of sample number.	34
Figure 14	Well logs.	36
Figure 15	Groundwater elevation plot during the study period.	39
Figure 16	October potentiometric map.	40
Figure 17a	Water level measurements in piezometer <i>ula</i> .	41
Figure 17b	Historical precipitation data collected at the Old Faithful weather station.	41
Figure 18	Location of hot spring that emerges in the creek.	41
Figure 19	Electromagnetic conductivity survey plot of study site conducted in August, 2001.	42
Figure 20	Groundwater chemistry stiff plot for October.	43
Figure 21	Major cation plots.	49
Figure 22	Temperature correlations plots with silica, chloride, and silica.	52
Figure 23	Ferrous to total iron ratios during the study.	58
Figure 24	Total iron (mg/L) using the ferrozine method, dissolved oxygen (mg/L), and pH plots for four months.	59
Figure 25	Groundwater and surface water pH.	60

Figure 26	Groundwater and surface water temperature.	60
Figure 27	Silica speciation derived from MinteqA2.	61
Figure 28a	Blank bead tube EDS spectra.	64
Figure 28b	Blank bead tube photograph.	64
Figure 29a	Groundwater bead tube (6) EDS spectra.	65
Figure 29b	Surface water bead tube (4) EDS spectra.	66
Figure 29c	Surface water (4) bead tube photograph.	66
Figure 30	Chemical precipitation box photograph showing sinter deposition.	68
Figure 31a	Lower precipitation box EDS spectra.	68
Figure 31b	Lower precipitation box SEM photograph showing cyanobacteria filament structure.	69
Figure 31c	Lower precipitation box SEM photograph showing diatoms.	69
Figure 32a	Subaqueous mineral deposit ( <i>rl3c</i> ) photograph.	71
Figure 32b	XRD scan of subaqueous mineral deposit ( <i>rl3c</i> ).	71
Figure 33a	XRD plots of sample <i>rl2a</i> .	72
Figure 33b	XRD plots of sample <i>rl3a</i> .	72
Figure 34a	Mineral deposit sample ( <i>rl1</i> ) photograph.	73
Figure 34b	XRD plot of mineral deposit sample ( <i>rl1</i> ).	73
Figure 35a	Sinter deposit thin section photomicrograph from piezometer <i>lra4</i> .	75
Figure 35b	Mineral deposit ( <i>rl3a</i> ) thin section photomicrograph.	75
Figure 36	Piezometer sinter deposit ( <i>ula30</i> ) SEM/BSE image.	76
Figure 37	Mineral deposit ( <i>rl4b</i> ) SEM/BSE image.	76
Figure 38	Elemental mapping images.	78
Figure 39	Average porosity measurements using PIA.	79
Figure 40	Longitudinal gradient measurements.	81
Figure 41	Location map of longitudinal gradient measurements.	81
Figure 42a	Cross section in single channel creek reach.	82
Figure 42b	Cross section in anastomosing channel creek reach.	82
Figure 43	Photograph of a single channel reach.	83
Figure 44	Photograph of a smaller terraced channel within the larger main channel in an upper anastomosing creek reach.	84
Figure 45a	Photograph of cyanobacteria in creek in February.	85
Figure 45b	Photograph of cyanobacteria in creek in June.	86
Figure 45c	Photograph of cyanobacteria in creek in July.	86
Figure 46	Near channel creek hydrology schematic.	88
Figure 47	Conceptual model of Rabbit Creek and the Rabbit Creek Basin.	97

## **1.0 Introduction**

Yellowstone National Park (YNP) contains the greatest concentration of hydrothermal features in North America. Magma is within 3-10 km of the land surface in Yellowstone (Fournier, 1989). Meteoric water enters into the subsurface through fractures in rhyolite (and secondarily basalt) and is heated to temperatures of 350°C or more (Brock, 1994, Ellis and Mahon, 1977, Friedman et al., 1974). The hot water rises to the surface and discharges from hot springs, geysers, and fumaroles. These hydrothermal features usually occur along faults, and are thus grouped linearly on the surface (Fournier, 1989).

Much of the hydrothermal water that discharges from the hot springs and geysers in YNP infiltrates into the nearby subsurface. In some cases hydrothermal water flows along outflow channels that are lined with mineral precipitates. These precipitates are typically composed of opal and quartz or calcium carbonate. It is believed that the formation of mineral precipitates along outflow channels occurs in response to cooling, oxidation, changes in solution concentration or ionic strength, or a combination of these factors (Langmuir, 1997). These physical and chemical factors vary depending on stream hydrology, geochemistry, geomorphology, and the types of biological populations present. Cyanobacterial mats often provide an important substrate for mineral deposition along outflow channels (Jones and Renaut, 1996). The combination of factors controlling mineral precipitate formation is complex and varies between sites.

The unusually high concentrations of dissolved constituents found in hydrothermal water provides a natural model for environmentally impacted sites. Anthropogenic inputs to

groundwater and rivers can significantly alter the biogeochemistry of the system through temperature changes, nutrient additions, and the introduction of toxic materials (Von Gunten et al., 1991). A thorough and critical understanding of river ecosystems at all catchment scales is integral to river conservation and preservation (Woessner, 2001, Stanford and Ward, 1993). Research conducted in hydrothermal environments may provide information that aids in the characterization, assessment, and remediation of contaminated streams and rivers.

Rabbit Creek is part of Midway Geyser Basin in the central part of Yellowstone National Park. Flow in Rabbit Creek is primarily maintained by discharge from one large hot spring at the head of the basin. The channel is lined with mineral precipitates.

### **1.1 Purpose of Research**

The purpose of this research was to determine the factors that control mineral-precipitate formation in the channel of Rabbit Creek, Yellowstone National Park. The mineral deposits in the creek have formed thick layers for several hundred meters from the hot spring source. Creek geomorphology is complex.

Temperature is hypothesized to be the driving factor for mineral precipitation in Rabbit Creek. Hydrogeology affects the location and geochemistry of the mineral deposits. Cyanobacterial mats provide an important substrate for mineral deposition. Creek geomorphology is an important control on both the locations of mineral deposition and

development of microbial mats. Mineral deposition onto microbial mats usually occurs in side eddies in stagnant water.

Work focused on hydrology and geochemistry of the surface water and groundwater systems. Groundwater exchange with the creek was examined using standard hydrogeological and hydrogeochemical techniques (piezometers, creek discharge, and water chemistry) and geophysical methods (ground conductivity). In addition, basin and stream geomorphology and biology were also examined.

## **1.2 Silica and Mineral Deposition in Hydrothermal Environments**

Rhyolite is the major source of silica in geothermal waters. Silica makes up about 75% of the chemical composition of rhyolite (Boyd, 1957), primarily in the form of  $\alpha$  quartz (Bohlmann, 1980). As hot water passes through fractures in the rhyolite, silica (quartz) goes into solution (Rimstidt and Cole, 1983). The concentration of silica in aqueous solution can be several hundred mg/L at the surface of hot springs (Morey et al., 1964). Precipitation and accumulation of silica occurs near the surface of hot springs due to cooling and evaporation (Hinman and Lindstrom, 1996).

Silica deposition in the subsurface creates low permeability barriers oriented in both vertical and horizontal directions (Becker and Blackwell, 1993). Gibson (1999) found sinter barriers in the subsurface near Octopus Spring, YNP. These barriers are low flow / no flow boundaries that separate the shallow groundwater into distinctly different

systems with contrasting geochemical characteristics. The groundwater systems are separated horizontally into subsurface hydrologic units or are separated vertically into perched and confined aquifers. Shallow aquifers tend to become confined or semi-confined as the upper and lower portions of the aquifer are sealed by silica (Healy and Hochstein, 1973). Silica precipitates in the subsurface along cooling margins where decreasing silica solubility controls deposition.

Laminated silica deposits are common in hydrothermal environments. These laminated deposits are termed “sinter” or “geyserite” (Mottana et al., 1978). Geologically young siliceous sinters tend to be amorphous (Herdianita et al., 2000) or a juvenile form of crystalline opal. Cementation occurs when silica polymers are deposited between grains of pre-existing sinter (Rimstidt and Cole, 1983). Ferric hydroxides aid in the cementation of siliceous deposits (Konhauser and Juniper, 1997, Dove and Rimstidt, 1994).

Sinter solubility is temperature dependent. In general, more soluble forms of silica are deposited first and must undergo recrystallization through a diagenetic sequence of decreasingly soluble silica phases (Figure 1). The typical sequence of diagenesis is amorphous silica to cristobalite to quartz. The sequence does not necessarily follow this path on the way to quartz, the thermodynamically stable form; this hierarchy has exceptions as some polymorphs are skipped due to temperature, pressure, and chemical factors. Most commonly, amorphous silica (opal-A) recrystallizes to opal-CT (cristobalite or tridymite), which recrystallizes to chalcedony or quartz ( $\alpha$  or  $\beta$  quartz,

depending on temperature and pressure) (Herdianita et al., 2000, Kastner et al., 1988, Williams et al., 1985, Iler, 1979, Jones and Segnit, 1971, Krauskopf, 1956).

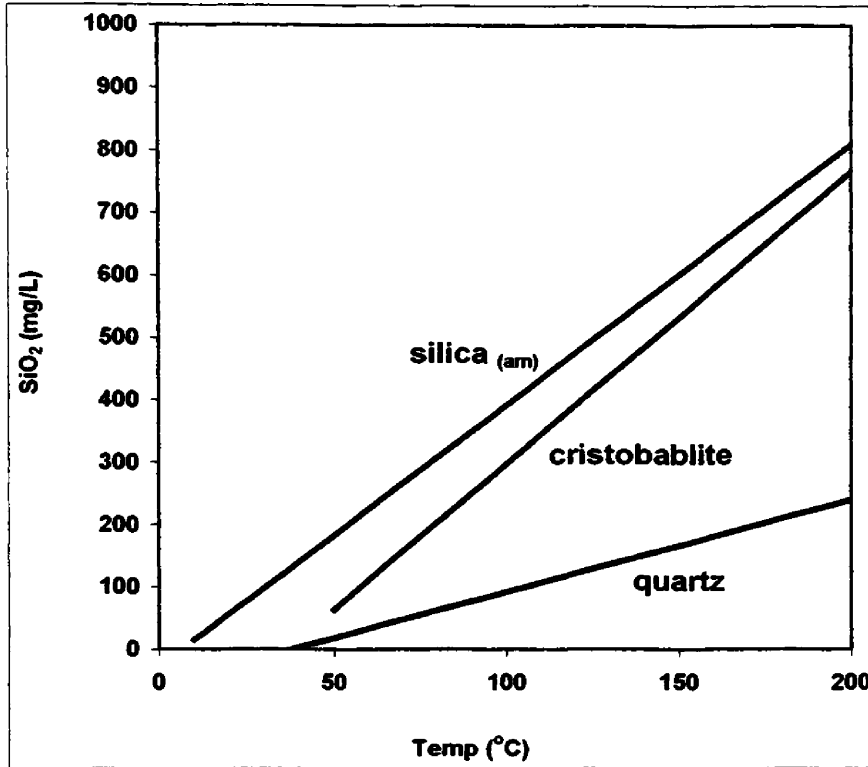


**Figure 1:** Quartz and cristobalite solubility plotted with amorphous silica. Crystalline phases of SiO<sub>2</sub> are less soluble than amorphous silica. The concentrations begins to decrease > 200°C (Rimstidt, 1997, Fournier, 1985, Rimstidt and Cole, 1983, and Alexander et al., 1954).

Temperature, pH, and the silica phase present control dissolved silica concentration (Rimstidt, 1997, Fournier, 1985). As water temperature decreases, silica solubility decreases and thus silica precipitates out of solution (Lowell et al., 1993). In most scenarios, water discharging from a hot spring will cool quickly leading to rapid precipitation (Rimstidt and Barnes, 1983).

The pH controls silica solubility through its effect on silica speciation. Between a pH of 1 to 9, silicic acid or silicate ( $\text{H}_4\text{SiO}_4$ ) is the dominant species (Figure 2) (White et al., 1956, Carrol et al., 1998, Siever, 1957). Above pH 9, silicic acid deprotonates to form  $\text{H}_3\text{SiO}_4^-$ . Silicate may also form into polymers that eventually grow to colloids or larger particles, often with the assistance of cations, particularly at higher pH.

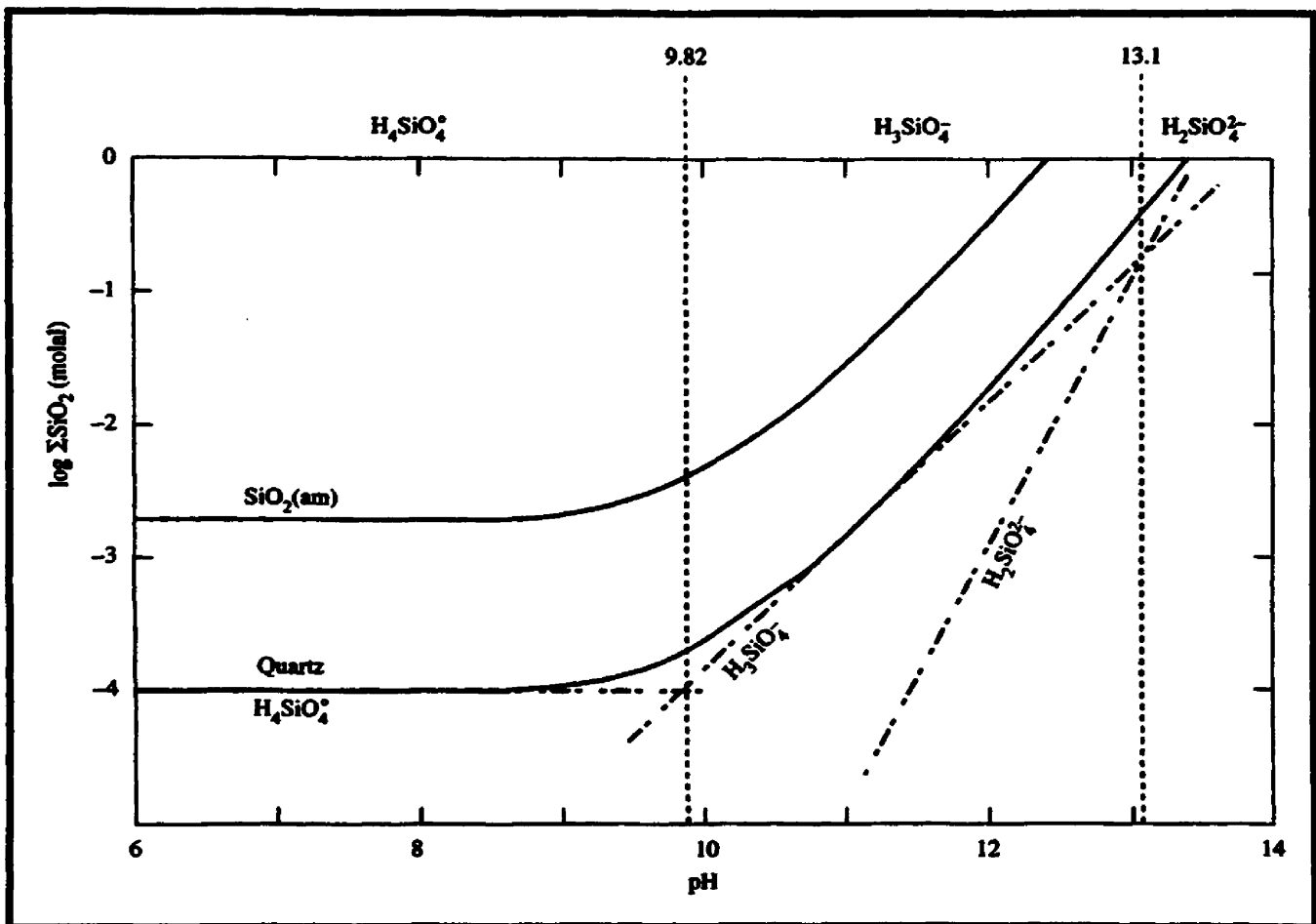


**Figure 2:** Speciation diagram for amorphous silica and quartz species. The opal equilibrium line is presumed to lie between the amorphous silica and quartz equilibrium lines.  $\text{H}_4\text{SiO}_4^0$  dissociates to  $\text{H}_3\text{SiO}_4^-$  at pH 9.82 and further dissociates into  $\text{H}_2\text{SiO}_4^{2-}$  at pH 13.1. As pH increases, solubility of  $\text{SiO}_2$  increases. Below pH 8.0, the solubility is constant to approximately pH 5.0. (from Langmuir, 1997, p. 246.)



Silica may not precipitate for several days, even under supersaturated conditions (Krauskopf, 1956). However, in undersaturated conditions, silica may deposit on microbial mats (Noffke et al., 2001, Jones and Renaut, 1996, Wiegart and Fraleigh, 1972). Microbial mats create stagnant environments within a moving water section. Silica polymerization takes place more readily in these stagnant water environments and eventually silica particles settle out of suspension within the mats. In moving water, the flow velocity may be too great for silica particles to adhere to substrates (Rimstidt and Barnes, 1983). Thus, silica can precipitate long distances from the vent in hot spring outflow channels. Other dissolved and solid components, like iron and aluminum oxides, affect silica speciation and deposition (Hinman, 1997, Iler, 1979, MacKenzie and Gees, 1971).

### **1.3 Previous Research**

The characteristics and behavior of silica have been studied in great detail in the field and the laboratory (Kinrade et al., 1999, Carroll et al., 1998, Akahane et al., 1997, Hinman and Lindstrom, 1996, Rimstidt and Barnes, 1980, Fournier and Rowe, 1977, Morey et al., 1964, Krauskopf, 1956, White et al., 1956, Alexander et al, 1954, and others). Silica solubility and deposition were intensively studied in the 1950s as geothermal energy sources were slated for development. Design of geothermal power plants had to incorporate the problem of silica depositing in the system mechanics. Some factors affecting silica behavior are not fully understood such as chemical reactions with other

elements (Mg, Al, Fe, etc.) and microbial mediation.

DeMonge (1999) found that “armoring”, mineral precipitates composed of silica, occurred in downwelling sections of Iron Springs Creek, YNP. She attributed the armoring to physical and chemical factors. Iron Springs Creek is a thermally influenced creek in Yellowstone. Gibson (1999) did not study stream channel armoring but stated that groundwater exchange with Sentinel Creek was limited due to channel armoring.

## **2.0 Description of Study Site**

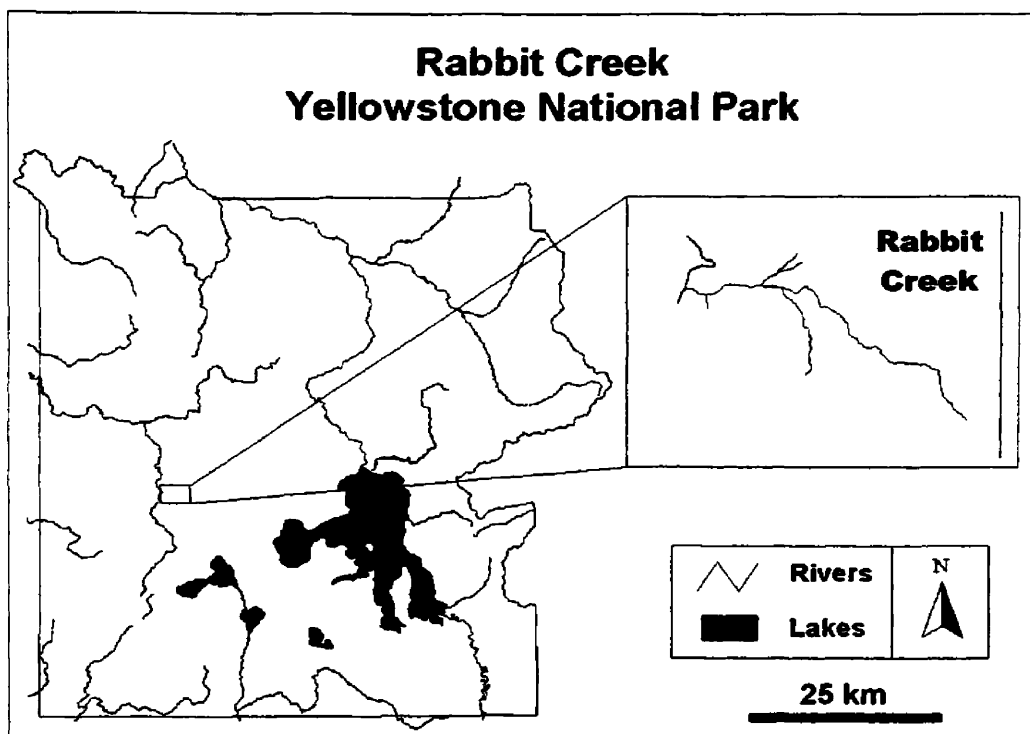
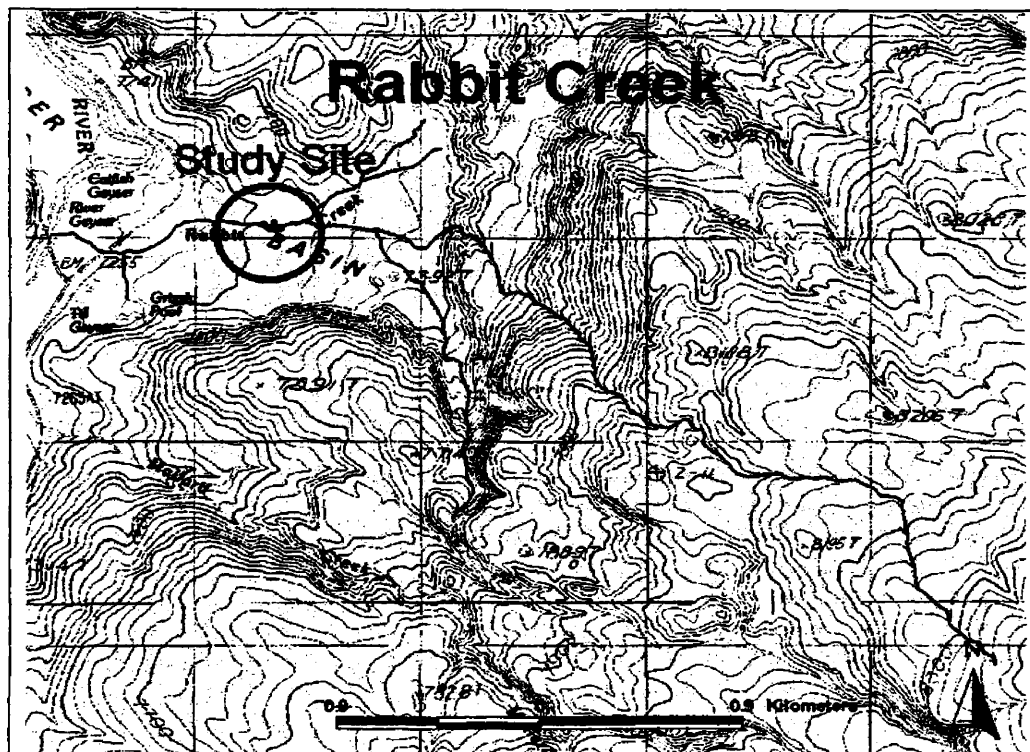
Rabbit Creek is 8 km north of Old Faithful Geyser in the Upper Geyser Basin (Figure 3). The low relief Rabbit Creek basin is up to half a kilometer wide. The basin elevation is ~2155 m (7000 ft) above sea level. Rabbit Creek flows for approximately 2 km long from its hot spring source to the confluence with the Firehole River.

### **2.1 Rabbit Creek Basin Geology**

The Rabbit Creek Basin lies within the Yellowstone Caldera where volcanism has occurred for over two million years (Fritz, 1985). The third and most recent Yellowstone pyroclastic caldera eruption deposited the Lava Creek Tuff during the Pleistocene Era approximately 600,000 years ago (Christiansen, 2001, Good and Pierce, 1996). Lava Creek Tuff consists predominantly of the rhyolitic tuff of the Yellowstone Group.

Yellowstone was affected by two major glacial periods: the Bull Lake, which began 150,000 years ago, and the Pinedale that began 80,000 years ago and ended 10-12,000 years ago (Fritz, 1985, Good and Pierce, 1996). Since the Pinedale Glacial Period removed most of the Bull Lake features, only debris from the Pinedale Glacial Period exists in the Rabbit Creek basin (Figure 4).

Research drilling was conducted in the Park in 1967 and hole Y-5 was drilled in the southwest part of the Rabbit Creek basin (Figure 5; inset of drill hole location)

*a**b*

**Figure 3:** Location map of Rabbit Creek in Yellowstone National Park (*a*) and location of the study site in the Rabbit Creek Basin with piezometer locations inside the circle (*b*). The hot spring source is the upper fork of Rabbit Creek.

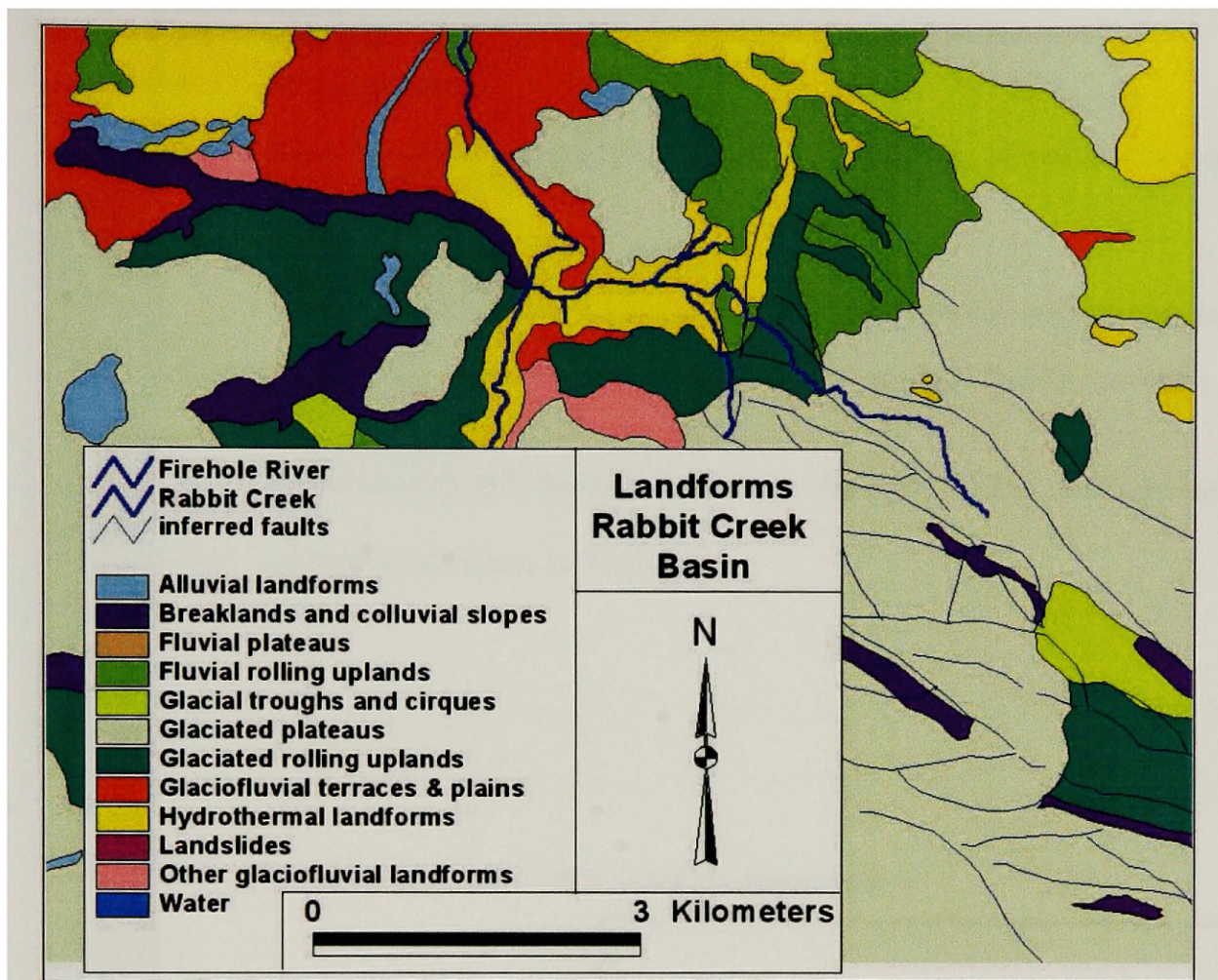


**Figure 4:** Landform map of the Rabbit Creek basin with surficial glacial material in the flat part of the basin. (Yellowstone Center for Resources Spatial Analysis Center, 2001)

(reported by White et al., 1975 and Keith and Muffler, 1978). The top five meters in research drill hole Y-5 intersected the Pinedale kame, consisting of sand and gravel with some opal cement but no defined sinter layer. Most of the opal has been mineralized to quartz and chalcedony (Keith and Muffler, 1978). Volcanic breccia was encountered between ~ 5 m and ~10 m depth. Lava Creek Tuff underlies this breccia at ~10 m to the bottom of the drill hole. This is the only known location of the Lava Creek Tuff in the western part of the Yellowstone Caldera (White et al., 1975, Keith and Muffler, 1978).

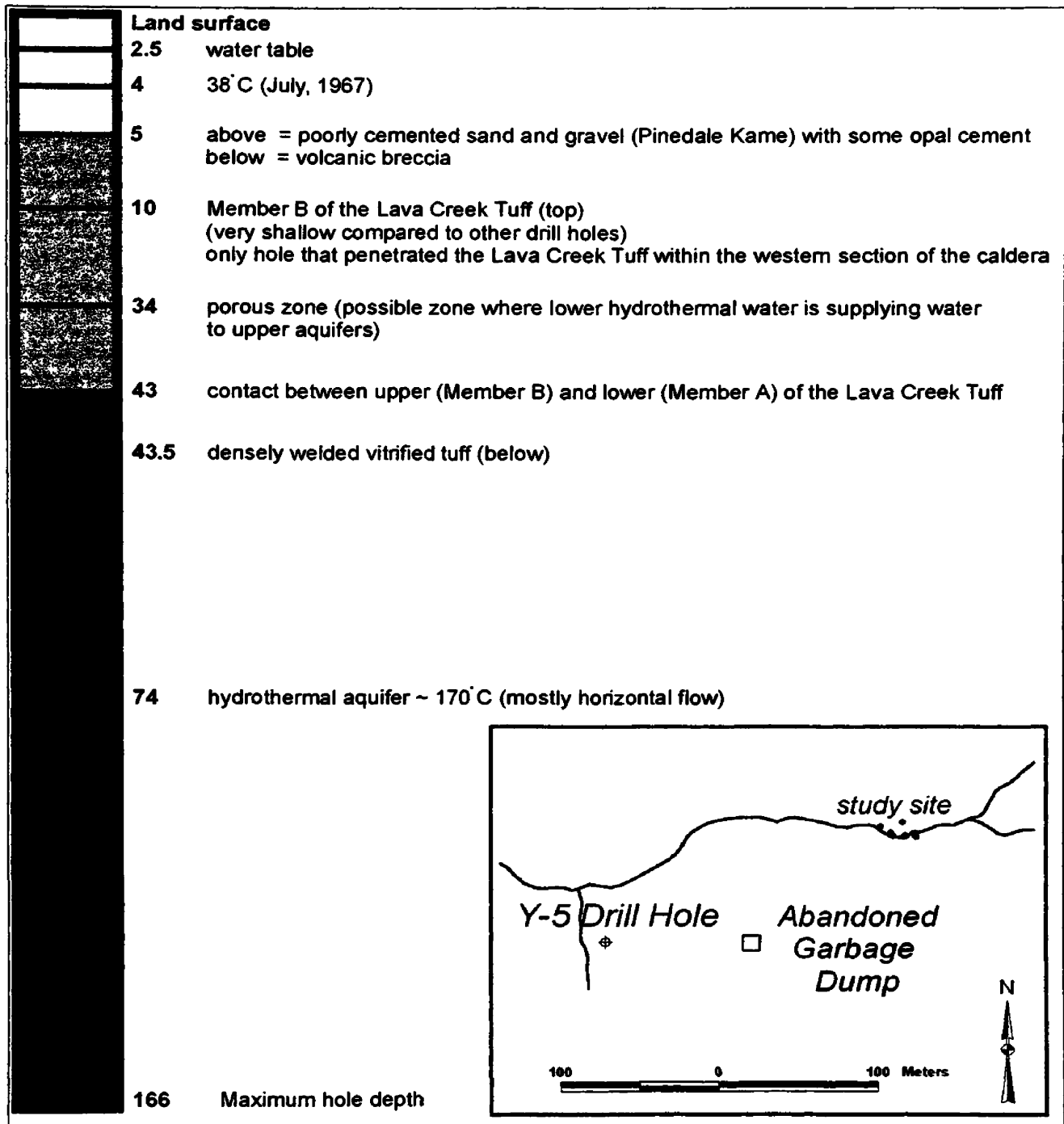


**Figure 5:** Rabbit Creek Basin Y-5 well log from research drilling in July and August, 1967. (Well log compiled from Christiansen, 2001, Keith and Muffler, 1978 and White et al., 1975). Units are in meters (relative scale).

The Lava Creek Tuff is the likely major source of ions, such as iron and copper, in the shallow groundwater.

The top of the hydrothermal aquifer in Rabbit Creek, composed of rhyolite bedrock, was encountered at 74 m depth in hole Y-5. Rhyolite provides high silica concentrations to hot springs in the basin. Flow in the basin is thought to be mostly horizontal because of the minimal upward vertical flow in the drill hole. This hydrothermal aquifer is semi-confined. Temperature and pressure were greater in the deepest aquifer than in the shallower aquifers (White et al., 1975).

## **2.2 Rabbit Creek**

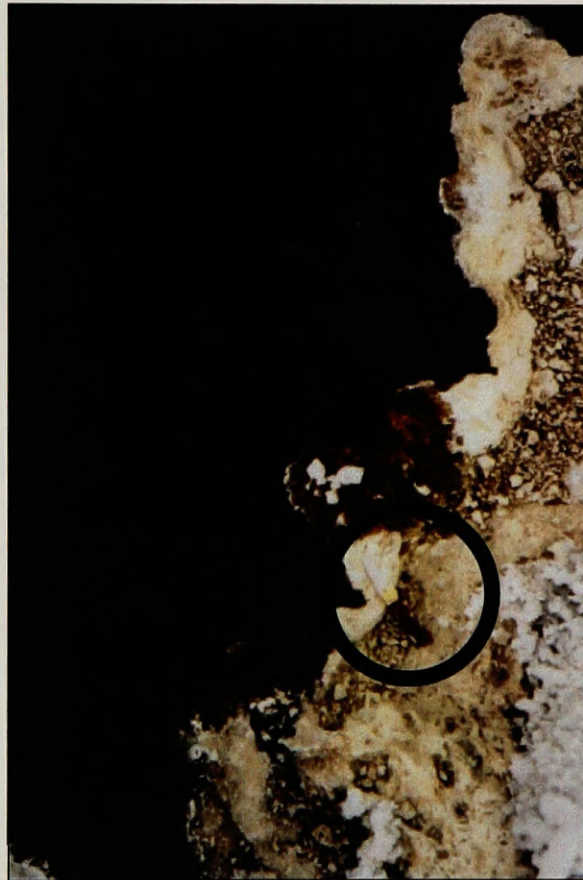
The siliceous alkaline hot spring source that supplies the majority of water to Rabbit Creek discharges water at a rate of approximately  $0.1 \text{ m}^3/\text{sec}$ . The water discharging from the spring has a pH of approximately 9-10 and a temperature over  $80^\circ \text{C}$  (Yellowstone Center for Resources, 2001). Siliceous mineral deposits have lined portions of the creek channel (Figures 6 and 7). Cyanobacterial populations grow along portions of the creek where silica was observed to precipitate onto the cyanobacterial mats.



*a**b*

**Figure 6:** Photo *a* shows a cyanobacterial mat in the creek near the hot spring source of Rabbit Creek. Photo *b* shows the typical creek channel where mineral deposits line the creek channel both vertically and horizontally.



*a**b*

**Figure 7:** Creek channel mineral lining. Photo *a* shows complex channel morphology in the lower portion of the study site (April). Photo *b* shows a close-up view of the deposits. Note the small knife in the center of the photo.

### **3.0 Methods**

Field work for this study was performed between August, 2001 and July, 2002. The following measurements were taken to assess existing hydrogeological and hydrogeochemical parameters in the creek and the near channel creek system and to both qualitatively and quantitatively describe seasonal changes.

The hydrology was analyzed in the creek using standard USGS techniques (i.e. discharge and stage). Piezometers were installed in the study site near the creek to determine surface water and groundwater interactions and resulting affects on the channel lining. A geophysics survey was employed over a larger portion of the study site to provide supporting evidence of the data collected from the piezometers.

Water samples were collected in the creek and the shallow groundwater to quantify water interaction and determine seasonal chemical changes. Silica saturation was calculated and silica components were modeled for phase differentiation. Silica concentration was measured and examined in areas of bacterial populations to assess biogeochemical interactions affecting silica precipitation and deposition. Instrumentation was installed in the creek to determine if silica and metals were currently precipitating out of solution and therefore if the channel lining was still forming. Geomorphological characteristics of the creek channel were measured and plotted. Mineral deposits were collected and analyzed to identify the channel lining composition. Photo documentation was conducted to

record existing conditions of the creek channel. Seasonal changes in bacterial populations were photographed for qualification.

### **3.1 Surface Hydrology**

Creek discharge and stage were measured to understand the biogeochemical system. Diurnal and seasonal variations aided in interpreting changes in the cyanobacterial communities and water chemistry.

A Marsh-McBierny Flo-Dar flow meter was used to measure surface water velocity. The flow meter, ideally suited for use in hot water, uses radar to measure the velocity at the water surface. Velocity was measured every fifteen minutes over a one week period in August, 2001. Data were exported to Excel where the measured cross sectional area of the creek was factored in to calculate discharge. Quality assurance and quality control on the Flo-Dar was conducted using a bobber test comparison. The bobber test was conducted using a floatable material (i.e. sticks) to determine the surface water velocity by recording the time it took for the bobber to travel a measured distance downstream. Water on the sides of a channel and the surface are slowed due to friction so a coefficient of 0.85 (Rantz, 1982) was used in the discharge calculation to compute for a representative creek velocity (i.e., multiplying the surface water velocity measurement by 0.85 is an estimate of this representative creek velocity at 0.6 depth). The bobber test consisted of ten trials over a three meter creek reach just below the Flo-Dar location. The velocity data from the bobber test was plotted against the Flo-Dar velocity measurements

for the same time of day and linear regression analysis was used to develop a relationship between the two methods.

Three stream staff gauges were installed in the creek in the study site. Staff gauges were made of 0.3 cm diameter solid stainless steel rods. The staff gauges were driven into the streambed and the top of the gauges were measured for relative elevation using a rod and transit. Measurements from the top of the gauge to the water surface were measured each sampling round to determine stage changes.

### **3.2 Hydrogeology**

The research permit issued by the National Park Service allowed for installation of a maximum of twelve piezometers in the Rabbit Creek Basin. Installation difficulties prevented placement of piezometers in some of the desired locations. Holes were not drilled near hydrothermal activity because of the threat of creating new hydrothermal features. Sinter could not be hand augured without first breaking up the cemented material with a rock bar and sledge hammer. Holes could be made if water was encountered above or at the sinter layer. However, if water was not encountered, the sinter was extremely hard and could not be broken with manual tools. Therefore, placement of piezometers coincided with water encounters.

All piezometers except three were installed within one meter of the creek channel. Four piezometers were installed in the upper section of a single channel reach, three

piezometers were installed at the lower part of the same single channel reach, and four piezometers were installed in the beginning of the braided reach. An equal number of piezometers were installed on each side of the creek (Figure 8).

When drilling holes, it was made sure that at least 10 cm of water in the hole was present before final installation to provide adequate water samples in the future. A 2.5 cm I. D. PVC pipe was used for casing. Holes (0.6 cm )were drilled at one end of the pipes and wrapped with nylon paint strainer material to serve as a well screen. Material taken out of the hole was used as backfill during installation. A thin layer of bentonite was placed at the top of the hole to prevent surface water infiltrating into the shallow holes.

Piezometers were surveyed for elevation at the top of each casing using rod and transit. They were mapped using GPS and tied into a USGS topographic map.

Water levels were measured in the piezometers during each of the sampling rounds. An electronic water level recorder was used. A steel tape was used when the water was too shallow to use an electronic water level recorder.

Slug tests were performed on several piezometers in June, 2002 to estimate hydraulic conductivity (Fetter, 1994, Driscoll, 1986). A steel tape was inserted into a piezometer and a known volume of deionized water was poured into the casing. Time was recorded with corresponding water level measurements. This field procedure was performed several times on each piezometer measured.

An estimate of hydraulic conductivity was calculated using Darcy's Law. An approximation of discharge ( $Q$ ) of groundwater to surface water was determined using chloride as a conservative tracer.

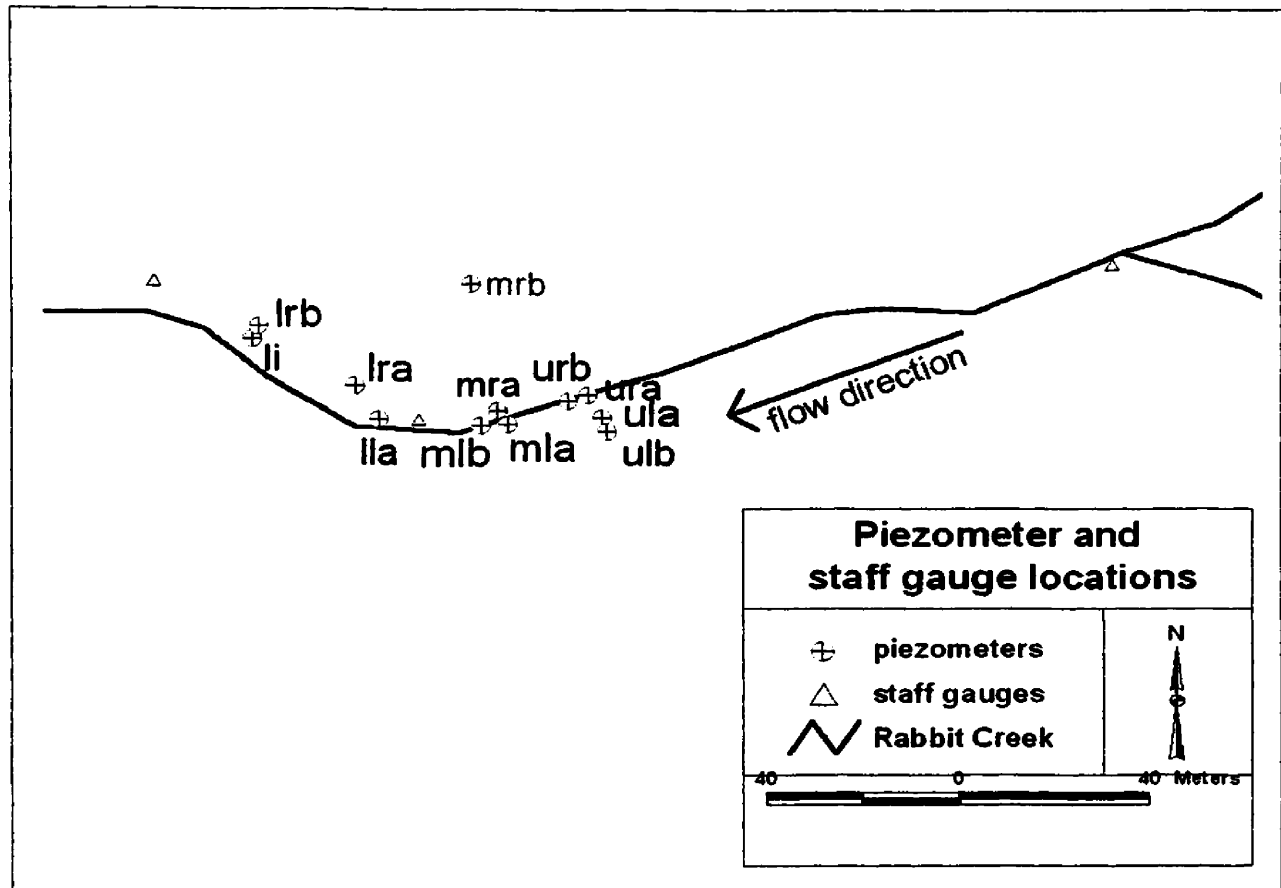


**Figure 8:** Piezometer and staff gauge locations in Rabbit Creek. Flow direction of creek is from east to west.

Electromagnetic conductivity measurements were conducted using a zig-zag type plot at the study site. A Geonics EM 31-K v. 2.00 ground conductivity meter with a DL600 data logger and DAT31W v. 1.02a software was used. Data were transferred to Surfer software where conductivity measurements were plotted using the Kriging method.

### 3.3 Geochemistry

Surface water and groundwater samples were collected in August and October (2001) and January, February, April, June, and July (2002). Water-level measurements were taken before piezometer sampling. Prior to sample collection, three bore casing volumes of water were purged and pH checked for consistent readings. This was done in order to assume shallow groundwater was being sampled. Surface water samples were taken at the source, below the source, and at various locations in the creek within the study reach (Figure 9).

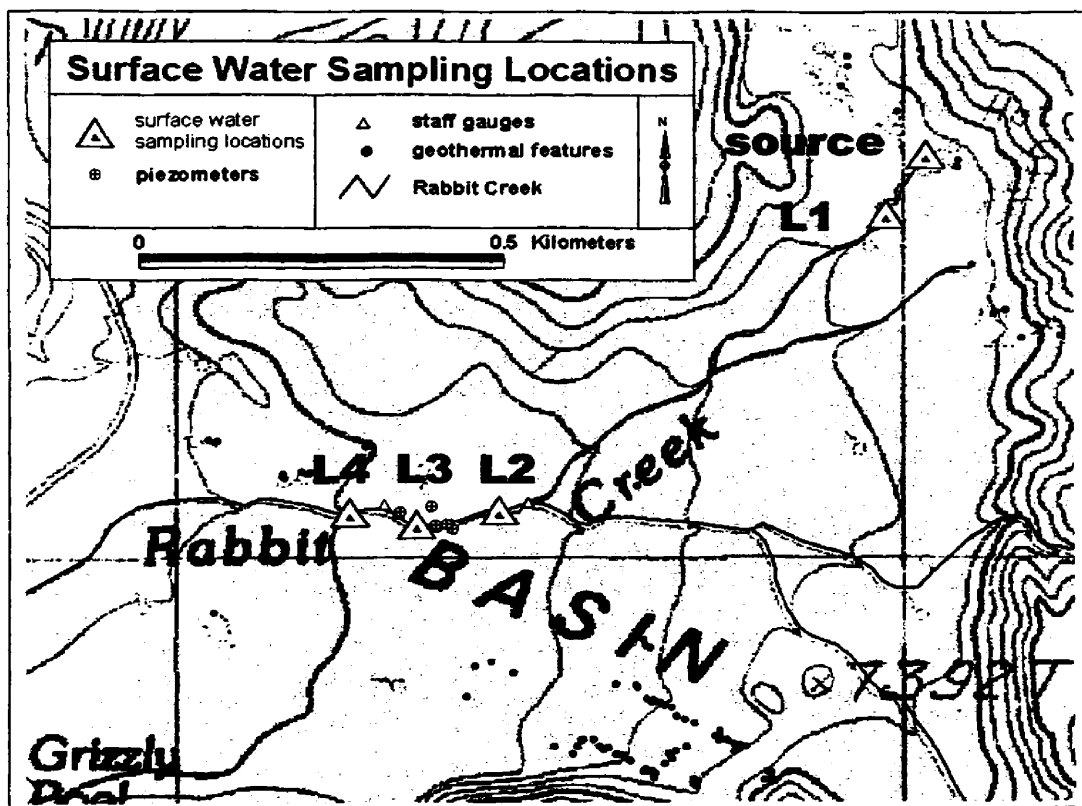


**Figure 9:** Surface water sample locations. Note the spatial extent of surface water sampling locations in relation to the piezometers in the study site. The source is the most right location on the map. Locations one through four are downstream of the source (right to left) with location one just to the left of the source.

Prior to sample collections, pH and temperature (Orion SA 250 meter with a Sensorex S200C combination pH and temperature probe), conductivity (Hach models 17250 and 44600), and dissolved oxygen (Orion model 820 and YSI model 95) measurements were taken with portable field meters using standard procedures. Water was sampled with a 100 ml syringe and filtered through a 0.2 micron filter (either Gellman or Whatman brands with a nylon filter membrane and polypropylene housing). The filtering process reduced particulates and microbes in the sample by providing a substrate for accumulation. The decrease in particulates and microbes is desired so minimal biogeochemical reactions take place before laboratory analysis. Sixty mL HDPE Level 1 EPA type water sample bottles were used. Cations were preserved with 0.2 N nitric acid within 48 hours of collection. All samples were kept in a cooler in the field (except for the winter season) and stored in a refrigerator until analysis. Alkalinity was analyzed by a Hach alkalinity kit (model AL-DT) for total alkalinity within three days of collection. Anions were analyzed by ion chromatography (Dionex ED40 electrochemical detector, GP40 gradient pump, and Peaknet software, EPA300 method using a 5  $\mu$ L loop) in the Murdock Environmental Biogeochemistry Laboratory at the University of Montana (August to January) and by the University of Wyoming Department of Zoology and Physiology (February to July). Cations were analyzed by XRAL Laboratories in Canada (EPA200 method). Sulfide was analyzed using the Hach Method in the field in July, 2002.

Iron samples were collected separately and preserved with 0.2 N nitric acid. Total iron and ferrous iron were analyzed by the Ferrozine method (Gibbs, 1979) using a Hach



Spectrophotometer Field Kit at the time of collection or within 48 hours of collection. Ferrozine reacts with iron to form a magenta color (Gibbs, 1979). The color intensity is directly proportional to the iron concentration. Hydroxylamine is used as a reducing agent for total iron analysis. Ferric iron was calculated by subtracting the ferrous iron amount by the total iron amount. It is highly recommended that ferrozine analyses be conducted in the field. If the analyses are not conducted in the field, actual iron concentration may vary due to oxygenation and photochemistry unless acidified (Waite et al., 1995, Hydes and Chapman, 1986).

Geochemical modeling was performed for surface water and groundwater samples using MINTEQA2 (Version 3.10, 1991, US Environmental Protection Agency). Field parameters (pH, temperature, dissolved oxygen), alkalinity, cations, anions, and  $\text{Fe}^{2+}$  /  $\text{Fe}^{3+}$  values were used in the input files. Silica speciation and mineral saturation indices were obtained.

### **3.4 Collection of Mineral Precipitates**

Six bead tubes were installed into the streambed to collect mineral precipitates. Silica was expected to be the primary precipitate. Tubes were constructed of 0.20 cm O. D., thin walled Plexiglas (Figure 10). Holes were drilled into the tubing (1.5 mm dia.) to allow sufficient water flow through the apparatus. Aluminosilicate beads (average 1 to 2 mm dia.) filled the tubes and aquarium cement sealed the ends. Foam inserts were installed within the tubes at the surface water and groundwater interface to prohibit water

mixing. Four tubes were 30 cm long and two tubes were 20 cm long. The long tubes were installed in deeper water in the single channel creek systems and the short tubes were installed in the shallow braided system. Fifteen centimeters of the tube was placed in the subsurface for both the short and long tubes. For the long tubes, 15 cm of the tube stuck out of the channel for surface water chemical precipitation. For the short tubes, 5 cm was allowed for surface water flow exposure.

Tubes were installed in October, 2001. They were collected in January, 2002. The beads were extracted from the tubes and then air dried. Sample beads were analyzed at 84 magnification using scanning electron microscopy (CamScan Series 3 SEM with EDAX EDS) at the Montana Crime Lab in Missoula, Montana. Photomicrographs of a blank bead and a bead with creek precipitates were taken for comparison. Three more tubes were installed in February, 2002: one near the source, one in the single channel section of the study site, and one in the braided section of the study site. A 50/50 mixture of aluminosilicate and soda lime glass beads was experimentally used.

Three chemical precipitation boxes were constructed. Numerous holes were drilled with a 0.6 cm drill bit in a small ( $\sim 100 \text{ cm}^3$ ) plastic box. The holes in the box were designed so the inside of the box would be open to the environment with the cover on. Glass plates were acid washed. Each box had two glass plates, one on the inside of the box and one on the top of the box. The boxes were attached to the creek channel substrate and submerged in the water. The purpose of the precipitation boxes was to determine if silica deposition would occur on the glass plates. Thereby, an estimate of the current rate of

silica deposition could be quantified by measuring the thickness of the silica layer. The boxes were installed in February and taken out in July, 2002. Photos of the boxes were taken during each round of water chemistry sampling to document any obvious changes. Precipitates from the second set of bead tubes and the boxes were analyzed by SEM July 29, 2002.

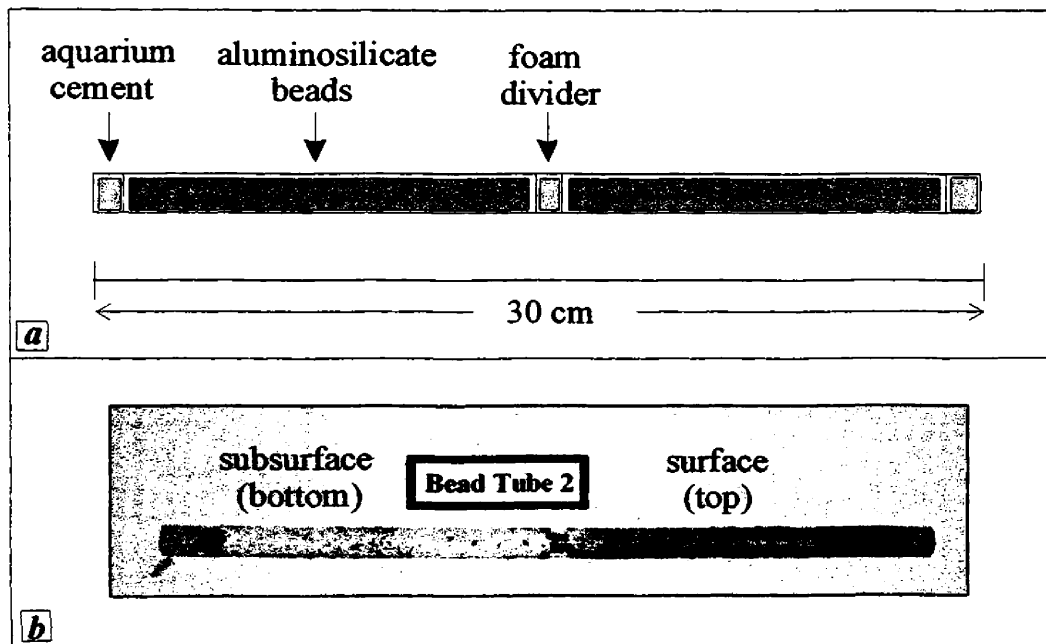


**Figure 10:** Schematic design of long bead tubes placed in the deeper creek sections (a) (not to scale). Bead tube 2 (b), after two months in the single channel section of the study site.

### 3.5 Mineral Identification

Twelve rock samples from the creek and the well bore holes were collected (Table 1).

Bore hole samples were chosen based on crystal observations in the field. Creek samples were chosen as representative samples of single type and anastomosing type creek

sections. Collected samples were taken from both aerial deposits and submerged deposits.

**Table 1:** Descriptions of rock samples and collection locations.

Sample ID	Description
m1a	43 cm depth (piezometer bore hole)
urb	<10 cm depth (piezometer bore hole)
ula30	30 cm depth (piezometer bore hole)
rl1	surface sample from <i>location 1</i> water sampling point near the source
rl2a	~ 100 m above study site from a braided creek section
rl2b	same as rl2a
rl3a	single channel section in study site near piezometer <i>lra</i> (partially submerged)
rl3b	same as rl3a
rl3c	same as rl3a
rl3d	sub-aqueous sample near piezometer <i>lla</i>
rl4a	braided section in study site near piezometer <i>li</i> ( <i>separated from channel lining</i> )
rl4b	braided section in study site near piezometer <i>li</i> ( <i>part of channel lining</i> )
rl4c	same as rl4a

Rock samples were dried at room temperature and ground with a mortar and pestle. A smaller sample set was prepared for clay analysis. Ultrasonic disaggregation of the sample was performed with chemical dispersement (sodium hexametaphosphate ( $\text{NaPO}_3$ )<sub>6</sub>). A centrifuge was used to separate the fraction that was  $<2 \mu\text{m}$ . Glycol solvate was used in the slide preparation.

Prepared samples were analyzed by x-ray diffraction (XRD) using the random powder method with a Philips XRG 3100 x-ray generator, APD 3720 recorder, and PW1877 V. 3.5B software. The start and end angles were  $2^\circ$  and  $65^\circ 2\theta$ , respectively. Scan time was 1 second per step and the step size was  $0.1^\circ 2\theta$  for initial scans. The scan time was increased up to 3 seconds per step and the step size was reduced down to  $0.01^\circ 2\theta$  on

subsequent scans for peak clarification. Diffraction scan data was transferred to MacDiff 4 v. 4.2.5 software for peak analysis and identification.

Petrographic microscopy was performed on a limited sample set. Rock samples were taken from the hot spring source, the creek channel lining, and the piezometer bore holes. Thin sections were made of five of these rock samples by San Diego Petrographics. The five samples were chosen based on x-ray diffraction patterns. The thin sections were photographed using a Carl Zeiss microscope with a 35 mm still camera. Layer morphology and microbe entombment were examined.

Scanning electron microscopy, energy dispersive spectrometry, and backscattered electron imaging (SEM/EDS/BEI) work was done on the thin sections at the Materials Characterization Laboratory at the Department of Geology and Geophysics, University of Wyoming. (Preliminary work was conducted at the Montana Crime Lab, Missoula, Montana). SEM/BEI images were taken and elemental mapping was performed. Two machines were used: a JEOL JXA-8900R WD/ED combined microanalyzer and a JEOL JSM-5800 LV Scanning Microscope (50 second spectral scans).

The hydraulic properties of the mineral precipitate are necessary for the quantification of surface water and groundwater interaction. Porosity ( $n$ ) was measured from protocol by Kendall (1999) after the theoretical work of Mowers and Budd (1996).

The porosity measurements were made by taking a still video image of a sample (Diagnostics Instruments 0.7X HRO70-CMT video camera attached to a Nikon Optiphot2-pol 70X microscope). The images were analyzed with NIH software where void space was delineated and porosity calculated. The field of view (FOV) represented a sample measurement. Seven sections on each sample were measured. The seven measurements covered the entire thin section sample.

Simple porosity statistics (average, mean, standard deviation, and 90% confidence interval) were performed on each sample set. Analysis of variance (ANOVA) was performed on the creek samples, the piezometer samples, and the entire sample set.

Permeability was calculated using equations and constants derived from Kendall (1999):

$$K_i = \frac{n^3}{[C(1-n)^2] [(4PP) / (\pi PA)]^2} \quad (1)$$

where  $k_i$  = intrinsic permeability ( $L^2$ )  
 $n$  = porosity  
 $C$  = shape factor (2.75 from Kendall, 1999)  
 $PP$  = pore perimeter ( $303,525 \mu m^2$ )  
 $PA$  = pore area

Hydraulic conductivity was calculated to account for water flowing through a porous medium (Fetter, 1994). Water temperature was estimated for all samples to be 35°C. Hydraulic conductivity is related to intrinsic permeability in the following equation:

$$K = k_i \left( \frac{\rho g}{u} \right) \quad (2)$$

where  $K$  = hydraulic conductivity  
 $\rho$  = water density  
 $g$  = acceleration of gravity  
 $u$  = water viscosity

### 3.6 Geomorphology

The channel in Rabbit Creek is complex. Mineral deposits are present in both single channel and anastomosing sections. Mineral deposits in the single channel sections are typically submerged and line the channel sides and creek bed. Thickness of deposits varies considerably. The mineral deposits have created step-pool systems. The mineral deposits in the anastomosing sections have confined several channels. Some channels are perched upon other channels. The channel morphology was characterized in order to establish patterns of mineral deposition taking place in the creek.

Longitudinal gradients were surveyed in the creek in two locations: at the study site and a creek reach just below the source. A Leica Wild T1610 theodolite mounted on a Leica Type GST 20-9 tripod was used to measure channel elevations. Relative elevations were tied into a base US Geological Survey map. The thalweg portion of the channel was chosen as the measuring point. Approximately every ten meters, a measurement was taken for elevation and for georeferencing. A Trimble Pro XR/XRS global positioning system unit was used to map the piezometers.

Channel cross sections in the study site were measured in June, 2002. A meter tape and meter stick were used. Depth from the surface water to the channel bottom was measured every 15 cm across the cross section. The most upstream cross section started at the upper stream staff gauge. A cross section was measured every 15 meters downstream from the previous cross section. The most downstream cross section was at the lower stream staff gauge.

### **3.7 Photographic Documentation**

Extensive photographs were taken during each of the water sampling rounds. The purpose of photo documentation was to qualify silica deposition, seasonal microbial community changes, and other unique geological features as observed. Three different cameras were used: an Epson PhototPC 850Z digital camera with max 6X zoom lens (JPEG format), an Olympus Stylus Epic (35 mm), and a Nikon N-70 camera with a Quantaray 28-80 mm zoom lens (35 mm). The 35 mm prints were scanned to JPEG images or digitally developed.



## 4.0 Results and Interpretation

### 4.1 Surface Hydrology

Discharge of Rabbit Creek was approximately  $0.1 \text{ m}^3/\text{sec}$  between August 19 and August 31, 2001 (Figure 11). A diel flow change of about  $0.01 \text{ m}^3/\text{sec}$  was observed during this period. Two factors could cause these diel fluctuations: evaporation or lunar gravity affects. It is unlikely that evaporation caused the discharge fluctuations seen because the water is approximately  $40^\circ\text{C}$ . The water evaporates significantly as soon as it leaves the source since the creek water temperature is so high. The water probably significantly evaporates whether the air temperature is warm or cold and thus would not cause these large diel changes. Barometric affects may influence evaporation but barometric data was not available. If several millimeters of water evaporated off the surface each day in the hot spring and the creek, the reduction in flow would still be negligible. The cross sectional area of the creek is large enough near the source, where the width to depth ratio is low, so a decrease in depth on the scale of millimeters would not significantly affect discharge.

Lunar gravity affects are the likely explanation for the fluctuations. The creek water supply comes from a hot spring. The source water is a confined hydrothermal reservoir that is likely sensitive to pressure changes. Other researchers have proposed and debated the concept of lunar gravitational affects in hydrothermal systems. Rinehart (1972) believes lunar gravitational affects are an important control on geyser periodicity. White and Marler (1972) disagree with Rinehart (1972) and believe geyser periodicity is

controlled by heat and pressure of hydrothermal water. Bredehoft (1967) thinks gravitational affects in aquifers are more dependent on the elastic properties of the earth as a whole rather than the elastic properties of an aquifer. Robinson and Bell (1971), in a discussion regarding the connectivity between ocean water and aquifers, claim a confined aquifer will receive negligible affects from nearby ocean tide fluctuations. Head changes in response to tidal fluctuations are too slow to accurately quantify. Robinson (1939) measured water levels in wells in New Mexico and Iowa, discounted barometric affects, and realized lunar gravitational affects acting on the system were responsible for the fluctuations. See Appendices for more lunar gravity data for evidence of diel flow changes in Rabbit Creek.

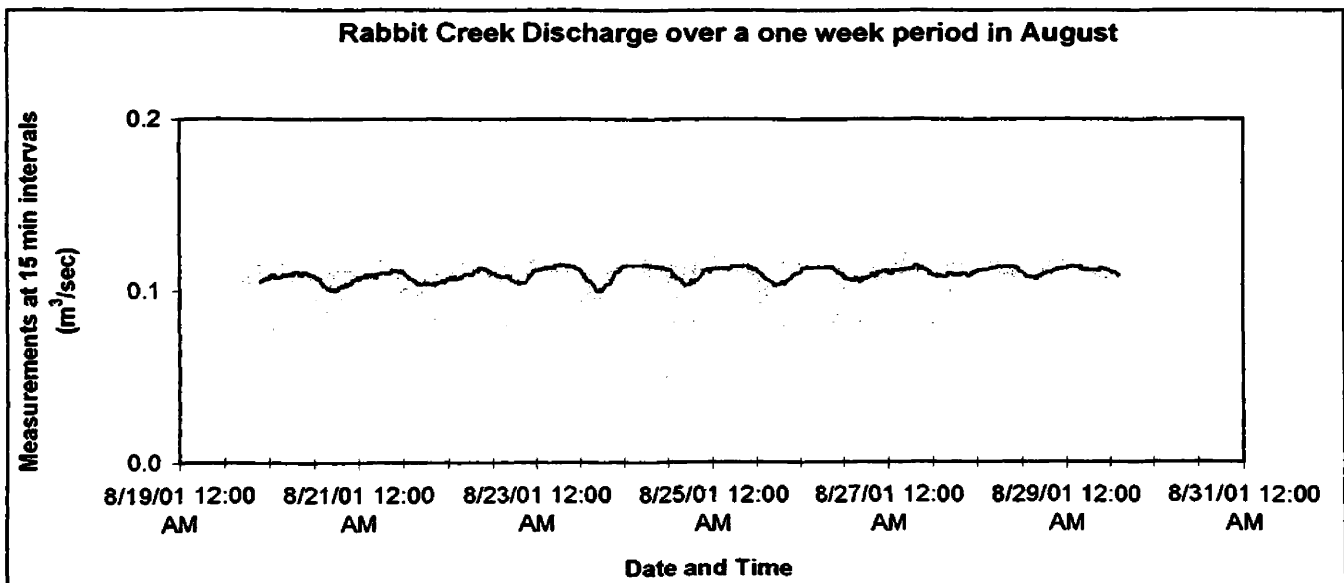


**Figure 11:** Flo-Dar hydrograph from August 19 – 31, 2001. The solid black line has a moving average value over 20 points.

Bobber tests performed monthly at the Flo-Dar site showed little variation in surface water velocity measurements (Figure 12). Variance is attributed to two factors: (1)

method or operator error and (2) seasonal affects. The bobber test uses tools and techniques that are approximate and so measurements have a large associated error. The measured discharge using the bobber test in August, 2001 is approximately the same as the Flo-Dar measurements made at the same time. The Flo-Dar is very precise; measurements are consistent. The bobber test hydrograph corresponds with a typical seasonal hydrograph where discharge is low in winter, increases in the spring, and then lowers again in the summer. However, with a one standard deviation error bar applied, there are no seasonal discharge fluctuations.

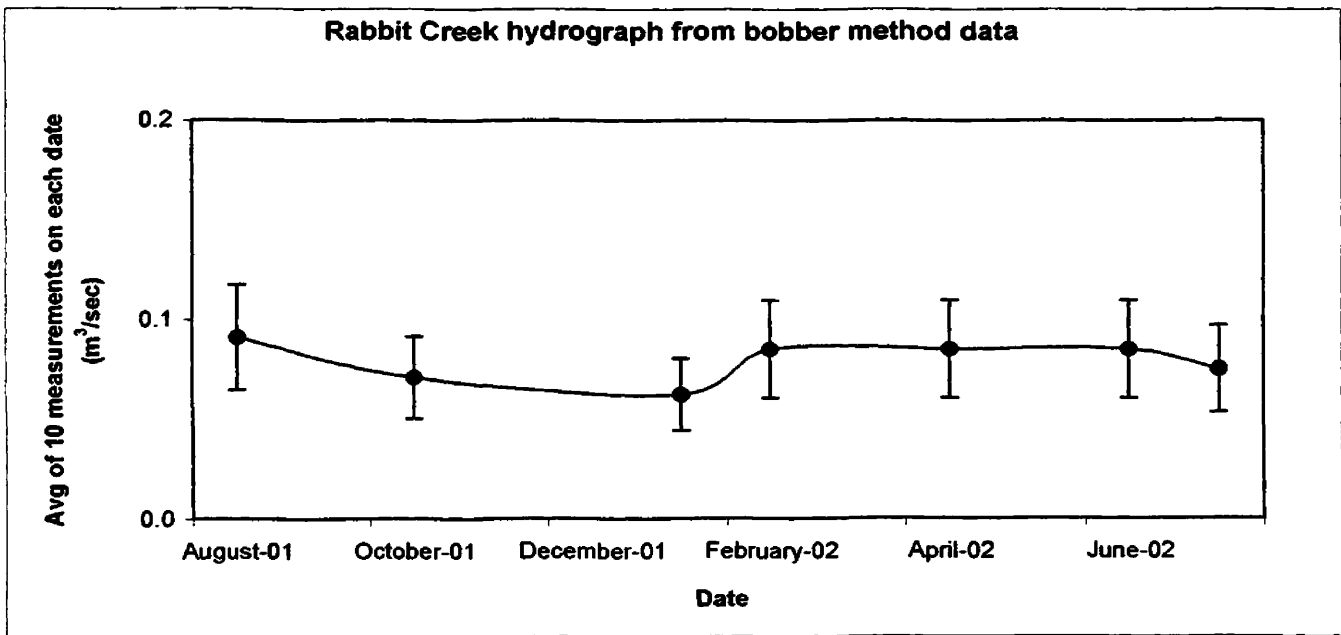


**Figure 12:** Bobber test creek hydrograph measured in the study site with one standard deviation error bars.

The Flo-Dar compared well with the bobber tests (Figure 13). The Flo-Dar was more precise but the bobber test provided consistent results. Since the Flo-Dar requires extensive setup time in the field, the bobber tests were particularly suited for quick

estimates of discharge. It would have been logistically difficult to use the Flo-Dar during the sampling days.

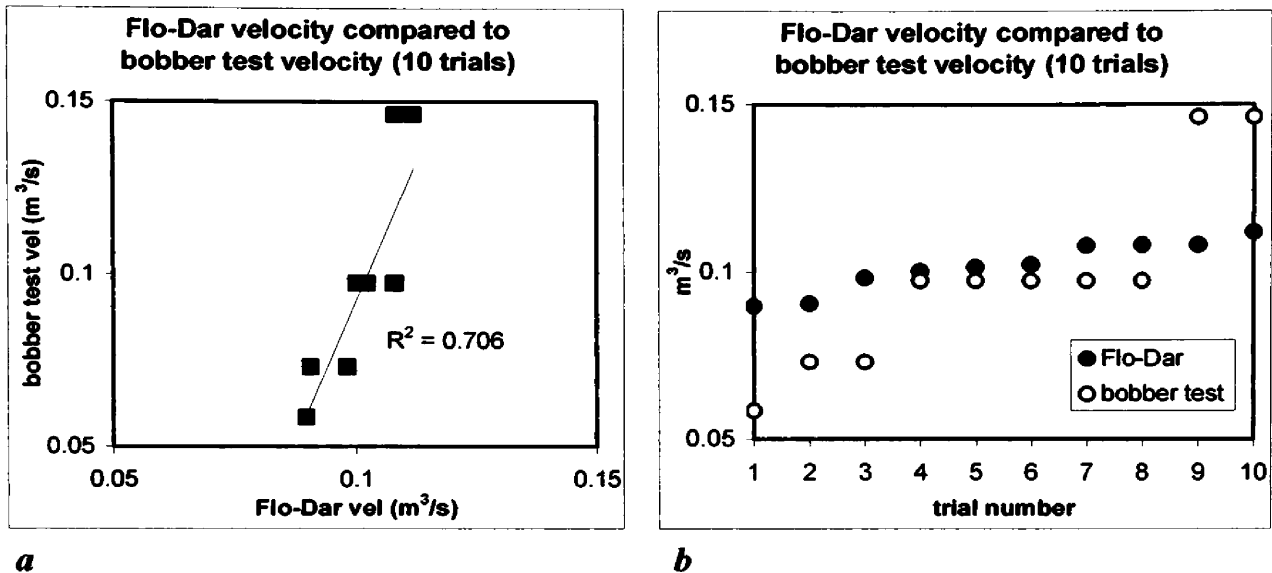


**Figure 13:** Discharge comparison between the Flo-Dar surface water velocity meter and a USGS bobber test. Data is sorted in ascending order. The correlation in plot *a* is good because the creek discharge is low and so associated error is acceptably high. The data for the Flo-Dar is plot *b* is more precise than the bobber test.

The three stream staff gauges showed minimal water level fluctuations during the study.

There was no trend in staff gauge measurements that could be attributed to discharge changes. For example, one staff gauge showed a slight increase in stage and another

showed a slight decrease in stage during the same month. Therefore, variance is

attributed to measurement resolution. A transducer installed on the staff gauges is needed to accurately measure stage in this small creek.

## 4.2 Hydrogeology

Hard sinter was encountered within 10 cm depth in each piezometer bore hole (Figure 14: well logs). The groundwater elevation in nearly all wells increased from August, 2001 to April, 2002 (Figure 15). A decrease in the water level elevation was measured from April to July, 2002. A decrease in the water table elevation and the absence of standing water on the ground surface persisted in the meadow from April to July. Figure 16 shows October 2001 groundwater head data where the groundwater elevation was higher than the creek water elevation.

The increase in groundwater elevation is from precipitation occurring in November and December, 2002. Much of the snow that accumulated in the meadow was melted by the warm shallow groundwater as winter progressed. The meadow became more inundated up to the April, 2002 and then started to dry. The meadow inundation observations correspond with the changes in water level measurements. Well *ula* was plotted individually (Figure 17) to show water level fluctuations corresponding to precipitation data. There is an anomaly in October where the groundwater elevation from the summer season. Precipitation does not follow this trend in October. However, the precipitation data set is an average of a half a century and not measurements taken during the study.

One piezometer, *li*, was dry when installed. However, measurable water was observed in January, February, April, and June: only 1 cm was in the piezometers. Enough water infiltrated into the piezometer to collect a full water sample in April. This water was

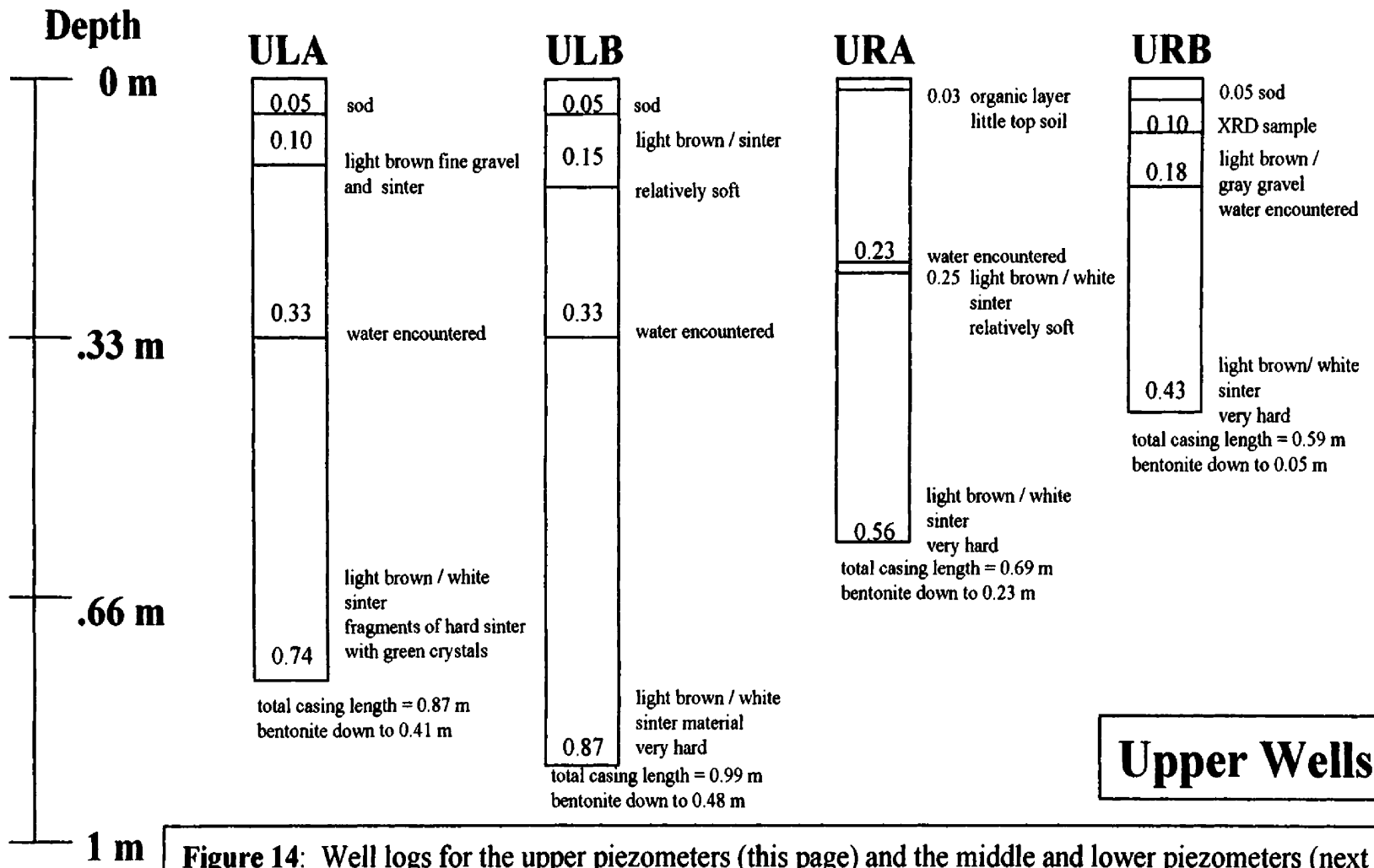
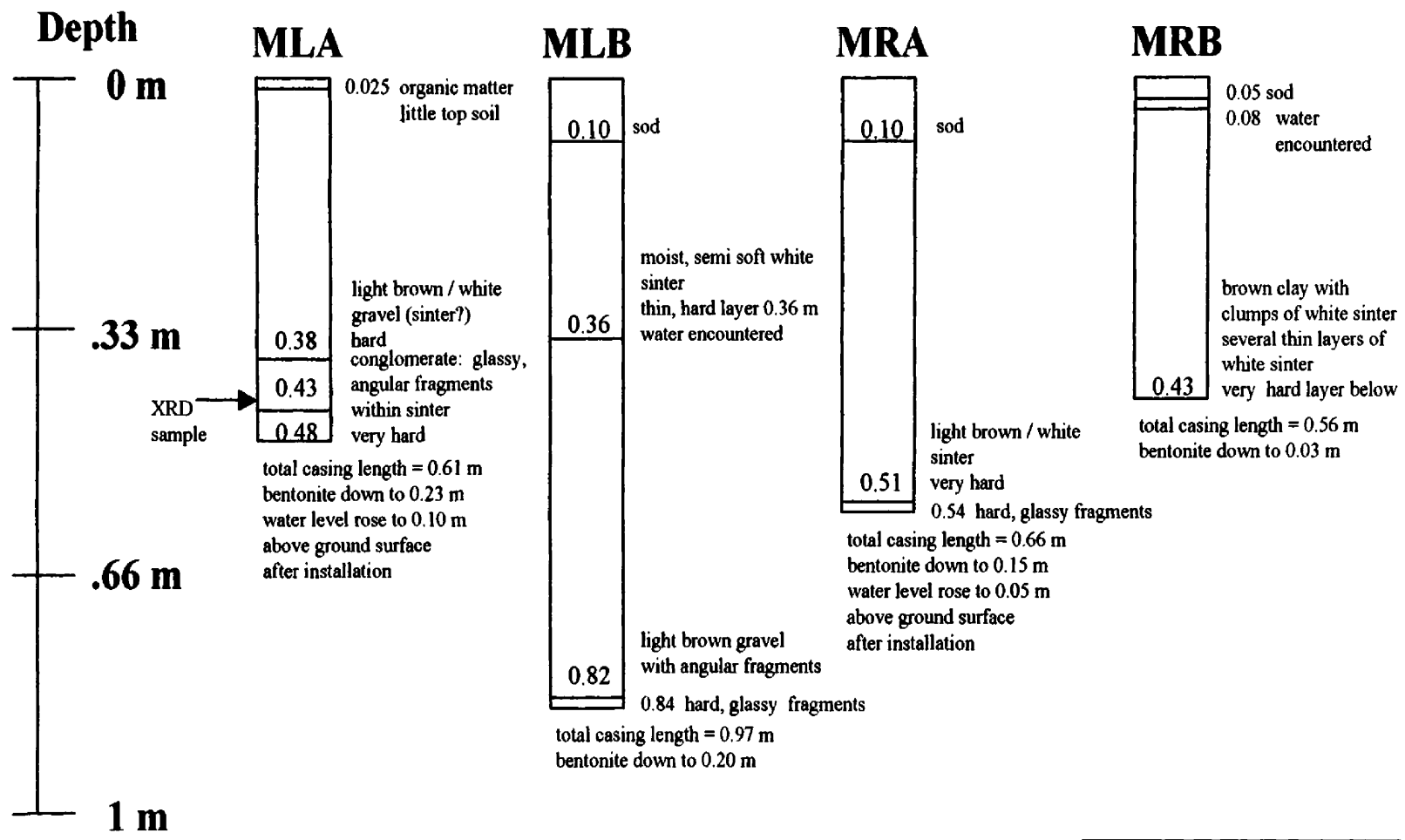
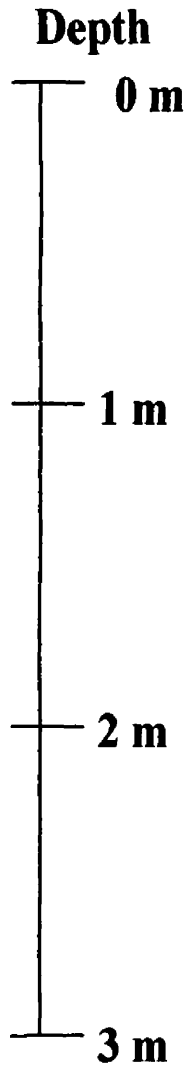


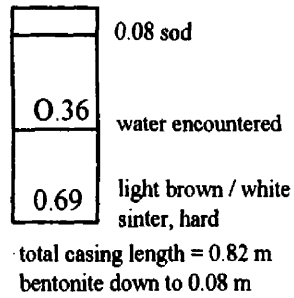
**Figure 14:** Well logs for the upper piezometers (this page) and the middle and lower piezometers (next two pages). All well casings are 0.13 m above ground surface. Screened intervals are 0.13 m in length, 0.03 m from the bottom. All holes were backfilled with material taken out when drilling.



**Middle Wells**

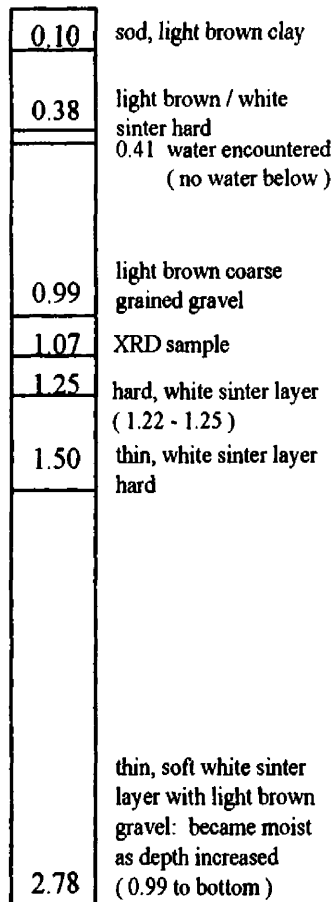


**LLA**



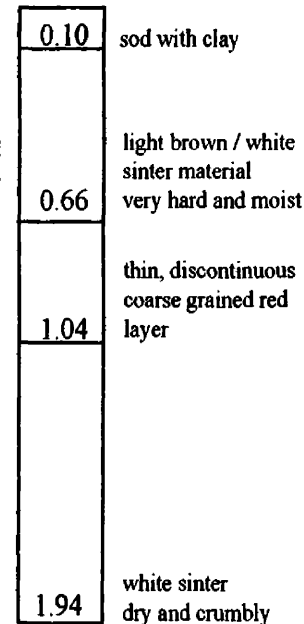
*Note different scale from Upper and Middle wells*

**LRA**



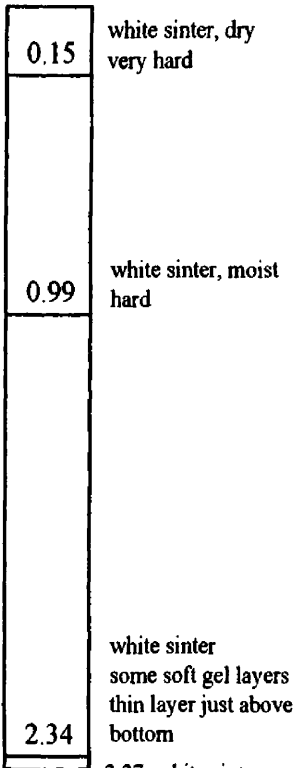
total casing length = 2.9 m  
bentonite down to 0.31 m  
dry well when installed

**LRB**



total casing length = 2.06 m  
bentonite down to 0.23 m  
dry well when installed

**LI**



total casing length = 2.50 m  
bentonite down to 0.05 m  
dry well when installed

**Lower Wells**



probably infiltrating vertically upward from a deeper groundwater system because the material above the bottom of the hole was dry during piezometer installation.

The small change in groundwater elevation, creek stage, and creek discharge indicates groundwater flux into the creek was constant during the study.

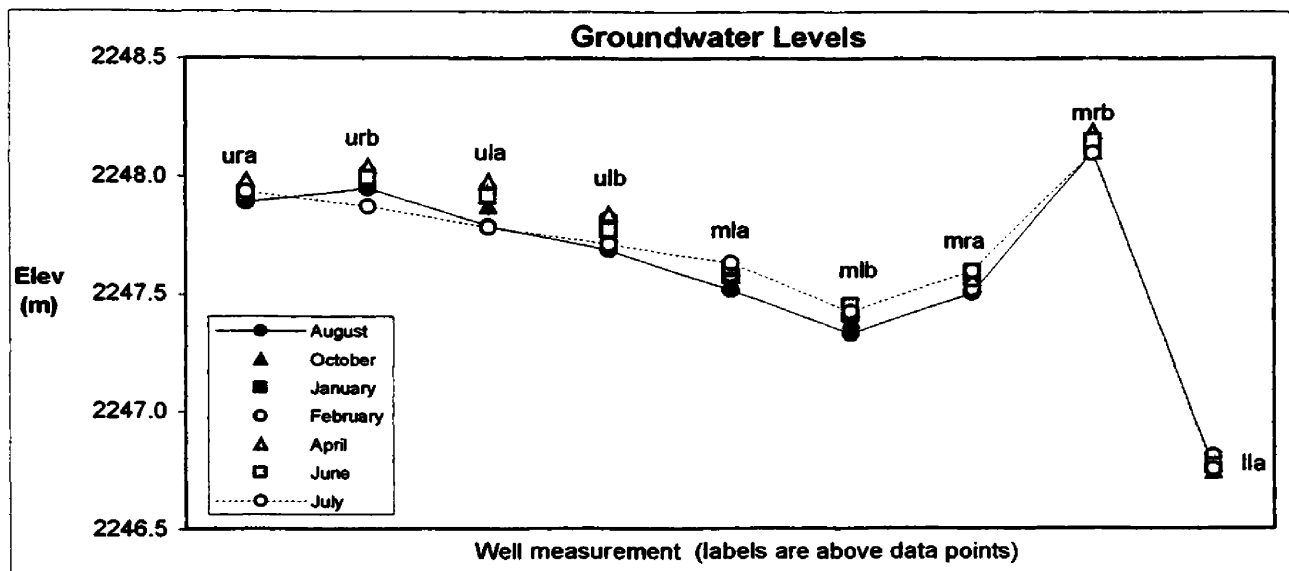


**Figure 15:** Groundwater elevation plot during the study period.

In the study site, a hot spring emerges in the single channel section (Figure 18). This hot spring water, as well as piezometers *mla* and *mra*, have elevated water temperatures in relation to the creek water temperature (a range of 5° – 15° C higher than the creek).

Water chemistry, pH, and conductivity are not similar but the geologic material likely affects these parameters. The head was above land surface in these piezometers during the study. It is inferred the two piezometers and the hot spring in the creek are probably coming from the same aquifer. This aquifer is different than the shallow groundwater system studied.

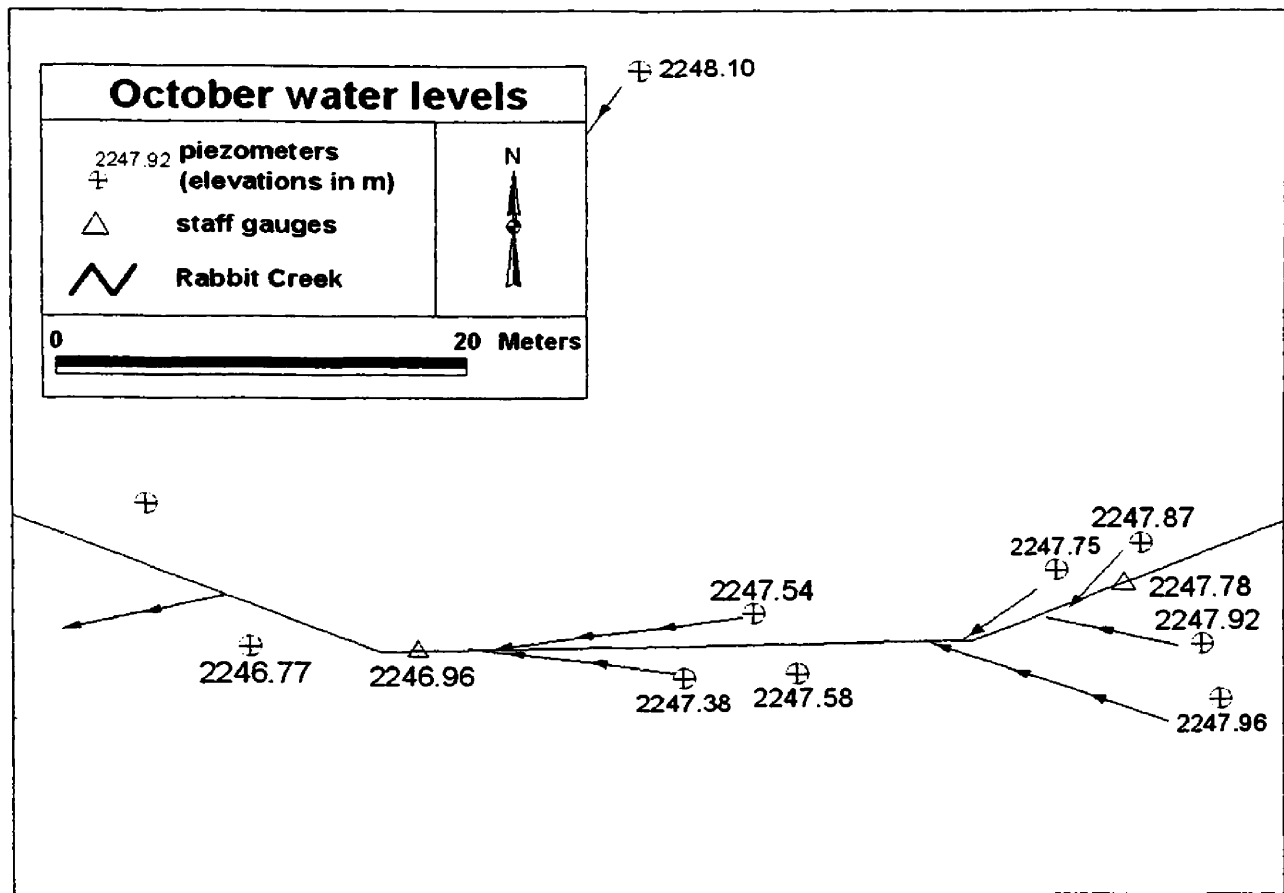


**Figure 16:** October potentiometric map showing water levels in piezometers and Staff gauges. Flow lines are drawn from locations of higher head to locations lower head. Similar trends occurred throughout the study.

Slug tests did not provide reliable data in any of the piezometers measured. Water injected into the piezometers drained too quickly to accurately record the water level. Water probably moved out of the bottom of the piezometers rapidly because the backfill material was highly permeable. The backfill material consists mostly of sinter fractured from the boring process. Since the piezometers are shallow, some of the water may have moved up into the soil zone that is probably highly permeable.

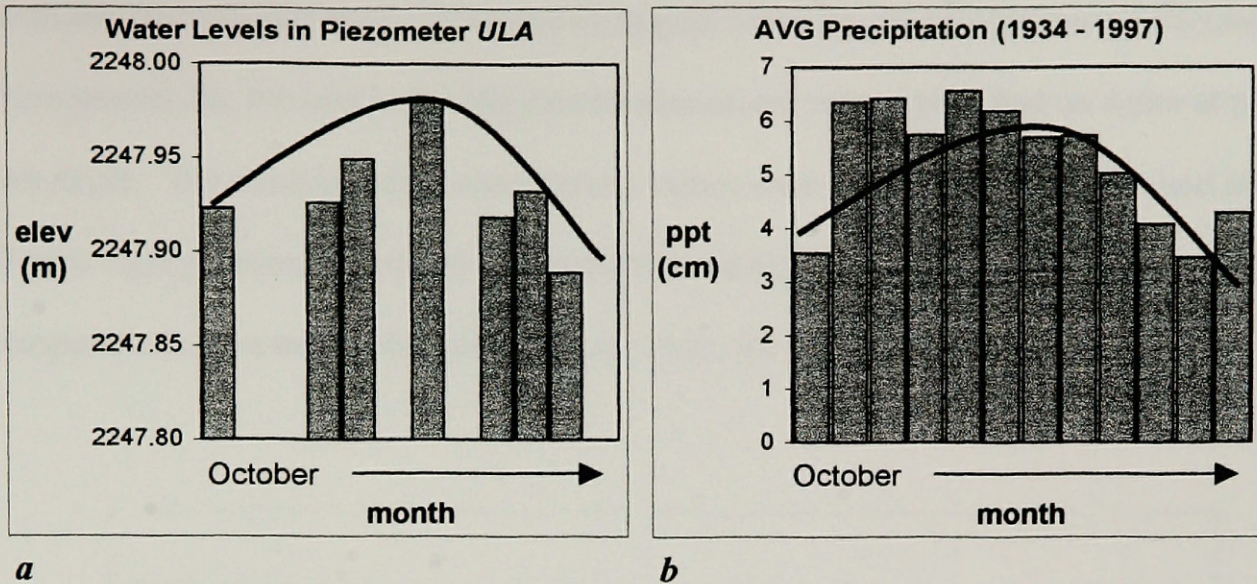


**Figure 17:** Water level measurements in piezometer *ula* (plot *a*). Historical precipitation data collected at the Old Faithful weather station is in plot *b*. (data downloaded from the National Climate Data Center Internet Web Site: <<<http://lwf.ncdc.noaa.gov>>>). Elevations and precipitation data correspond by increasing during the winter and early spring and decreasing in summer.

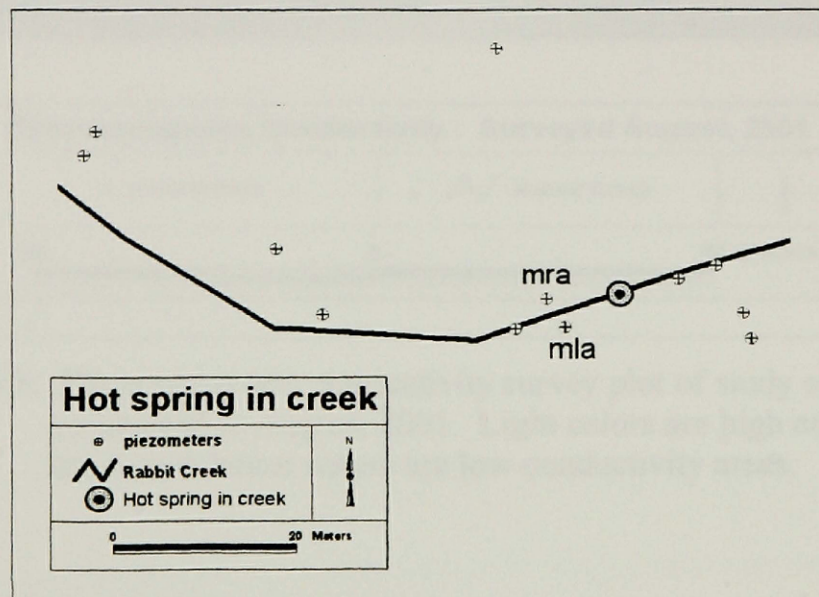


**Figure 18:** Location of hot spring that emerges in the creek in relation to piezometers *mla* and *mra*.

Electromagnetic conductivity (em) data showed variation in conductivity values throughout the surveyed area (Figure 19). The conductivity values appeared to correlate



with the groundwater levels measured in August when the em surveys were performed. Piezometers *lra*, *lrb* and *li* (far left piezometers on em survey plot) had no water at nearly 3m depth. The corresponding conductivity values were low. Piezometers *ula* and *ulb* (lower right piezometers on em survey plot) had a high water table with warmer temperatures than most other piezometers. Here, the conductivity values were high.

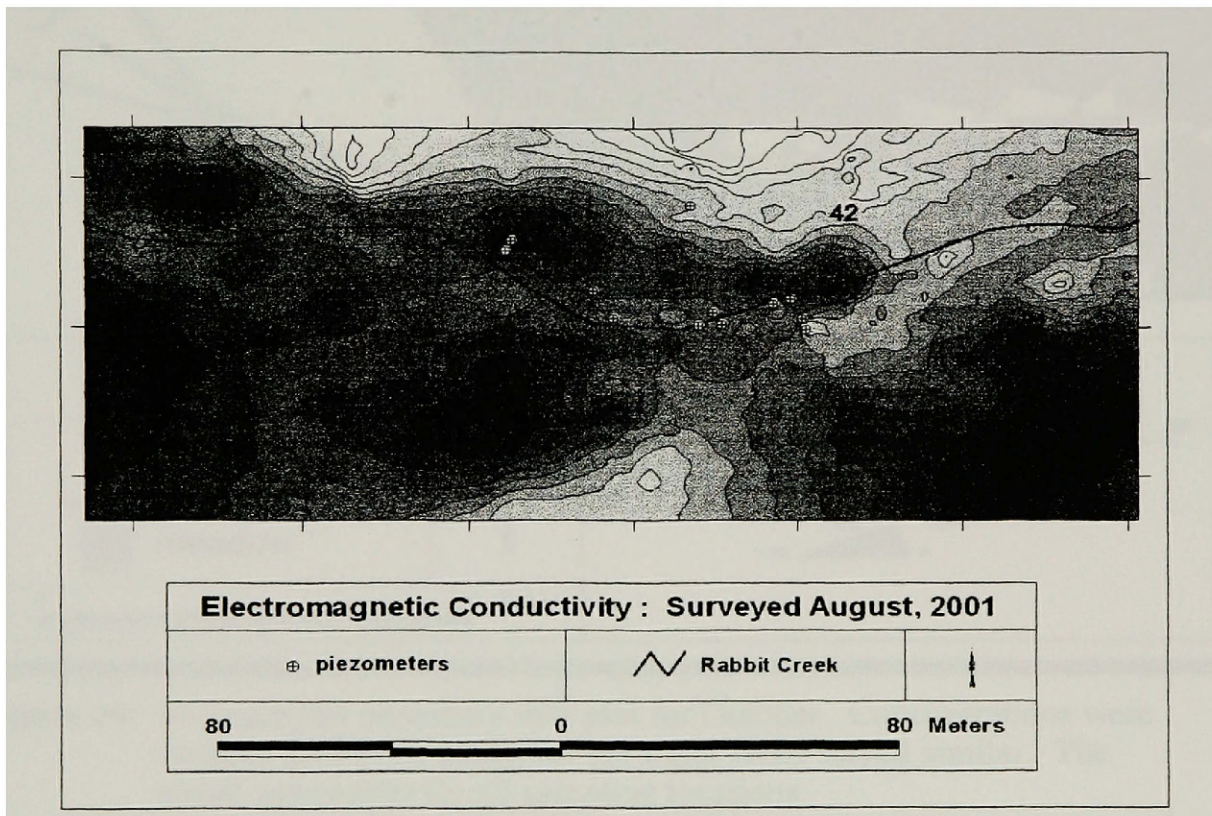


**Figure 19:** Electromagnetic conductivity survey plot of study site conducted in August, 2001. Light colors are high conductivity areas and darker colors are low conductivity areas.

### 4.3 Geochemistry

Figure 20 is a stiff diagram of the groundwater. All waters were sodium-chloride-

bicarbonate type waters with high concentrations of silica. The meq/L are similar for all symbols. The surface water showed the same type waters.

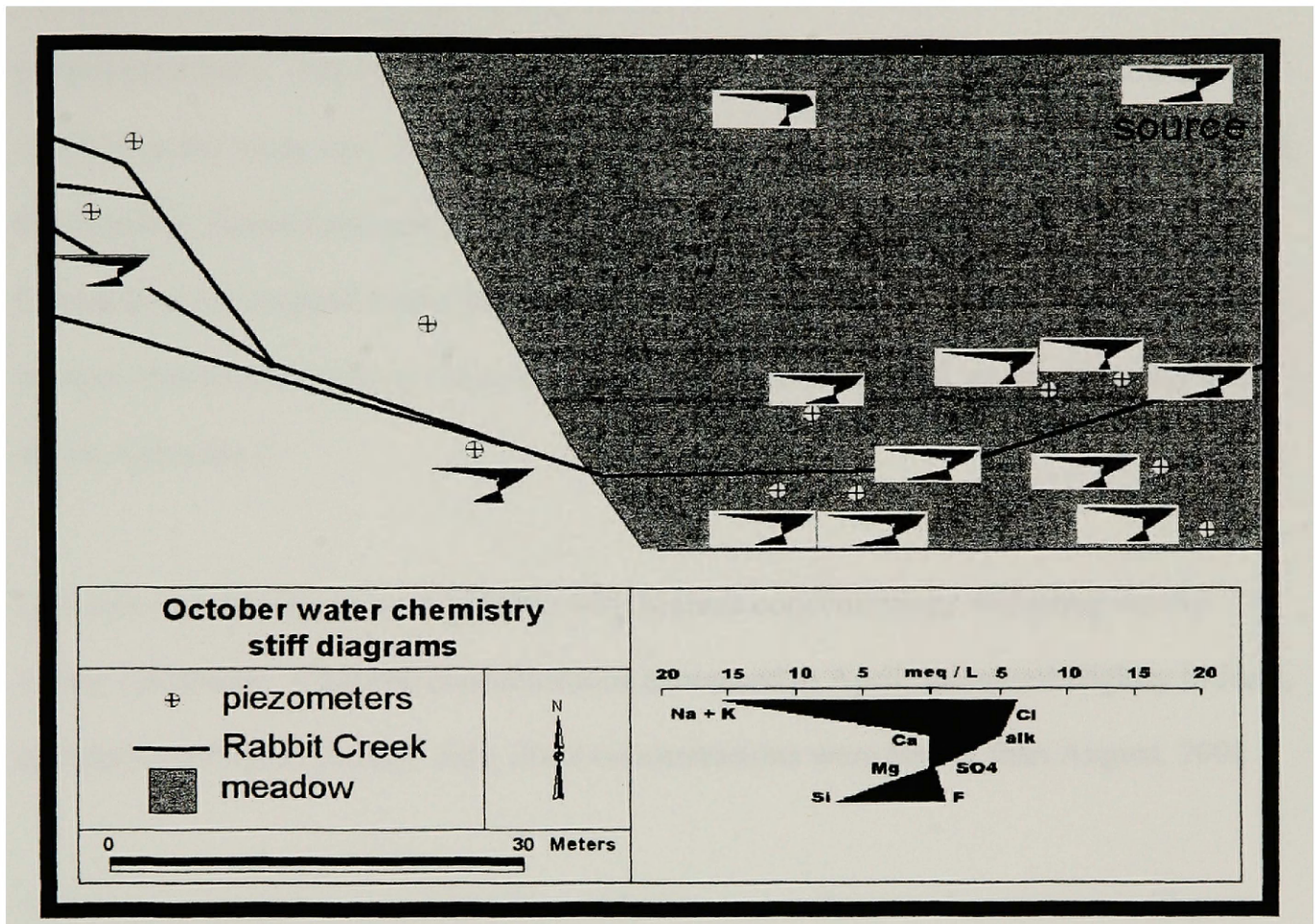


**Figure 20:** Groundwater chemistry stiff plot for October. Concentrations were variable during the study but the water types stayed similar. The meq/L are similar for all sampling locations.

There was a large variance in analyte concentrations in both the surface water and groundwater during the study. The analyte concentrations compared well with archived chemical data (Appendix E). However, silica concentrations were higher in the Rabbit Creek source area when measured in 1971 as compared to this study. This may be due to differences in analytical procedure where this study used technologically advanced tools. During the winter months, concentrations of analytes increased both in the surface water



and the groundwater. Major cation concentrations (Al, Ca, Fe, K, Mg, Na, and Si,) were higher during the winter (Table 2 and Figure 21, preceding pages). Silica and chloride increased in both surface water and groundwater. Ferrous and ferric iron increased in the groundwater only. The only measurable iron in the surface water was just below the meadow in the study site. Piezometers *ura* and *urb*, both on the north side of the creek in the meadow, showed anomalously high concentrations of the major analytes in January. Concentrations dropped back down to the beginning August, 2001 conditions by the second summer field season (June and July water chemistry). All water chemistry data are in Appendix C.

Chloride concentrations were variable with highest concentrations occurring during winter conditions. Chloride concentrations decreased to April, increased slightly in June, and decreased again in July. July, 2002 concentrations were higher than August, 2001.

Temperature was plotted against silica, chloride, and sodium to observe trends (Figure 22). In the groundwater, as temperature increases, silica concentration increases which is a function of silica solubility. However, there is no correlation between silica and temperature in the hot spring source or the creek. This indicates silica is not behaving conservatively in the surface water. The non-conservative behavior is attributed to silica precipitation and dissolution of the creek channel mineral deposits and the sinter that the creek runs through. There were observable trends of chloride and sodium to temperature in the groundwater, though the  $r^2$  values were low. There is no correlation of chloride and sodium to temperature in the surface water.

**Table 2: Major cations and chloride. Concentrations are in mg/L.**  
There are no surface water samples in August.

---

**August**

Element	Al	Ca	Fe	K	Mg	Na	Si	Cl
<b>Well ID</b>								
082101 ula	0.00	0.95	0.06	12.12	0.14	311.00	82.86	202.51
082101 ulb	0.00	1.47	0.24	11.79	0.29	305.00	71.78	199.51
082101 ura	0.00	1.52	0.09	12.81	0.21	357.00	58.76	234.89
082101 urb	0.00	1.30	0.06	14.92	0.29	341.00	77.19	224.49
082101 mla	0.00	0.83	0.00	11.95	0.05	317.00	107.00	202.96
082101 mlb	0.00	0.77	0.00	12.42	0.06	340.00	98.62	224.90
082101 mra	0.00	0.72	0.00	12.41	0.09	346.00	96.81	222.39
082101 mrb	0.00	2.51	0.23	20.06	0.32	481.00	52.13	171.01
082101 lla	0.00	0.97	0.00	12.68	0.13	323.00	81.74	205.01

---

**October**

Element	Al	Ca	Fe	K	Mg	Na	Si	Cl
<b>Well ID</b>								
100601 ula	0.00	0.80	0.00	12.08	0.11	319.00	82.84	191.87
100601 ulb	0.00	1.38	0.19	11.42	0.28	312.00	71.59	187.06
100601 ura	0.00	1.45	0.13	13.48	0.26	355.00	63.43	235.32
100601 urb	0.00	1.18	0.07	12.68	0.35	342.00	71.12	220.71
100601 mla	0.00	0.68	0.00	12.30	0.11	322.00	106.70	190.83
100601 mlb	0.00	0.96	0.15	12.69	0.17	341.00	91.12	209.65
100601 mra	0.00	0.67	0.00	13.12	0.08	333.00	102.00	221.15
100601 mrb	0.00	3.03	0.59	21.03	0.51	570.00	46.75	159.66
100601 lla	0.00	1.05	0.06	12.76	0.18	303.00	79.26	193.01

**Surface Water**

100701 source	0.14	0.34	0.00	13.31	0.00	455.00	130.00	278.36
100701 location 1	0.16	0.41	0.00	13.64	0.00	444.00	128.00	284.74
100701 location 2	0.00	0.48	0.00	14.17	0.07	430.00	134.80	284.34
100701 location 3	0.00	0.49	0.00	13.89	0.07	433.00	139.80	279.11
100701 location 4	0.00	0.50	0.00	14.00	0.00	431.00	133.70	282.00

---

**January**

Element	Al	Ca	Fe	K	Mg	Na	Si	Cl
---------	----	----	----	---	----	----	----	----

Well ID	Al	Ca	Fe	K	Mg	Na	Si	Cl
---------	----	----	----	---	----	----	----	----

011302 ula	0.00	3.97	1.35	10.90	0.78	378.00	70.45	318.73
011302 ulb	0.09	4.11	1.72	9.37	0.78	365.00	64.35	290.42
011302 ura	0.12	6.08	0.85	25.70	0.73	636.00	47.65	576.01
011302 urb	0.06	5.04	0.73	19.20	0.78	575.00	56.55	318.89
011302 mla	0.00	0.98	0.00	9.74	0.09	313.00	119.95	216.14
011302 mlb	0.06	2.01	0.53	12.70	0.19	383.00	96.95	282.48
011302 mra	0.00	0.86	0.00	11.90	0.08	326.00	102.95	242.86
011302 mrb	0.08	2.58	0.87	17.70	0.41	493.00	42.05	217.30
011302 lla	0.20	3.85	0.23	9.58	0.65	316.00	69.05	254.15

**Surface Water**

011402 source	0.26	0.52	0.00	10.50	0.00	418.00	147.95	305.77
011402 location 1	0.25	0.50	0.00	11.40	0.00	462.00	152.95	328.67
011402 location 2	0.13	0.58	0.00	12.10	0.00	429.00	153.95	315.02
011402 location 3	0.19	0.57	0.00	10.30	0.00	432.00	159.95	314.89
011402 location 4	0.16	0.74	0.00	12.60	0.00	430.00	152.95	321.31

---

**February**

Element	Al	Ca	Fe	K	Mg	Na	Si	Cl
---------	----	----	----	---	----	----	----	----

Well ID	Al	Ca	Fe	K	Mg	Na	Si	Cl
---------	----	----	----	---	----	----	----	----

022302 ula	0.05	6.15	2.65	15.65	1.50	383.35	57.36	374.36
022302 ulb	0.00	6.07	3.06	14.80	1.07	358.70	53.86	342.43
022302 ura	0.12	4.04	0.74	17.72	0.46	456.82	43.34	460.93
022302 urb	0.00	5.29	0.77	20.55	0.77	527.37	45.99	537.23
022302 mla	0.00	0.72	0.00	11.45	0.00	261.51	99.77	208.42
022302 mlb	0.00	2.00	0.62	13.81	0.21	321.57	80.70	272.70
022302 mra	0.00	0.76	0.00	11.96	0.11	281.89	87.82	241.53
022302 mrb	0.07	2.36	1.00	16.69	0.50	409.39	35.95	318.03
022302 lla	0.43	4.40	0.48	12.17	0.83	270.21	54.50	238.43

**Surface Water**

022302 source	0.22	0.25	0.00	12.42	0.00	348.94	113.92	298.41
022302 location 1	0.18	0.48	0.00	12.49	0.00	352.13	126.42	160.80
022302 location 2	0.12	0.55	0.00	12.92	0.00	362.68	122.45	222.24
022302 location 3	0.14	0.51	0.00	12.84	0.00	353.35	121.05	295.20
022302 location 4	0.13	0.54	0.00	12.72	0.00	340.97	122.83	296.94



---

**April**

Element	Al	Ca	Fe	K	Mg	Na	Si	Cl
---------	----	----	----	---	----	----	----	----

Well ID	Al	Ca	Fe	K	Mg	Na	Si	Cl
---------	----	----	----	---	----	----	----	----

040802 ula	0.07	5.02	1.92	14.14	1.15	342.79	58.70	277.42
040802 ulb	0.17	8.63	4.21	17.08	1.37	400.08	55.06	301.56
040802 ura	0.44	4.46	1.23	17.99	0.53	457.04	43.68	316.72
040802 urb	0.13	3.47	0.59	15.89	0.67	398.06	52.85	298.87
040802 mla	0.00	0.74	0.00	11.46	0.00	265.75	100.58	213.05
040802 mlb	0.00	1.24	0.25	11.79	0.10	291.69	87.43	224.14
040802 mra	0.00	1.00	0.00	12.16	0.12	299.98	82.40	242.49
040802 mrb	0.06	2.70	0.66	18.21	0.43	389.76	41.15	275.69
040802 lla	0.34	4.33	0.46	11.45	0.81	262.91	51.82	223.17

**Surface Water**

040802 source	0.22	0.29	0.00	12.34	0.00	354.43	114.74	265.87
040802 location 1	0.18	0.39	0.00	12.26	0.00	356.02	122.68	263.60
040802 location 2	0.13	0.64	0.00	12.65	0.00	350.74	124.14	265.87
040802 location 3	0.13	0.51	0.00	12.82	0.00	352.88	121.84	261.18
040803 location 4	0.10	0.50	0.00	12.66	0.00	344.98	121.53	260.67

---

**June**

Element	Al	Ca	Fe	K	Mg	Na	Si	Cl
---------	----	----	----	---	----	----	----	----

Well ID	Al	Ca	Fe	K	Mg	Na	Si	Cl
---------	----	----	----	---	----	----	----	----

060402 ula	0.00	4.78	2.05	15.50	0.81	328.26	68.00	331.18
060402 ulb	0.28	4.30	2.10	13.88	0.72	291.91	60.57	268.44
060402 ura	0.35	2.89	0.79	15.03	0.38	353.67	48.13	324.10
060402 urb	0.17	3.12	0.61	14.59	0.58	324.35	57.21	286.76
060402 mla	0.00	0.67	0.00	11.74	0.05	252.39	99.64	235.50
060402 mlb	0.08	1.10	0.32	12.62	0.14	276.55	86.06	239.02
060402 mra	0.00	0.98	0.00	12.11	0.12	288.99	85.84	272.87
060402 mrb	0.00	2.47	0.52	19.49	0.40	392.08	47.79	333.30
060402 lla	0.13	1.61	0.20	11.88	0.26	259.04	63.19	229.06

**Surface Water**

060402 source	0.23	0.43	0.00	12.70	0.00	356.62	115.76	333.57
060402 location 1	0.19	0.40	0.00	12.67	0.00	352.72	127.34	337.07
060402 location 2	0.14	0.47	0.00	12.82	0.00	347.68	122.85	170.42
060402 location 3	0.13	0.52	0.00	13.21	0.00	357.73	118.95	321.45
060402 location 4	0.14	0.51	0.00	12.88	0.00	351.62	120.68	330.03

---

**July**

**Element**                      **Al**      **Ca**      **Fe**      **K**      **Mg**      **Na**      **Si**      **Cl**

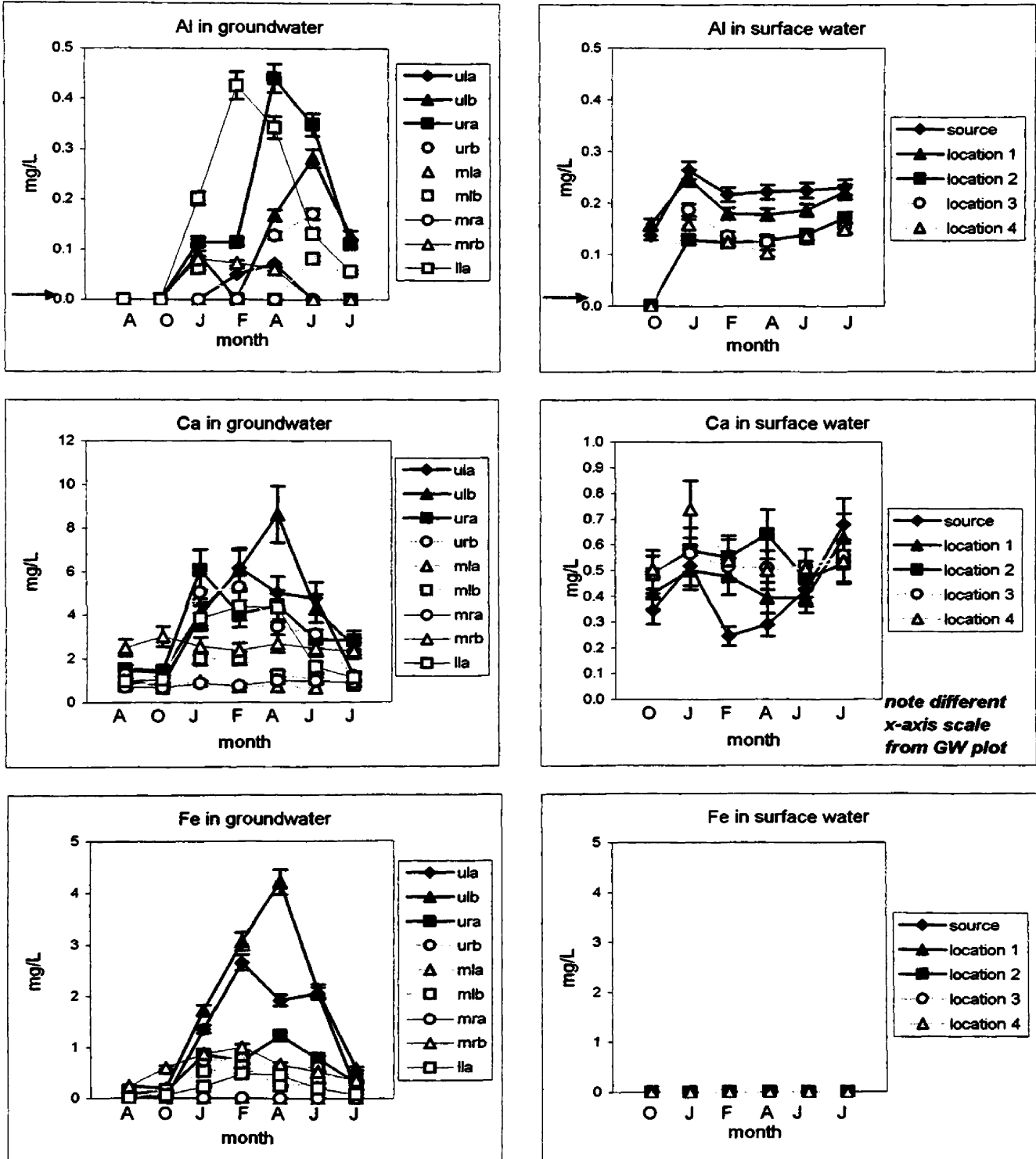
**Well ID**

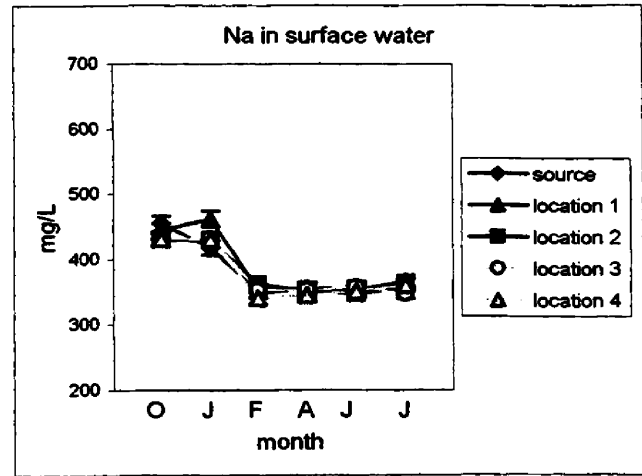
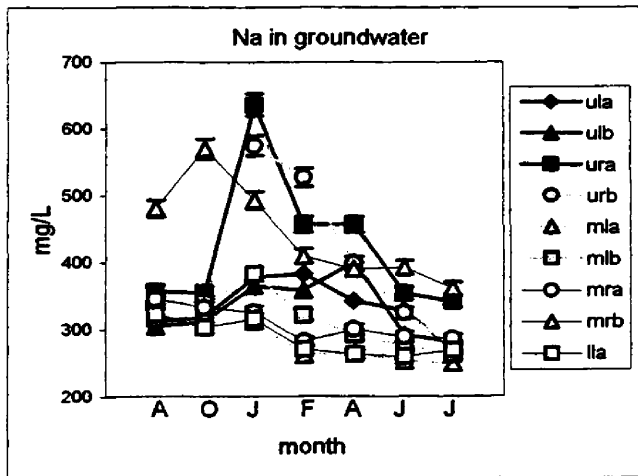
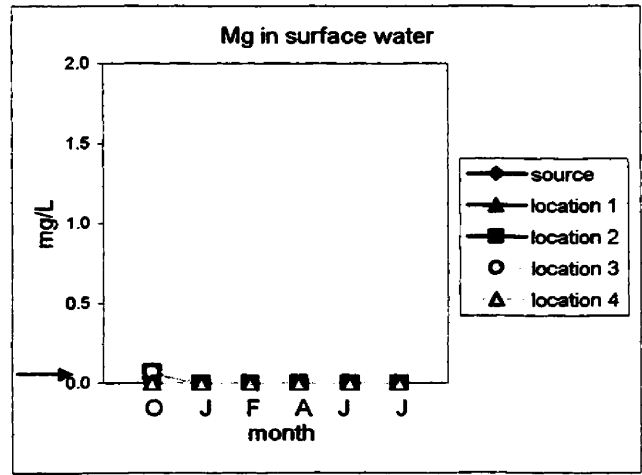
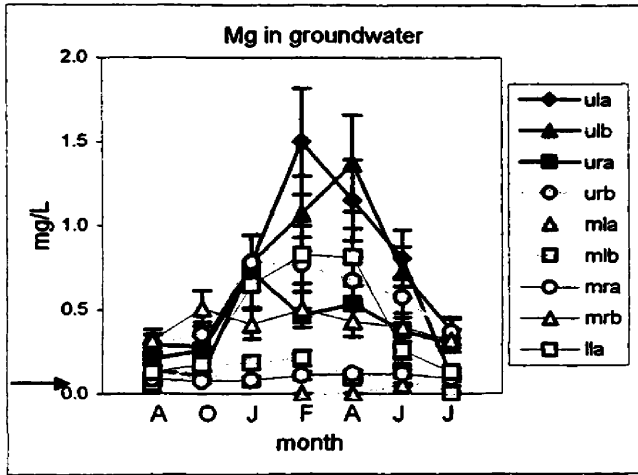
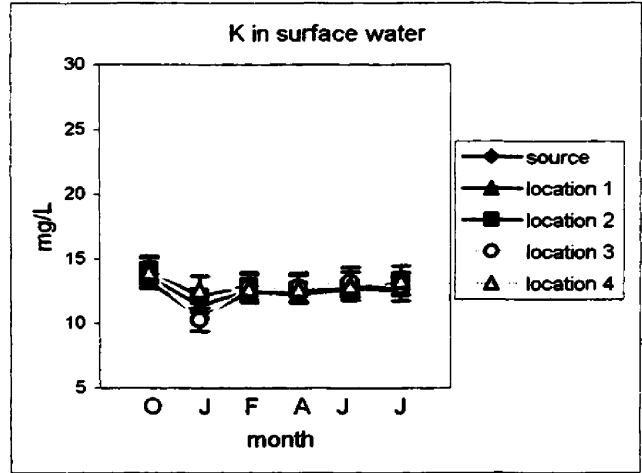
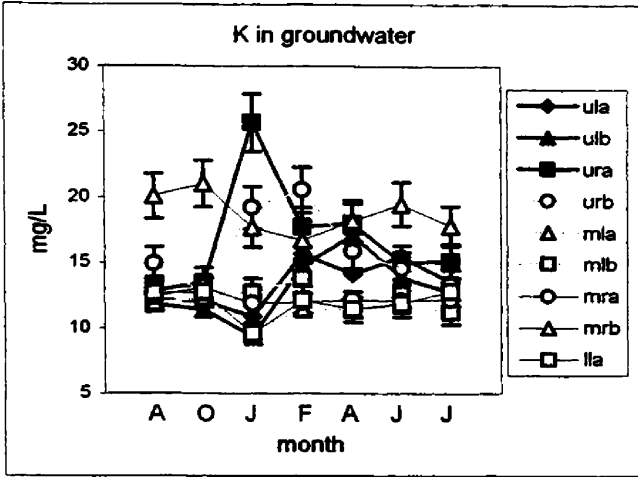
<b>071602 ula</b>	0.00	1.22	0.17	13.53	0.11	270.58	88.70	203.02
<b>071602 ulb</b>	0.13	2.55	0.59	12.77	0.38	281.22	70.41	220.79
<b>071602 ura</b>	0.11	2.83	0.31	15.14	0.30	341.89	57.19	287.61
<b>071602 urb</b>	0.00	1.17	0.08	13.30	0.37	273.94	84.56	215.85
<b>071602 mla</b>	0.00	1.01	0.00	11.32	0.06	249.20	102.44	197.94
<b>071602 mlb</b>	0.00	0.78	0.00	11.26	0.00	262.24	94.19	212.09
<b>071602 mra</b>	0.00	0.89	0.00	12.21	0.09	285.19	90.55	208.66
<b>071602 mrb</b>	0.00	2.35	0.35	17.83	0.32	360.86	51.18	281.94
<b>071602 lla</b>	0.06	1.11	0.08	12.80	0.13	268.88	78.76	207.46

**Surface Water**

<b>071602 source</b>	0.23	0.68	0.00	12.62	0.00	349.46	120.07	295.22
<b>071602 location 1</b>	0.22	0.63	0.00	12.87	0.00	366.31	130.40	307.32
<b>071602 location 2</b>	0.17	0.53	0.00	13.16	0.00	355.41	128.34	299.94
<b>071602 location 3</b>	0.15	0.56	0.00	12.84	0.00	347.62	125.90	299.34
<b>071602 location 4</b>	0.15	0.54	0.00	13.32	0.00	360.74	129.78	299.80

**Figure 21:** Major cations plots. There are consistent increases in element concentrations in the groundwater during the winter season. January experienced increased concentrations in the surface water except for iron, potassium, and magnesium. Concentrations decrease from January to the second summer field season. Note the iron concentration difference from the ferrozine method. (Arrows = detection limit at low concentrations.)





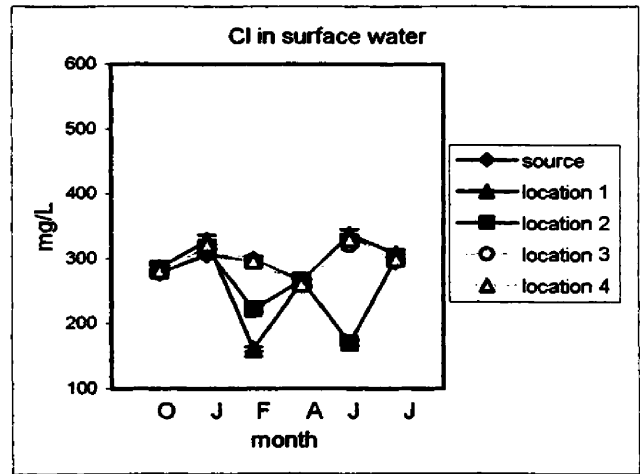
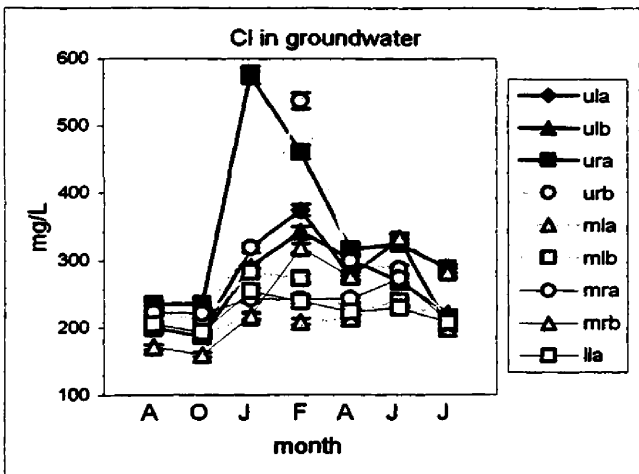
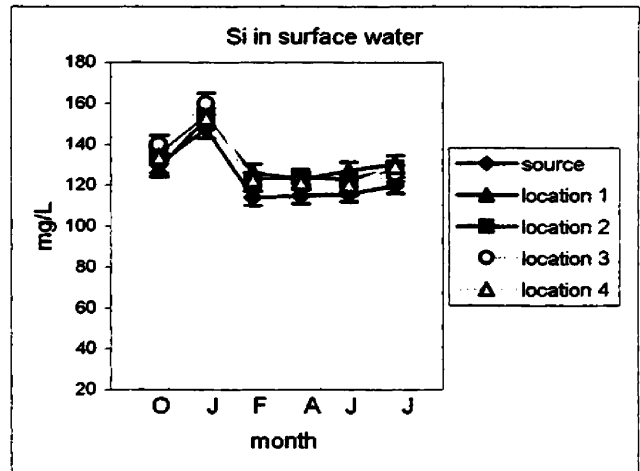
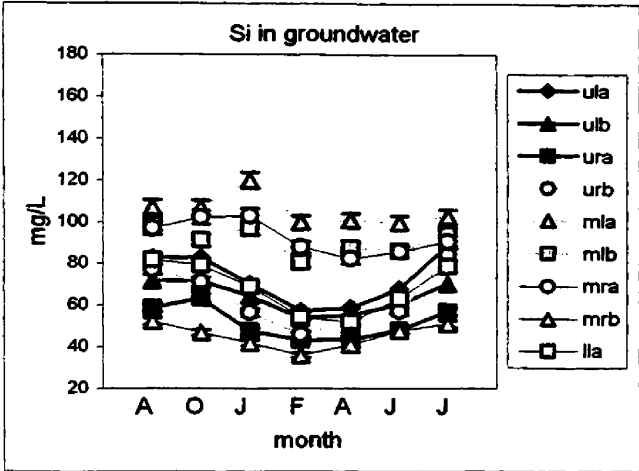
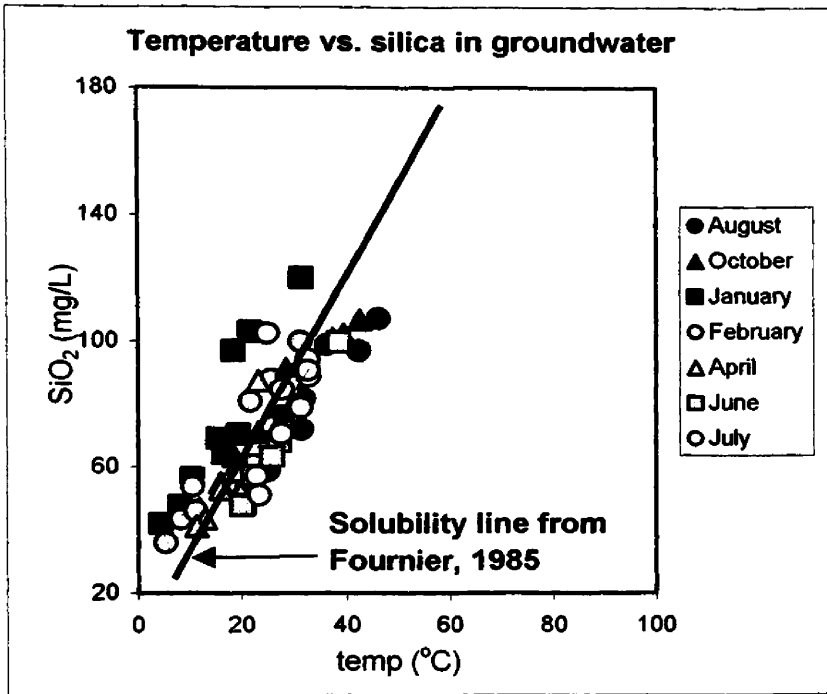
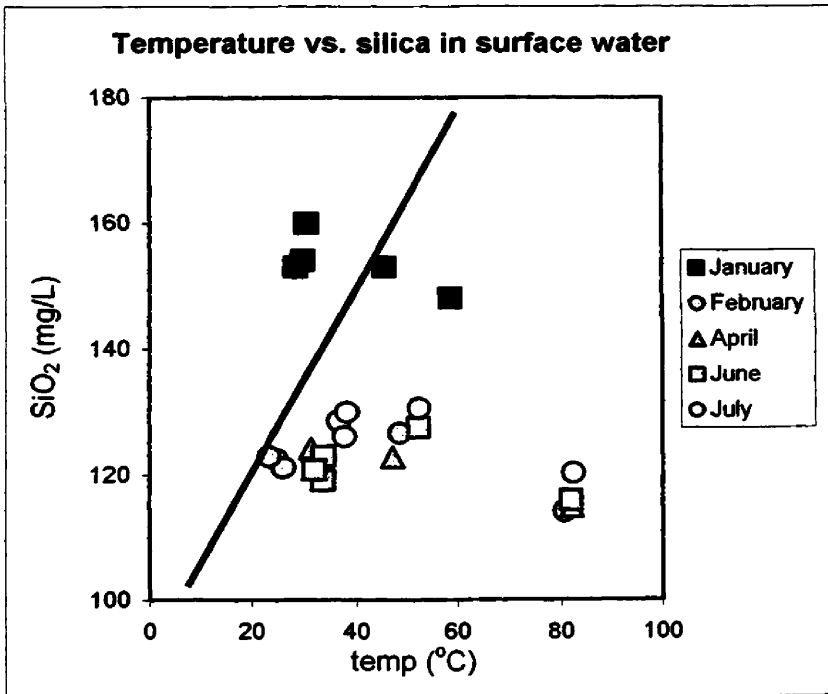


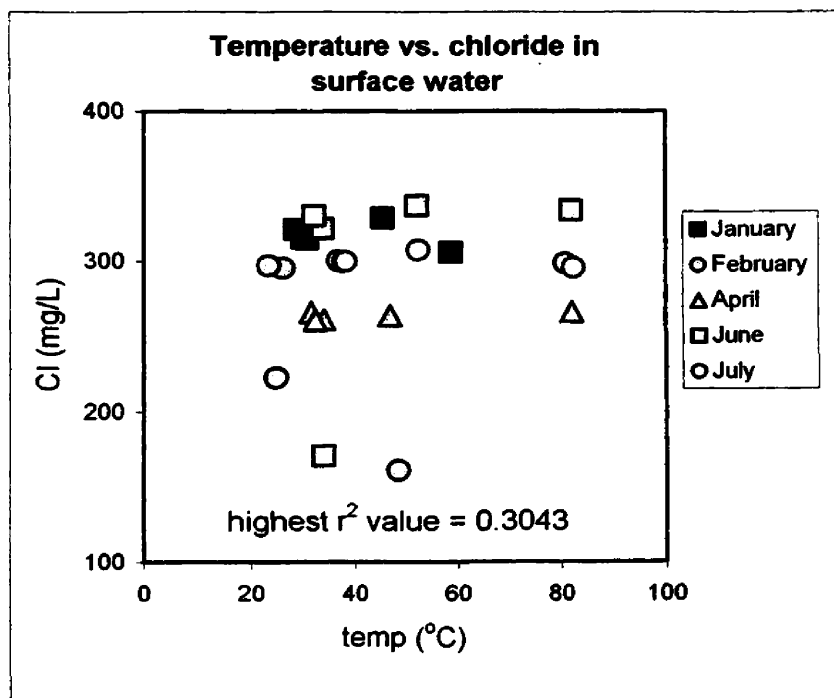
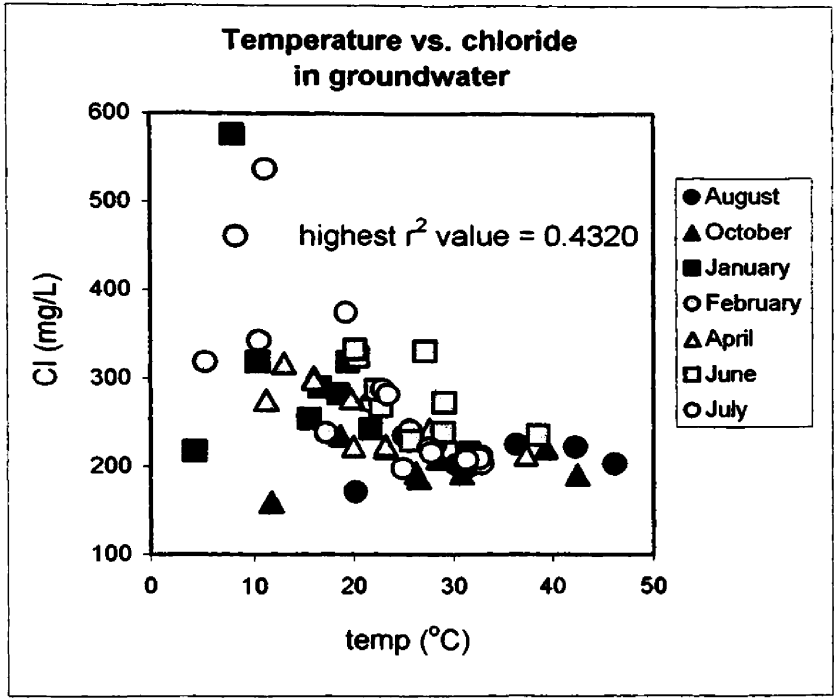
**Figure 22:** Temperature correlations plots with silica, chloride, and sodium. There are no surface water correlations for August because water samples were not collected. There are no surface water samples for October because field meter data was not reliable.

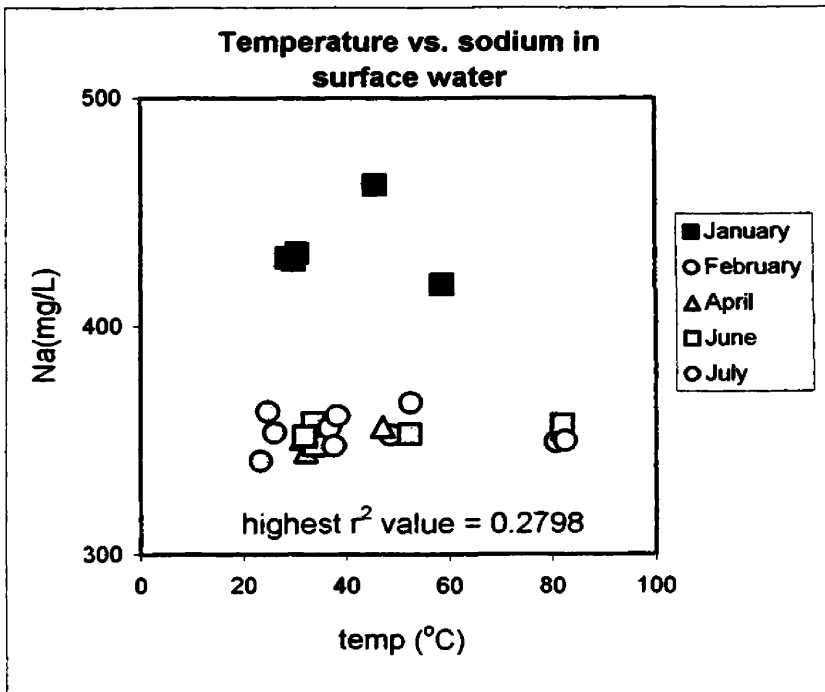
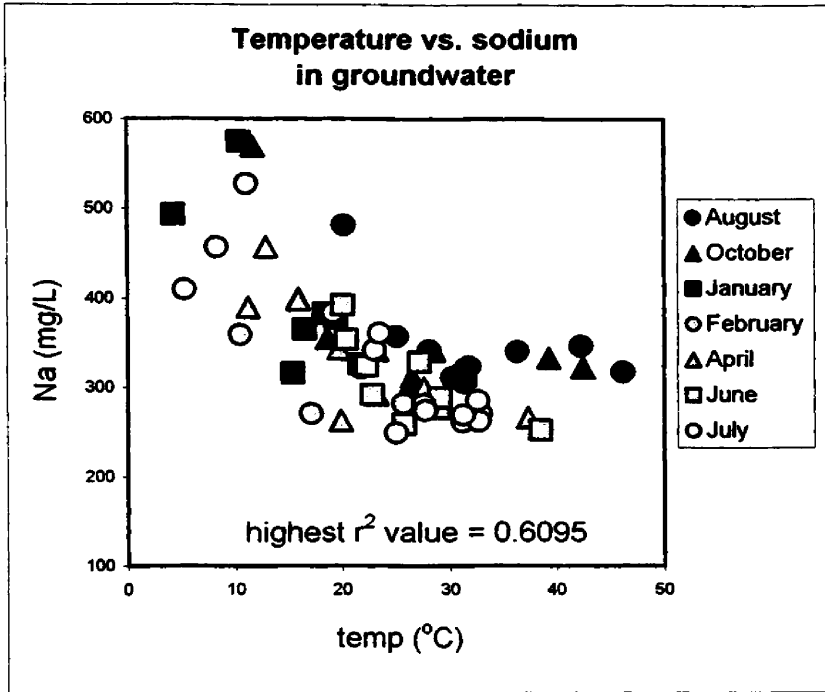


month	r <sup>2</sup> value
August	0.8870
October	0.9466
January	0.8711
February	0.9206
April	0.8761
June	0.9090
July	0.3606



month	r <sup>2</sup> value
January	0.5379
February	0.4304
April	0.8436
June	0.1476
July	0.604







Chloride is a conservative anion in most natural environments (Damm, 1995). Chloride plumes in the groundwater were apparent in the shallow system that shifted slightly. These shifts were detected in piezometers *ura* and *urb*. The chloride concentrations increased and then decreased several hundred mg/L in these piezometers from January to February. The chloride concentration increased 245% from October to January in piezometer *ura* and 164% from January to February in piezometer *urb* (Table 3).

**Table 3:** Chloride concentrations in piezometers *ura* and *urb*.

<b>Chloride (mg/l)</b>	<b>October</b>	<b>January</b>	<b>February</b>
<b>piezometer <i>ura</i></b>	235	576	432
<b>piezometer <i>urb</i></b>	221	319	524

Temperature and pressure changes at depth likely affected both the hot spring source and the shallow groundwater. Aquifers at different depths may mix seasonally changing the chloride concentration. Temperature and pressure changes in aquifers may cause one aquifer to seep into another aquifer. One explanation could be the result of colder meteoric water entering the system during the winter. The addition of cooler water would decrease pressure in an aquifer allowing a higher pressure aquifer to discharge water into the aquifer at lower pressure. Pressure changes on the scale of  $10^3$  bars would be expected to account for the chloride concentration changes (as seen in the Wairakei Geothermal Field in New Zealand) (Ellis and Mahon, 1977). Hot springs in Norris Geyser Basin, YNP have experienced seasonal water chemistry variability. It is thought that during the winter, meteoric water cools the hot spring system and causes silica to precipitate in and seal hydrothermal fractures. During the dry season in summer, the water table lowers and temperature in the hydrothermal aquifers increase. The increase

in temperature causes increased pressure and then cracks the silica sealed fractures allowing aquifers to mix. Tectonic events may also contribute to this hydrofracturing (White et al., 1988). Dilution of meteoric waters entering the system may explain the decreases in chloride concentration. Chloride concentration fluctuations, particularly the increase in concentrations observed in June, 2002, may be a result of meteoric water flushing chloride out of the soil zone (White et al., 1988).

An estimate of hydraulic conductivity in the meadow where groundwater likely discharges to the creek was calculated using Darcy's Law:

$$K = \frac{-Q}{A (dh / dl)} \quad (3)$$

An estimate of 1.4% (+/- 0.2%) of the creek discharge (~0.1 m<sup>3</sup> / sec) is from groundwater. This estimate was derived with a chemical dilution calculation using groundwater, upper creek reach, and lower creek reach chloride concentrations from January ( $X_1/X_2 = Y_1/Y_2$ ). Chloride concentration increased from location 2 to location 4 approximately 2-3 mg/L. The chloride concentration increase is thought to be from groundwater discharge into the creek. Estimates of other variables used were  $A = 100$  m<sup>2</sup>,  $dh = 0.2$  m, and  $dl = 0.5$  m. The calculated hydraulic conductivity is  $3.5 \times 10^{-5}$  m/sec (3.0 m/day). This hydraulic conductivity value fits in the range for unfractured limestone (Driscoll, 1986, p 75). The calculated K value compares with Gibson (1999) who used in-situ falling head permeameter tests.

Table 4 lists iron concentrations analyzed using the ferrozine method. The detection limit was 0.1 mg/L. Figure 23 shows ferrous to total iron ratios that increased during the

winter. The increase in these ratios is indicative of reducing groundwater conditions. The only location where iron was present in solution in the creek was just below the study site.

Concentrations of iron in piezometers were low in August, 2001 (0-1 mg/L) as analyzed by ICP). Iron concentrations increased to over 2 mg/L in some piezometers in January and February, 2002. Ferrous iron concentrations increased to 7 mg/L in one piezometer (April, 2002). One piezometer (mlb) measured ferrous iron concentration higher than the total iron concentration; the explanation for this analysis caveat is unknown ( $\text{Fe (II)} = 0.47 \text{ mg/L}$  and  $\text{Total Fe} = 0.00 \text{ mg/L}$ ). Dissolved oxygen concentrations range from 1-3 mg/L in January, February, and April (see appendices for complete data set). The pH of the waters during April, when the iron concentrations were highest, were consistently about half a pH unit lower than all other winter sampling rounds. In June, iron concentrations ranged from not detectable to just over 1 mg/L and dissolved oxygen concentrations were 1-2 mg/L higher than during the winter. No iron was detected in June. June dissolved oxygen concentrations were more than double the concentrations during the winter and the pH had increased approximately one unit. It is apparent that a slight decrease in oxygen and pH seem to affect iron solubility by reducing  $\text{Fe(III)}$  to  $\text{Fe(II)}$  (Figure 24). When there is an oxygen depletion in the system,  $\text{O}_2^{2-}$  is weakly bonded to  $\text{Fe}^{2+}$  and thus oxygen in the iron oxide compound will be broken apart and used by other biogeochemical processes (Sung and Morgan, 1980, Tamura et al., 1976). However, Emmenegger and others (1998) studied an open system in a eutrophic lake and found that pH between 6.8 and 7.3 did not have an affect on the iron oxidation kinetics.

**Table 4:** Iron concentration (ferrous and total iron ) from January to July, 2002 using the ferrozine method. Error is < 5%.

Sample Location Well ID	January Ferrous	Total	February Ferrous	Total	April Ferrous	Total	June Ferrous	Total	July Ferrous	Total
ula	1.23	1.58	2.26	2.38	2.68	2.81	0.90	1.34	<dl	<dl
ulb	1.30	1.79	2.60	2.89	6.27	7.76	0.90	1.17	<dl	<dl
ura	0.73	1.08	0.53	0.65	1.26	1.45	<dl	<dl	<dl	<dl
urb	0.57	0.95	0.66	0.74	0.50	0.69	<dl	<dl	<dl	<dl
mia	0.00	0.26	<dl	<dl	0.14	0.26	<dl	<dl	<dl	<dl
mlb	0.31	0.65	<dl	0.42	0.34	0.51	<dl	<dl	<dl	<dl
mra	0.00	0.22	<dl	<dl	0.20	0.26	<dl	<dl	<dl	<dl
mrB	0.71	1.02	<dl	0.63	0.86	0.94	0.15	<dl	<dl	<dl
lla	0.12	0.39	<dl	0.14	0.40	0.69	<dl	<dl	<dl	<dl
li	---	---	---	---	0.24	0.69	---	---	---	---
<b>Surface Water</b>										
source	<dl	0.19	<dl	<dl	<dl	<dl	<dl	<dl	<dl	<dl
location 1	---	---	<dl	<dl	<dl	<dl	<dl	<dl	<dl	<dl
location 2	<dl	0.18	<dl	<dl	<dl	<dl	<dl	<dl	<dl	<dl
location 3	<dl	0.16	<dl	<dl	<dl	<dl	<dl	<dl	<dl	<dl
location 4	0.01	0.51	<dl	<dl	<dl	<dl	<dl	<dl	<dl	<dl

detection limit = 0.1 mg/L

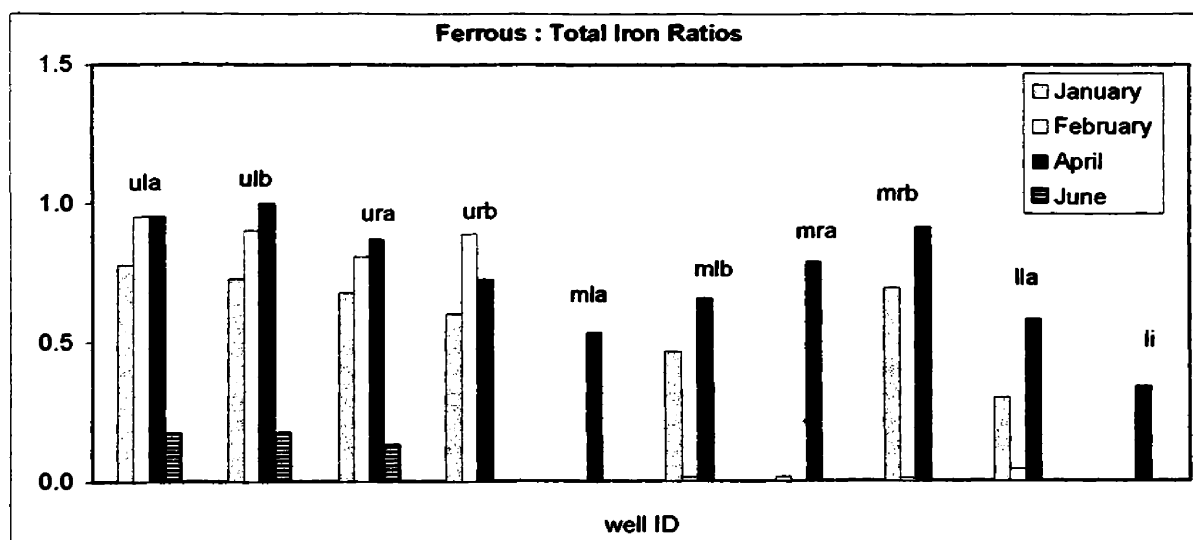


**Figure 23:** Ferrous to total iron ratios during the study.

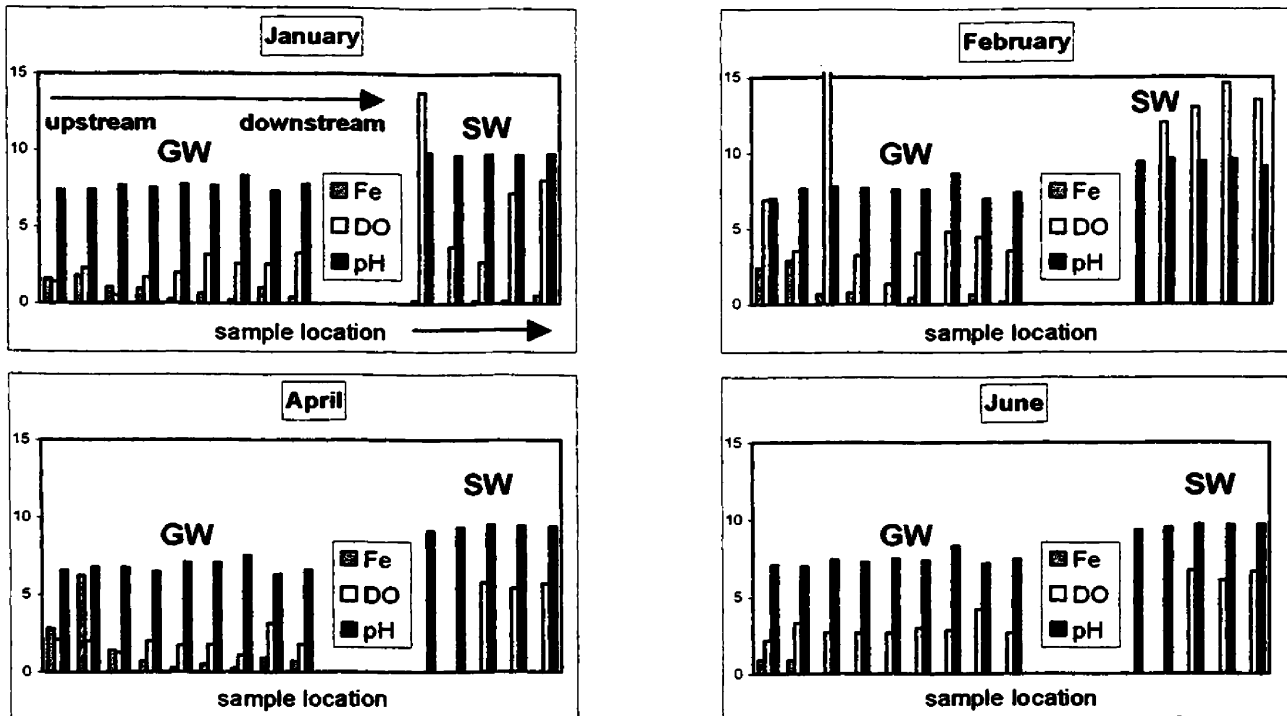


**Figure 24:** Total iron (mg/L) using the ferrozine method, dissolved oxygen (mg/L), and pH plots for four months (labeled in each box). The groundwater samples are displayed as upstream to the left moving downstream to the right. The surface water samples start with the source on the left and move downstream to the right in the plots. The plots show that as dissolved oxygen decreases, total iron concentration increases. The pH decreases in April where iron concentrations are highest. August, 2001 data not shown because iron was analyzed by ICP, no dissolved oxygen are available, and no surface water measurements were taken. October data are not shown because dissolved oxygen concentrations were not measured due to equipment failure. Detection limit is 0.1 mg/L. The spectrophotometer measures consistent readings.

The groundwater pH was near neutral and the surface water was alkaline (pH 9-10). The pH decreased by ~0.5 unit during the winter. Figure 25 is a plot of pH in surface water and groundwater during the study. A change of 1 pH unit was measured between January and April. Temperature decreased in both surface water and groundwater during the winter (Figure 26). This variation was expected due to atmospheric cooling and snow accumulation/runoff.

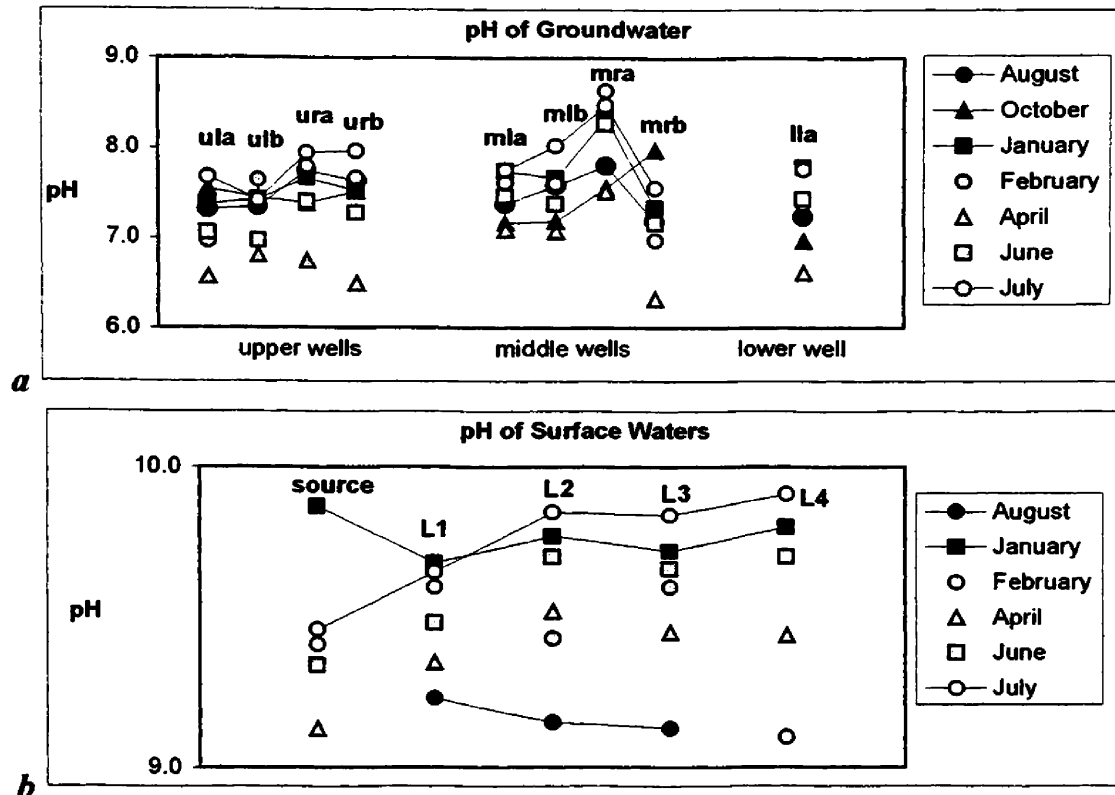


**Figure 25:** Groundwater pH (a) and surface water pH (b).

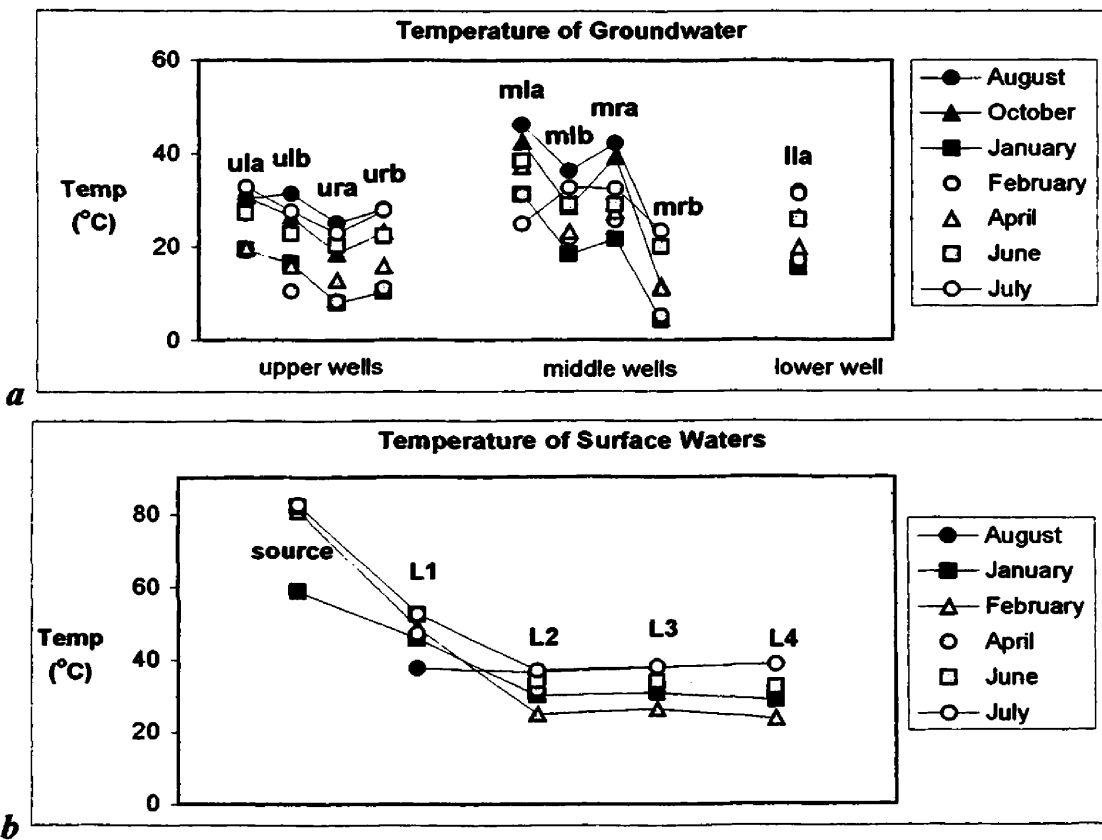


**Figure 26:** Surface water temperature (a) and groundwater temperature (b).

### MINTEQA2 Geochemical Modeling

Silica speciation was modeled and plotted (Figure 27). The hot spring source had the highest temperature and pH while percent unionized  $\text{H}_4\text{SiO}_4^\circ$  concentrations were least.  $\text{H}_4\text{SiO}_4^\circ$  percentages increased as distance from the source increased while temperature and pH decreased. This indicates that silica more readily precipitates out of solution as distance from the source increases since  $\text{H}_4\text{SiO}_4^\circ$  percentages increase downstream.  $\text{H}_4\text{SiO}_4^\circ$  is the silica species that is a precipitate. All months showed similar model results.  $\text{H}_4\text{SiO}_4^\circ$  percentages in the groundwater were near 100%.

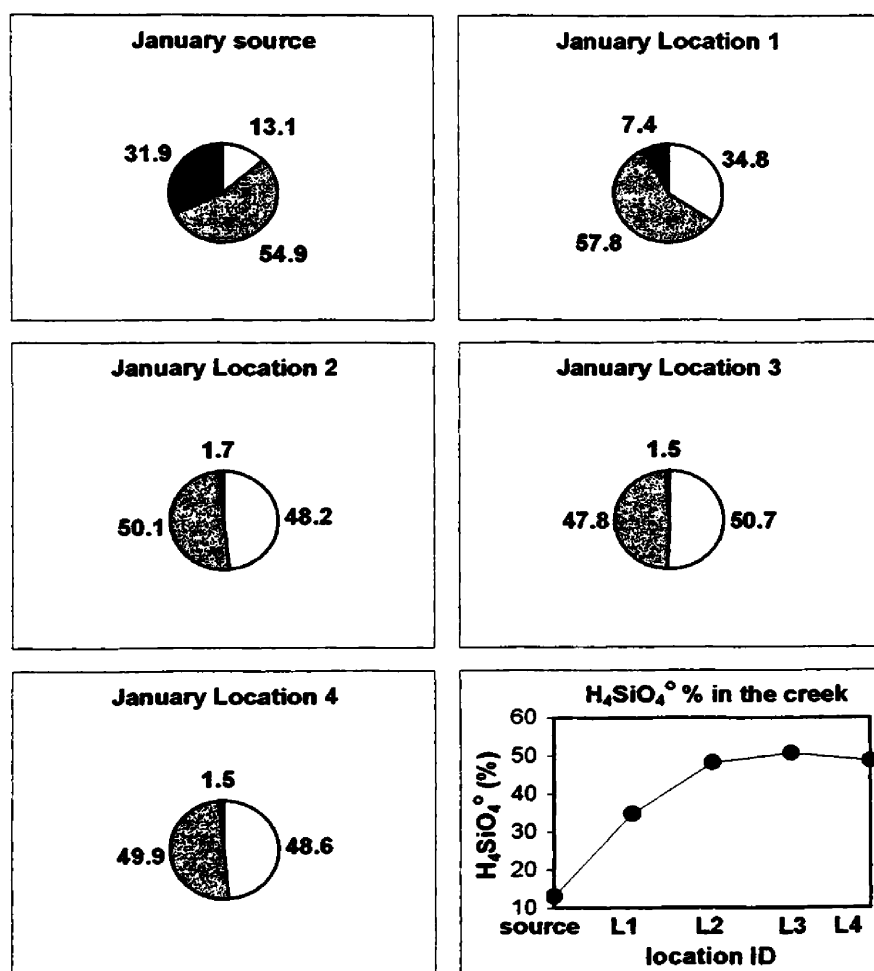


**Figure 27:** Silica speciation derived from MinteqA2.  $\text{H}_4\text{SiO}_4^\circ$  (white) increases as distance from the source increases.  $\text{H}_3\text{SiO}_4^-$  is gray and  $\text{H}_2\text{SiO}_4^{2-}$  is black. Values are in percent.

Mineral saturation indices were compared with x-ray diffraction patterns. Very few saturated minerals (from a relatively large list provided in the MINTEQA2 output file) were identified by x-ray diffraction. Aluminum was not detectable in most samples previous to January, 2002. However, January water chemistry had detectable concentrations of aluminum and thus several aluminum bearing minerals were saturated in the model (*albite, analcime, annite, diaspore, halloysite, illite, imogolite, kaolinite, laumontite, leonhardite, leucite, microcline, montmorillite, muscovite, phillipsite, pyrophyllite, and sanidine*).

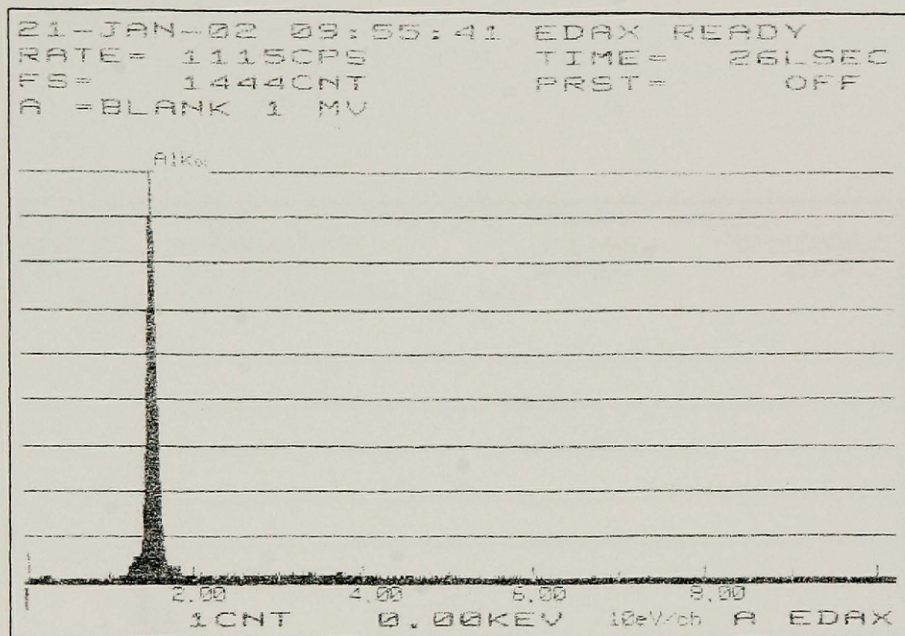


#### 4.4 Collection of Mineral Precipitates

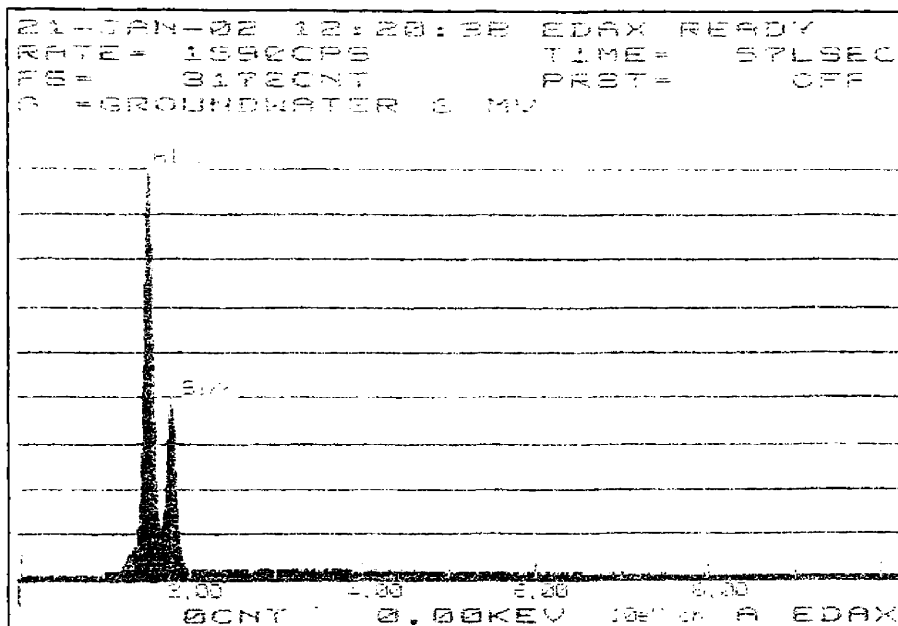
*Bead tubes:* The beads in the bead tubes had mostly solid silica as analyzed by scanning electron microscopy and energy dispersive spectrometry (SEM/EDS) for both sets of bead tubes (those installed in October, 2001 and February, 2002). A blank bead was scanned and no silica was present (Figure 28). Silica peaks on the EDS scan showed a significant amount of silica had precipitated onto the bead surfaces installed in the creek (Figure 29). Green cyanobacteria grew on the surface water section of all bead tubes but not in the subsurface section.

Iron and copper were detected in the surface water portion of a bead tube. The bead tube was installed in the anastomosing creek section in the study site. Other elements were not detected at other sites. Soluble iron and copper in the groundwater likely discharged into the creek in reduced form and were oxidized and coprecipitated rapidly.

The soda lime glass bead experiment was not successful. There was no visual precipitation on the beads when they were taken out of the creek. The glass beads were installed in the creek for the same time period as the aluminosilicate beads. An EDS scan of a glass bead from a creek sample showed the same pattern as a blank bead that had not been installed in the creek. The glass beads were made mostly of silica so any silica that may have precipitated was not detectable. Other elements like aluminum, for example, that may have precipitated onto the beads would be undetectable since aluminum was also present on the blank bead. No other major elements were observed.

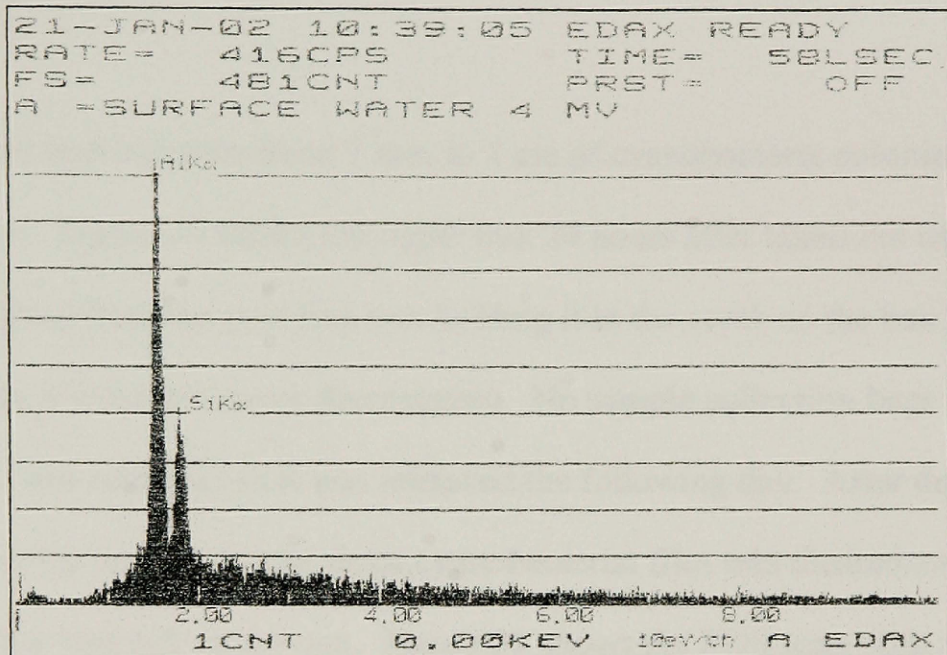
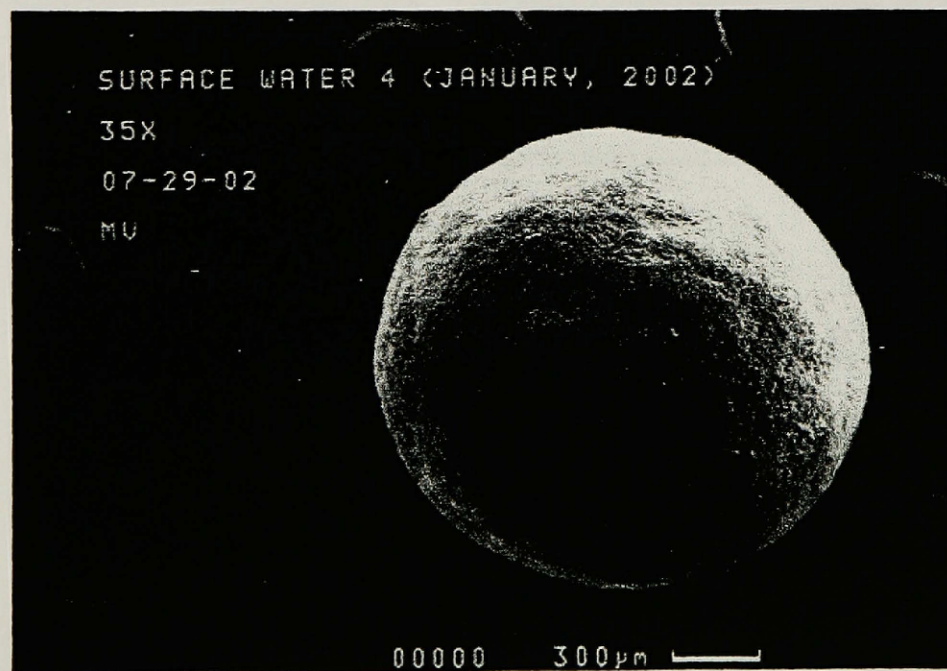
*a**b*

**Figure 28:** Blank bead analyzed by SEM/EDS. (Plot *a* has no silica. Photo *b* is a blank bead at 35X magnification).



**a**

**Figure 29:** SEM/EDS plots showing silica peaks. The aluminum peak is from the aluminosilicate bead composition. Plot *a* is a groundwater sample from below the meadow in the study site. Plot *b* (next page) is a surface water sample from the single channel section in the middle of the study site (see accompanying photo). Photo (*c*) is an aluminosilicate bead from the surface water 4 location in plot *b*.

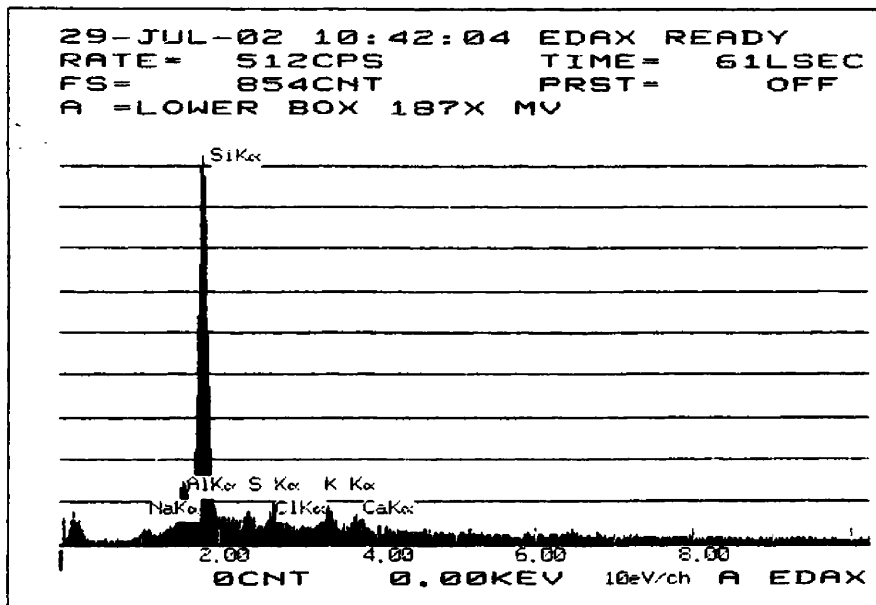
**b****c**

**Chemical precipitation boxes:** The chemical precipitation boxes showed no silica precipitation directly on the glass plates. If given enough time with over-saturated (with respect to silica) conditions, silica polymorphs would probably deposit onto the plates (Akahane et al., 1997).

All three boxes had between about 1 mm to 1 cm of cyanobacteria colonization on the top part of the box. Figure 30 shows the upper box 24 hours after taken out of the creek. The box had detached from the post that was holding it in the creek so the box was taken out of the creek so it wouldn't move downstream. No sample collection bags were available when the box was removed so it was retrieved the following day. After drying at room temperature in the laboratory, the dried cyanobacterial film was cleared away and a powdered sinter was left on the box. Figure 31 shows the EDS scan with a sharp silica peak and SEM photos for the lower box. The upper and middle boxes also showed the sharp silica peaks. The results indicate that water is trapped within the cyanobacteria and thus the water becomes stagnant and so the suspended load of silica settles out of solution.



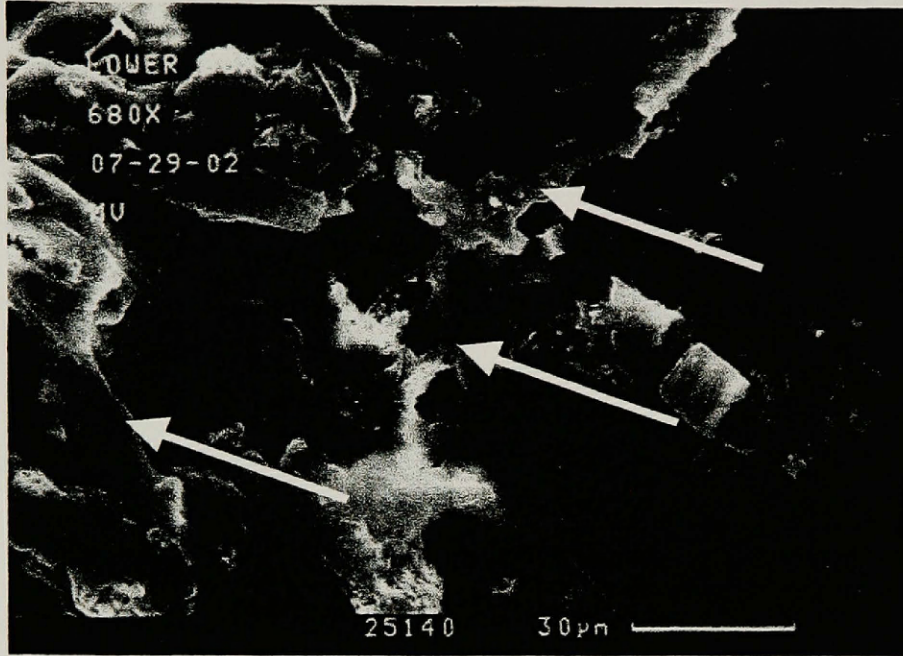
**Figure 30:** Chemical precipitation box shows sinter deposition. Deposition is likely due to cyanobacteria causing water to become stagnant within the cyanobacteria and thus silica settles out of solution.



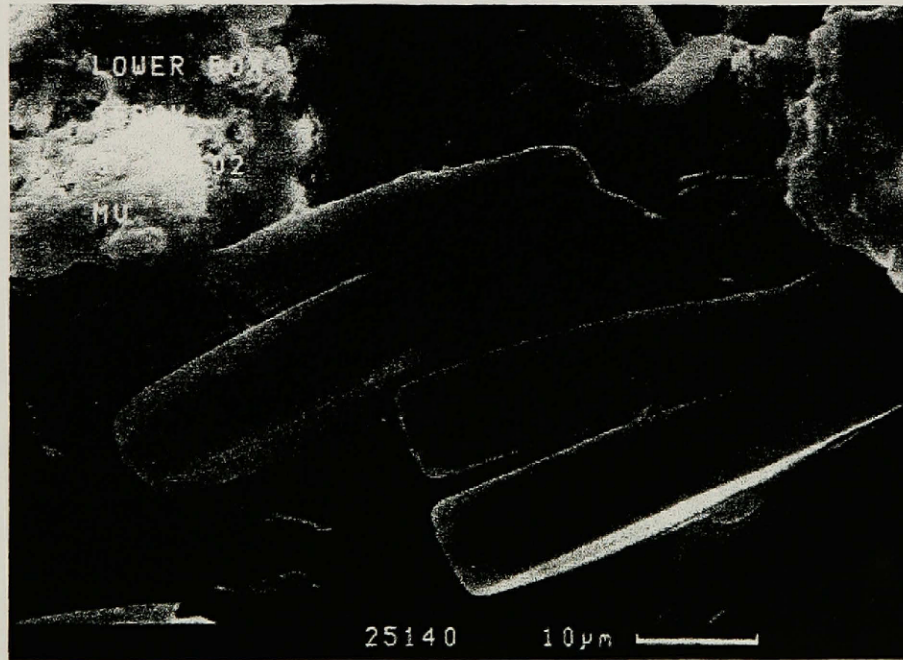
*a*

**Figure 31:** EDS scan of the lower box with a sharp silica peak (*a*). The cyanobacteria filament structure can be seen in photo *b* (next page), see arrows. Diatoms are present in photo *c*. Diatoms were entombed in silica in all samples.





*b*



*c*

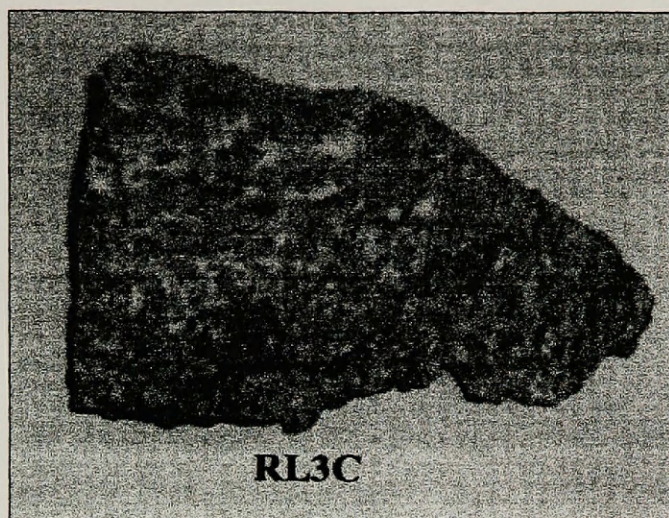
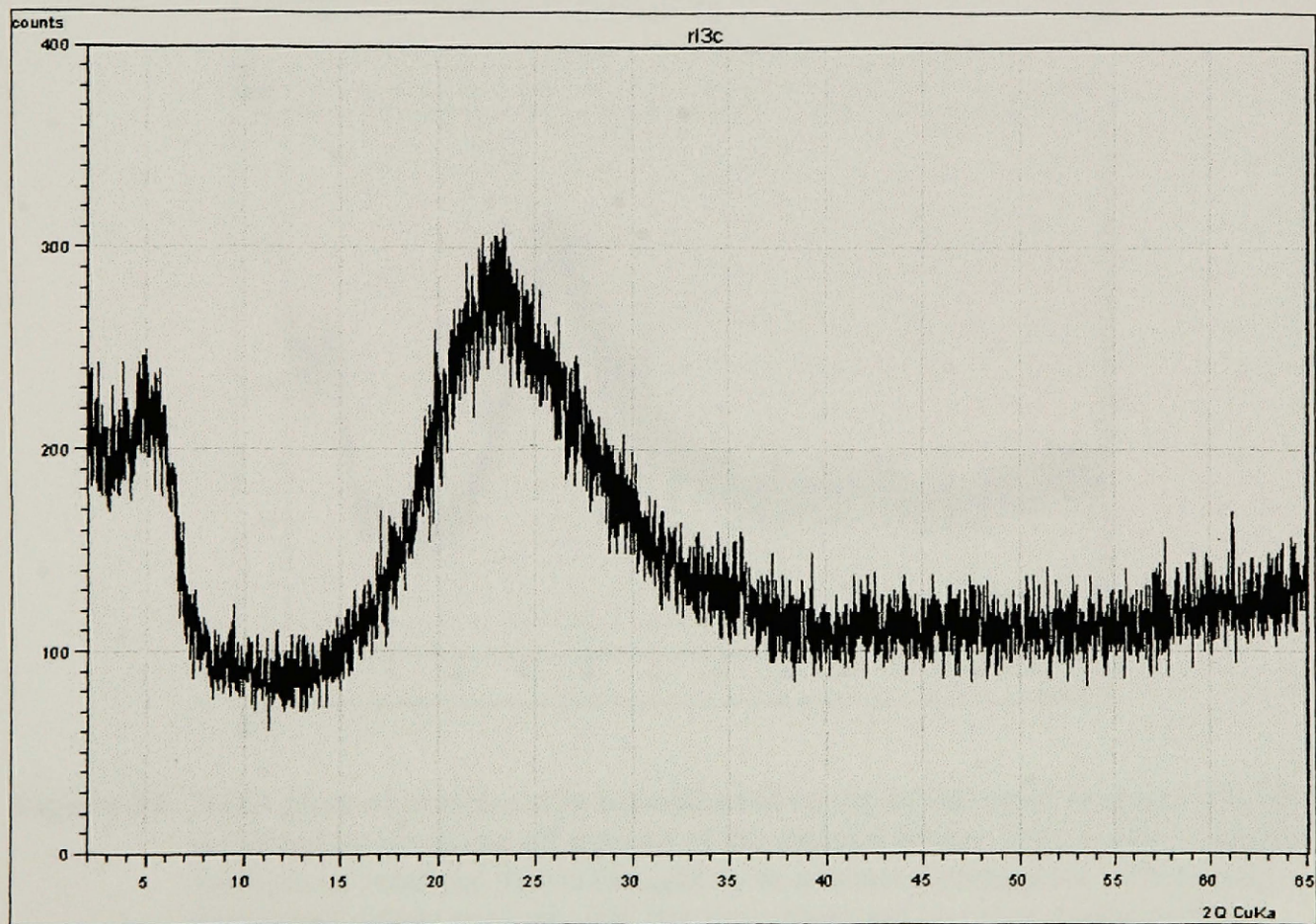
#### 4.5 Mineral Identification

X-ray diffraction (XRD) showed amorphous silica in most of the mineral precipitates. Some crystallization was present in the samples but was not identifiable (see XRD plots in Figure 32 and the appendices). Nearly all rocks in the creek channel, taken from the surface, were composed only of amorphous silica. Small amounts of quartz, cristobalite, and tridymite were clearly distinguishable by the XRD peaks in two samples.

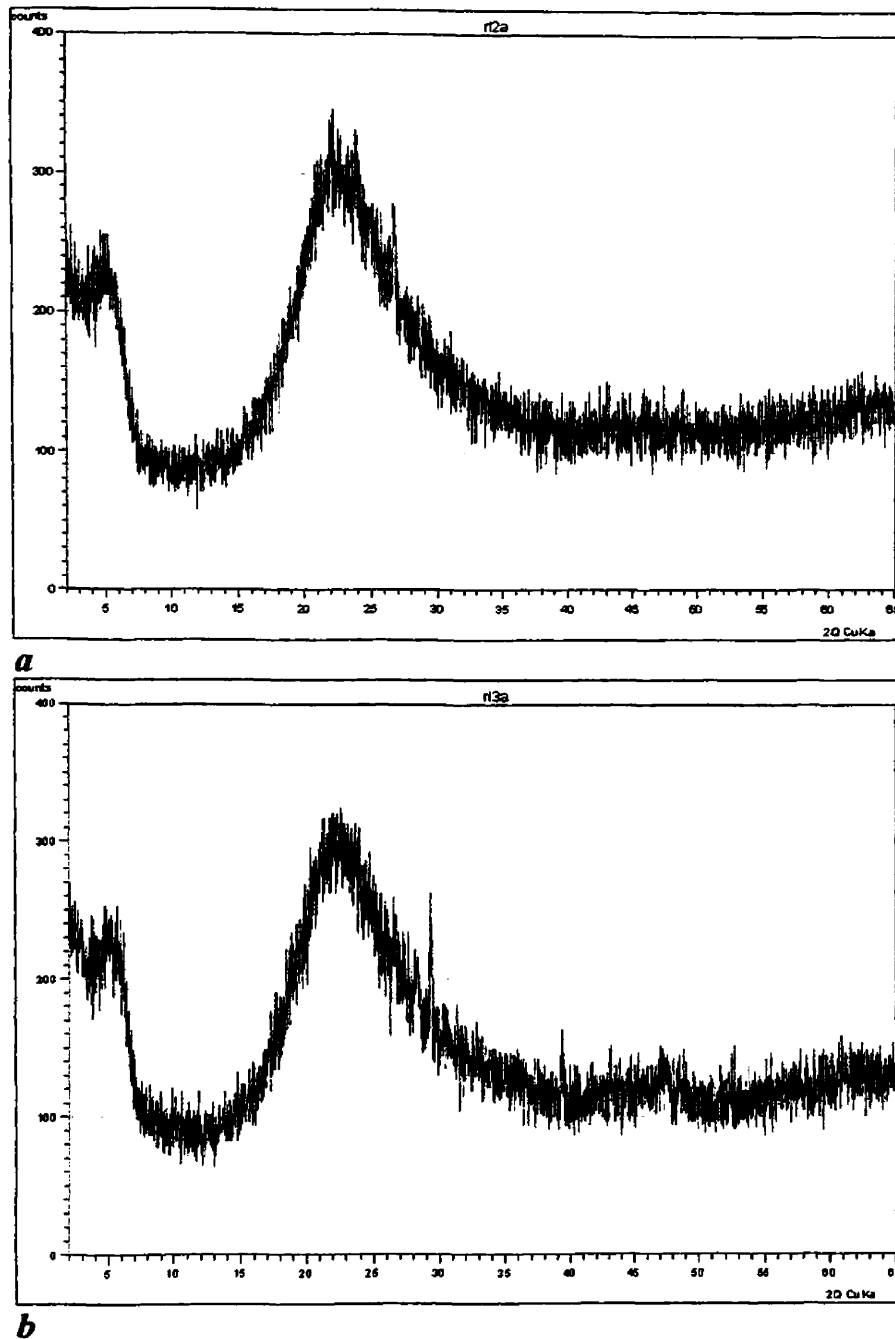
Some samples were clearly more amorphous than others (Figure 33). It is thought that the more amorphous samples are deposits where silica precipitates from the creek. The slightly less amorphous samples are thought to be existing sinter that the creek runs through. Thus, XRD patterns has the potential to be a reliable tracer to identify where dissolution and precipitation is taking place.

One sample with quartz, cristobalite, and tridymite was located just below the source above the water surface of the creek (Figure 34). Table 5 lists reference angles and d-spaces with measured d-spaces for comparison. A small amount of kaolinite was identified in this sample. Quartz probably formed when the hot spring was much larger or the creek was at a higher stage. The second sample with quartz, cristobalite, and tridymite was collected from *m1a* piezometer bore hole at 43 cm depth. Metal oxides, particularly iron oxides that bind onto the silica deposits, may inhibit crystal growth that may help explain why most of the creek channel mineral deposits are amorphous.



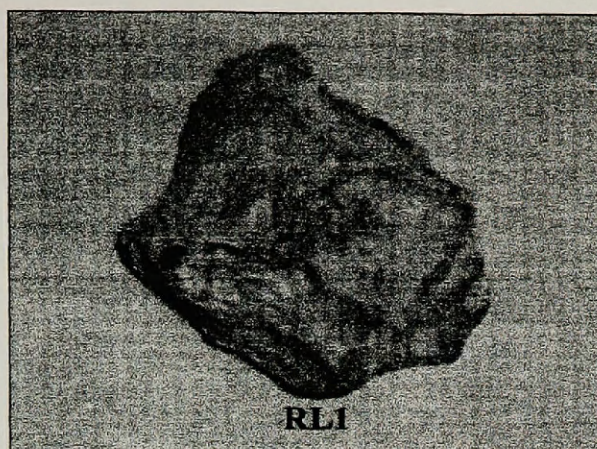
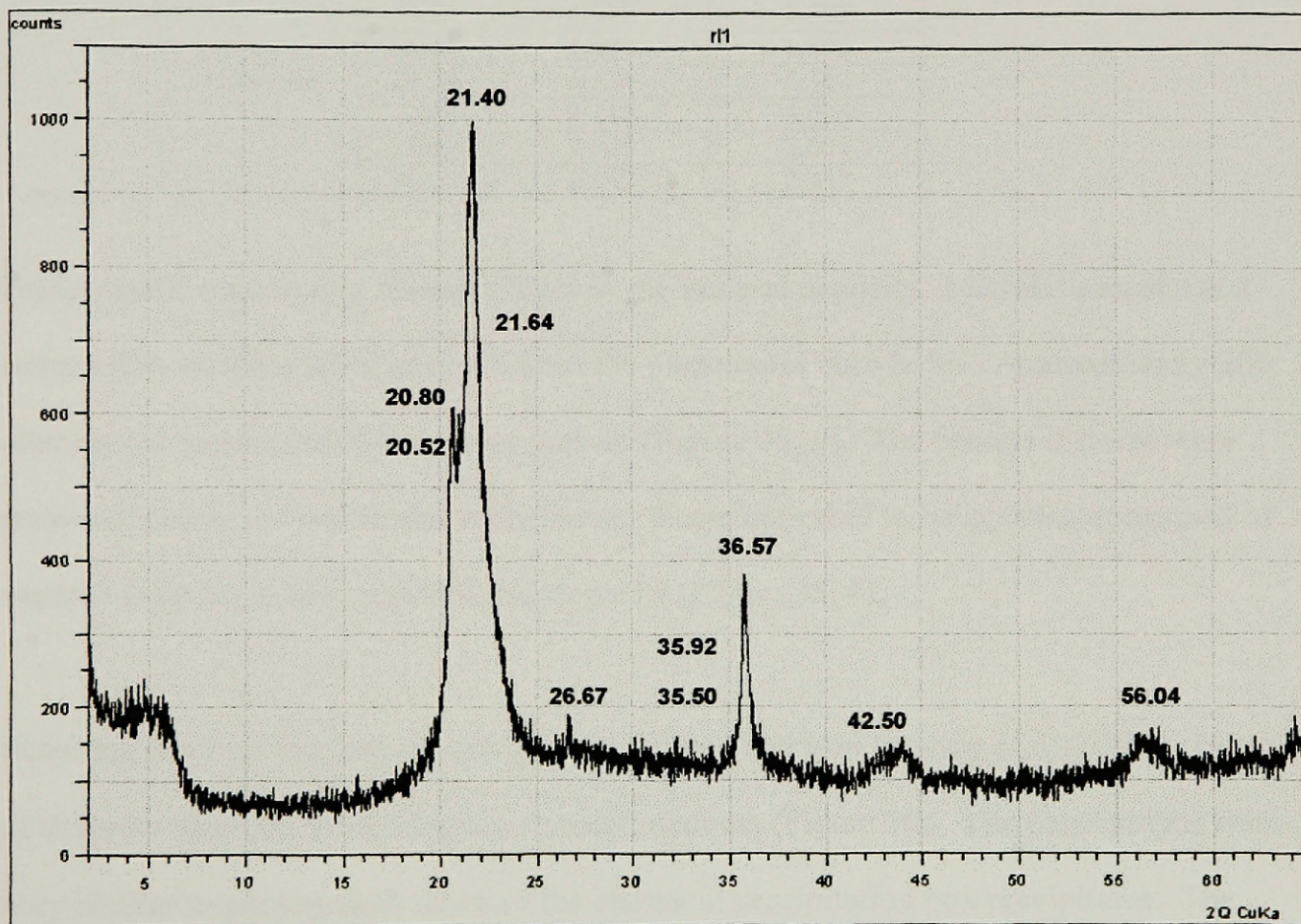
*a**b*

**Figure 32:** Photo *a* is a subaqueous sample taken in the single channel section of the study site. The section seen is the bedding surface as it occurred in the creek. Plot *b* is the coinciding XRD scan where the tall peak indicates amorphous silica. The x-axis is  $^{\circ}2\theta$  and the y-axis is intensity (counts).



**Figure 33:** XRD plots of samples r12a (*a*) collected on top of the creek bed and r13a (*b*) collected by breaking off a piece of the channel lining. Plot *a* shows mostly amorphous material that is thought to be a mineral precipitate. There may be a small quartz peak at  $\sim 26^\circ$  but since there are no other quartz peaks, identification was not determined. Plot *b* shows the same amorphous material with more noise in the diffraction pattern and is thought to be pre-existing sinter that the creek runs through. There may be calcite and goethite present but the peaks represent a weak signal. Goethite and calcite were saturated in the MINTEQA model.



*a**b*

**Figure 34:** Rock sample *r11* collected just below the source *location 1*. The photo is viewed from the top of the sample (*a*). Plot *b* is the coinciding XRD scan where the quartz, cristobalite, and tridymite peaks are labeled ( $^{\circ} 2\theta$ ).

**Table 5:** XRD reference angles and d-spaces (angstroms) with measured d-spaces for comparison for sample *r11*. Measured angles are labeled in Figure 34. Sample *m1a43* is similar to *r11* (located in the appendices). Reference values from PDF cards 4-359, 18-1170, and 5-490 reprinted in Moore and Reynolds (1997).

Sample ID	mineral	$2\theta$ (°)	d (reference)	d (measured)
<i>r11</i>	quartz	20.80	4.270	4.337
		26.67	3.342	3.342
		36.57	2.457	2.510
		42.50	2.128	2.237
	cristobalite	21.40	4.150	4.099
		35.50	2.530	2.507
		56.04	1.640	1.692
	tridymite	20.52	4.330	4.312
		21.64	4.110	4.095
		35.92	2.500	2.501
		36.57	2.457	2.457

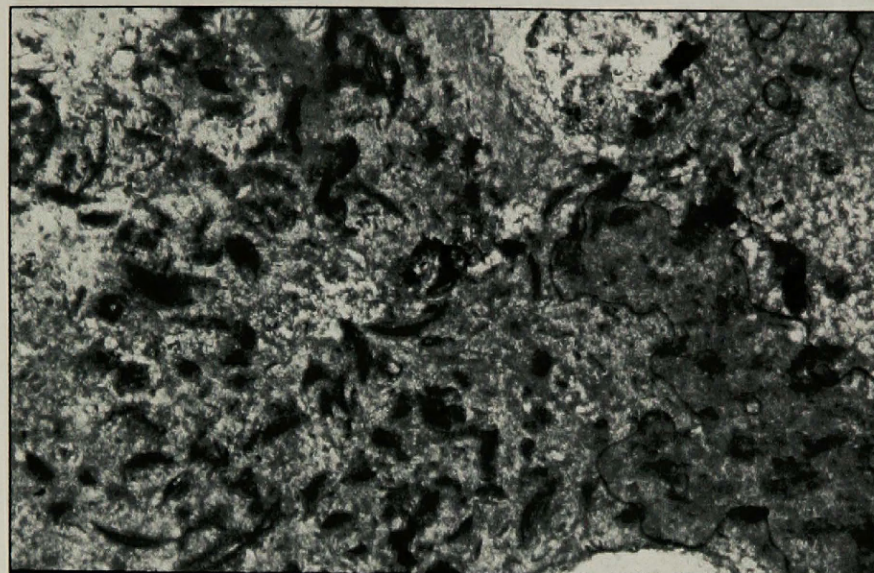
Petrographic microscopy revealed biota in the mineral deposits. Microbe entombment occurred in samples taken at depth from the piezometer bore holes. Approximately 200 diatoms per square centimeter were present (Figure 35, *a*). The opaque diatoms were very well preserved within the white sinter. There appeared to be layering composed of organic material in the creek channel deposits (Figure 35, *b*).

Scanning electron microscopy using backscattered electron imaging (SEM/BSE) photos of deposits taken on some samples revealed diatoms (Figure 36). The photographs were very similar to photographs taken of the chemical precipitation box precipitates. The diatoms were the same and were very well preserved in the deposits. The channel deposits in the braided section of the creek below the meadow revealed similar biota in the thin section photomicrographs as the chemical precipitation boxes (Figure 35).

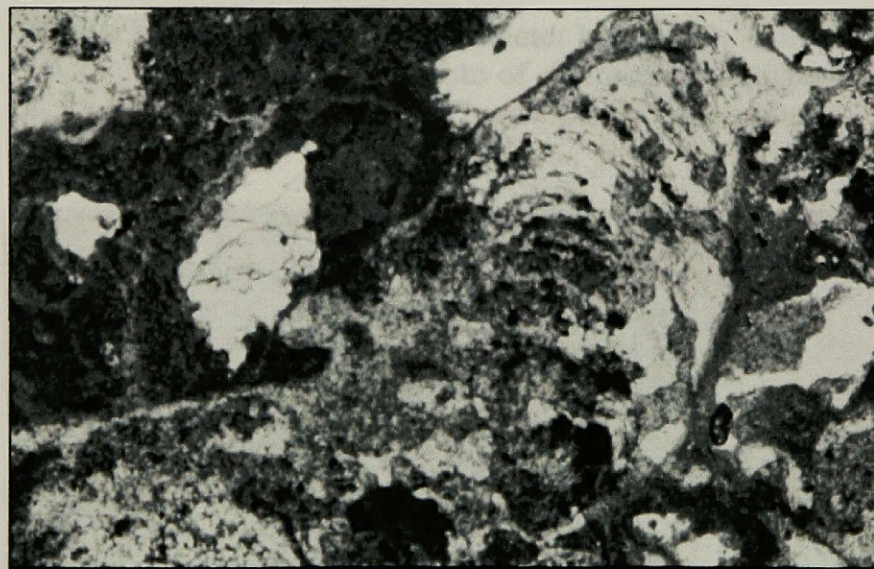
Figure 37 shows a mineral deposit SEM/BSE image with diatoms and iron oxide. Again, the diatoms are similar as seen in other samples. The iron oxide detected corresponds



well with iron found in the bead tube installed in the same section of creek. The iron is likely derived from groundwater.



*a*



*b*

**Figure 35:** Thin section photomicrographs at different scales. Sample *lra4* (*a*) (FOV ~ 1 cm) and is from piezometer *lra* at 10 cm depth. Random microbe entombment in silica is mostly present with some silica layering in different sections of the sample. Photo *a* matches well with the random microbe (diatoms) entombment found in the SEM photographs (*figure 31*). Sample *rl3a* (*b*) (FOV ~ 1 cm) and is located in the creek in the meadow area. Silica and cyanobacteria layering are seen.



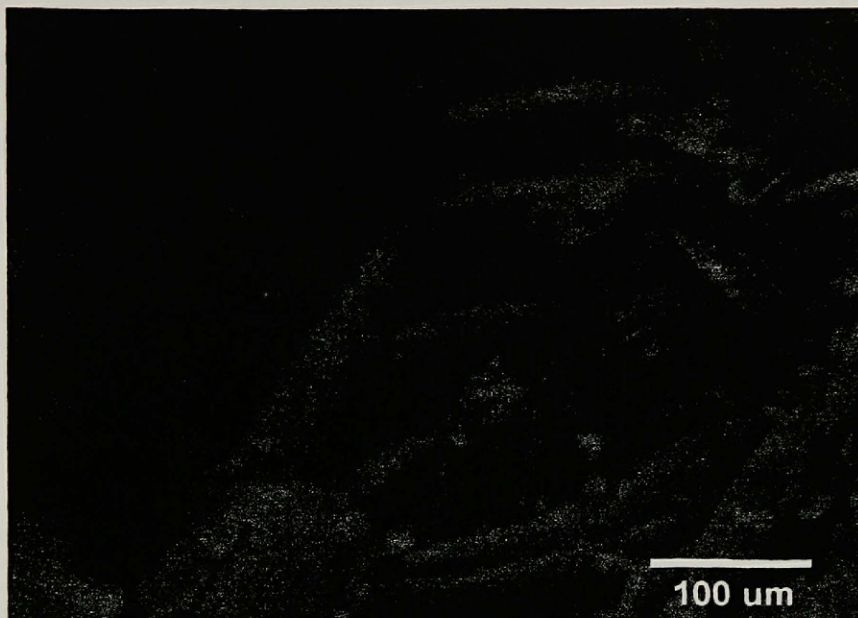


**Figure 36:** Sample *ula30* (piezometer bore hole). Compare with Figure 31 photo of chemical precipitation box precipitates. The diatoms are the same.

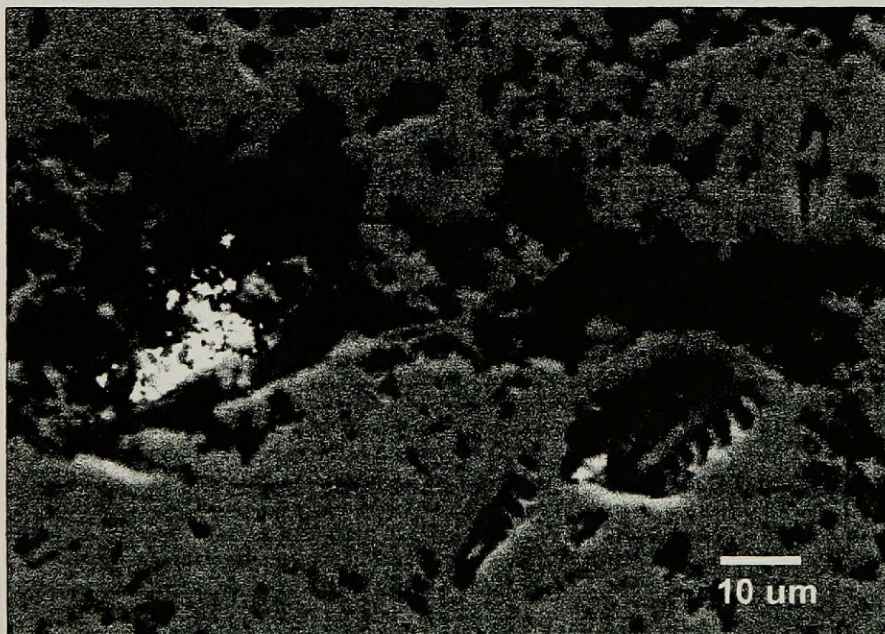


**Figure 37:** Sample *rl4b* (collected in the braided section of the study site). The white coloring on the left is iron. Note the microbe cast on the right.

Elemental mapping was performed on the thin sections where mostly SiO<sub>2</sub> with trace amounts of other elements was present (Figure 38). Aluminum, sodium, potassium, and magnesium were in layered sequences. Iron was only present in spots and was not part of layering. Several spectral scans were done on the samples and SiO<sub>2</sub> was the dominant compound present in most scans. There were some small spots of NaCl and calcium but in no systematic order. Samples from the piezometer bore holes were composed only of SiO<sub>2</sub>.

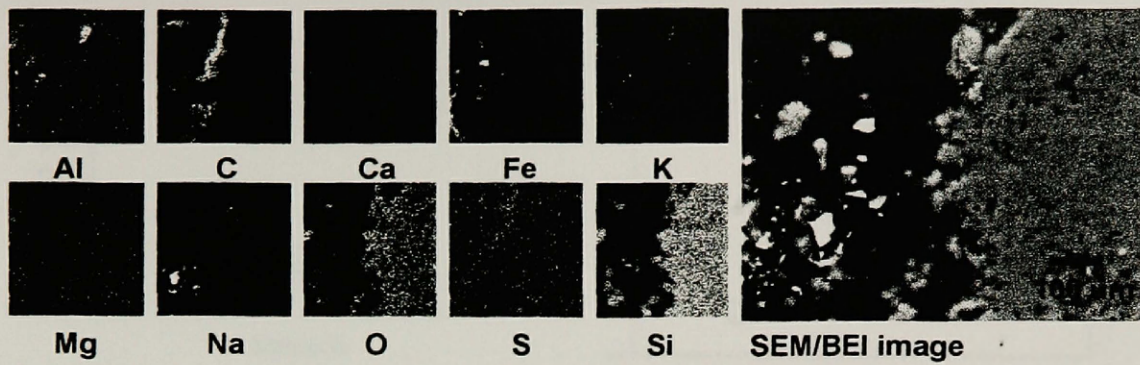
Porosity ( $n$ ) measurements were low for both the channel deposits and the subsurface sinter (see Table 6 for descriptions). The piezometer bore sample porosity was less than 12% while the creek channel deposit porosity ranged from 13.4-15.4% (Figure 39). Standard deviations were large. Thus, porosity was variable in the samples. This was expected since the thin section samples were small in size and there was observed variability in each thin section. Variability was expected because the samples were collected in different creek reaches.

Calculated permeability values ( $K$ ) were lower than other sinter facies types (Table 7). Values for this study are three orders of magnitude lower than previous studies. Gibson (1999) and Kendall (1999) hydraulic conductivity measurements were  $10^{-1}$  -  $10^{-2}$  m/s.

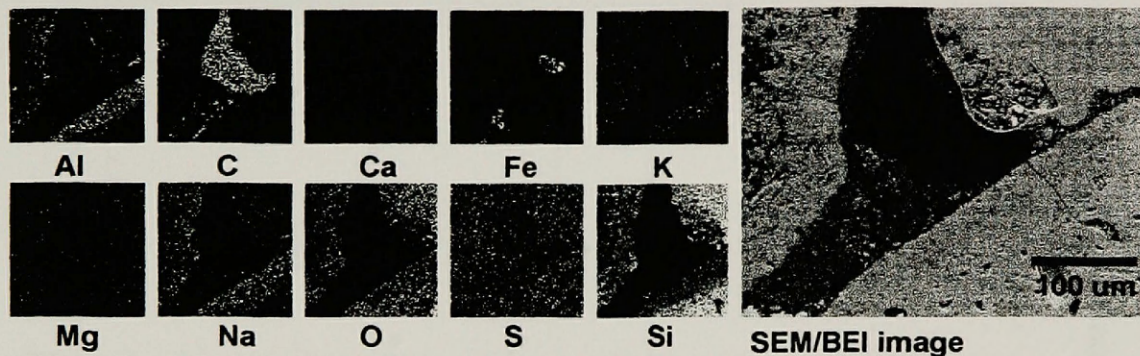
**Table 6:** Deposit sample location descriptions.

<b>Sample ID</b>	<b>description</b>
mla17	piezometer <i>mla</i> , 43 cm depth
lra4	piezometer <i>lra</i> , 10 cm depth
rl2	above meadow, in creek
rl3a	in meadow, in creek
rl4b	below meadow, in creek

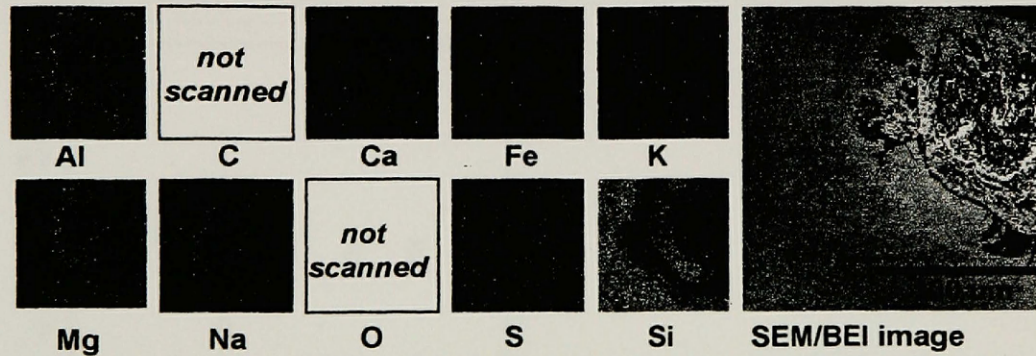




Sample *r/2a* (collected above the meadow in the creek).



Sample *r/3a* (collected in single channel section of meadow).



Microprobe elemental map of sample *r/3a*  
(collected in single channel section of meadow).

**Figure 38:** Elemental mapping of selected creek channel mineral deposits from thin sections.



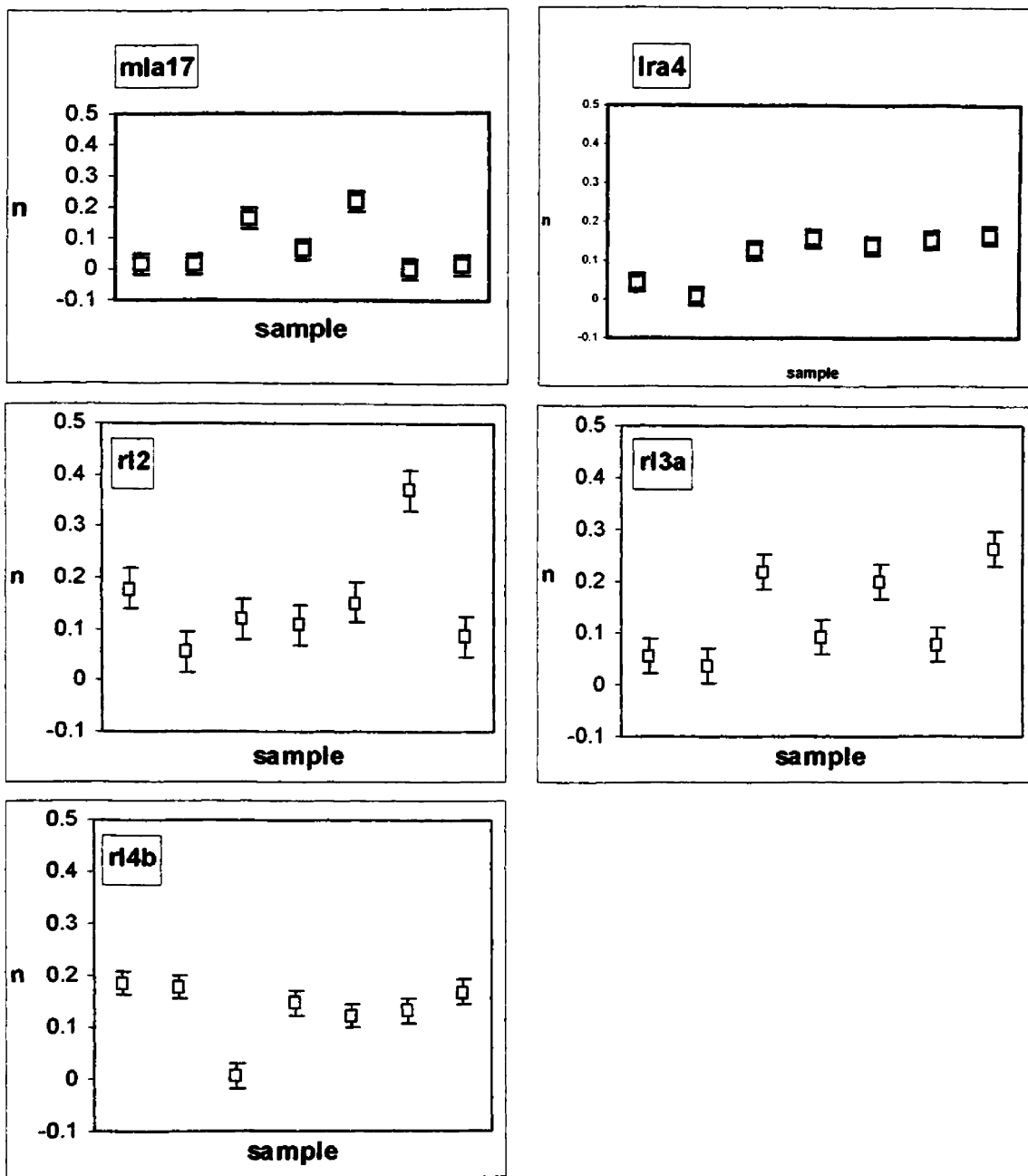


**Figure 39:** Average porosity ( $n$ ) measurements for rock samples with SE bars. Seven measurements were conducted on each sample

**Table 7:** Porosity statistics for thin sections samples. FOV (field of view) is  $303, 525 \mu\text{m}^2$ . Seven measurements were made on each sample.

Sample ID	Porosity ( $n$ ) (avg of 7 measurements)	SD	mean	90% C.I.	K (m/s)
mla17	.070	.086	.108	.004	$1.553 \times 10^{-5}$
lra4	.113	.062	.079	.003	$2.767 \times 10^{-5}$
rl2	.154	.104	.315	.005	$4.133 \times 10^{-5}$
rl3a	.135	.09	.163	.004	$3.491 \times 10^{-5}$
rl4b	.134	.061	.179	.002	$3.449 \times 10^{-5}$

The  $\rho$ -value for the creek sample set is 0.896. The  $\rho$ -value for the piezometer sample and the total sample set is  $< 0.4$  (Table 8).

**Table 8:** Mineral precipitate porosity  $\rho$ -values.

Sample set	$\rho$ -value
creek	0.896
piezometers	0.302
creek and piezometers	0.390

This indicates that the creek sample porosity is similar throughout the length of the creek. The piezometer samples are not similar according to  $\rho$ -value statistics. The piezometer samples and the creek samples are not similar. However, all sample permeability measurements are the same order of magnitude.

#### 4.6 Geomorphology

Longitudinal gradients of two creek sections showed a uniform slope in the single channel creek sections (right side of plots in Figure 40) and a slight convex downward slope in the anastomosing sections (left side of plot in Figure 40) (see James, 1989). Figure 41 shows the locations where the longitudinal gradient measurements were taken. Both single channel sections drained through meadows. Both anastomosing sections drained through dry parts of the basin where lodgepole pines and sinter slickens were present.

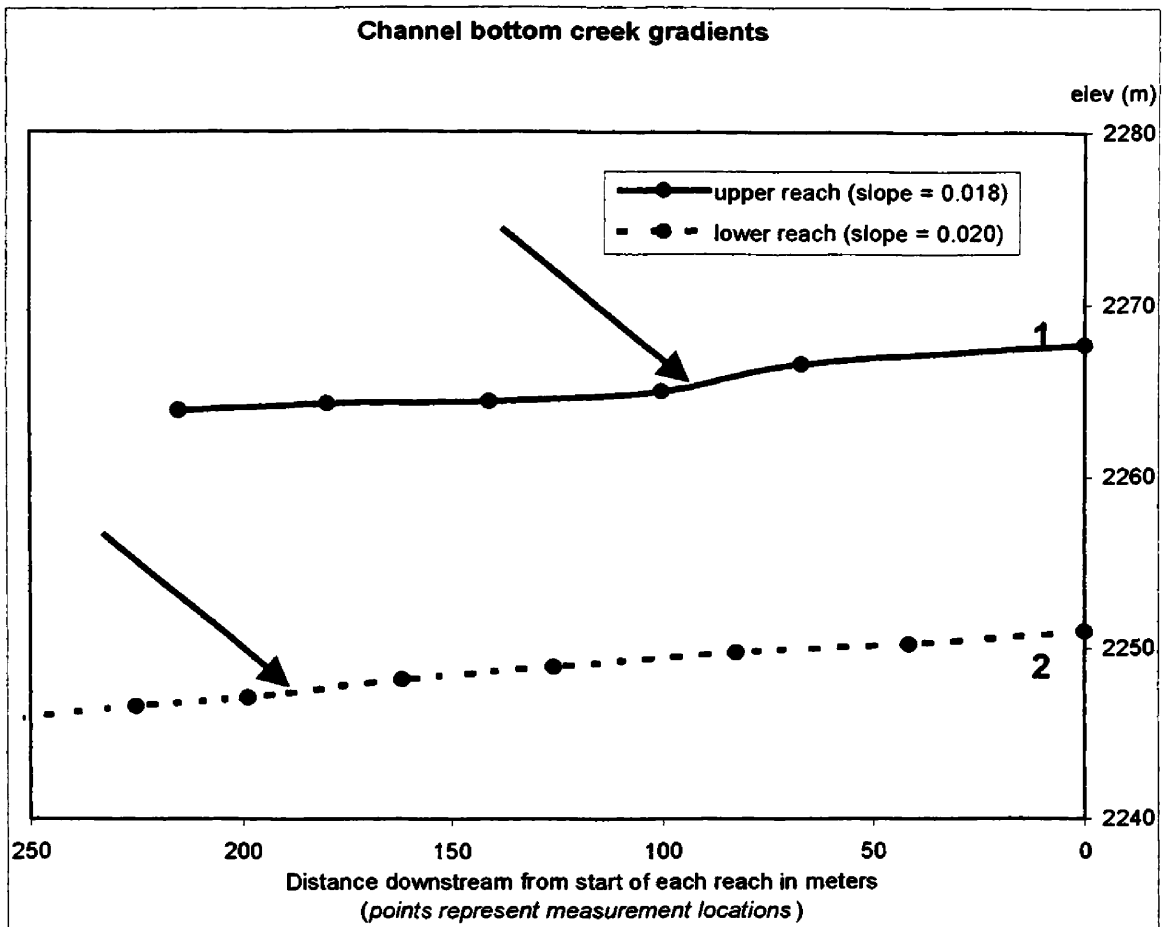


**Figure 40:** Longitudinal gradients of the study site (bottom) and a morphologically similar site (top) just below the source of Rabbit Creek. Arrows point to convexity of line where the single channel sections form into anastomosing sections. There are no error bars associated with these measurements because the rod and transit used provided consistent measurements.

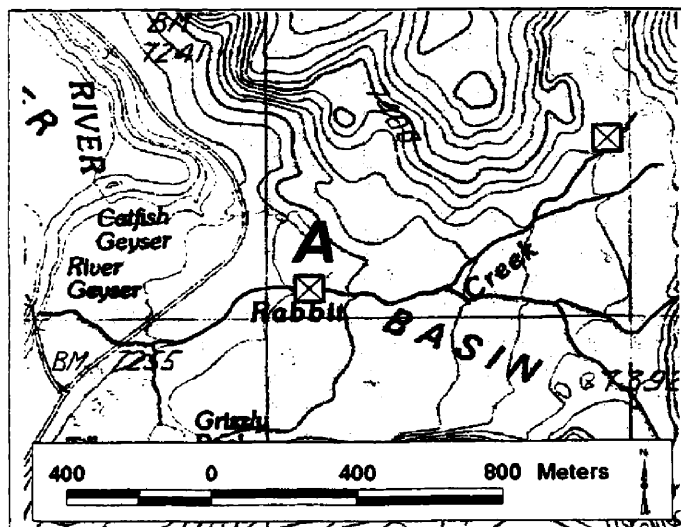


**Figure 41:** Location map of longitudinal gradient measurements (X in square).

Cross sections of the creek showed the dramatic vertical changes in channel morphology due to sinter deposition (Figure 42; the locations in the creek underlie the left square (A) in Figure 41). The single channel sections are likely where the creek eroded the channel through pre-existing sinter (Figure 43). Perched channels (channels at a higher elevation than the main channel) in the single channel section are seen where there are numerous drops in water levels throughout the reach. The channels are armored that prevent lateral movement.

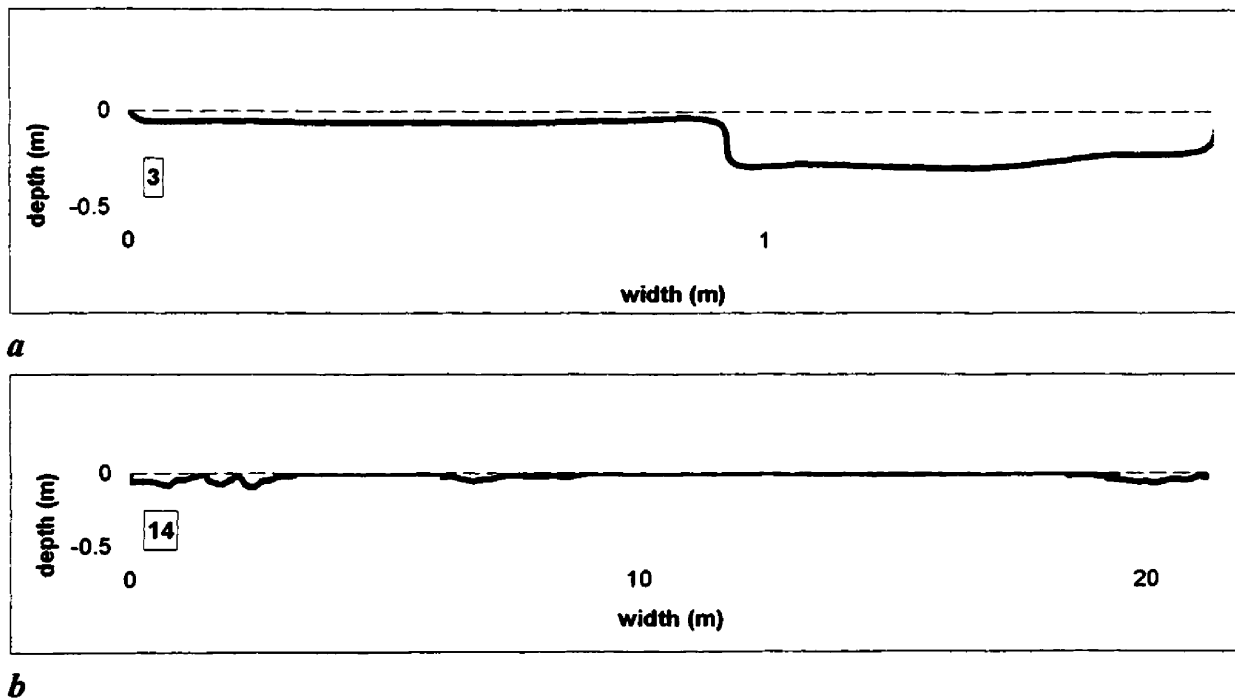


**Figure 42:** Cross section 3 (a) is in the single channel of the creek. Note the sharp drop in the middle of the creek that is a result of sinter deposition. Plot b is in the anastomosing section of the creek (*note different x-axis scale*). The channels are narrow and shallow. Sinter islands are between the channels. These two cross-sections are approximately 100 m apart.

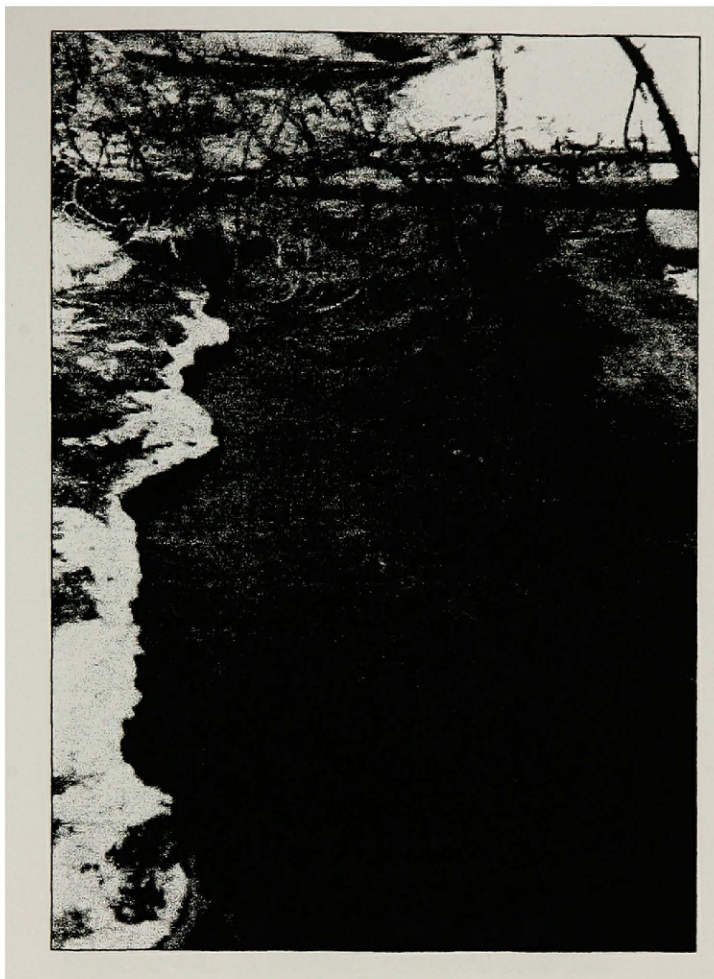


**Figure 43:** Single channel reach where the creek likely eroded the channel through pre-existing sinter. The white color on the upper right is snow. Sinter is on the left.

The channel morphology is most complex in the anastomosing sections. The anastomosing sections show silica in between the channels. Within the channels of the anastomosing sections, sinter has formed vertical barriers that separate water flow in the same channel as the water flows downstream. Many of these channels are not able to move laterally. In some reaches, terraces have formed that are higher than the surrounding channel bed (Figure 44). See Appendix F for all cross section plots.

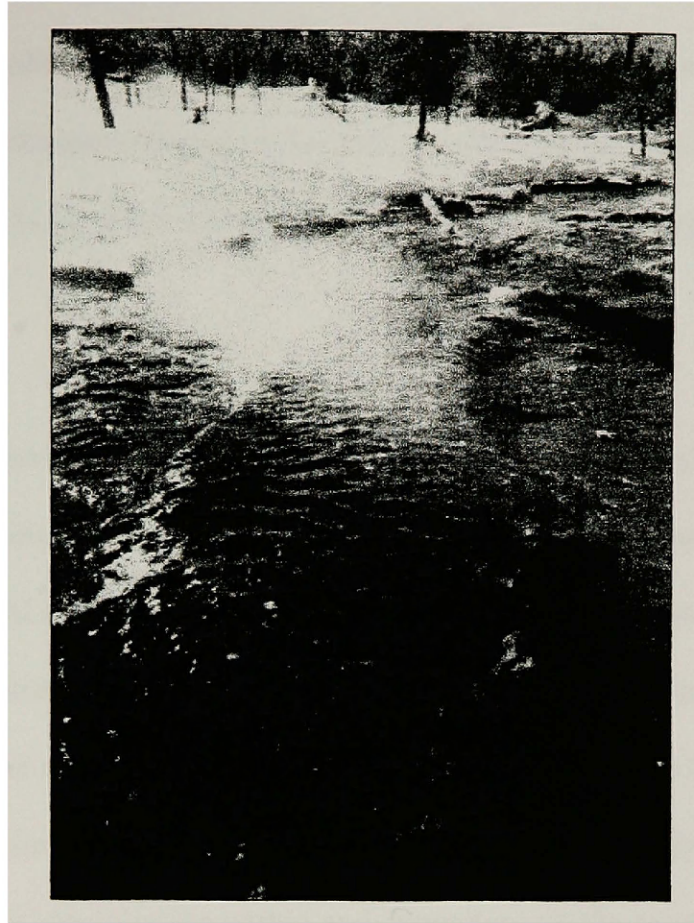


**Figure 44:** A smaller terraced channel within the larger main channel.

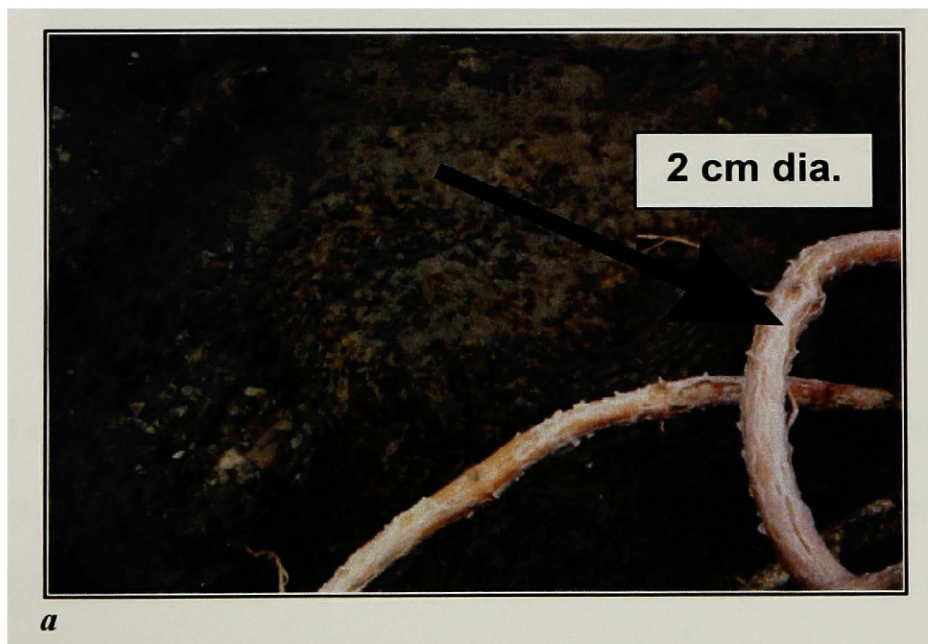
#### **4.7 Photographic Documentation**

The important results from photographic documentation reveal changes in the creek channel between summer and winter. Figure 45 shows photos of the same location, in the braided section of the study site, where one photo was taken in the winter, spring, and summer. In the winter, a thick cyanobacterial mat (~1-2cm) was present. By the following June, only a thin biofilm was present on the bottom of the creek channel. In winter, cyanobacteria covered a larger spatial area in the creek. Cyanobacteria in the creek have not been identified but probably include *Oscillatoria* and / or *Phormidium* (Yellowstone Center for Resources, Thermophilic Microorganism Survey).

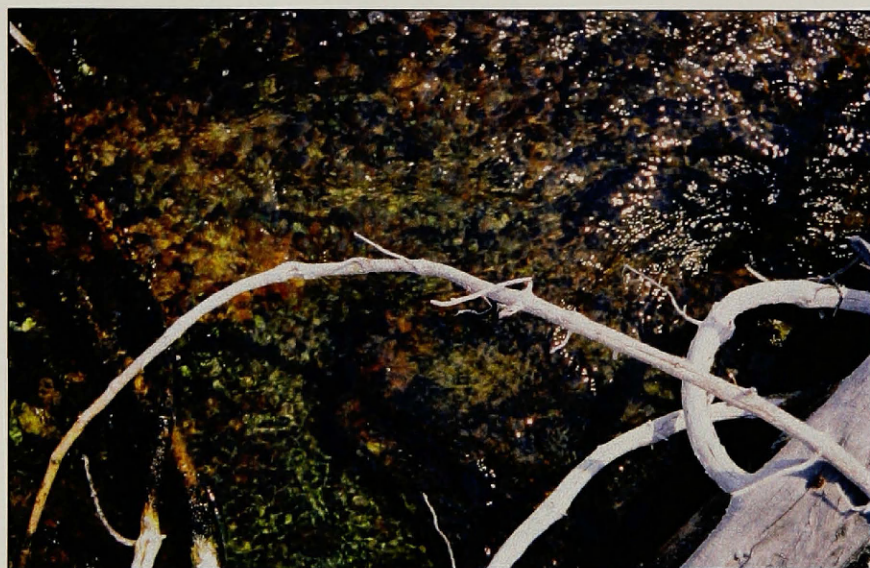


Temperature is probably the driving factor for the seasonal biotic community changes. Photosynthesis and chemosynthesis likely have an affect on the biota. Iron concentrations were highest during the winter and may provide an energy source during this season.

During the winter months, the creek water temperature decreased by  $\sim 15^{\circ}\text{C}$  and cyanobacteria and other biota thrived on the bottom of the creek channel. This is also when silica and metal concentrations are the highest. During the summer season, when creek water temperatures are approximately  $30^{\circ}\text{C}$  and analyte concentrations are lower, biotic populations are much smaller. In the winter, silica saturation increased in the creek water as air temperature decreased and silica precipitated onto the cyanobacteria. So the combination of silica precipitating within and depositing on the cyanobacteria is occurring mostly in winter.



**Figure 45:** Photo *a* with thick, green biota was taken in February of 2002. Photo *b* (next page) with only a thin biofilm present was taken in June of 2002. By July, 2002, a different microbial mat existed in the creek channel (*c*).

*b**c*

Fine-grained creek sediment was photographed in the winter and the summer in several locations (not shown). The photographs show that minimal sediment transport occurred. This was expected since the spring hydrograph did not have large discharge fluctuations.



## **5.0 Discussion**

The formation of mineral deposits in the channel of Rabbit Creek is controlled by hydrological, geochemical, thermal, geomorphological, and biological factors. Some or all of these factors need to occur simultaneously for silica and metal oxides to precipitate. At a large scale, hydrology determines the locations for mineral deposition. Creek temperature is the driving factor because temperature controls mineral saturation and subsequent precipitation. Geochemistry controls the details of the processes through its effect on silica deposition rates. Biota in the form of cyanobacterial mats act as a substrate for mineral deposition.

### **5.1 Hydrologic Controls on Mineral Precipitation**

Water level data from the piezometers and staff gauges suggest that the upper, single channel reach of Rabbit Creek is a gaining reach and the lower, anastomosing reach is losing to groundwater (Figure 46). The single channel reach runs through a meadow. The head in the near-channel piezometers along the single channel reach was approximately 0.1 m higher in elevation than the water levels at the staff gauges in the creek (Figure 40). In this single channel reach, groundwater is shallow and flows through the soil zone into the creek where the channel deposits are lower in elevation. In the lower, anastomosing reach, some surface water exits the creek above the channel deposits. Where water level in the creek is below the channel deposits, no interaction occurs.

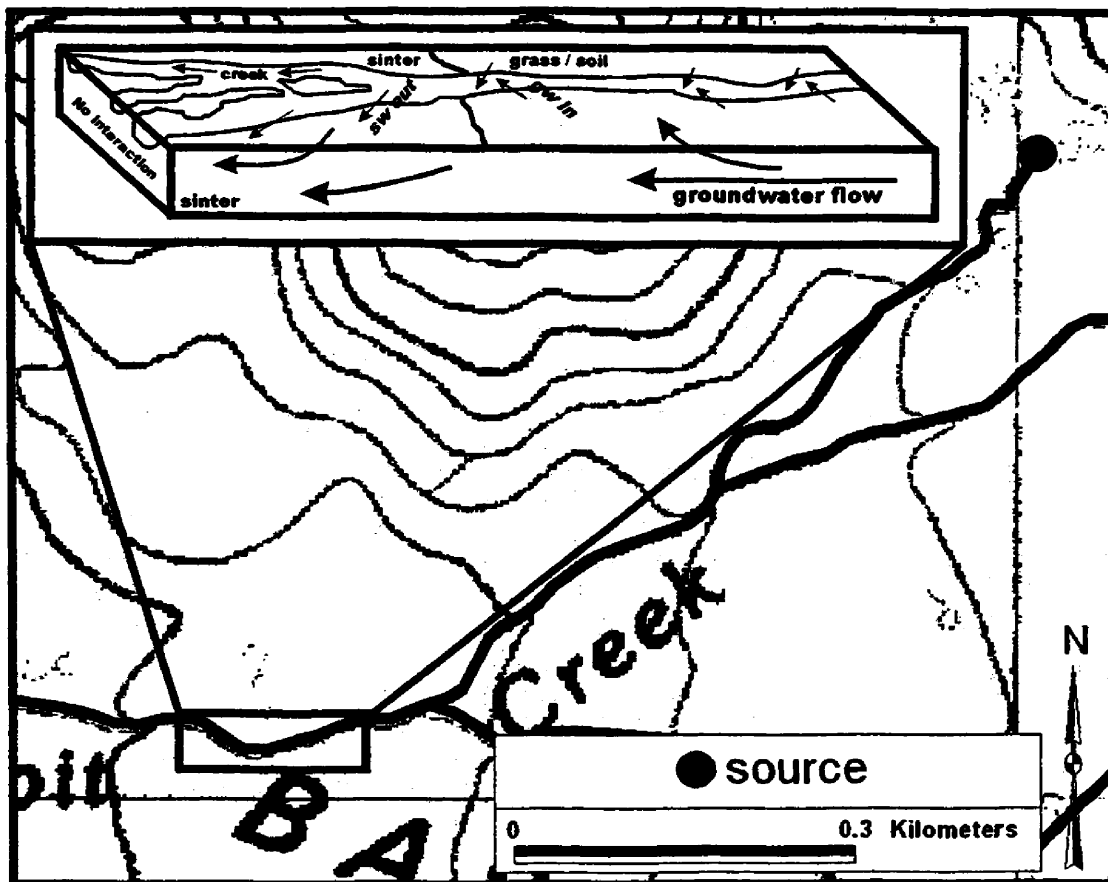


**Figure 46:** Near channel creek hydrology schematic estimated from piezometric and staff gauge head data in context within the basin.

It appears, and a thorough petrographic study would likely confirm, that the single channel reach, where groundwater discharges to surface water, runs through pre-existing sinter. The lower section is lined with silica precipitates. The implication is that precipitation only occurs along the lower, losing reach.

Essentially, as surface water infiltrates into the subsurface in the losing creek reach, silica precipitates as a result of physical processes. Dissolved silica is forced into the creekbed where polymerization and deposition takes place. Since silica has a higher tendency to deposit on substrates that have previous silica deposits, the rate of silica deposition is

enhanced in the losing creek reach. Differences in chemistry between surface and groundwater enhance the deposition process.

Other streams in Yellowstone are also lined with mineral precipitates. Sentinel Creek (Gibson, 1999) and Iron Spring Creek (DeMonge, 1999) have irregular streambed armoring. Rabbit Creek, however, has nearly continuous armoring along its length. Interaction with groundwater is restricted to connections with the soil zone above the top part of channel armoring and along streambed fractures. Gibson's (1999) study showed minor groundwater interaction with Sentinel Creek along armored sections. Sentinel Creek is mainly fed by meteoric and shallow groundwater and drains a large meadow that is marshy for most of the year. Gibson did not address what controls mineral deposition or when mineral deposition occurs. However, DeMonge (1999) also found that mineral deposition was occurring in losing sections of Iron Spring Creek but the chemical processes driving deposition in Rabbit Creek are different than those for Iron Spring Creek.

## **5.2 Chemical Controls on Mineral Precipitation**

The physical and chemical characteristics of the surface water in Rabbit Creek were distinctly different from the groundwater at the near channel scale. This illuminates groundwater and surface water interaction. Calculations using chloride concentrations indicated that 1.4 % (+/- 0.2%) of the water in Rabbit Creek comes from groundwater discharge during the winter.

### *Effects of temperature*

Cooling affects silica precipitation in the creek, particularly in the anastomosing sections. As water temperature cools, precipitation rates increase (Williams and Crerar, 1985). Temperature of the creek drops 50°C in the uppermost creek reach to 35°C in the lowest creek reach studied. In Octopus Spring (Yellowstone National Park) silica starts precipitating from solution at 30°C (Stauffer et al., 1980) so major inorganic silica precipitation in Rabbit Creek may be occurring downstream of the lowest creek reach studied. The anastomosing sections promote silica deposition as water spreads over a relatively large surface area with shallow depth. The creek water cools quickly due to an increase in surface to volume ratio. Silica precipitation is now occurring where substrate surface area is greatest.

### *Effects of pH*

The pH affects silica speciation and thus solubility and deposition rates in surface water. But measured pH did not fluctuate downstream from the source. Instead, silicic acid dissociation constants increase at elevated temperatures, which leads to increased concentrations of easily polymerized anionic forms of silica. Silica speciation was calculated using MINTEQA2 (Version 3.10, 1991, US Environmental Protection Agency). Because of the high pH in the surface water (9 to 10), a large percentage of  $\text{H}_3\text{SiO}_4^-$  was present in solution instead of  $\text{H}_4\text{SiO}_4^0$ , which is present at lower pH. In the presence of cations, the rate of  $\text{H}_3\text{SiO}_4^-$  polymerization is faster than  $\text{H}_4\text{SiO}_4^0$ . In losing

reaches, these polymerized forms of silica are driven through the silica-rich creekbed leading to deposition. In groundwater, where pH is lower and silicic acid is only slightly dissociated, little or no deposition occurs as dissolved silica passes across the silicified streambed. Thus, the most rapid rates of silica deposition should and do occur where  $\text{H}_3\text{SiO}_4^-$  is present in significant concentrations.

#### *Effects of changes in water chemistry*

The shallow groundwater experienced seasonal variations in redox conditions due to the effect of winter snow and ice cover. During the winter, snow covered the ground in the meadow and created a nearly closed system. As warm groundwater melted the snow, the water table rose slightly (Figure 15) and a layer of ice developed over the ground surface. This layer of snow and ice likely sealed off exchange of oxygen with the atmosphere. Subsequent organic matter decomposition lowered dissolved oxygen concentration and pH (Harris, 1967).

In a comparable physical environment, Hoehn and von Gunten (1989) found radon concentrations increased dramatically in their one winter of sampling. They attributed the concentration changes to snow pack over a moist unsaturated zone that prohibited exchange with the atmosphere. Applin and Zhao (1989) studied iron redox geochemistry in an alluvial aquifer of the Missouri River and found that reducing conditions mobilized iron as iron oxides were reduced to soluble ferrous iron. Coprecipitated and adsorbed ions were also mobilized (i.e. aluminum, magnesium, copper, etc.), resulting in elevated

concentrations of these ions in groundwater. In Rabbit Creek, a pulse of reduced iron was observed in piezometer *ulb*. This reduced iron provided a qualitative tracer as it moved from groundwater to surface water. Once the reduced iron entered the creek, rapid oxidation occurred resulting in deposition on the channel lining.

Groundwater discharge, although small, likely has a significant affect on the creek channel mineral deposits. Ferrous iron in discharging groundwater precipitates onto the existing sinter deposits upon oxidation in the alkaline solution ( $\text{pH} > 9$ ) and is incorporated into the rock material (Williamson, 1999, Tamura et al., 1976). Aluminum concentrations in surface water were also probably increased from groundwater discharge. Aluminum deposits on the mineral lining affecting the area of sorbing sites for future silica deposition. The ionized species of silicic acid may polymerize with metal oxides that subsequently deposit on the creek channel lining. Iron and aluminum ions reduce the concentration and solubility of dissolved silica and so opal-C or quartz may precipitate (Hinman, 1998, Chang and Yortsos, 1994, Iler, 1973). Iron and aluminum concentrations observed in Rabbit Creek probably affect silica in both dissolved and solid form.

#### *Mineral-precipitate collection instrumentation*

The bead tubes and chemical precipitation boxes were installed in the creek just below the hot spring source, in the single channel reach that runs through the meadow, and in the lower anastomosing reach. Both sets that were installed in the fall and in the

following spring collected silica precipitates. However, precipitation rates could not be determined. Amorphous silica was saturated during all months sampled, regardless of temperature, according to MINTEQA2 geochemical modeling (Version 3.10, 1991, US Environmental Protection Agency). The saturation index (SI) gives an indication of whether a solid will precipitate from solution. An SI greater than zero indicates saturated conditions with respect to that mineral phase. Values greatly in excess of zero are common for minerals not actively forming. The SI for amorphous silica in Rabbit Creek was less than one indicating that silica was only slightly saturated and likely actively precipitating. The highest saturation index values for silica occurred in January.

Silica deposited on the creekbed is mostly amorphous silica as analyzed by X-ray diffraction. A creek channel deposit sample collected just below the hot spring source was composed of opal-C and quartz. Controlling factors on silica deposition are a combination of temperature, pH, geochemistry, and biological mediation (Akahane et al., 1997, Change and Yortsos, 1994, Rimstidt and Cole, 1983). Temperature is the dominant controlling factor (Herdianita et al., 2000, Carroll et al., 1998, Fournier and Rowe, 1977, White et al., 1956) that likely explains the deposition of opal-C and quartz near the source. If silica was not deposited in crystal form, accelerated diagenesis may have occurred in these deposits due to higher creek water temperatures.

Iron and copper only precipitated onto the bead tubes (below the meadow in the creek) when there were elevated concentrations of these ions present in the groundwater during winter. Ferrous iron and copper were present in the groundwater during the reducing

winter conditions at near neutral pH. Iron discharged to the alkaline creek likely oxidizes rapidly depositing iron oxides on the silica. Some trace amounts of iron, aluminum, potassium, and sodium were present in the deposits, as analyzed by SEM/EDS. Iron oxides on the surface of the mineral deposits likely affect the affinity for silica to deposit in the creek channel.

### **5.3 Microbial Influences on Precipitation**

Cyanobacterial mats provide a substrate for silica deposition (Jones and Renaut, 1996). Cyanobacterial mat existence depends on a particular species' temperature range. The mats mostly grow in stagnant pools or along the sides of the channel in Rabbit Creek. Silica deposits were observed on the mats in the creek.

When water is trapped and becomes stagnant in the mats, silica particles form and settle out of solution, even when undersaturated with respect to silica (Phoenix and Konhauser, 1999, Wiegart and Fraleigh, 1972, White et al., 1956). The chemical precipitation boxes in Rabbit Creek that were analyzed by SEM collected only silica precipitates. The boxes showed that, even though no minerals deposited directly onto the glass substrate, silica precipitates settled out of solution within the cyanobacteria that had colonized the boxes. Thin section photomicrographs of the mineral deposits were composed of similar microbes that had colonized the boxes. Thus, cyanobacteria and microorganisms are incorporated into the channel lining.



#### **5.4 Seasonal Timing of Mineral Precipitate Formation**

Photographic documentation revealed changes in cyanobacteria mat populations. The mats, as well as an abundance of other microbes like diatoms, had more extensive populations during the winter season (Figure 45). The cyanobacterial mats were thicker and covered a larger spatial area therefore creating a more sites for the deposition and entrapment of minerals. During the summer season, only thin biofilms existed where relatively thick cyanobacterial mats were present during the winter. Cyanobacteria thrive in optimal thermal regimes (Castenholz, 1969) so the population increase in winter is likely driven by temperature.

The creek channel mineral deposits are formed mostly during the winter season, particularly in January. This is the time of year when silica concentration and saturation are highest. The air temperature is colder than the rest of the year and that in turn lowers the creek water temperature. Decreasing water temperature affects silica solubility and so silica precipitates more readily. Microbial mat populations are thicker and more extensive in the creek providing a high affinity substrate for silica deposition. The groundwater experiences reducing conditions where soluble metals discharge to the creek, quickly become oxidized, and are incorporated into the existing mineral deposits.

#### **5.5 Conceptual Model of Rabbit Creek and the Rabbit Creek Basin**

Groundwater flow in the Rabbit Creek basin is probably mostly horizontal (White et al.,

1975). The unconsolidated material (Becker and Blackwell, 1993) consists of an unconfined aquifer. Groundwater in this unconfined aquifer flows from the head of the basin to the west, approximately parallel to the creek (Figure 47). A hot spring emerges in the creek just upstream of piezometers *m1a* and *m1a*. It is likely the water in the piezometers and the spring are coming from the same source, a semi-confined aquifer within the unconfined aquifer.

Hot spring water seeps into the local groundwater where there is radial flow away from spring sources (Gibson, 1999). The soil zone is a sink for metals that mobilize upward from the gravel and tuff layers in the basin. Groundwater enters the creek mostly through the soil zone since the mineral deposits have relatively low porosity. According to chemical dilution calculations, approximately 1.4% of the creek flow is from groundwater. Metals derived from groundwater contribute to the creek channel deposit mineralogy. Creek channel mineral deposits occur in losing reaches.

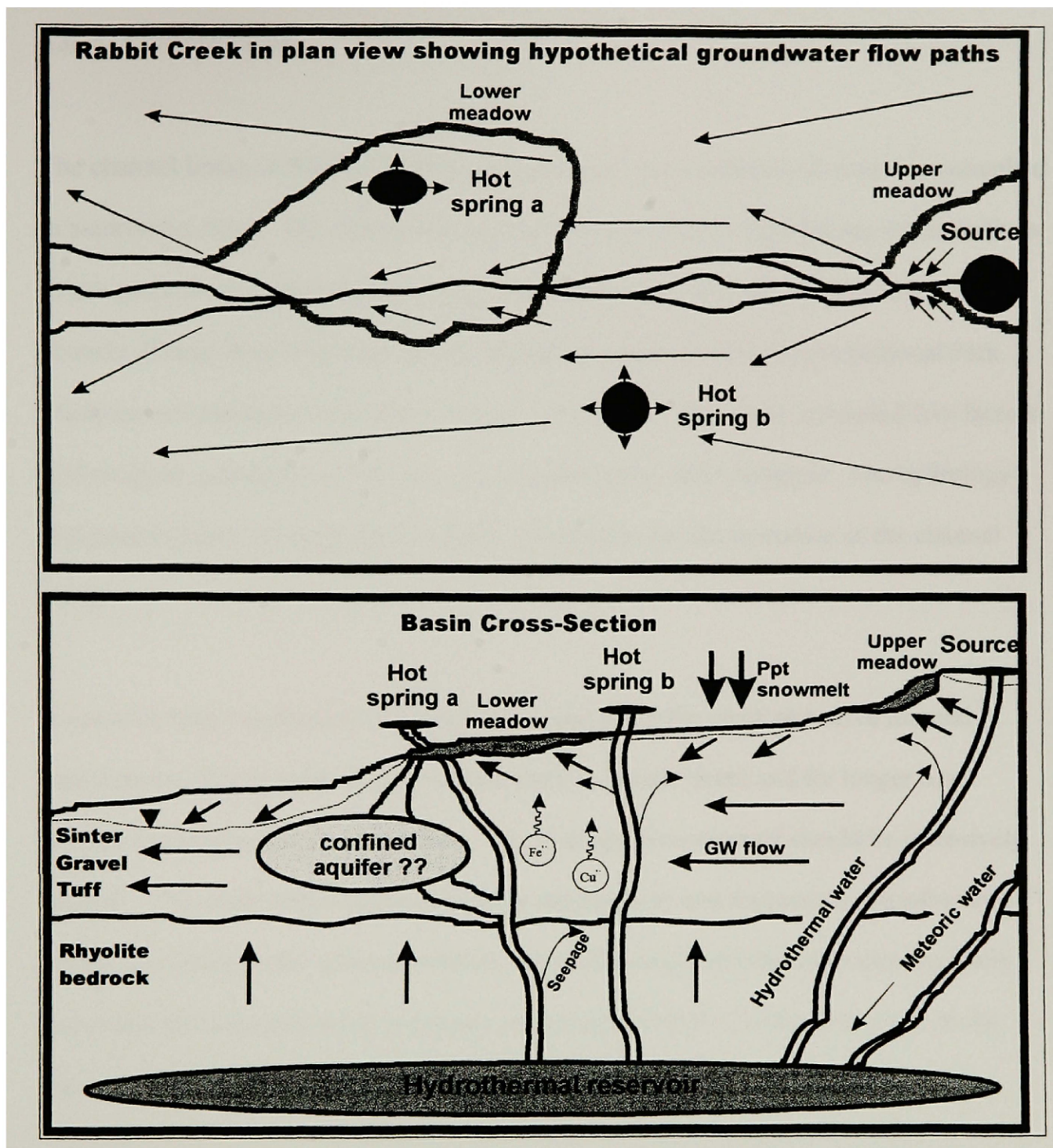


**Figure 47:** Conceptual model of Rabbit Creek and the Rabbit Creek Basin. Stratigraphy after Keith and Muffler, 1978 and White et al., 1975.

## 6.0 Conclusions

The channel lining in Rabbit Creek is composed of cyanobacteria and microbes entombed in amorphous silica. The channel lining appears in perched, anastomosing creek sections where groundwater discharge is absent. The mineralization of the channel lining is visually distinct from other hot spring outflow channels in Yellowstone National Park. There are several factors that affect mineral deposition. This study examined five factors: hydrological, geochemical, thermal, geomorphological, and biological. The hydrology and geochemistry of the system is mostly responsible for the formation of the channel lining.

In order to better understand the processes occurring in the creek that drive mineral precipitation, future work should be conducted in greater detail and for longer time periods to examine the studied factors. The biological component should be intensively studied. This study only examined biology qualitatively and focused on cyanobacteria acting as a substrate for silica deposition. Cyanobacteria and other microbes are likely important for biogeochemical processes occurring in Rabbit Creek, particularly at the surface water and groundwater interface.

Seasonal water chemistry variability in the surface water and groundwater was not expected in this study. Analytes in both the surface water and the groundwater significantly increased during the winter. These analytes, like magnesium, aluminum, and iron, may affect silica solubility and thus the channel lining in the creek. A more

thorough petrographic study of the creek channel mineral deposits would provide detailed data regarding the precipitate formation.

Chloride variability was also substantial. The chloride concentrations increased up to 245% in the shallow groundwater where these increases have never been observed in Yellowstone. Chloride is a good hydrothermal water indicator and so suggests the hydrothermal system in the basin is dynamic. The variability in water chemistry may provide new information about the Yellowstone National Park hydrothermal system as a whole.

## References Cited

- Akahane, H., I. Yasuda, H. Miyajima, K. Goto, and H. Honoki. 1997. Precipitation of silica sinter in hot spring water. *Journal of the Geological Society of Japan*, v 103, no 2, p 154-162.
- Alexander, G., W. Heston, and R. Iler. 1954. The solubility of amorphous silica in water. *Journal of the American Chemical Society*, v 75, p. 453-455.
- Allaby, M. 1994. *The Concise Oxford Dictionary of Ecology*. Oxford University Press, New York. 415 p.
- Applin, K. and N. Zhao. 1989. The kinetics of Fe(II) oxidation and well screen encrustation. *Ground Water*, v 27, no 2, p 168-174.
- Bates, R. and J. Jackson, editors. 1984. *Dictionary of Geological Terms*. Anchor Books, Doubleday: New York. 571 p.
- Becker, D. and D. Blackwell. 1993. Gravity and hydrothermal modeling of the Roosevelt Hot Springs Area, Southwestern Utah. *Journal of Geophysical Research*, v 98, no B10, p 17,787-17,800.
- Bohlmann, E., R. Mesmer, and P. Berlinski. 1980. Kinetics of silica deposition from simulated geothermal brines. Chemistry Division of the Oak Ridge National Laboratory, Oak Ridge, Tennessee, 34 p.
- Borrok, D., S. Kesler, E. Essene, and R. Boer. 1997. Fluid inclusion evidence for a magmatic-hydrothermal model for massive iron oxide deposits. *Abstracts with Programs – Geological Society of America*, v 29, no 6, p 208.
- Boyd, F. 1957. *Geology of the Yellowstone Rhyolite Plateau*. PhD Thesis, Harvard University. 128 p.
- Braunstein, D. and D. Lowe. 2001. Relationship between spring and geyser activity and the deposition and morphology of high temperature (>73 degrees C) siliceous sinter, Yellowstone National Park, Wyoming, USA. *Journal of Sedimentary Research*, v 71, no 5, p 747-763.
- Bredehoft, J. 1967. Well-aquifer systems and earth tides. *Journal of Geophysical Research*, v 72, p 3075-3087.

- Bridge, T. and D. Johnson. 1998. Reduction of soluble iron and reductive dissolution of ferric iron-containing minerals by moderately thermophilic iron-oxidizing bacteria. *Journal of Applied and Environmental Microbiology*, v 64, no 6, p 2181-2186.
- Brock, T. 1994. *Life at High Temperatures*. Yellowstone Association for Natural Science, History, and Education, Inc., Yellowstone National Park, Wyoming. 31 p.
- Cady, S., D. Des Marais, L. Jahnke, R. Summons, C. Blank, and M. Walter. 1997. Biogenic signatures of modern subaerial hydrothermal deposits formed near life's upper temperature limit; a comprehensive model for ancient analog studies. *Abstracts with Programs – Geological Society of America*, v 29, no 6, p 194-195.
- Carroll, S., E. Mroczek, M. Alai, and M. Ebert. 1998. Amorphous silica precipitation (60 to 120°C): Comparison of laboratory and field rates. *Geochimica et Cosmochimica Acta*, v 62, No 8, p 1379-1396.
- Castenholz, R. 1969. Thermophilic blue-green algae and the thermal environment. *Bacteriological Reviews*, v 33, no 4, p 476-504.
- Chang, J. and Y. Yortsos. 1994. Lamination during silica diagenesis-effects of clay content and Ostwald Ripening. *American Journal of Science*, v 294, p 137-172.
- Christiansen, R. 2001. *The Quaternary and Pliocene Yellowstone Plateau Volcanic Field of Wyoming, Idaho, and Montana*. US Geological Survey Professional Paper 729-G, 145 p.
- Cox, E. 1978. Iron in wastewater lagoons in Yellowstone National Park, Wyoming. *Journal of Research, U.S. Geological Survey*, v 6, no 3, p 319-324.
- Crerar, D., E. Axtmann, and R. Axtmann. 1981. Growth and ripening of silica polymers in aqueous solutions. *Geochimica et Cosmochimica Acta*, v 45, p 1259-1266.
- Damm, K. 1995. Controls on the chemistry and temporal variability of seafloor hydrothermal fluids. In *Seafloor Hydrothermal Systems: Physical, Biological, and Geological Interactions*. S. Humphris, R. Zierenberg, L. Mullineaux, and R. Thomson, Editors. American Geophysical Union, p 222-247.
- Danielpol, D. 1989. Groundwater fauna associated with riverine aquifers. *Journal of the North American Benthological Society*, v 8, no 1, p 18-35.
- Davison, W. and G. Seed. 1983. The kinetics of ferrous iron in synthetic and natural waters. *Geochimica et Cosmochimica Acta*, v 47, p 67-79.

- DeMonge, J. 1999. Streambed armoring in Iron Spring Creek, Yellowstone National Park: ground water-surface water interactions. Master's Thesis, University of Montana. 267 p.
- Dove, P. and J. Rimstidt. 1994. Silica-water interactions. In *Silica, Physical Behavior, Geochemistry and Materials Applications*. Reviews in Mineralogy, v 29, p 259-308.
- Driscoll, F. 1986. *Groundwater and Wells*. Johnson Screens, St. Paul, Minnesota. 1089 p.
- Ehrlich, H. 1996. *Geomicrobiology*, 3<sup>rd</sup> Edition. Marcel Dekker, Inc., New York, 719 p.
- Ellis, A. and W. Mahon. 1977. *Chemistry and Geothermal Systems*. Academic Press, 392 p.
- Emmenegger, L., D. King, L. Sigg, and B. Sulzberger. 1998. Oxidation kinetics of Fe(II) in a eutrophic Swiss Lake. *Environmental Science and Technology*, v 32, p 2990-2996.
- Fournier, R. 1985. The behavior of silica in hydrothermal solutions. In *Geology and Geochemistry of Epithermal Systems: Volume 2*. Reviews in Economic Geology, p 45-61.
- Fournier, R. 1989. Geochemistry and dynamics of the Yellowstone National Park hydrothermal system. *Annual Review of Earth and Planetary Sciences*, v 17, p 13-53.
- Fournier, R. and J. Rowe. 1977. The solubility of amorphous silica in water at high temperatures and high pressures. *American Mineralogist*, v 62, p 1052-1056.
- Fox, L. 1988. Solubility of colloidal ferric hydroxide. *Letters to Nature*, v 333, p 442-444.
- Friedman, I., P. Lipman, J. Obradovich, and J. Gleason. 1974. Meteoric water in magmas. *Science*, v 184, p 1069-1072.
- Fritz, W. 1985. *Roadside Geology of the Yellowstone Country*. Mountain Press Publishing Company, Missoula, Montana, 149 p.
- Gibbs, M. 1979. A simple method for the rapid determination of iron in natural waters. *Water Research*, v 13, no 3, p 295-297.
- Gibson, M. 1999. Hydrothermal water/groundwater interaction: a comparative study of electromagnetic terrain-conductivity mapping and standard hydrogeochemical techniques. Master's Thesis, University of Montana. 153 p.



- Goldschmidt, V. 1954. *Geochemistry*. Oxford at the Clarendon Press, London. 730 p.
- Good, J. and K. Pierce. 1996. Recent and ongoing geology of Grand Teton and Yellowstone National Parks. Grand Teton Natural History Association, Grand Teton National Park, Moose, Wyoming, 58 p.
- Hannington, M., I. Jonasson, P. Herzig, and S. Petersen. 1995. Physical and chemical processes of seafloor mineralization at mid-ocean ridges. In *Seafloor Hydrothermal Systems: Physical, Biological, and Geological Interactions*. S. Humphris, R. Zierenberg, L. Mullineaux, and R. Thomson, Editors. American Geophysical Union, p 115-152.
- Harris, R. 1967. Silica and chloride in interstitial waters of river and lake sediments. *Limnology and Oceanography*, v 12, no 1, p 8-12.
- Healy, J. and M. Hochstein. 1973. Horizontal flow in hydrothermal systems. *Journal of Hydrology (New Zealand)*, v 12, no 2, p 71-82.
- Henley, R., A. Truesdell, P. and Barton, Jr. 1984. Fluid-mineral equilibria in hydrothermal systems. *Reviews in Economic Geology: Society of Economic Geologists*, v 1, 268 p.
- Herdianita, N., P. Browne, K. Rodgers, and K. Campbell. 2000. Mineralogical and textural changes accompanying ageing of silica sinter. *Mineralium Deposita*, v 35, p 48-62.
- Hinman, N. 1998. Sequences of silica phase transitions: effects of Na, Mg, K, Al, and Fe ions. *Marine Geology*, v 147, p 13-24.
- Hinman, N. and B. Lindstrom. 1996. Seasonal changes in silica deposition in hot spring systems. *Chemical Geology*, v 132, p 237-246.
- Hoganson, C. and G. Babcock. 1997. A metalloradical mechanism for the generation of oxygen from water in photosynthesis. *Science*, v 277, p 1953-1956.
- Hydes, D. and E. Chapman. 1986. Methods for the shipboard determination of dissolved iron and manganese in samples of sediment interstitial water. Institute of Oceanographic Sciences, Taunton, United Kingdom. 35 p.
- Iler, R. 1973. Effect of adsorbed alumina on the solubility of amorphous silica in water. *Journal of Colloid and Interface Science*, v 43, no 2, p 399-408.
- Iler, R. 1979. *The Chemistry of Silica*. John Wiley and Sons, New York. 866 p.

- James, A. 1989. Sustained storage and transport of hydraulic gold mining sediment in the Bear River, California. *Annals of the Association of American Geographers*, v 79, no 4, p 570-592.
- Jones, B. and R. Renaut. 1996. Influence of thermophilic bacteria on calcite and silica precipitation in hot springs with water temperatures above 90°C: evidence from Kenya and New Zealand. *Canadian Journal of Earth Sciences*, v 33, p 72-83.
- Jones, B., R. Renaut, and M. Rosen. 1998. Microbial biofacies in hot-spring sinters: a model based on Ohaaki Pool, North Island, New Zealand. *Journal of Sedimentary Research*, v 68, no 3, p 413-434.
- Jones, B. and E. Segnit. 1971. The nature of opal, I. Nomenclature and constituent phases. *Journal of the Geological Society of Australia*, v 18, p 57-68.
- Jorgensen, B., and N. Revsbech. 1983. Photosynthesis and structure of benthic microbial mats: microelectrode and SEM studies of four cyanobacterial communities. *Limnology and Oceanography*, v 28, no 6, p 1075-1093.
- Kastner, M., J. Gieskes, and E. Bromley. 1988. Hydrothermal experiments on silica diagenesis. *Eos, Transactions of the American Geophysical Union*, v 44.
- Kendall, T. 1999. Early diagenesis of thermal spring deposits. Master's Thesis, University of Montana, 176 p.
- Kent, D. 1983. On the surface chemical properties of synthetic and biogenic amorphous silica. PhD Dissertation, University of California, San Diego, 420 p.
- Keenan, J., F. Keyes, P. Hill, and J. Moore. 1969. *Steam Tables*. John Wiley and Sons: New York. 162 p.
- Keith, T. and L. Muffler. 1978. Minerals produced during cooling and hydrothermal alteration of ash flow tuff from Yellowstone Drill Hole Y-5. *Journal of Volcanology and Geothermal Research*, v 3, p 373-402.
- Kinrade, S., J. Del Nin, A. Schach, T. Sloan, K. Wilson, and C. Knight. 1999. Stable five- and six-coordinated silicate anions in aqueous solution. *Science*, v 285, p 1542-1545.
- Konhauser, K. and K. Juniper. 1997. Hydrothermal biomineralization at terrestrial hot springs and deep sea vents. *Abstracts with Programs – Geological Society of America*, v 29, no 6, p 294-295.
- Kramer, J. and H. Allen. 1988. *Metal Speciation: Theory, Analysis and Application*. Lewis Publishers, Chelsea, Michigan. 357 p.

- Krauskopf, K. 1956. Dissolution and precipitation of silica at low temperatures. *Geochimica et Cosmochimica Acta*, v 10, p 1-26.
- Krauskopf, K. 1979. *Introduction to Geochemistry*. McGraw-Hill, Inc.: New York. 617 p.
- Krumbein, W., and D. Werner. 1983. The Microbial Silica Cycle. Chapter 5 in *Microbial Geochemistry*, W. Krumbein, ed. Blackwell Scientific Publications, Oxford, p 125-157.
- Kump, L. 1990. Precambrian shales, iron formations, and the global iron cycle. *Eos*, Annual Meeting, Dallas Texas.
- Kurtz, A. and L. Derry. 1998. Mineral aerosols and the marine silica cycle; constraints from Ge/Si. *Abstracts with Programs – Geological Society of America*, v 30, no 7, p 99.
- Langmuir, D. 1997. *Aqueous Environmental Geochemistry*. Prentice Hall, Upper Saddle River, New Jersey, 600 p.
- Lowell, R., P. Cappellen, and L. Germanovich. 1993. Silica precipitation in fractures and the evolution of permeability in hydrothermal upflow zones. *Science*, v 260, p 192-194.
- Maliva, R., A. Knoll, and R. Siever. 1990. Secular change in chert distribution: a reflection of evolving biological participation in the silica cycle. *Research Reports, Society for Sedimentary Geology*, p 519-532.
- Marshall, C and R. Fairbridge, Editors. 1999. Iron. (M. Williamson, author). In *Encyclopedia of Geochemistry*, Kluwer Academic Publishers: Dordrecht, Netherlands. P 348-353.
- Marshall, C and R. Fairbridge, Editors. 1999. Silicon, Silica. (N. Hinman, author). In *Encyclopedia of Geochemistry*, Kluwer Academic Publishers: Dordrecht, Netherlands. P 572-575.
- McKay, C. and H. Hartman. 1991. Hydrogen peroxide and the evolution of oxygenic photosynthesis. *Origins of Life and Evolution of the Biosphere*, v 21, p 157-163.
- Moore, D. and R. Reynolds. 1997. *X-ray diffraction and the identification and analysis of clay minerals*. Oxford University Press, New York: 378 p.
- Morey, G., R. Fournier, and J. Rowe. 1964. The solubility of amorphous silica at 25°C. *Journal of Geophysical Research*, v 69, no 10, p 1995-2002.

- Mottana, A., R. Crespi, and G. Liborio. Guide to Rocks and Minerals. Simon and Schuster, Inc.: New York. 607 p.
- Mowers, T. and D. Budd. 1996. Quantification of porosity and permeability reduction due to calcite cementation using computer-assisted petrographic image analysis techniques. AAPG Bulletin, v 80, no 3, p 309-322.
- Muffler, L. D. White, A. Truesdell, and R. Fournier. 1982. Geologic map of Lower Geyser Basin, Yellowstone National Park, Wyoming. Map, 1:24,000.
- Nealson, K. 1983. The Microbial Iron Cycle. Chapter 6 in Microbial Geochemistry, W. Krumbein, ed. Blackwell Scientific Publications, Oxford, p 159-190.
- Nelson, Y., W. Lo, L. Lion, M. Shuler, and W. Ghiorse. 1995. Lead distribution in a simulated aquatic environment: effects of bacterial biofilms and iron oxide. Water Research, v 29, no 8, p 1934-1944.
- Noffke, N., G. Gerdes, T. Klenke, and W. Krumbein. 2001. Microbially induced sedimentary structures – a new category within the classification of primary sedimentary structures. Journal of Sedimentary Research, v 71, no 5, p 649-656.
- Oehler, J. and J. Schopf. 1971. Artificial microfossils: experimental studies of permineralization of blue-green algae in silica. Science, v 174, p 1229-1231.
- Pentecost, A. 1996. High temperature ecosystems and their chemical interactions with their environment. In Evolution of Hydrothermal Ecosystems on Earth (and Mars?). Wiley, Chichester (Ciba Foundation Symposium 202), p 99-111.
- Phoenix, V. and K. Konhauser. 1999. Rates and processes of cyanobacterial silicate mineralisation. Abstracts with Programs – Geological Society of America, v 31, no 7, p 392-393.
- Prescott, G. 1977. The Diatoms. Coward, McGann & Geoghegan, Inc., New York, 47 p.
- Rantz, S. 1982. Measurement and Computation of Streamflow: Volume 1. Measurement of Stage and Discharge. US Geological Survey WSP 2175. 284 p.
- Rimstidt, J. 1997. Quartz solubility at low temperatures. Geochimica et Cosmochimica Acta, v 61, no 13, p 2553-2558.
- Rimstidt, J. and D. Cole. 1983. Geothermal mineralization I: the mechanism of formation of the Beowawe, Nevada, siliceous sinter deposit. American Journal of Science, v 283, p 861-875.

- Rinehart, J. 1972. Fluctuations in geyser activity caused by variations in Earth tidal forces, barometric pressure, and tectonic stresses. *Journal of Geophysical Research*, v 77, no 2, p 342-350.
- Robinson, E. and R. Bell. 1971. Tides in confined well-aquifer systems. *Journal of Geophysical Research*, v 76, no 8, p 1857-1869.
- Robinson, T. 1939. Earth-tides shown by fluctuations of water-levels in wells in New Mexico and Iowa. *Transactions of the American Geophysical Union*, v 20, p 656-666.
- Siever, R. 1957. The silica budget in the sedimentary cycle. *The American Mineralogist*, v 42, p 821-841.
- Simonson, B. 1987. Early silica cementation and subsequent diagenesis in arenites from four early Proterozoic iron formations of North America. *Journal of Sedimentary Petrology*, v 57, no 3, p 494-511.
- Smith, R. and A. Martell. 1976. *Critical Stability Constants; Volume 4: Inorganic Complexes*. Plenum Press, New York, 257 p.
- Snoeyink, V. and D. Jenkins. 1980. *Water Chemistry*. John Wiley and Sons, New York, 463 p.
- Stanford, J., and J. Ward. 1993. An ecosystem perspective of alluvial rivers: connectivity and the hyporheic corridor. *Journal of the North American Benthological Society*, v 12, no 1, p 48-60.
- Stauffer, R., E. Jenne, and J. Ball. 1980. Chemical studies of selected trace elements in hot-spring drainages of Yellowstone National Park. US Geological Survey Professional Paper 1044-F, 20 p.
- Sung, W. and J. Morgan. 1980. Kinetics and product of ferrous iron oxygenation in aqueous systems. *Environmental Science and Technology*, v 14, no 5, p 561-568.
- Taillefert, M. and J. Gaillard. 2001. Reactive transport modeling of trace elements in the water column of a stratified lake: iron cycling and metal scavenging. *Journal of Hydrology*, v 256, p 16-34.
- Takahashi, K. 1988. Opal flux dynamics and partition for silica cycle. *Eos, Transactions of the American Geophysical Union*, v 44.
- Tamura, H., K. Goto, and M. Nagayama. 1976. The effect of ferric hydroxide on the oxygenation of ferrous ions in neutral solutions. *Corrosion Science*, v 16, p 197-207.

- Von Gunten, H., G. Karametaxas, U. Krahenbuhl, M. Kuslys, R. Geovanoli, E. Hoehn, and R. Keil. 1991. Seasonal biogeochemical cycles in riverborne groundwater. *Geochimica et Cosmochimica Acta*, v 55, p 3597-3609.
- Waite, T., R. Szymczak, Q. Espey, and M. Furnas. 1995. Diel variations in iron speciation in northern Australian shelf waters. *Marine Chemistry*, v 50, no 1-4, p 79-91.
- Walter, M. 1976. Geyserites of Yellowstone National Park: an example of abiogenic "stromatolites". In *Stromatolites*, Elsevier Scientific Publishing Company: Amsterdam, p 87-112.
- Walter, M., J. Bauld, and T. Brock. 1972. Siliceous algal and bacterial stromatolites in hot springs and geyser effluents of Yellowstone National Park. *Science*, v 178, p 402-405.
- Webster's Ninth New Collegiate Dictionary. 1990. Merriam-Webster, Inc. Springfield, Massachusetts. 1564 p.
- Wedepohl, K. 1969. *Handbook of Geochemistry: V II/I*. Springer-Verlag, Berlin, p 26, A-1 to A-14.
- White, D., W. Brannock, and K. Murata. 1956. Silica in hot-spring waters. *Geochimica et Cosmochimica Acta*, v 10, p 27-59.
- White, D. and G. Marler. 1972. Comments on paper by John S. Rinehart, 'fluctuations in geyser activity caused by variations in earth tidal forces, barometric pressure, and tectonic stresses'. *Journal of Geophysical Research*, v 77, no 29, p 5825-5829.
- White, D., R. Fournier, L. Muffler, and A. Truesdell. 1975. Physical results of research drilling in thermal areas of Yellowstone National Park, Wyoming. US Geological Survey Professional Paper 892, 70 p.
- White, D., R. Hutchinson, and T. Keith. 1988. The geology and remarkable thermal activity of Norris Geyser Basin, Yellowstone National Park, Wyoming. US Geological Survey Professional Paper 1456, 84 p.
- Wiegart, R. and P. Fraleigh. 1972. Ecology of Yellowstone thermal effluent systems: net primary production and species diversity of a successional blue-green algal mat. *Limnology and Oceanography*, v 17, no 2, p 215-228.
- Williams, L., G. Parks, and D. Crerar. 1985. Silica diagenesis, I. Solubility controls. *Journal of Sedimentary Petrology*, v 55, no 3, p 301-311.

- Williams, L. and D. Crerar. 1985. Silica diagenesis, II. General mechanisms. *Journal of Sedimentary Petrology*, v 55, no 3, p 312-321.
- Williamson, M. 1999. Iron. In *Encyclopedia of Geochemistry*, C. Marshall and R. Fairbridge, Editors. Kluwer Academic Publishers: Dordrecht, Netherlands. P 348-353.
- Woessner, W. 2000. Stream and fluvial plain ground water interactions; rescaling hydrogeologic thought. *Groundwater*, v 38, p 423-429.
- Yellowstone Center for Resources. 2001. Spatial Analysis Center Geographic Information System Database. National Park Service: Yellowstone National Park, Wyoming.
- Yellowstone Center for Resources. Thermophilic Microorganisms Survey, Yellowstone National Park, Wyoming. 26 p.
- Zhang, J. and G. Nancollas. 1990. Mechanisms of growth and dissolution of sparingly soluble salts. *Reviews in Mineralogy*, v 23, p 365-396.

## Glossary

<b>amorphous</b> <sup>1</sup>	Literally, without form; applied to rocks and minerals having no definite crystalline structure.
<b>colloid</b> <sup>1</sup>	A particle-size range of less than $2.4 \times 10^{-5}$ mm, i.e. smaller than clay size. Any extremely fine-grained material in suspension, or that can be easily suspended, commonly having peculiar properties because of its very high surface area.
<b>crystalite</b> <sup>1</sup>	A mineral: $\text{SiO}_2$ . It is a high-temperature polymorph of quartz and tridymite, and occurs as white octahedrons in acidic volcanic rocks. Cristobalite is stable only above $1,470^\circ\text{C}$ .
<b>eukaryote</b> <sup>2</sup>	An organism whose cells have a distinct nucleus enveloped by a double membrane, and other features including double-membraned mitochondria and 80S ribosomes in the fluid of the cytoplasm (i.e. all protists, fungi, plants, and animals). The first eukaryotes were almost certainly green algae (Chlorophyceae) and what appear to be their microscopic remains appear in Precambrian sediments dating from a little less than 1,500 million years ago.
<b>free energy</b> <sup>1</sup>	The capacity of a system to perform work, a change in free energy being measured by the maximum work obtainable from a given process. ( <i>Gibbs Free Energy</i> )
<b>iron</b> <sup>6</sup>	$\text{Fe}^0$ (elemental iron), $\text{Fe}^{2+}$ (ferrous iron), and $\text{Fe}^{3+}$ (ferric iron).
<b>monomer</b> <sup>4</sup>	A chemical compound that can undergo polymerization.
<b>opal-A</b>	Amorphous silica.
<b>opal-CT</b> <sup>3</sup>	Cristobalite and tridymite intergrowths.
<b>polymerization</b> <sup>4</sup>	A chemical reaction in which two or more small molecules combine to form larger molecules that contain repeating structural units of the original molecules. <i>Polymer is the resulting compound.</i>
<b>polymorphism</b> <sup>1</sup>	The characteristic of a chemical substance to crystallize in more than one form.



- quartz**<sup>1</sup> Crystalline silica, an important rock-forming mineral, SiO<sub>2</sub>. It is, next to feldspar, the commonest mineral, occurring either in transparent, hexagonal crystals or in crystalline or cryptocrystalline masses. Quartz is the commonest gangue mineral of ore deposits, forms the major proportion of most sands, and has a widespread distribution in igneous (esp. granitic), metamorphic, and sedimentary rocks. It has a vitreous to greasy luster, a conchoidal fracture, an absence of cleavage and a hardness of 7 on the Mohs scale.
- reaction affinity**<sup>5</sup> The equilibrium state defined by the change in Gibb's Free energy.
- silica**<sup>1</sup> Silicon dioxide, SiO<sub>2</sub>. It occurs as crystalline quartz, cryptocrystalline chalcedony, and amorphous opal; dominantly in sand, diatomite, and chert; and combined in silicates as an essential constituent of many minerals.
- silicate**<sup>1</sup> A compound whose crystal structure contains SiO<sub>4</sub> tetrahedra, either isolated or joined through one or more of the oxygen atoms to form groups, chains, sheets, or three-dimensional structures with metallic elements. Silicates are classified according to crystal structure.
- siliceous sinter**<sup>1</sup> The lightweight porous opaline variety of silica, white or nearly white, deposited as an incrustation by precipitation from the waters of geysers and hot springs.
- tridymite**<sup>1</sup> A mineral, SiO<sub>2</sub>. It is a high-temperature polymorph of quartz, and usually occurs as minute tabular white or colorless crystals or scales, in cavities in acidic volcanic rocks. Tridymite is stable between 870°C and 1,470°C.

*Complete or partial definitions quoted or paraphrased from the following references:*

- <sup>1</sup> Bates and Jackson, 1984.
- <sup>2</sup> Allaby, 1994.
- <sup>3</sup> Marshall and Fairbridge, 1999.
- <sup>4</sup> Webster's Ninth New Collegiate Dictionary. 1990.
- <sup>5</sup> Langmuir, 1997.
- <sup>6</sup> Williamson, 1999.

**Appendix A: An extensive review of silica and iron geochemistry.**

A discussion of silica and iron geochemistry follows since these analytes were important in this study. Silica is a major constituent in many hot spring waters and iron is an important component in most natural systems. The creek channel mineral deposits are composed mostly of silica and so an extensive review follows, beyond what was stated in the introduction, to make clear the importance and extensive work done on silica and how it pertains to this study.

## Silica

### Global silica cycle

Chemical and biological weathering of silicate minerals is the major global source of aqueous silica. Silicate rocks are chemically and physically weathered in the oceans, rivers, subsurface waters, and in hot springs (Figure A1). Silica concentrations in surface waters are usually only a few mg/L but silica concentrations may be higher than 50 mg/L in some groundwaters depending on water-rock interactions and residence time.

Hot springs and diatoms provide the greatest amount of amorphous silica in aqueous solutions (Siever, 1957, Maliva, 1990). Silica in aerosol dust is only a small part of the silica cycle (Kurtz and Derry, 1998). Many hot springs are supersaturated with respect to silica, and so inorganic precipitation is common.

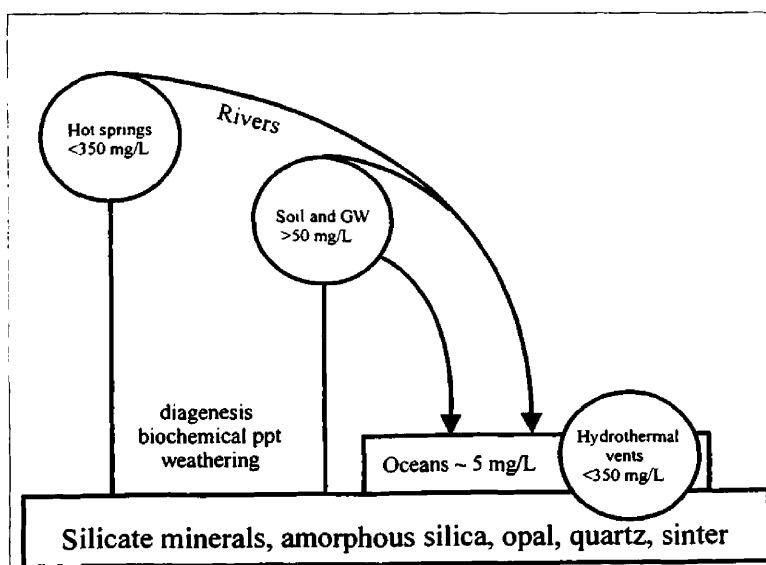


**Figure A1:** A simplified global silica cycle with approximate concentrations in major sinks (excluding the aerosol component).

## Diagenesis

There are several diagenetic forms of SiO<sub>2</sub> minerals. Amorphous silica requires the least amount of energy to form. Quartz is the last diagenetic form of SiO<sub>2</sub>, is the most stable, and takes longest to form. Quartz takes an extremely long time to precipitate out of solution. There are several crystalline forms in between amorphous silica and quartz. The diagenetic sequence does not necessarily pass through all diagenetic forms on the way to quartz. There is a hierarchy of forms although some may be skipped due to temperature, pressure, and chemical factors that alter the mineralogical sequence. Possible SiO<sub>2</sub> minerals include amorphous silica (opal-A), which recrystallizes to opal-CT (cristobalite or tridymite), which recrystallizes again to chalcedony or quartz ( $\alpha$  or  $\beta$  quartz, depending on temperature and pressure) (Kastner et al., 1988, Williams et al., 1985, Iler, 1979, Jones and Segnit, 1971, Krauskopf, 1956).

Opal exists at low temperatures (usually below boiling) with fast rates of precipitation. Silica polymers may go through a growth period, Ostwald Ripening, where many small polymers nucleate into fewer large silica particles (Chang and Yortsos, 1994, Rimstidt and Cole, 1983). Spherical silica particles rapidly grow in size on the time scale of hours (Williams and Crerar, 1985) where smaller particles are replaced by larger particles (Chang and Yortsos, 1994, Crerar et al., 1981). Bladed particles then replace amorphous spheres of opal-A (Herdianita et al., 2000, Chang and Yortsos, 1994).

Opal is usually powdery, although it may become hard if periodically submerged. Submerged opal usually forms hard rock (White et al., 1956) where porosity is between 35% and 60%. Opal-A is amorphous silica and may contain “seed” crystals that are the beginning phase of opal-CT (Williams et al., 1985). Opal-CT has a crystal pattern of cristobalite or tridymite, as analyzed by x-ray diffraction (Figure A2) (Fournier, 1985, Williams et al., 1985, White et al., 1956). The formation of opal-CT is enhanced by magnesium (Hinman, 1997, Kastner et al., 1988) and alkalinity (Kastner et al., 1988). Opal-C, an undeveloped form of opal-CT, may be present for short time periods (Herdianita et al., 2000).

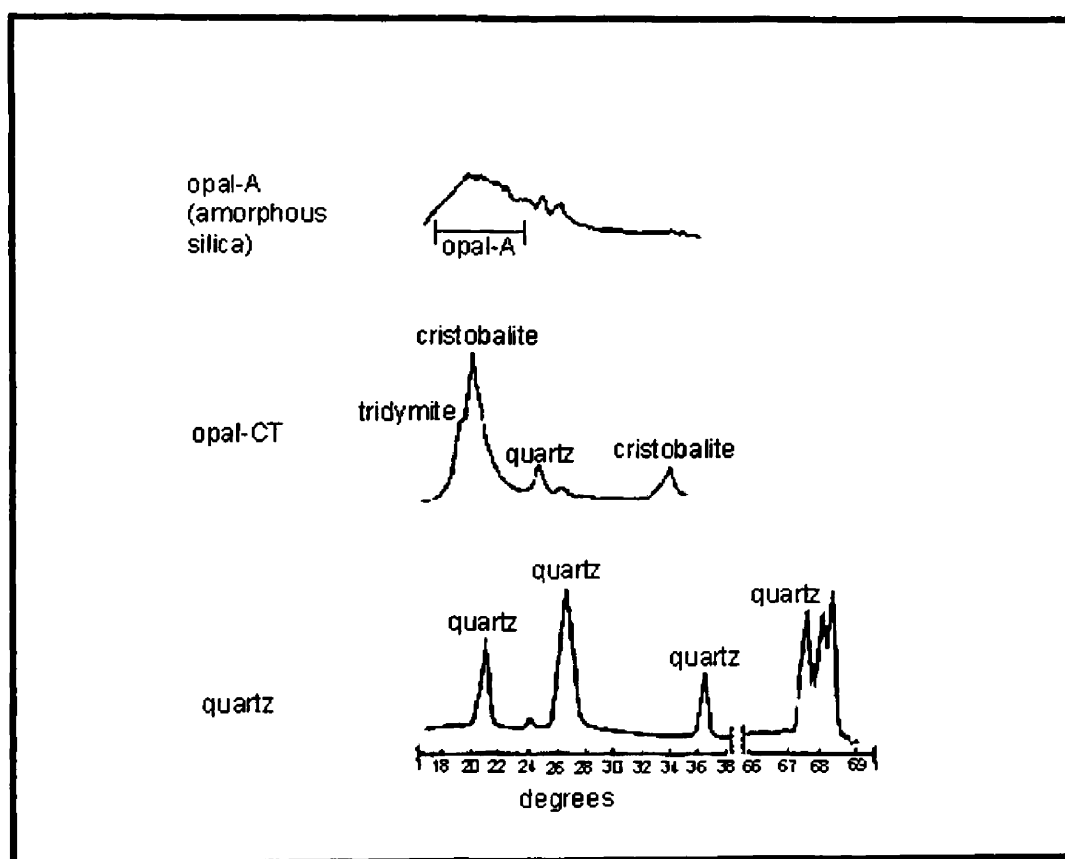


**Figure A2:** X-ray diffraction peaks of opal-A, opal-CT, and quartz. The amorphous opal-A has no defined peak. The opal-CT pattern can vary depending on the minerals present. The quartz peak is unmistakable since four peaks are common. It can have up to 22 separate peaks in a mature crystalline sample. The x-axis is degrees  $2\theta$ , using  $\text{CuK}\alpha$  x-rays. (Williams et al., 1985).

Chalcedony is rare in sinter deposits. It forms when silica supersaturation is high and precipitation rates are rapid. Chalcedony may precipitate out of solution without going through an amorphous stage (Fournier, 1985).

Opal-CT dissolution is slow and thus produces a low concentration of silica. This allows microcrystalline quartz crystals to grow slowly in solution (Williams et al, 1985). At high temperatures, coarse quartz grains will result if precipitated directly as amorphous silica (Fournier, 1985). All other forms of silica below 573 °C should eventually alter to a stable  $\alpha$ -quartz.  $\beta$ -quartz is stable from 573 °C to 870 °C (Langmuir, 1997, White et al., 1956).

### **Precipitation**

Temperature, pH, and reaction affinity are the primary controlling factors in silica precipitation. Amorphous silica precipitation rate increases as temperature decreases (Iler, 1979). Silica precipitates out of solution below pH 10 and precipitation kinetics increase as pH decreases. (Carroll et al., 1998). The size of silica particles and reactions with hydroxides, particularly ferric hydroxides, catalyze silica precipitation (Rimstidt and Cole, 1983).

Two main steps for silica precipitation are coagulation and nucleation (Rimstidt and Cole, 1983, Iler 1979). Silica colloids grow and coagulate or flocculate out of solution (Fournier, 1985). Nucleation involves the formation of particles by the polymerization of

$\text{Si(OH)}_4$ . Once nucleation takes place, precipitates are in the suspended load and will eventually settle out and deposit on substrates.

### **Deposition**

Substrate is a strong control on deposition (Carroll et al., 1998) and deposition is dependent on the substrate surface area. Substrates may be biological (Akahane et al., 1997). For example, cyanobacteria mats, held together by mucous, trap water where silica subsequently settles out of suspension. If a solution is only slightly oversaturated with silica and polymerization does not take place, precipitates may only deposit on substrates previously deposited with silica (Herdianita et al., 2000). Silica substrates are negatively charged above pH 2 (Iler, 1979). The negatively charged surface site attracts cations and positively charged silica complexes. Ferric (Rimstidt and Cole, 1983) and magnesium (Change and Yortsos, 1994) hydroxides adsorb onto silica substrates at pH<9 (Kent, 1983).

### **Biological Factors**

Microbes fix silica and subsequently release it to the environment (Kinrade et al., 1999, Siever, 1957). Diatoms are the most abundant organisms that fix silica (Prescott, 1977, Siever, 1990). Radiolarians are responsible for about 25 % of silica fixation (Ehrlich, 1996, Takahashi, 1988). Silica polymerization is enhanced by the presence of bacteria (Konhauser and Juniper (1997, White et al., 1956).

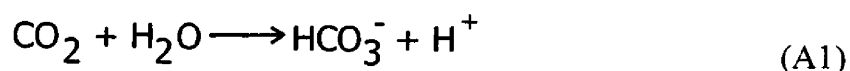
Thermophilic organisms live between 30° and 70° C (Pentecost, 1996, Walter et al., 1972, White et al., 1956). Fewer species of thermophilic bacteria exist above 70° C (Jones and Renault, 1996). These organisms are mostly phototrophic and chemotrophic bacteria and archaea of the Prokaryote Kingdom. The populations make up microbial mats where phototrophs exist in the upper section of the mat and heterotrophs exist at depth. Photosynthetic bacteria and cyanobacteria dominate in hot spring outflow channels.

Organisms produce mucous that aids in stabilizing microbial mats and also causes particulates to become easily trapped (Jones and Renault, 1996). Thicknesses of mats vary but is generally a few millimeters to several centimeters thick. Thickness is limited by water depth (Pentecost, 1996, Walter et al., 1972, Wiegart and Fraleigh, 1972). Thus, mineralized microbial mats are relatively thin layers in the geologic record.

Biodiversity is low within single outflow channels (Pentecost, 1996, Cady et al., 1997). Biodiversity increases as distance from the source increases. This is mainly due to hydrological factors like flow velocity and depth (Wiegart and Fraleigh, 1972). There are species variations between different channels. These variations are controlled by temperature, dissolved oxygen, chemistry, hydrology, and geographic location (Wiegart and Fraleigh, 1972, Pentecost, 1996). Various species of organisms have different effects on the rate of silica fixation. Particular microbes, like cyanobacteria, are important substrates for silica deposition where silica becomes trapped in the cyanobacteria mucous and settles out of suspension.



Most species of (thermophilic) bacteria conduct photosynthesis using water with a byproduct of oxygen (Hoganson and Babcock, 1997, McKay and Hartman, 1991, Jorgensen et al., 1983. Some cyanobacterial chemosynthesis conducted at temperatures greater than 73°C may not release oxygen (Walter, 1976, Walter et al., 1972). With the presence of high concentrations of dissolved CO<sub>2</sub> and certain species of cyanobacteria, the water in hydrated silica (SiO<sub>2</sub> • nH<sub>2</sub>O) will react with the CO<sub>2</sub>:



Cyanobacteria mediates this reaction that promotes silica precipitation (Pentecost, 1996).

Silica can be brought up to the surface of microbial mats in outflow channels by capillary action. Water level fluctuations induce desiccation that results in microbial mat silicification (Hinman and Lindstrom, 1996). Silicification is aided by the presence of ferric iron (Phoenix and Konhauser, 1999). Autotrophs then oxidize any reduced iron in the aqueous system forming auxiliary minerals like Fe<sub>2</sub>O<sub>3</sub> (ferrihydrite, hematite, or maghemite). Silica depositing on mats will cause mortality to the organisms and will eventually take over the mat by excessive precipitation (Pentecost, 1996). Silica is deposited on mat surfaces, between cyanobacterial cells, and within previously deposited silica spheres (Krumbein and Werner, 1983). Eventually, silica will replace all organic matter. This silicification may or may not preserve an organism's structure (Jones and Renault, 1996). The potential for the identification of microbial structures in sinter

decreases as deposits age. Diagenesis progresses, as sinter ages, until quartz crystals are the only observable structures (Krumbein and Werner, 1983).

Fabric bedforms in subaerial laminated sinter deposits are usually a result of microbial mats that functioned as substrates (Herdianita et al., 2000, Cady et al., 1997) although sinter may form abiogenically (Walter, 1976). Microbes provide an initial site for silica nucleation and so control the initial fabric laminations (Jones et al., 1998). After decomposition of the microbial mats, the resulting sinter is porous (Walter and Des Marais, 1993). Other laminated fabrics systematically include plants, woody debris, and filamentous microbes (Herdianita et al., 2000, Walter and Des Marais, 1993). Microbial mats mainly affect the micro-structure of the laminations; the macro-structure is controlled mainly by the hydrochemical factors of deposition and diagenesis (Braunstein and Lowe, 2001).

### **Solubility and kinetics**

Solubility, pH, temperature, and the initial form of silica are the controlling factors on silica concentration (Rimstidt, 1997, Fournier, 1985). These factors have little effect over a time scale of hours or even days.

Temperature affects on silica solubility have been studied in great detail (Carroll et al., 1998, Rimstidt, 1997, Rimstidt and Barnes, 1980, Fournier, 1977, Krauskopf, 1956, White et al., 1956, Alexander et al., 1954). Temperature has a direct affect on silica

concentration and is usually the main control on silica solubility (Figures A3 and A4) (Williams et al, 1985). See table A1 below for calculated silica concentrations at low temperature. Silica solubility is related to temperature (from Langmuir, 1997, p. 243):

$$\log K_{sp} = -0.26 - [731 / T(K)] \quad (A2)$$

Silica transport in hydrothermal systems is dependent on quartz solubility (Rimstidt, 1997). Amorphous silica is the most soluble form of SiO<sub>2</sub> and therefore usually

**Table A1:** Calculated silica solubility concentrations at low temperatures (from Langmuir, 1997).

Temp (°C)	SiO <sub>2</sub> (aq) (mg/L)
0	67
25	116
50	183
100	372

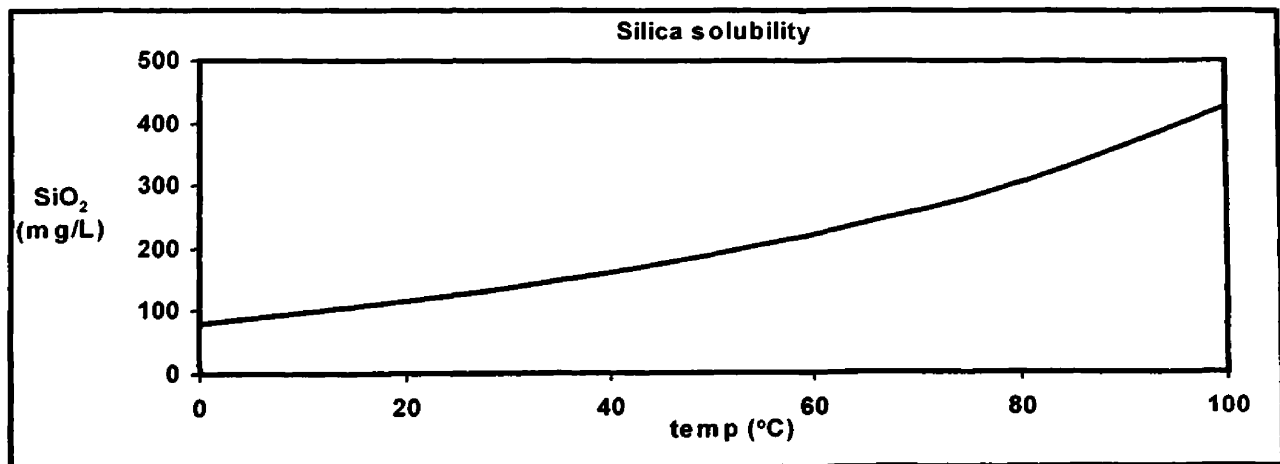


**Figure A3:** Silica solubility versus temperature creates an asymptotic curve up to 100°C. (Modified from Rimstidt and Cole, , and Alexander et al., 1954).

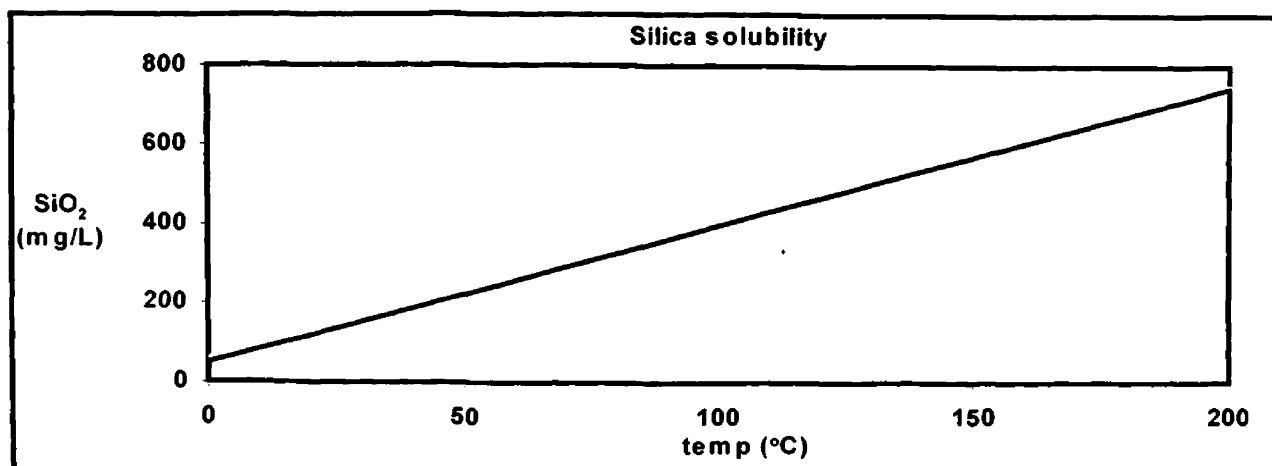


**Figure A4:** Silica solubility versus temperature creates a more linear curve when the temperature scale is increased to 200°C. Plot area is 320% of Figure 2. (Modified from Rimstidt and Cole, 1983, and Alexander et al., 1954).

precipitates out of solution first (Fournier, 1985). Normally, amorphous silica alters to quartz at around 200 °C in hydrothermal environments after going through a cristobalite phase (Langmuir, 1997, Fournier, 1985).

Silica solubility is governed by the following reaction below pH 9 (from Langmuir, 1997, Krumbein and Werner, 1983, Iler, 1979, Morey et al., 1964, and Siever, 1957):



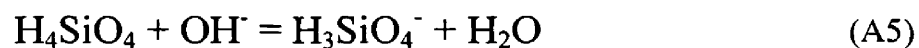
This reaction is completely reversible (Carroll et al., 1998) where precipitation moves to the left and dissolution moves to the right. The solubility constant for silica is  $10^{-3.64}$  at 25°C (Smith and Martell, 1976 and Siever, 1957).

Particle size of amorphous solids affects the solubility (Zhang and Nancollas, 1990, Williams et al., 1985, Krauskopf, 1956). Polymerization is rapid in alkaline waters

(White et al., 1956, Carrol et al., 1998). Polymerization rate becomes faster as initial supersaturation increases (Krauskopf, 1956). The equilibrium equation for silica in solution at 25 °C is (Langmuir, 1997):

$$K = 9.82 = \frac{\{H_4SiO_4^{\circ}\}}{\{H^+\} \{H_3SiO_4^-\}} \quad (A4)$$

Silica becomes more soluble as pH increases above 9 (Krumbein and Werner, 1983, Alexander et al., 1954). Silicic acid dissociates into monomeric silica at a pH value slightly lower than 10:



Solubility changes little when the pH is higher than 10 (Siever, 1957).

Even though silica has been thoroughly studied during the past half century, there are still details that are not fully understood; ie interactions with other elements like aluminum and iron, microbial mediation, etc. Silica studied in the field can never be fully duplicated in the laboratory and so new field rates and constants will continually be added to the literature.

## Iron

### Oxidation

Iron is one of the most abundant and reactive elements on earth and its transport and deposition depends on redox states. There are two main states of iron occurring in nature:  $\text{Fe}^{2+}$  (reduced ferrous), and  $\text{Fe}^{3+}$  (oxidized ferric). Ferrous iron is present in anoxic water systems and may also be present even when there are measureable dissolved oxygen concentrations. Ferric iron occurs mostly in surface water. Iron oxidation is primarily dependent on the oxygen concentration and pH of solution (Taillefert and Gaillard, 2001, Emmenegger et al., 1998, Langmuir, 1997, Sung and Morgan, 1980) but can also be microbially mediated (Marshall and Fairbridge, 1999).

Iron behavior in aqueous systems can be generalized to distinguish between reduced and oxidized iron species. Oxidizing conditions promote iron precipitation and reducing conditions promote soluble iron. Acidic conditions promote soluble iron and alkaline conditions promote iron precipitation (Figure A5) (Marshall and Fairbridge, 1999). In the literature, iron solubility data ranges over three orders of magnitude in natural environments (Fox, 1988) and the kinetics of iron oxidation is not fully understood in the field (Davison and Seed, 1983). Thus, various iron species may be present over a wide range of pH and dissolved oxygen concentrations. For example, ferrous iron can dominate in oxidized conditions when the Eh value is low (Cox, 1978). Carbonate

alkalinity has a significant affect on iron redox products by forming iron hydroxide complexes (Krauskopf, 1979).

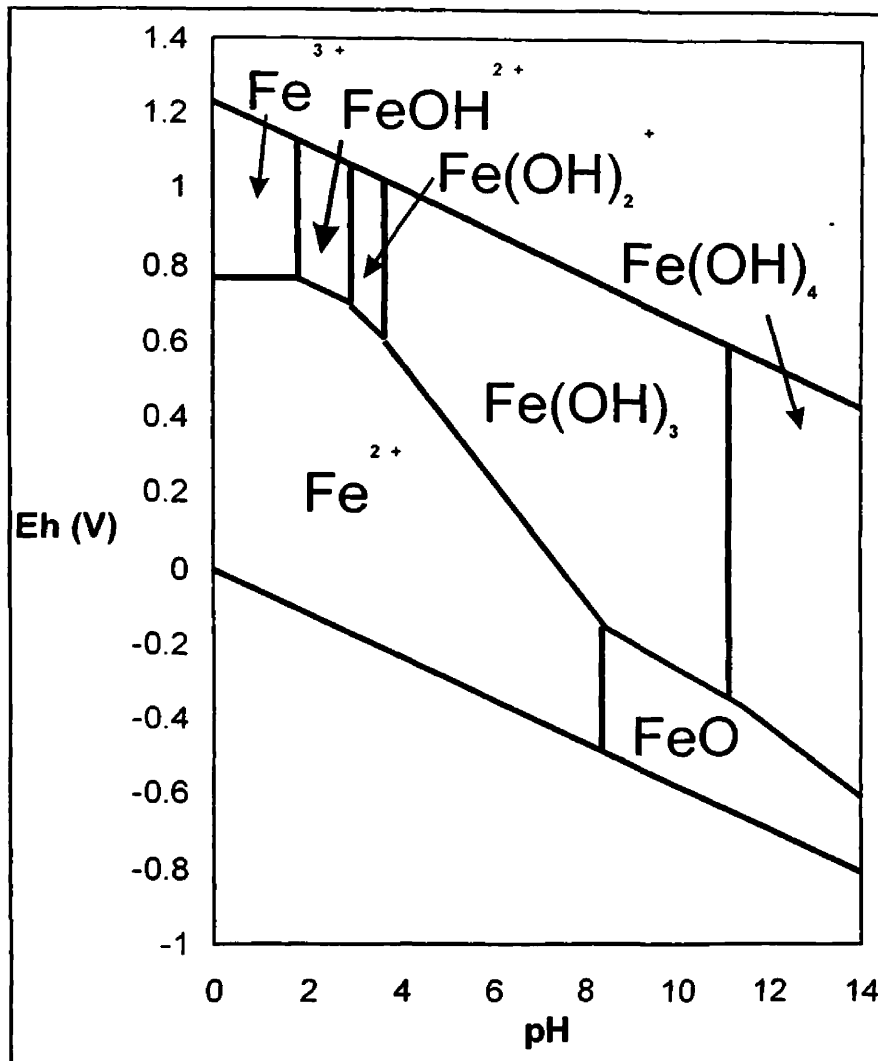


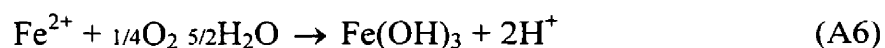
**Figure A5:** Eh-pH diagram of iron. Ferrous iron is present in acidic, reducing conditions and ferric iron dominates in alkaline, oxidized conditions. There is a wide range of Eh and pH values where each species can be present. This diagram is at standard pressure and 25°C.

At alkaline pH, iron oxidation is rapid but is limited by the availability of oxygen in the gas phase (Snoeyink and Jenkins, 1980). Therefore, oxidation in surface water should reach equilibrium quicker than in groundwater since the surface water is in direct contact with the atmosphere. Groundwater ferrous iron concentrations are normally several mg/L

higher than in surface water since groundwater can be slightly reduced (Marshall and Fairbridge, 1999). Ferrous iron in a soil zone that is waterlogged can be transported to shallow groundwater causing elevated iron concentrations (Goldschmidt, 1954).

Colloidal oxides, transported from groundwater or anaerobic portions of surface water, may travel long distances in rivers before suspension settle out occurs (Krauskopf, 1979).

Iron oxides normally precipitate as amorphous ferrihydrite,  $\text{Fe}(\text{OH})_3$  (Figure A6) (Langmuir, 1997).  $\text{Fe}_2\text{O}_3$  is a common crystalline oxide that can be hematite or maghemite (Wedepohl, 1969). Iron complexes may form but that depends on other species present and the ionic strength of the solution. Quartz usually only has trace amounts of ferric iron. Certain anions, like  $\text{SO}_4^{2-}$  and  $\text{Cl}^-$ , retard iron oxidation (Nealson, 1983) that may be important in hydrothermal environments. Iron oxidation occurs by the following reaction in standard atmospheric conditions where oxygen limits the reaction rate (from Langmuir, 1997):



### **Biological Factors**

Microorganisms, particularly cyanobacteria and heterotrophs, are important in iron cycling (Taillefert and Gaillard, 2002, Bridge and Johnson, 1998, Emmenegger et al., 1998, Hannington et al., 1995, Kramer and Allen, 1988). These organisms use iron as an energy source and can oxidize or reduce iron. Iron is taken up or oxidized as a result of microbial processes in reducing conditions (Nealson, 1983). In systems with an



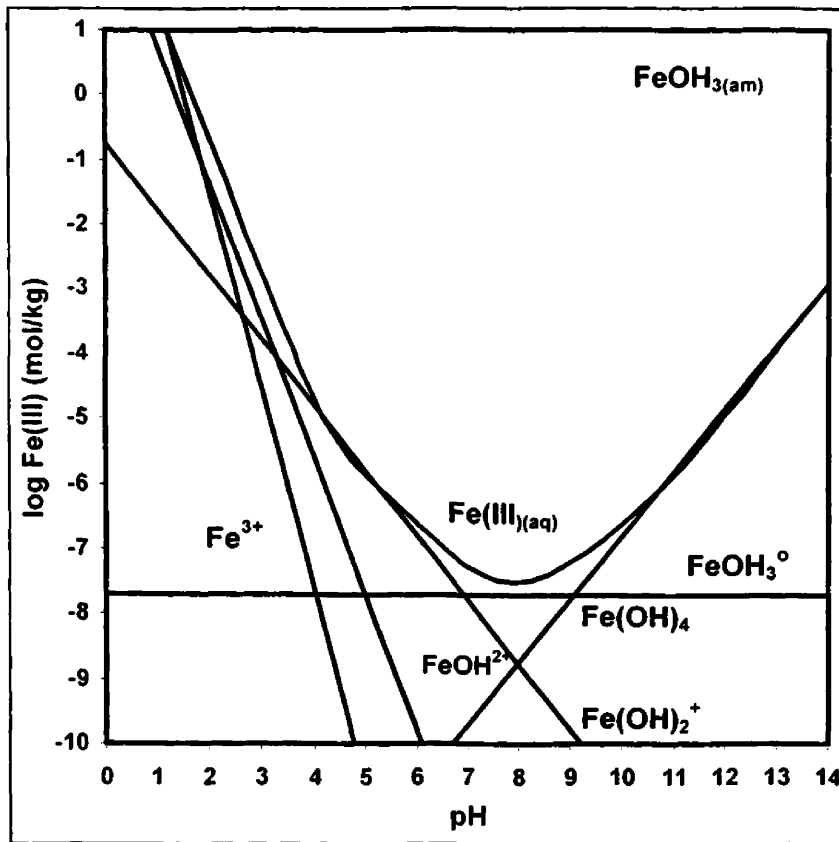


**Figure A6:** Iron speciation diagram. Iron is in solid form above neutral pH. Iron may be soluble if pH is near neutral.

abundance of organic material, reducing conditions often result and oxidized iron reduces to soluble form (Marshall and Fairbridge, 1999).

## Appendix B: Measured hydrological data.

The following data was collected at 15 minute intervals by the Flo-Dar flow meter. Measured surface water velocity was multiplied by a 0.85 coefficient to account for a representative flow velocity. Then the representative flow velocity was multiplied by the cross sectional area in the creek to derive discharge in m<sup>3</sup>/sec.

Date and Time	measured Vel (fps)	calculated m3/sec
08/19/2001 4:59 PM	3.72	9982.763736
08/19/2001 5:14 PM	2.87	12940.42662
08/19/2001 5:29 PM	3.66	10145.12464
08/19/2001 5:44 PM	3.41	10889.89065
08/19/2001 5:59 PM	2.93	12670.84507
08/19/2001 6:14 PM	3.79	9797.837034
08/19/2001 6:29 PM	3.66	10145.13602
08/19/2001 6:44 PM	3.76	9873.394078
08/19/2001 6:59 PM	3.64	10200.44018
08/19/2001 7:14 PM	2.65	14013.85752
08/19/2001 7:29 PM	3.76	9873.40239
08/19/2001 7:44 PM	3.86	9619.640299
08/19/2001 7:59 PM	3.82	9719.567376
08/19/2001 8:14 PM	3.81	9746.828513
08/19/2001 8:29 PM	3.70	10036.34109
08/19/2001 8:44 PM	3.90	9521.760321
08/19/2001 8:59 PM	3.79	9797.867276
08/19/2001 9:14 PM	3.88	9570.460769
08/19/2001 9:29 PM	3.76	9873.424554
08/19/2001 9:44 PM	3.71	10007.45575
08/19/2001 9:59 PM	3.91	9495.757905
08/19/2001 10:14 PM	3.21	11568.30175
08/19/2001 10:29 PM	3.79	9797.883772
08/19/2001 10:44 PM	3.80	9770.342262
08/19/2001 10:59 PM	2.81	13214.6437
08/19/2001 11:14 PM	3.85	9642.55485
08/19/2001 11:29 PM	3.82	9719.605558
08/19/2001 11:44 PM	3.79	9797.897519
08/19/2001 11:59 PM	3.80	9770.35597
08/20/2001 12:14 AM	3.81	9746.872272
08/20/2001 12:29 AM	3.63	10230.52986
08/20/2001 12:44 AM	3.90	9521.80307
08/20/2001 12:59 AM	3.75	9901.592866
08/20/2001 1:14 AM	3.95	9400.394319
08/20/2001 1:29 AM	2.72	13652.20389
08/20/2001 1:44 AM	3.81	9746.888682
08/20/2001 1:59 AM	3.81	9746.891417
08/20/2001 2:14 AM	3.81	9746.894152
08/20/2001 2:29 AM	3.89	9544.234849
08/20/2001 2:44 AM	3.91	9495.808531
08/20/2001 2:59 AM	3.91	9495.811195
08/20/2001 3:14 AM	3.88	9570.52522
08/20/2001 3:29 AM	3.83	9696.405714
08/20/2001 3:44 AM	3.96	9375.063107
08/20/2001 3:59 AM	2.92	12717.35263
08/20/2001 3:29 PM	3.07	12097.76708

Date and Time	Vel (fps)	m3/sec
08/20/2001 4:14 AM	3.78	9821.68043
08/20/2001 4:29 AM	3.82	9719.6601
08/20/2001 4:44 AM	3.73	9954.30281
08/20/2001 4:59 AM	3.94	9422.27843
08/20/2001 5:14 AM	3.89	9544.26431
08/20/2001 5:29 AM	3.90	9521.85383
08/20/2001 5:44 AM	3.91	9495.8405
08/20/2001 5:59 AM	3.86	9619.75097
08/20/2001 6:14 AM	3.68	10090.567
08/20/2001 6:29 AM	3.58	10370.1466
08/20/2001 6:44 AM	3.76	9873.52706
08/20/2001 6:59 AM	3.82	9719.68738
08/20/2001 7:14 AM	3.82	9719.6901
08/20/2001 7:29 AM	3.88	9570.57087
08/20/2001 7:44 AM	3.83	9696.45197
08/20/2001 7:59 AM	3.00	12374.5701
08/20/2001 8:14 AM	3.83	9696.45741
08/20/2001 8:29 AM	3.79	9797.99374
08/20/2001 8:44 AM	3.87	9593.22764
08/20/2001 8:59 AM	3.79	9797.99924
08/20/2001 9:14 AM	3.79	9798.00199
08/20/2001 9:29 AM	3.91	9495.88047
08/20/2001 9:44 AM	3.84	9669.49626
08/20/2001 9:59 AM	3.79	9798.01024
08/20/2001 10:14 AM	3.75	9901.69567
08/20/2001 10:29 AM	3.41	10890.0954
08/20/2001 10:44 AM	3.75	9901.70122
08/20/2001 10:59 AM	3.88	9570.60847
08/20/2001 11:14 AM	3.59	10343.7473
08/20/2001 11:29 AM	3.69	10061.4146
08/20/2001 11:44 AM	3.54	10490.9475
08/20/2001 11:59 AM	3.62	10256.5405
08/20/2001 12:14 PM	3.14	11827.1856
08/20/2001 12:29 PM	3.66	10145.341
08/20/2001 12:44 PM	3.49	10637.7501
08/20/2001 12:59 PM	3.31	11216.4783
08/20/2001 1:14 PM	3.77	9849.61464
08/20/2001 1:29 PM	2.75	13500.8629
08/20/2001 1:44 PM	3.35	11083.6273
08/20/2001 1:59 PM	3.64	10200.6577
08/20/2001 2:14 PM	3.32	11185.5519
08/20/2001 2:29 PM	3.10	11978.6225
08/20/2001 2:44 PM	3.83	9696.52815
08/20/2001 2:59 PM	3.50	10609.9415
08/20/2001 3:14 PM	3.43	10827.1485
08/21/2001 4:14 AM	3.98	9328.5881

08/20/2001 3:44 PM	3.70	10036.55793
08/20/2001 3:59 PM	3.69	10061.46537
08/20/2001 4:14 PM	3.47	10698.60602
08/20/2001 4:29 PM	3.36	11053.44703
08/20/2001 4:44 PM	3.70	10036.5692
08/20/2001 4:59 PM	3.66	10145.39223
08/20/2001 5:14 PM	2.66	13957.92162
08/20/2001 5:29 PM	3.74	9930.067027
08/20/2001 5:44 PM	3.57	10401.31297
08/20/2001 5:59 PM	3.68	10090.70007
08/20/2001 6:14 PM	3.53	10518.23809
08/20/2001 6:29 PM	3.46	10731.66807
08/20/2001 6:44 PM	3.67	10115.88289
08/20/2001 6:59 PM	3.74	9930.083745
08/20/2001 7:14 PM	3.58	10370.29497
08/20/2001 7:29 PM	3.29	11284.19241
08/20/2001 7:44 PM	3.59	10343.84594
08/20/2001 7:59 PM	3.60	10313.15493
08/20/2001 8:14 PM	3.72	9983.069064
08/20/2001 8:29 PM	3.77	9849.694791
08/20/2001 8:44 PM	2.99	12418.96527
08/20/2001 8:59 PM	3.60	10313.16651
08/20/2001 9:14 PM	3.86	9619.915624
08/20/2001 9:29 PM	3.58	10370.32116
08/20/2001 9:44 PM	3.80	9770.594485
08/20/2001 9:59 PM	3.76	9873.696061
08/20/2001 10:14 PM	3.85	9642.803773
08/20/2001 10:29 PM	3.82	9719.856471
08/20/2001 10:44 PM	3.91	9496.021691
08/20/2001 10:59 PM	3.86	9619.934519
08/20/2001 11:14 PM	3.69	10061.54724
08/20/2001 11:29 PM	3.74	9930.133899
08/20/2001 11:44 PM	3.93	9448.091215
08/20/2001 11:59 PM	2.73	13599.12896
08/21/2001 12:14 AM	3.77	9849.736248
08/21/2001 12:29 AM	3.85	9642.828124
08/21/2001 12:44 AM	3.85	9642.83083
08/21/2001 12:59 AM	3.79	9798.175196
08/21/2001 1:14 AM	3.77	9849.747303
08/21/2001 1:29 AM	3.74	9930.156189
08/21/2001 1:44 AM	3.80	9770.638349
08/21/2001 1:59 AM	2.91	12757.68029
08/21/2001 2:14 AM	3.92	9473.87194
08/21/2001 2:29 AM	3.94	9422.505798
08/21/2001 2:44 AM	3.88	9570.777654
08/21/2001 2:59 AM	3.89	9544.497302
08/21/2001 3:14 AM	3.73	9954.554193
08/21/2001 3:29 AM	3.97	9353.685996
08/21/2001 3:44 AM	3.84	9669.691614
08/21/2001 3:59 AM	3.81	9747.175853
08/21/2001 7:13 PM	3.61	10287.25873
08/21/2001 7:28 PM	3.11	11937.86738
08/21/2001 7:43 PM	3.72	9983.332187
08/21/2001 7:58 PM	3.70	10036.87598
08/21/2001 8:13 PM	3.85	9643.041694
08/21/2001 8:28 PM	2.77	13404.62866
08/21/2001 8:43 PM	3.79	9798.392205
08/21/2001 8:58 PM	3.84	9669.878646
08/21/2001 9:13 PM	3.71	10007.9891

08/21/2001 4:29 AM	2.64	14062.9853
08/21/2001 4:44 AM	3.82	9719.92465
08/21/2001 4:59 AM	3.96	9375.3288
08/21/2001 5:14 AM	3.96	9375.33143
08/21/2001 5:29 AM	3.96	9375.33406
08/21/2001 5:44 AM	3.96	9375.33669
08/21/2001 7:59 AM	3.95	9400.71876
08/21/2001 8:14 AM	3.86	9620.03439
08/21/2001 8:29 AM	3.92	9473.9384
08/21/2001 8:44 AM	3.80	9770.71511
08/21/2001 8:59 AM	3.89	9544.56158
08/21/2001 9:14 AM	3.80	9770.7206
08/21/2001 9:29 AM	3.81	9747.23602
08/21/2001 9:44 AM	3.89	9544.56961
08/21/2001 9:59 AM	3.77	9849.84403
08/21/2001 10:14 AM	3.76	9873.83181
08/21/2001 10:29 AM	3.83	9696.74309
08/21/2001 10:44 AM	3.80	9770.73705
08/21/2001 10:59 AM	3.74	9930.26207
08/21/2001 11:14 AM	3.68	10090.8954
08/21/2001 11:29 AM	3.36	11053.6827
08/21/2001 11:44 AM	3.69	10061.6884
08/21/2001 11:59 AM	3.66	10145.6086
08/21/2001 12:14 PM	3.15	11787.3916
08/21/2001 12:29 PM	3.53	10518.4535
08/21/2001 12:44 PM	3.69	10061.6997
08/21/2001 12:59 PM	3.72	9983.25674
08/21/2001 1:14 PM	3.55	10459.6748
08/21/2001 1:29 PM	3.48	10670.7063
08/21/2001 1:44 PM	3.70	10036.8058
08/21/2001 1:59 PM	3.68	10090.9266
08/21/2001 2:14 PM	3.52	10550.4036
08/21/2001 2:29 PM	3.60	10313.3691
08/21/2001 2:44 PM	3.64	10200.9411
08/21/2001 2:59 PM	3.52	10550.4125
08/21/2001 3:14 PM	3.47	10698.8822
08/21/2001 3:29 PM	3.32	11185.8689
08/21/2001 3:44 PM	3.42	10856.4354
08/21/2001 4:13 PM	3.59	10344.0837
08/21/2001 4:28 PM	3.71	10007.9357
08/21/2001 4:43 PM	3.35	11083.9629
08/21/2001 4:58 PM	3.66	10145.6653
08/21/2001 5:13 PM	3.67	10116.1382
08/21/2001 5:28 PM	3.67	10116.141
08/21/2001 5:43 PM	3.69	10061.756
08/21/2001 5:58 PM	3.62	10256.8856
08/21/2001 6:13 PM	3.23	11497.7975
08/21/2001 6:28 PM	3.65	10175.3854
08/21/2001 6:43 PM	3.37	11018.7288
08/21/2001 6:58 PM	3.79	9798.37296
08/22/2001 9:13 AM	3.74	9930.50986
08/22/2001 9:28 AM	3.89	9544.82385
08/22/2001 9:43 AM	3.83	9696.99594
08/22/2001 9:58 AM	3.81	9747.50387
08/22/2001 10:13 AM	3.78	9822.27552
08/22/2001 10:28 AM	3.79	9798.54342
08/22/2001 10:43 AM	3.53	10518.716
08/22/2001 10:58 AM	3.79	9798.54891
08/22/2001 11:13 AM	3.51	10578.1756

08/21/2001 9:28 PM	3.70	10036.89287
08/21/2001 9:43 PM	3.60	10313.4528
08/21/2001 9:58 PM	3.81	9747.372587
08/21/2001 10:13 PM	3.85	9643.063339
08/21/2001 10:28 PM	3.86	9620.188071
08/21/2001 10:43 PM	3.91	9496.277306
08/21/2001 10:58 PM	2.91	12757.98075
08/21/2001 11:13 PM	3.82	9720.126293
08/21/2001 11:28 PM	3.78	9822.157019
08/21/2001 11:43 PM	3.88	9571.003054
08/21/2001 11:58 PM	3.80	9770.882165
08/22/2001 12:13 AM	3.76	9873.986776
08/22/2001 12:28 AM	3.77	9850.004147
08/22/2001 12:43 AM	2.77	13404.6926
08/22/2001 12:58 AM	3.86	9620.215064
08/22/2001 1:13 AM	3.83	9696.903436
08/22/2001 1:28 AM	3.76	9874.000628
08/22/2001 1:43 AM	3.95	9400.905864
08/22/2001 1:58 AM	2.72	13652.9468
08/22/2001 2:13 AM	3.78	9822.187335
08/22/2001 2:28 AM	3.79	9798.455439
08/22/2001 2:43 AM	3.76	9874.014481
08/22/2001 2:58 AM	3.98	9328.826115
08/22/2001 3:13 AM	3.97	9353.935153
08/22/2001 3:28 AM	3.92	9474.140249
08/22/2001 3:43 AM	3.92	9474.142908
08/22/2001 3:58 AM	3.92	9474.145566
08/22/2001 4:13 AM	3.92	9474.148224
08/22/2001 4:43 AM	3.93	9448.409164
08/22/2001 5:58 AM	3.79	9798.493929
08/22/2001 6:13 AM	3.89	9544.789035
08/22/2001 6:28 AM	3.78	9822.234186
08/22/2001 6:43 AM	3.91	9496.36257
08/22/2001 6:58 AM	3.84	9669.987174
08/22/2001 7:13 AM	3.84	9669.989888
08/22/2001 7:28 AM	3.81	9747.476516
08/22/2001 7:43 AM	3.87	9593.733521
08/22/2001 7:58 AM	3.87	9593.736213
08/22/2001 8:13 AM	3.90	9522.396032
08/22/2001 8:28 AM	3.92	9474.193415
08/22/2001 8:43 AM	3.79	9798.524171
08/22/2001 8:58 AM	3.86	9620.30144
08/22/2001 9:58 PM	3.96	9375.760046
08/22/2001 10:13 PM	3.96	9375.762676
08/22/2001 10:28 PM	3.81	9747.640613
08/22/2001 10:43 PM	3.90	9522.550997
08/22/2001 10:58 PM	3.86	9620.452599
08/22/2001 11:13 PM	3.95	9401.132709
08/22/2001 11:28 PM	3.91	9496.541092
08/22/2001 11:43 PM	3.89	9544.976502
08/22/2001 11:58 PM	3.95	9401.140622
08/23/2001 12:13 AM	2.88	12893.56585
08/23/2001 12:28 AM	3.95	9401.145897
08/23/2001 12:43 AM	3.96	9375.788982
08/23/2001 12:58 AM	3.98	9329.056455
08/23/2001 1:13 AM	3.91	9496.559743
08/23/2001 1:28 AM	3.95	9401.156448
08/23/2001 1:43 AM	3.85	9643.360965
08/23/2001 1:58 AM	3.99	9307.653612

08/22/2001 11:28 AM	3.74	9930.53494
08/22/2001 11:43 AM	3.04	12213.7638
08/22/2001 11:58 AM	3.94	9422.8599
08/22/2001 12:13 PM	3.87	9593.78197
08/22/2001 12:28 PM	3.82	9720.27084
08/22/2001 12:43 PM	3.80	9771.02198
08/22/2001 12:58 PM	3.53	10518.7426
08/22/2001 1:13 PM	3.49	10638.329
08/22/2001 1:28 PM	3.80	9771.03021
08/22/2001 1:43 PM	3.86	9620.35273
08/22/2001 1:58 PM	3.52	10550.6847
08/22/2001 2:13 PM	3.84	9670.06586
08/22/2001 2:28 PM	3.61	10287.481
08/22/2001 2:43 PM	3.84	9670.07128
08/22/2001 2:58 PM	3.77	9850.16444
08/22/2001 3:13 PM	3.83	9697.0558
08/22/2001 3:28 PM	3.79	9798.5984
08/22/2001 3:43 PM	3.79	9798.60115
08/22/2001 3:58 PM	3.77	9850.1755
08/22/2001 4:13 PM	3.83	9697.06668
08/22/2001 4:28 PM	2.80	13266.0562
08/22/2001 4:43 PM	3.82	9720.3172
08/22/2001 4:58 PM	2.82	13165.5632
08/22/2001 5:13 PM	3.20	11602.2735
08/22/2001 5:28 PM	3.86	9620.39322
08/22/2001 5:43 PM	3.79	9798.62314
08/22/2001 5:58 PM	2.87	12941.483
08/22/2001 6:13 PM	3.39	10954.5227
08/22/2001 6:28 PM	3.80	9771.08504
08/22/2001 6:43 PM	3.87	9593.85196
08/22/2001 6:58 PM	3.85	9643.28791
08/22/2001 7:13 PM	2.77	13404.9709
08/22/2001 7:28 PM	3.89	9544.93097
08/22/2001 7:43 PM	3.84	9670.12555
08/22/2001 7:58 PM	3.80	9771.10149
08/22/2001 8:13 PM	3.88	9571.22326
08/22/2001 8:28 PM	3.99	9307.59616
08/22/2001 8:43 PM	3.68	10091.2747
08/22/2001 8:58 PM	3.87	9593.87619
08/22/2001 9:13 PM	3.78	9822.39679
08/22/2001 9:28 PM	3.74	9930.64639
08/22/2001 9:43 PM	3.94	9422.96301
08/23/2001 11:28 AM	3.83	9697.27618
08/23/2001 11:43 AM	3.85	9643.46919
08/23/2001 11:58 AM	3.78	9822.55939
08/23/2001 12:13 PM	3.63	10231.4913
08/23/2001 12:28 PM	3.23	11498.3427
08/23/2001 12:43 PM	3.73	9955.19643
08/23/2001 12:58 PM	3.40	10920.3352
08/23/2001 1:13 PM	2.78	13361.0729
08/23/2001 1:28 PM	3.87	9594.05385
08/23/2001 1:43 PM	2.73	13600.0712
08/23/2001 1:58 PM	3.58	10371.0717
08/23/2001 2:13 PM	3.69	10062.2585
08/23/2001 2:28 PM	3.78	9822.58695
08/23/2001 2:43 PM	3.81	9747.81839
08/23/2001 2:58 PM	3.72	9983.81679
08/23/2001 3:13 PM	3.42	10857.014
08/23/2001 3:30 PM	2.88	12893.787

08/23/2001 2:13 AM	3.94	9423.0106
08/23/2001 2:28 AM	3.98	9329.07216
08/23/2001 2:43 AM	3.90	9522.593746
08/23/2001 2:58 AM	3.91	9496.578395
08/23/2001 3:13 AM	3.87	9593.943483
08/23/2001 3:28 AM	3.95	9401.17755
08/23/2001 3:43 AM	3.93	9448.642457
08/23/2001 3:58 AM	3.86	9620.506585
08/23/2001 4:13 AM	3.90	9522.609777
08/23/2001 4:28 AM	3.98	9329.0931
08/23/2001 4:43 AM	3.95	9401.190739
08/23/2001 4:58 AM	3.82	9720.450843
08/23/2001 5:13 AM	3.93	9448.658363
08/23/2001 5:28 AM	3.93	9448.661014
08/23/2001 5:43 AM	3.93	9448.663665
08/23/2001 5:58 AM	3.93	9448.666316
08/23/2001 6:58 AM	3.96	9375.854748
08/23/2001 7:13 AM	3.96	9375.857378
08/23/2001 7:28 AM	3.96	9375.860009
08/23/2001 7:43 AM	3.93	9448.684874
08/23/2001 7:58 AM	3.77	9850.352379
08/23/2001 8:13 AM	3.94	9423.074052
08/23/2001 8:28 AM	3.81	9747.750012
08/23/2001 8:43 AM	3.77	9850.36067
08/23/2001 8:58 AM	4.00	9282.86825
08/23/2001 9:13 AM	3.77	9850.366198
08/23/2001 9:28 AM	3.81	9747.760952
08/23/2001 9:43 AM	3.88	9571.368278
08/23/2001 9:58 AM	3.93	9448.708733
08/23/2001 10:13 AM	3.88	9571.373649
08/23/2001 10:28 AM	3.80	9771.260498
08/23/2001 10:43 AM	3.50	10610.74813
08/23/2001 10:58 AM	3.76	9874.371873
08/23/2001 11:13 AM	3.74	9930.799641
08/24/2001 12:15 AM	3.87	9594.169955
08/24/2001 12:30 AM	3.79	9798.961673
08/24/2001 12:45 AM	3.92	9474.621752
08/24/2001 1:00 AM	3.92	9474.62441
08/24/2001 1:15 AM	3.92	9474.627069
08/24/2001 1:30 AM	3.92	9474.629727
08/24/2001 6:00 AM	3.98	9329.360435
08/24/2001 6:15 AM	3.94	9423.307065
08/24/2001 6:30 AM	3.92	9474.682892
08/24/2001 6:45 AM	3.78	9822.766449
08/24/2001 7:00 AM	3.93	9448.931775
08/24/2001 7:15 AM	3.79	9799.035903
08/24/2001 7:30 AM	3.90	9522.90136
08/24/2001 7:45 AM	3.90	9522.904031
08/24/2001 8:00 AM	3.90	9522.906703
08/24/2001 8:15 AM	3.90	9522.909375
08/24/2001 8:30 AM	3.90	9522.912047
08/24/2001 8:45 AM	3.93	9448.950332
08/24/2001 9:00 AM	3.89	9545.333045
08/24/2001 9:15 AM	3.87	9594.266861
08/24/2001 9:30 AM	3.91	9496.903819
08/24/2001 9:45 AM	3.77	9850.637414
08/24/2001 10:00 AM	3.81	9748.029342
08/24/2001 10:15 AM	3.84	9670.543746
08/24/2001 10:30 AM	3.83	9697.52686

08/23/2001 3:45 PM	3.63	10231.5319
08/23/2001 4:00 PM	2.72	13653.5296
08/23/2001 4:15 PM	2.72	13653.5334
08/23/2001 4:30 PM	3.34	11120.0198
08/23/2001 4:45 PM	3.75	9902.56826
08/23/2001 5:00 PM	3.81	9747.84337
08/23/2001 5:15 PM	3.86	9620.65001
08/23/2001 5:30 PM	3.85	9643.53178
08/23/2001 5:45 PM	3.73	9955.25267
08/23/2001 6:00 PM	2.74	13554.6765
08/23/2001 6:15 PM	3.82	9720.59575
08/23/2001 6:30 PM	3.81	9747.85977
08/23/2001 6:45 PM	3.82	9720.60121
08/23/2001 7:00 PM	3.87	9594.11343
08/23/2001 7:15 PM	3.76	9874.46367
08/23/2001 7:30 PM	3.84	9670.38367
08/23/2001 7:45 PM	3.73	9955.27501
08/23/2001 8:00 PM	3.90	9522.77846
08/23/2001 8:15 PM	3.97	9354.36593
08/23/2001 8:30 PM	3.89	9545.19914
08/23/2001 8:45 PM	3.87	9594.13227
08/23/2001 9:00 PM	3.76	9874.48306
08/23/2001 9:15 PM	3.94	9423.21189
08/23/2001 9:30 PM	4.02	9237.18296
08/23/2001 9:45 PM	3.92	9474.58985
08/23/2001 10:00 PM	3.96	9376.01294
08/23/2001 10:15 PM	3.91	9496.78392
08/23/2001 10:30 PM	3.94	9423.22511
08/23/2001 10:45 PM	3.96	9376.02083
08/23/2001 11:00 PM	3.92	9474.60314
08/23/2001 11:15 PM	3.95	9401.38628
08/23/2001 11:30 PM	4.01	9261.81748
08/23/2001 11:45 PM	4.03	9212.72297
08/24/2001 12:00 AM	3.90	9522.82121
08/24/2001 5:15 PM	3.64	10201.7942
08/24/2001 5:30 PM	3.85	9643.79153
08/24/2001 5:45 PM	3.75	9902.8461
08/24/2001 6:00 PM	3.82	9720.85485
08/24/2001 6:15 PM	3.87	9594.36377
08/24/2001 6:30 PM	3.77	9850.73414
08/24/2001 6:45 PM	2.87	12942.1916
08/24/2001 7:00 PM	3.93	9449.05903
08/24/2001 7:15 PM	3.88	9571.72849
08/24/2001 7:30 PM	3.90	9523.02961
08/24/2001 7:45 PM	3.91	9497.01306
08/24/2001 8:00 PM	3.85	9643.81859
08/24/2001 8:15 PM	3.89	9545.45356
08/24/2001 8:30 PM	3.95	9401.61049
08/24/2001 8:45 PM	3.92	9474.83441
08/24/2001 9:00 PM	3.90	9523.04564
08/24/2001 9:15 PM	3.91	9497.02905
08/24/2001 9:30 PM	3.91	9497.03172
08/24/2001 9:45 PM	3.85	9643.83753
08/24/2001 10:00 PM	3.90	9523.05632
08/24/2001 10:15 PM	3.88	9571.76071
08/24/2001 10:30 PM	3.96	9376.27074
08/24/2001 10:45 PM	3.91	9497.04504
08/24/2001 11:00 PM	3.78	9822.94559
08/24/2001 11:15 PM	3.91	9497.05037

08/24/2001 10:45 AM	3.83	9697.529581
08/24/2001 11:00 AM	3.84	9670.551886
08/24/2001 11:15 AM	3.75	9902.773859
08/24/2001 11:30 AM	3.80	9771.535019
08/24/2001 11:45 AM	3.82	9720.786665
08/24/2001 12:00 PM	3.75	9902.782194
08/24/2001 12:15 PM	3.67	10116.89924
08/24/2001 12:30 PM	3.84	9670.568165
08/24/2001 12:45 PM	3.77	9850.670579
08/24/2001 1:00 PM	3.66	10146.44001
08/24/2001 1:15 PM	2.85	13032.22816
08/24/2001 1:30 PM	2.88	12894.10536
08/24/2001 1:45 PM	3.84	9670.581731
08/24/2001 2:00 PM	3.88	9571.672093
08/24/2001 2:15 PM	3.91	9496.954445
08/24/2001 2:30 PM	2.93	12672.50214
08/24/2001 2:45 PM	3.82	9720.819393
08/24/2001 3:00 PM	3.89	9545.39732
08/24/2001 3:15 PM	3.83	9697.578555
08/24/2001 3:30 PM	3.34	11120.30686
08/24/2001 3:45 PM	3.52	10551.27417
08/24/2001 4:00 PM	3.56	10429.16634
08/24/2001 4:15 PM	2.98	12464.78069
08/24/2001 4:30 PM	3.79	9799.137626
08/24/2001 4:45 PM	2.82	13166.26924
08/24/2001 5:00 PM	3.76	9874.704699
08/25/2001 6:45 AM	3.95	9401.718638
08/25/2001 7:00 AM	3.89	9545.568717
08/25/2001 7:15 AM	3.97	9354.733367
08/25/2001 7:30 AM	3.96	9376.365439
08/25/2001 7:45 AM	3.99	9308.215432
08/25/2001 8:00 AM	3.87	9594.511817
08/25/2001 8:15 AM	3.87	9594.514508
08/25/2001 8:30 AM	3.92	9474.959353
08/25/2001 8:45 AM	4.00	9283.366061
08/25/2001 9:00 AM	3.77	9850.894442
08/25/2001 9:15 AM	3.96	9376.383853
08/25/2001 9:30 AM	3.99	9308.233713
08/25/2001 9:45 AM	3.95	9401.750291
08/25/2001 10:00 AM	2.91	12759.16968
08/25/2001 10:15 AM	3.84	9670.804215
08/25/2001 10:30 AM	3.87	9594.538735
08/25/2001 10:45 AM	3.85	9643.978223
08/25/2001 11:00 AM	3.81	9748.302838
08/25/2001 11:15 AM	3.83	9697.796218
08/25/2001 11:30 AM	3.78	9823.083382
08/25/2001 11:45 AM	3.90	9523.203273
08/25/2001 12:00 PM	3.89	9545.622279
08/25/2001 12:15 PM	3.20	11603.14641
08/25/2001 12:30 PM	3.51	10579.04558
08/25/2001 12:45 PM	3.74	9931.351702
08/25/2001 1:00 PM	3.63	10232.05151
08/25/2001 1:15 PM	3.68	10092.00553
08/25/2001 1:30 PM	3.49	10639.19202
08/25/2001 1:45 PM	3.49	10639.195
08/25/2001 2:00 PM	3.41	10891.6051
08/25/2001 2:15 PM	3.53	10519.60771
08/25/2001 2:30 PM	3.71	10008.99196
08/25/2001 2:45 PM	3.73	9955.755434

08/24/2001 11:30 PM	2.78	13361.587
08/24/2001 11:45 PM	3.91	9497.0557
08/25/2001 12:00 AM	3.83	9697.67378
08/25/2001 12:15 AM	3.99	9308.13709
08/25/2001 12:30 AM	3.96	9376.29178
08/25/2001 12:45 AM	4.07	9123.1661
08/25/2001 1:00 AM	3.90	9523.08839
08/25/2001 1:15 AM	3.89	9545.50712
08/25/2001 1:30 AM	3.94	9423.51064
08/25/2001 1:45 AM	4.07	9123.17634
08/25/2001 2:00 AM	3.86	9621.00361
08/25/2001 2:15 AM	3.86	9621.00631
08/25/2001 2:30 AM	3.86	9621.00901
08/25/2001 2:45 AM	3.86	9621.01171
08/25/2001 3:45 AM	3.93	9449.15181
08/25/2001 4:00 AM	3.81	9748.22626
08/25/2001 4:15 AM	3.87	9594.47144
08/25/2001 4:30 AM	3.95	9401.6949
08/25/2001 4:45 AM	3.90	9523.12846
08/25/2001 5:00 AM	3.83	9697.7282
08/25/2001 5:15 AM	3.88	9571.83591
08/25/2001 5:30 AM	3.76	9874.84322
08/25/2001 5:45 AM	3.90	9523.13915
08/25/2001 6:00 AM	3.92	9474.93277
08/25/2001 6:15 AM	4.01	9262.13711
08/25/2001 6:30 AM	4.00	9283.34262
08/25/2001 7:37 PM	2.80	13267.1751
08/25/2001 7:52 PM	3.83	9697.88999
08/25/2001 8:07 PM	3.91	9497.27276
08/25/2001 8:22 PM	3.88	9571.99829
08/25/2001 8:37 PM	3.85	9644.08501
08/25/2001 8:52 PM	3.75	9903.14746
08/25/2001 9:07 PM	3.84	9670.92215
08/25/2001 9:22 PM	3.86	9621.21271
08/25/2001 9:37 PM	3.92	9475.09882
08/25/2001 9:52 PM	3.86	9621.21811
08/25/2001 10:07 PM	3.85	9644.10124
08/25/2001 10:22 PM	3.81	9748.42719
08/25/2001 10:37 PM	3.88	9572.02246
08/25/2001 10:52 PM	3.84	9670.94114
08/25/2001 11:07 PM	3.81	9748.43539
08/25/2001 11:22 PM	3.89	9545.74404
08/25/2001 11:37 PM	3.89	9545.74672
08/25/2001 11:52 PM	3.90	9523.33277
08/26/2001 12:07 AM	3.87	9594.68535
08/26/2001 12:22 AM	3.79	9799.48807
08/26/2001 12:37 AM	3.88	9572.04394
08/26/2001 12:52 AM	3.93	9449.37574
08/26/2001 1:07 AM	3.92	9475.13604
08/26/2001 1:22 AM	3.98	9329.81449
08/26/2001 1:37 AM	4.07	9123.4207
08/26/2001 1:52 AM	3.84	9670.9737
08/26/2001 2:07 AM	3.84	9670.97641
08/26/2001 2:22 AM	3.84	9670.97913
08/26/2001 2:37 AM	3.84	9670.98184
08/26/2001 8:07 AM	3.87	9594.77149
08/26/2001 8:22 AM	3.89	9545.84045
08/26/2001 8:37 AM	3.90	9523.42628
08/26/2001 8:52 AM	3.85	9644.21759

08/25/2001 3:00 PM	3.15	11788.69821
08/25/2001 3:15 PM	3.37	11019.87316
08/25/2001 3:30 PM	3.63	10232.08022
08/25/2001 3:45 PM	3.72	9984.363392
08/25/2001 4:00 PM	3.47	10700.04416
08/25/2001 4:15 PM	3.79	9799.398808
08/25/2001 4:30 PM	3.41	10891.63566
08/25/2001 4:52 PM	2.98	12465.12504
08/25/2001 5:07 PM	3.73	9955.781876
08/25/2001 5:22 PM	3.58	10371.66996
08/25/2001 5:37 PM	3.59	10345.21452
08/25/2001 5:52 PM	3.68	10092.05781
08/25/2001 6:07 PM	3.72	9984.38991
08/25/2001 6:22 PM	3.83	9697.87367
08/25/2001 6:37 PM	3.73	9955.798635
08/25/2001 6:52 PM	3.90	9523.279331
08/25/2001 7:07 PM	3.76	9874.994122
08/25/2001 7:22 PM	3.44	10795.02766
08/26/2001 1:37 PM	3.72	9984.608401
08/26/2001 1:52 PM	3.72	9984.611203
08/26/2001 2:07 PM	3.69	10063.07044
08/26/2001 2:22 PM	3.73	9956.019294
08/26/2001 2:37 PM	2.77	13406.34599
08/26/2001 2:52 PM	3.76	9875.21299
08/26/2001 3:07 PM	3.83	9698.099495
08/26/2001 3:22 PM	3.79	9799.653024
08/26/2001 3:37 PM	3.82	9721.352491
08/26/2001 3:52 PM	3.60	10314.7741
08/26/2001 4:07 PM	3.71	10009.2797
08/26/2001 4:22 PM	2.84	13074.99504
08/26/2001 4:37 PM	3.84	9671.133781
08/26/2001 4:52 PM	3.70	10038.19283
08/26/2001 5:07 PM	3.83	9698.121261
08/26/2001 5:22 PM	3.83	9698.123982
08/26/2001 5:37 PM	3.72	9984.65322
08/26/2001 5:52 PM	3.83	9698.129424
08/26/2001 6:07 PM	3.79	9799.683266
08/26/2001 6:22 PM	3.87	9594.881852
08/26/2001 6:37 PM	3.77	9851.266074
08/26/2001 6:52 PM	3.88	9572.23998
08/26/2001 7:07 PM	3.90	9523.538496
08/26/2001 7:22 PM	3.86	9621.45025
08/26/2001 7:37 PM	3.84	9671.166339
08/26/2001 7:52 PM	3.87	9594.898003
08/26/2001 8:07 PM	3.83	9698.153911
08/26/2001 8:22 PM	2.80	13267.54361
08/26/2001 8:37 PM	3.90	9523.554527
08/26/2001 8:52 PM	3.95	9402.120804
08/26/2001 9:07 PM	3.92	9475.348703
08/26/2001 9:22 PM	3.85	9644.352871
08/26/2001 9:37 PM	3.70	10038.24634
08/26/2001 9:52 PM	3.88	9572.272206
08/26/2001 10:07 PM	3.86	9621.479942
08/26/2001 10:22 PM	3.82	9721.426129
08/26/2001 10:37 PM	4.02	9237.940937
08/26/2001 10:52 PM	3.87	9594.930305
08/26/2001 11:07 PM	3.90	9523.581245
08/26/2001 11:22 PM	3.92	9475.372627
08/26/2001 11:37 PM	3.86	9621.496138

08/26/2001 9:07 AM	3.91	9497.41132
08/26/2001 9:22 AM	3.77	9851.16382
08/26/2001 9:37 AM	2.86	12984.195
08/26/2001 9:52 AM	3.75	9903.29193
08/26/2001 10:07 AM	3.85	9644.23112
08/26/2001 10:22 AM	3.02	12295.3016
08/26/2001 10:37 AM	3.88	9572.15136
08/26/2001 10:52 AM	3.79	9799.60354
08/26/2001 11:07 AM	3.73	9955.98298
08/26/2001 11:22 AM	3.78	9823.34648
08/26/2001 11:37 AM	3.87	9594.80917
08/26/2001 11:52 AM	3.53	10519.8629
08/26/2001 12:07 PM	3.88	9572.16747
08/26/2001 12:22 PM	2.79	13310.9719
08/26/2001 12:37 PM	3.79	9799.62278
08/26/2001 12:52 PM	3.62	10258.2083
08/26/2001 1:07 PM	3.78	9823.36577
08/26/2001 1:22 PM	3.80	9772.08187
08/27/2001 4:07 AM	3.78	9823.53113
08/27/2001 4:22 AM	3.86	9621.54742
08/27/2001 4:37 AM	4.07	9123.69714
08/27/2001 4:52 AM	4.00	9283.82567
08/27/2001 5:07 AM	3.87	9594.9976
08/27/2001 5:22 AM	3.97	9355.21751
08/27/2001 5:37 AM	3.95	9402.21313
08/27/2001 5:52 AM	3.90	9523.65338
08/27/2001 6:07 AM	3.97	9355.22538
08/27/2001 6:22 AM	3.88	9572.36351
08/27/2001 6:37 AM	3.82	9721.51613
08/27/2001 6:52 AM	3.86	9621.57442
08/27/2001 7:07 AM	3.93	9449.69652
08/27/2001 7:22 AM	3.92	9475.45769
08/27/2001 7:37 AM	3.93	9449.70182
08/27/2001 7:52 AM	3.93	9449.70447
08/27/2001 8:07 AM	3.93	9449.70712
08/27/2001 8:22 AM	2.75	13503.3311
08/27/2001 8:37 AM	3.84	9671.30743
08/27/2001 8:52 AM	3.96	9376.8849
08/27/2001 9:07 AM	3.90	9523.68812
08/27/2001 9:22 AM	3.85	9644.48274
08/27/2001 9:37 AM	3.85	9644.48545
08/27/2001 9:52 AM	3.87	9595.04875
08/27/2001 10:07 AM	3.76	9875.42632
08/27/2001 10:22 AM	3.85	9644.49357
08/27/2001 10:37 AM	3.76	9875.43186
08/27/2001 10:52 AM	3.72	9984.8465
08/27/2001 11:07 AM	3.71	10009.4931
08/27/2001 11:22 AM	2.73	13601.5006
08/27/2001 11:37 AM	3.83	9698.3226
08/27/2001 11:52 AM	3.83	9698.32532
08/27/2001 12:07 PM	3.80	9772.33135
08/27/2001 12:22 PM	3.66	10147.2527
08/27/2001 12:37 PM	3.83	9698.33348
08/27/2001 12:52 PM	3.79	9799.88946
08/27/2001 1:07 PM	3.77	9851.47059
08/27/2001 1:22 PM	3.24	11461.6765
08/27/2001 1:37 PM	3.79	9799.89771
08/27/2001 1:52 PM	3.81	9748.85931
08/27/2001 2:07 PM	3.80	9772.35328

08/26/2001 11:52 PM	3.89	9546.006496
08/27/2001 12:07 AM	3.95	9402.155095
08/27/2001 12:22 AM	2.74	13555.86864
08/27/2001 12:37 AM	3.87	9594.949148
08/27/2001 12:52 AM	3.80	9772.207978
08/27/2001 1:07 AM	3.85	9644.393457
08/27/2001 1:22 AM	3.93	9449.635541
08/27/2001 1:37 AM	3.93	9449.638192
08/27/2001 1:52 AM	3.93	9449.640843
08/27/2001 2:07 AM	3.93	9449.643494
08/27/2001 4:52 PM	3.82	9721.62795
08/27/2001 5:07 PM	3.73	9956.318161
08/27/2001 5:22 PM	3.76	9875.50666
08/27/2001 5:37 PM	3.46	10733.68118
08/27/2001 5:52 PM	3.40	10921.57184
08/27/2001 6:07 PM	3.78	9823.685463
08/27/2001 6:22 PM	3.46	10733.69021
08/27/2001 6:37 PM	3.89	9546.207353
08/27/2001 6:52 PM	3.67	10117.79184
08/27/2001 7:07 PM	3.82	9721.652496
08/27/2001 7:22 PM	3.87	9595.151034
08/27/2001 7:37 PM	3.80	9772.413594
08/27/2001 7:52 PM	3.79	9799.966442
08/27/2001 8:07 PM	3.87	9595.15911
08/27/2001 8:22 PM	3.93	9449.837021
08/27/2001 8:37 PM	3.73	9956.357265
08/27/2001 8:52 PM	3.87	9595.167185
08/27/2001 9:07 PM	3.83	9698.42599
08/27/2001 9:22 PM	3.84	9671.445801
08/27/2001 9:37 PM	2.82	13167.40501
08/27/2001 9:52 PM	3.85	9644.618029
08/27/2001 10:07 PM	3.84	9671.45394
08/27/2001 10:22 PM	3.87	9595.183336
08/27/2001 10:37 PM	3.92	9475.619847
08/27/2001 10:52 PM	3.77	9851.578378
08/27/2001 11:07 PM	3.95	9402.397767
08/27/2001 11:22 PM	3.86	9621.752569
08/27/2001 11:37 PM	3.90	9523.843081
08/27/2001 11:52 PM	3.93	9449.874136
08/28/2001 12:07 AM	3.92	9475.635797
08/28/2001 12:22 AM	3.92	9475.638455
08/28/2001 12:37 AM	3.99	9308.893029
08/28/2001 12:52 AM	3.89	9546.274306
08/28/2001 1:07 AM	3.89	9546.276984
08/28/2001 1:22 AM	3.83	9698.472243
08/28/2001 1:37 AM	3.87	9595.21833
08/28/2001 1:52 AM	3.87	9595.221022
08/28/2001 2:07 AM	3.87	9595.223713
08/28/2001 2:22 AM	3.87	9595.226405
08/28/2001 4:22 AM	3.70	10038.59273
08/28/2001 4:37 AM	3.90	9523.896517
08/28/2001 4:52 AM	3.95	9402.458434
08/28/2001 5:07 AM	3.92	9475.688962
08/28/2001 5:22 AM	3.81	9749.028879
08/28/2001 5:37 AM	3.97	9355.472091
08/28/2001 5:52 AM	3.94	9424.318255
08/28/2001 6:07 AM	3.93	9449.940412
08/28/2001 6:22 AM	3.97	9355.479964
08/28/2001 6:37 AM	3.84	9671.54619

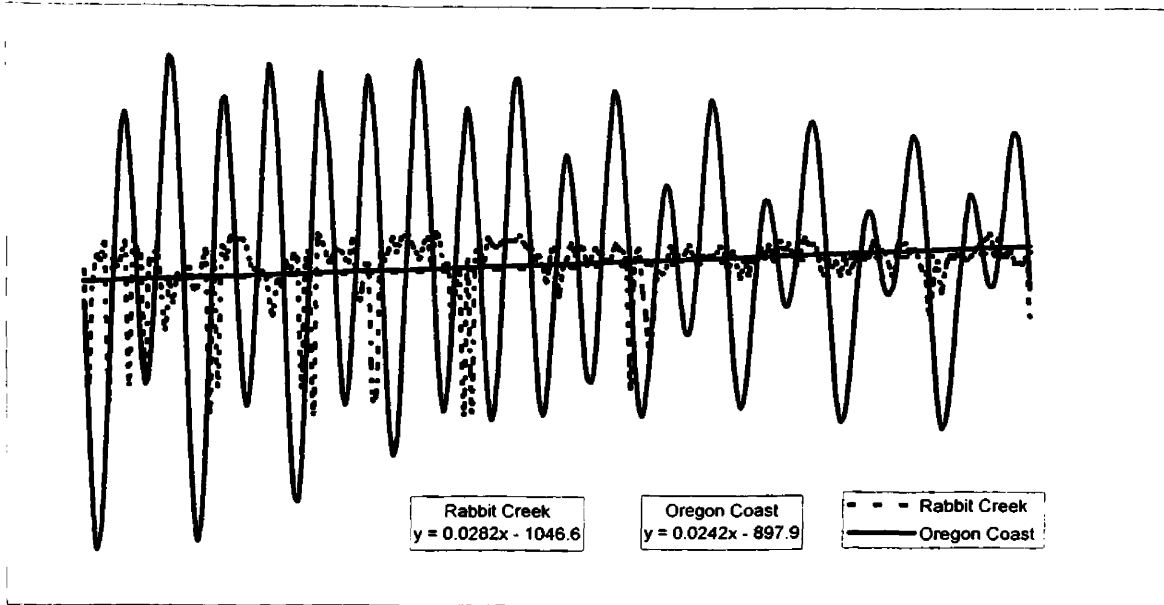
08/27/2001 2:22 PM	3.74	9931.90469
08/27/2001 2:37 PM	3.86	9621.65809
08/27/2001 2:52 PM	3.85	9644.54227
08/27/2001 3:07 PM	3.71	10009.538
08/27/2001 3:22 PM	3.81	9748.87572
08/27/2001 3:37 PM	3.64	10202.5998
08/27/2001 3:52 PM	3.89	9546.17789
08/27/2001 4:07 PM	3.84	9671.38882
08/27/2001 4:22 PM	3.84	9671.39154
08/27/2001 4:37 PM	3.77	9851.50928
08/28/2001 7:22 AM	3.93	9449.95367
08/28/2001 7:37 AM	3.87	9595.28293
08/28/2001 7:52 AM	3.81	9749.05623
08/28/2001 8:07 AM	3.87	9595.28832
08/28/2001 8:22 AM	3.87	9595.29101
08/28/2001 8:37 AM	3.87	9595.2937
08/28/2001 8:52 AM	3.96	9377.13744
08/28/2001 9:07 AM	3.90	9523.94461
08/28/2001 9:22 AM	3.70	10038.6491
08/28/2001 9:37 AM	3.84	9671.57875
08/28/2001 9:52 AM	3.83	9698.56475
08/28/2001 10:07 AM	3.85	9644.75061
08/28/2001 10:22 AM	3.78	9823.8646
08/28/2001 10:37 AM	3.84	9671.5896
08/28/2001 10:52 AM	3.90	9523.96331
08/28/2001 11:07 AM	3.76	9875.70336
08/28/2001 11:22 AM	2.88	12895.4637
08/28/2001 11:37 AM	3.71	10009.7683
08/28/2001 11:52 AM	3.81	9749.09999
08/28/2001 12:07 PM	3.73	9956.53044
08/28/2001 12:22 PM	3.71	10009.7767
08/28/2001 12:37 PM	3.43	10829.45
08/28/2001 12:52 PM	3.62	10258.7609
08/28/2001 1:07 PM	3.44	10795.8242
08/28/2001 1:22 PM	3.50	10612.2087
08/28/2001 1:37 PM	3.82	9721.85432
08/28/2001 1:52 PM	3.83	9698.60828
08/28/2001 2:07 PM	3.66	10147.5459
08/28/2001 2:22 PM	3.83	9698.61372
08/28/2001 2:37 PM	3.78	9823.91145
08/28/2001 2:52 PM	3.80	9772.62469
08/28/2001 3:07 PM	3.81	9749.13554
08/28/2001 3:22 PM	3.62	10258.7897
08/28/2001 3:37 PM	3.72	9985.16864
08/28/2001 3:52 PM	3.72	9985.17144
08/28/2001 4:02 PM	3.59	10346.032
08/28/2001 4:17 PM	3.77	9851.77092
08/28/2001 4:32 PM	3.79	9800.19372
08/28/2001 4:47 PM	3.92	9475.81302
08/28/2001 5:02 PM	3.77	9851.77921
08/28/2001 5:17 PM	3.77	9851.78197
08/28/2001 5:32 PM	3.79	9800.20471
08/28/2001 5:47 PM	3.80	9772.65668
08/28/2001 6:02 PM	3.85	9644.83629
08/28/2001 6:17 PM	3.76	9875.78278
08/28/2001 6:32 PM	3.81	9749.17292
08/28/2001 6:47 PM	3.85	9644.84441
08/28/2001 7:02 PM	3.83	9698.66451
08/28/2001 7:17 PM	3.86	9621.96761



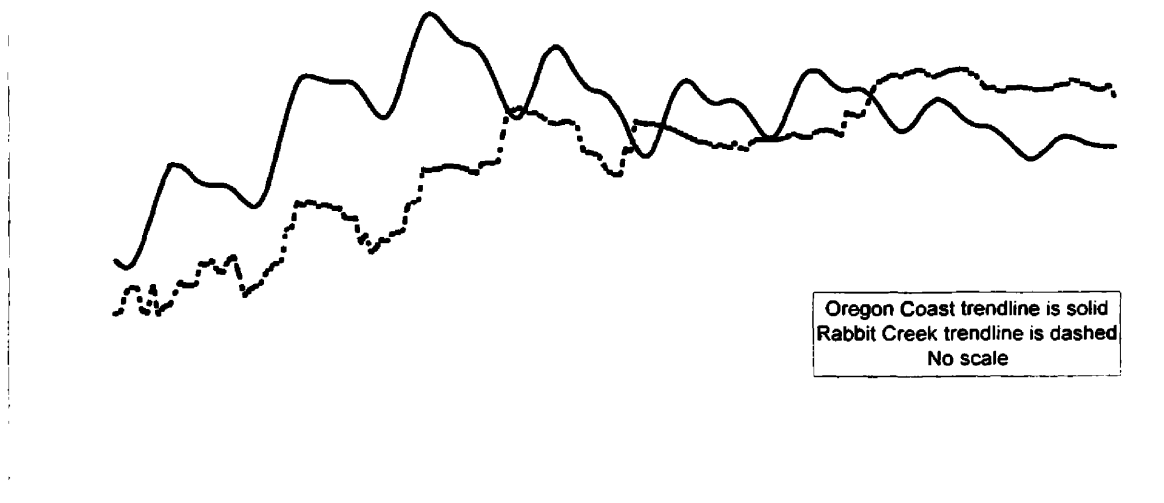
08/28/2001 6:52 AM	3.93	9449.948365
08/28/2001 7:07 AM	3.94	9424.331474
08/28/2001 8:02 PM	3.85	9644.857934
08/28/2001 8:17 PM	3.93	9450.090638
08/28/2001 8:32 PM	3.88	9572.773493
08/28/2001 8:47 PM	3.92	9475.855548
08/28/2001 9:02 PM	3.84	9671.702652
08/28/2001 9:17 PM	3.94	9424.481293
08/28/2001 9:32 PM	3.80	9772.697801
08/28/2001 9:47 PM	3.83	9698.694441
08/28/2001 10:02 PM	3.82	9721.946136
08/28/2001 10:17 PM	3.92	9475.871497
08/28/2001 10:32 PM	3.96	9377.281245
08/28/2001 10:47 PM	3.92	9475.876814
08/28/2001 11:02 PM	3.84	9671.724358
08/28/2001 11:17 PM	3.91	9498.073892
08/28/2001 11:32 PM	3.86	9622.013498
08/28/2001 11:47 PM	3.87	9595.457005
08/29/2001 12:02 AM	3.88	9572.81109
08/29/2001 12:17 AM	3.99	9309.140251
08/29/2001 12:32 AM	3.92	9475.895422
08/29/2001 12:47 AM	3.87	9595.467772
08/29/2001 1:02 AM	3.92	9475.900738
08/29/2001 1:17 AM	3.95	9402.673849
08/29/2001 1:32 AM	3.95	9402.676487
08/29/2001 1:47 AM	3.95	9402.679125
08/29/2001 2:02 AM	3.95	9402.681763
08/29/2001 3:47 AM	3.72	9985.30496
08/29/2001 4:02 AM	4.00	9284.31706
08/29/2001 4:17 AM	2.70	13755.90833
08/29/2001 4:32 AM	3.83	9698.767902
08/29/2001 4:47 AM	3.89	9546.573359
08/29/2001 5:02 AM	3.85	9644.955339
08/29/2001 5:17 AM	3.89	9546.578716
08/29/2001 5:32 AM	3.87	9595.518917
08/29/2001 5:47 AM	3.92	9475.951246
08/29/2001 6:02 AM	3.97	9355.728422
08/29/2001 6:17 AM	3.89	9546.589428
08/29/2001 6:32 AM	3.74	9932.352358
08/29/2001 6:47 AM	3.89	9546.594784
08/29/2001 7:02 AM	3.85	9644.976984
08/29/2001 7:17 AM	3.95	9402.737155
08/29/2001 7:32 AM	3.88	9572.891654
08/29/2001 7:47 AM	3.92	9475.972512
08/29/2001 8:02 AM	3.84	9671.822034
08/29/2001 8:17 AM	3.84	9671.824747
08/29/2001 8:32 AM	3.74	9932.374649
08/29/2001 8:47 AM	3.91	9498.175143
08/29/2001 9:02 AM	3.89	9546.618887
08/29/2001 9:17 AM	3.93	9450.228493
08/29/2001 9:32 AM	3.73	9956.76972
08/29/2001 9:47 AM	3.76	9875.954554

08/28/2001 7:32 PM	3.80	9772.67587
08/28/2001 7:47 PM	3.83	9698.67267
08/29/2001 10:17 AM	3.74	9932.39415
08/29/2001 10:32 AM	3.73	9956.78089
08/29/2001 10:47 AM	3.88	9572.92656
08/29/2001 11:02 AM	3.80	9772.84585
08/29/2001 11:17 AM	3.76	9875.97118
08/29/2001 11:32 AM	3.81	9749.3589
08/29/2001 11:47 AM	3.60	10315.5603
08/29/2001 12:02 PM	3.79	9800.40816
08/29/2001 12:17 PM	3.70	10038.9523
08/29/2001 12:32 PM	3.50	10612.4846
08/29/2001 12:47 PM	3.75	9904.12452
08/29/2001 1:02 PM	3.83	9698.86041
08/29/2001 1:17 PM	3.82	9722.1125
08/29/2001 1:32 PM	3.72	9985.41421
08/29/2001 1:47 PM	3.80	9772.876
08/29/2001 2:02 PM	3.40	10922.1131
08/29/2001 2:17 PM	3.58	10372.7514
08/29/2001 2:32 PM	3.87	9595.61582

Rabbit Creek velocity hydrograph plotted with Oregon coast tide stage data. The measurements are plotted over time; the same one week period for each data set is plotted as the beginning of the week on the left. Data was zeroed to fit on the same y-axis scale (velocity and stage as arbitrary values). The second plot on the bottom shows the data with a moving average to better represent data correlation.



Rabbit Creek and Oregon Coast Hydrographs  
 (Data is a moving average with a factor of 50)



## Bobber Tests

3:30 pm on 08-25-01	
Trial	Time (sec)
1	4
2	2
3	3
4	3
5	3
6	2
7	3
8	4
9	5
10	3
AVG time (sec)	3.2
AVG vel (ft/sec)	3.1
x-sect A (sq ft)	1.215
0.85 coef	0.85
Q (cfs)	3.2
m <sup>3</sup> /sec	0.091

2:00 pm on 01-13-02	
Trial	Time (sec)
1	4
2	4
3	6
4	4
5	6
6	3
7	4
8	5
9	4
10	6
AVG time (sec)	4.6
AVG vel (ft/sec)	2.17
x-sect A (sq ft)	1.215
0.85 coef	0.85
Q (cfs)	2.2
m <sup>3</sup> /sec	0.0623

12:25 pm on 04-08-02	
Trial	Time (sec)
1	4
2	3
3	3
4	4
5	3
6	3
7	4
8	4
9	3
10	3
AVG time (sec)	3.4
AVG vel (ft/sec)	2.94
x-sect A (sq ft)	1.215
0.85 coef	0.85
Q (cfs)	3.0
m <sup>3</sup> /sec	0.085

12:30 pm on 07-16-02	
Trial	Time (sec)
1	4
2	3
3	4
4	4
5	4
6	4
7	4
8	4
9	4
10	4
AVG time (sec)	3.9
AVG vel (ft/sec)	2.56
x-sect A (sq ft)	1.215
0.85 coef	0.85
Q (cfs)	2.6
m <sup>3</sup> /sec	0.075

1:45 pm on 10-05-01	
Trial	Time (sec)
1	4
2	4
3	5
4	5
5	4
6	4
7	4
8	4
9	4
10	4
AVG time (sec)	4.2
AVG vel (ft/sec)	2.38
x-sect A (sq ft)	1.215
0.85 coef	0.85
Q (cfs)	2.5
m <sup>3</sup> /sec	0.071

12:45 pm on 02-23-02	
Trial	Time (sec)
1	3.5
2	4
3	3.5
4	4
5	3.5
6	3
7	3.5
8	3
9	3.5
10	3.5
AVG time (sec)	3.5
AVG vel (ft/sec)	2.86
x-sect A (sq ft)	1.215
0.85 coef	0.85
Q (cfs)	3.0
m <sup>3</sup> /sec	0.085

11:50 am on 06-04-02	
Trial	Time (sec)
1	3
2	3
3	4
4	3
5	3
6	4
7	4
8	4
9	3
10	4
AVG time (sec)	3.5
AVG vel (ft/sec)	2.86
x-sect A (sq ft)	1.215
0.85 coef	0.85
Q (cfs)	3.0
m <sup>3</sup> /sec	0.085

## Water Level Elevations

(height in meters above sea level)

Well ID	August	October	January	February	April	June	July
ULA	2247.88923	2247.92308	2247.92615	2247.94929	2247.98006	2247.91852	2247.93
ULB	2247.94769	2247.96308	2247.98462	2248.01698	2248.0416	2247.99237	2247.87
URA	2247.78769	2247.87385	2247.91385	2247.94929	2247.97822	2247.91545	2247.78
URB	2247.68615	2247.75385	2247.80308	2247.82006	2247.84006	2247.77083	2247.71
MLA	2247.51615	2247.57769	2247.58615	2247.58006	2247.60868	2247.61391	2247.63
MLB	2247.32923	2247.38462	2247.40923	2247.42314	2247.43237	2247.45083	2247.42
MRA	2247.50385	2247.53769	2247.52923	2247.5216	2247.56437	2247.59545	2247.60
MRB	2248.10077	2248.10385	2248.14062	2248.15545	2248.19175	2248.14929	2248.10
LLA	2246.76308	2246.77077	2246.79231	2246.81083	2246.74622	2246.76775	2246.75
LI	no water	no water	2243.62677	2243.63237	2243.70006	2243.6416	no water
LRA	no water	no water	no water	no water	no water	no water	no water
LRB	no water	no water	no water	no water	no water	no water	no water

Staff Gauges	August	October	January	February	April	June	July
USG	2249.58462	2249.57538	2249.57148	2249.57908	2249.57938	2249.57231	2249.58
MSG	2246.96308	2246.95692	2246.96148	2246.95662	2246.96308	2246.96	2246.96
LSG	2244.85231	2244.84	2244.84769	2244.96	2244.85108	2244.84615	2244.91
MSG2	-----	2247.77846	2247.78114	2247.67692	2247.78769	2247.78462	2247.78

## Appendix C: Water chemistry data: cations, anions, and field meter data.

All data are reported in mg/L.

Cation analyses by ICP 200 at XRAL Laboratories, Don Mills, Ontario, Canada.

August

Element	Be	Na	Mg	Al	P	K	Ca	Sc	Ti	V	Cr	Mn
Detection Limit	0.01	0.05	0.05	0.05	0.05	0.10	0.05	0.00	0.01	0.01	0.01	0.01

Well ID

082101 ula	<dl	311.00	0.14	<dl	<dl	12.12	0.95	<dl	<dl	<dl	<dl	0.02
082101 ula field dup	<dl	305.00	0.16	<dl	0.08	12.49	0.99	<dl	<dl	<dl	<dl	0.02
082101 ulb	<dl	305.00	0.29	<dl	<dl	11.79	1.47	<dl	<dl	<dl	<dl	0.09
082101 ura	<dl	357.00	0.21	<dl	<dl	12.81	1.52	<dl	<dl	<dl	<dl	0.02
082101 urb	<dl	341.00	0.29	<dl	<dl	14.92	1.30	<dl	<dl	<dl	<dl	0.02
082101 urb field dup	<dl	337.00	0.27	<dl	<dl	13.36	1.09	<dl	<dl	<dl	<dl	0.02
082101 mla	<dl	317.00	0.05	<dl	<dl	11.95	0.83	<dl	<dl	<dl	<dl	0.01
082101 mla field dup	<dl	316.00	0.06	<dl	<dl	12.05	0.71	<dl	<dl	<dl	<dl	0.01
082101 mlb	<dl	340.00	0.06	<dl	0.05	12.42	0.77	<dl	<dl	<dl	<dl	0.03
082101 mra	<dl	346.00	0.09	<dl	<dl	12.41	0.72	<dl	<dl	<dl	<dl	0.02
082101 mrb	<dl	481.00	0.32	<dl	<dl	20.06	2.51	<dl	<dl	<dl	<dl	0.14
082101 lla	<dl	323.00	0.13	<dl	<dl	12.68	0.97	<dl	<dl	<dl	<dl	0.03
082101 lla field dup	<dl	330.00	0.19	<dl	<dl	12.44	0.94	<dl	<dl	<dl	<dl	0.03

continued

Element	Fe	Co	Ni	Cu	Zn	As	Sr	Y	Zr	Mo	Ag	Cd
Detection Limit	0.05	0.01	0.01	0.01	0.01	0.03	0.00	0.01	0.01	0.01	0.00	0.01

Well ID

082101 ula	0.06	0.03	<dl	0.01	0.01	1.19	0.00	<dl	<dl	0.02	<dl	<dl
082101 ula field dup	<dl	<dl	<dl	<dl	0.01	1.22	0.00	<dl	<dl	0.03	<dl	<dl
082101 ulb	0.24	0.02	<dl	<dl	0.01	1.37	0.01	<dl	<dl	0.02	0.00	0.01
082101 ura	0.09	0.02	<dl	<dl	0.02	1.20	0.01	<dl	<dl	0.03	<dl	0.02
082101 urb	0.06	0.03	<dl	0.01	0.03	1.35	0.01	<dl	<dl	0.03	<dl	0.02
082101 urb field dup	0.06	0.03	<dl	<dl	0.02	1.40	0.01	<dl	<dl	0.03	0.01	0.01
082101 mla	<dl	0.02	<dl	0.01	0.08	1.34	0.00	<dl	<dl	0.02	0.02	0.02
082101 mla field dup	<dl	0.03	<dl	<dl	0.06	1.22	0.00	<dl	<dl	0.02	0.00	0.01
082101 mlb	<dl	0.01	<dl	0.01	0.01	1.49	0.00	<dl	<dl	0.03	0.01	<dl
082101 mra	<dl	0.03	<dl	<dl	0.03	1.52	0.00	<dl	<dl	0.03	<dl	0.03
082101 mrb	0.23	<dl	<dl	<dl	0.05	0.70	0.01	<dl	<dl	0.01	0.01	0.03
082101 lla	<dl	<dl	<dl	<dl	0.03	1.26	0.00	<dl	<dl	0.02	0.01	<dl
082101 lla field dup	<dl	<dl	<dl	<dl	0.05	1.28	0.00	<dl	<dl	0.02	0.00	<dl

continued

Element	Sn	Sb	Ba	La	W	Pb	Bi	B	Si
Detection Limit	0.05	0.05	0.01	0.01	0.05	0.03	0.05	0.01	0.10

Well ID

082101 ula	<dl	<dl	0.03	0.01	0.25	<dl	<dl	2.01	82.86
082101 ula field dup	<dl	0.11	0.04	0.02	0.23	<dl	<dl	1.98	81.47
082101 ulb	<dl	<dl	0.05	<dl	0.24	<dl	<dl	1.95	71.78
082101 ura	<dl	0.08	0.02	<dl	0.28	<dl	<dl	2.25	58.76
082101 urb	<dl	<dl	0.05	0.02	0.29	<dl	<dl	2.19	77.19
082101 urb field dup	<dl	<dl	0.04	<dl	0.26	<dl	<dl	2.22	76.11
082101 mla	<dl	<dl	0.04	<dl	0.25	<dl	<dl	2.09	107.00
082101 mla field dup	<dl	0.13	0.05	<dl	0.24	<dl	<dl	2.05	104.90
082101 mlb	<dl	<dl	0.04	<dl	0.29	<dl	<dl	2.31	98.62
082101 mra	<dl	<dl	0.03	<dl	0.30	<dl	<dl	2.22	96.81
082101 mrb	<dl	<dl	0.28	0.01	0.27	<dl	<dl	3.14	52.13
082101 lla	<dl	0.18	0.03	<dl	0.28	<dl	<dl	2.09	81.74
082101 lla field dup	<dl	0.11	0.07	0.01	0.27	<dl	<dl	2.07	81.61

October

Element	Be	Na	Mg	Al	P	K	Ca	Sc	Ti	V	Cr	Mn
Detection Limit	0.01	0.05	0.05	0.05	0.05	0.10	0.05	0.00	0.01	0.01	0.01	0.01

Well ID

100601 ula	<dl	319.00	0.11	<dl	<dl	12.08	0.80	<dl	<dl	<dl	<dl	0.01
100601 ulb	<dl	312.00	0.28	<dl	<dl	11.42	1.38	<dl	<dl	<dl	<dl	0.08
100601 ulb field dup	<dl	313.00	0.31	<dl	<dl	12.02	1.35	<dl	<dl	<dl	<dl	0.06
100601 ura	<dl	355.00	0.26	<dl	0.05	13.48	1.45	<dl	<dl	<dl	<dl	0.03
100601 ura field dup	<dl	374.00	0.27	<dl	<dl	13.54	1.43	<dl	<dl	<dl	<dl	0.03
100601 urb	<dl	342.00	0.35	<dl	<dl	12.68	1.18	<dl	<dl	<dl	<dl	0.02
100601 mla	<dl	322.00	0.11	<dl	<dl	12.30	0.68	<dl	<dl	<dl	<dl	0.01
100601 mlb	<dl	341.00	0.17	<dl	0.05	12.69	0.96	<dl	<dl	<dl	<dl	0.07
100601 mra	<dl	333.00	0.08	<dl	<dl	13.12	0.67	<dl	<dl	<dl	<dl	0.02
100601 mra field dup	<dl	345.00	0.07	<dl	<dl	13.01	0.65	<dl	<dl	<dl	<dl	0.02
100601 mrb	<dl	570.00	0.51	<dl	<dl	21.03	3.03	<dl	<dl	<dl	<dl	0.18
100601 lla	<dl	303.00	0.18	<dl	<dl	12.76	1.05	<dl	<dl	<dl	<dl	0.03

Surface Water

100701 source	<dl	455.00	<dl	0.14	<dl	13.31	0.34	<dl	<dl	<dl	<dl	<dl
100701 source field dup	<dl	453.00	<dl	0.08	<dl	13.26	0.33	<dl	<dl	<dl	<dl	<dl
100701 location 1	<dl	444.00	<dl	0.16	<dl	13.64	0.41	<dl	<dl	<dl	<dl	<dl
100701 location 2	<dl	430.00	0.07	<dl	<dl	14.17	0.48	<dl	<dl	<dl	<dl	<dl
100701 location 3	<dl	433.00	0.07	<dl	<dl	13.89	0.49	<dl	<dl	<dl	<dl	<dl
100701 location 4	<dl	431.00	<dl	<dl	<dl	14.00	0.50	<dl	<dl	<dl	<dl	<dl

continued

Element	Fe	Co	Ni	Cu	Zn	As	Sr	Y	Zr	Mo	Ag	Cd
Detection Limit	0.05	0.01	0.01	0.01	0.01	0.03	0.00	0.01	0.01	0.01	0.00	0.01

Well ID

100601 ula	<dl	<dl	<dl	<dl	0.03	1.22	0.00	<dl	0.01	0.02	<dl	<dl
100601 ulb	0.19	0.03	<dl	<dl	0.01	1.26	0.01	<dl	<dl	0.02	<dl	0.02
100601 ulb field dup	0.15	0.02	<dl	<dl	0.01	1.23	0.01	<dl	0.01	0.02	<dl	0.02
100601 ura	0.13	<dl	<dl	<dl	0.01	1.49	0.01	<dl	<dl	0.03	<dl	0.02
100601 ura field dup	0.13	<dl	<dl	<dl	0.01	1.42	0.01	<dl	<dl	0.03	0.01	<dl
100601 urb	0.07	0.04	<dl	<dl	<dl	1.40	0.01	<dl	<dl	0.03	<dl	0.02
100601 mla	<dl	0.04	<dl	<dl	0.05	1.29	0.00	<dl	<dl	0.02	0.00	<dl
100601 mlb	0.15	0.04	<dl	<dl	0.01	1.53	0.00	<dl	<dl	0.03	0.00	<dl
100601 mra	<dl	<dl	<dl	<dl	0.02	1.38	0.00	<dl	<dl	0.03	0.01	<dl
100601 mra field dup	<dl	<dl	<dl	<dl	0.02	1.46	0.00	<dl	<dl	0.03	0.01	0.01
100601 mrb	0.59	<dl	<dl	<dl	0.03	0.47	0.02	<dl	<dl	<dl	<dl	0.02
100601 lla	0.06	0.03	<dl	<dl	0.04	1.32	0.00	<dl	0.01	0.02	0.01	0.02

Surface Water

100701 source	<dl	0.01	<dl	<dl	0.03	1.67	0.00	<dl	<dl	0.03	0.00	0.01
100701 source field dup	<dl	0.03	<dl	<dl	0.02	1.79	0.00	<dl	<dl	0.03	0.01	0.02
100701 location 1	<dl	<dl	<dl	<dl	0.02	1.79	0.00	<dl	<dl	0.02	<dl	0.03
100701 location 2	<dl	0.02	<dl	<dl	0.01	1.82	0.00	<dl	<dl	0.03	0.00	<dl
100701 location 3	<dl	0.02	<dl	<dl	0.02	1.71	0.00	<dl	<dl	0.03	0.01	0.02
100701 location 4	<dl	0.03	<dl	<dl	0.01	1.83	0.00	<dl	<dl	0.03	<dl	<dl

continued

Element	Sn	Sb	Ba	La	W	Pb	Bi	B	Si
Detection Limit	0.05	0.05	0.01	0.01	0.05	0.03	0.05	0.01	0.10

Well ID

100601 ula	<dl	<dl	0.18	<dl	0.26	<dl	<dl	2.06	82.84
100601 ulb	<dl	<dl	0.05	<dl	0.23	<dl	<dl	1.98	71.59
100601 ulb field dup	<dl	<dl	0.05	<dl	0.21	<dl	<dl	2.10	76.60
100601 ura	<dl	<dl	0.07	0.02	0.29	<dl	0.07	2.51	63.43
100601 ura field dup	<dl	<dl	0.05	<dl	0.30	<dl	0.07	2.47	62.68
100601 urb	<dl	<dl	0.04	<dl	0.27	<dl	<dl	2.31	71.12
100601 mla	<dl	<dl	0.07	<dl	0.24	<dl	0.06	2.07	106.70
100601 mlb	<dl	0.11	0.05	<dl	0.29	<dl	<dl	2.27	91.12
100601 mra	<dl	<dl	0.05	<dl	0.28	<dl	<dl	2.30	102.00
100601 mra field dup	<dl	0.08	0.05	<dl	0.27	<dl	<dl	2.26	99.54
100601 mrb	<dl	<dl	0.38	<dl	0.16	<dl	<dl	3.49	46.75
100601 lla	<dl	<dl	0.09	<dl	0.22	<dl	<dl	2.02	79.26

Surface Water

100701 source	<dl	0.06	0.08	0.01	0.38	<dl	<dl	2.97	130.00
100701 source field dup	<dl	<dl	0.10	<dl	0.36	<dl	<dl	2.90	127.00
100701 location 1	<dl	0.10	0.06	<dl	0.37	<dl	<dl	2.88	128.00
100701 location 2	<dl	0.19	0.04	<dl	0.39	<dl	<dl	2.94	134.80
100701 location 3	<dl	0.22	0.04	<dl	0.32	<dl	<dl	3.11	139.80
100701 location 4	<dl	0.17	0.05	<dl	0.36	<dl	<dl	2.97	133.70

## January

Element	Be	Na	Mg	Al	P	K	Ca	Sc	Ti	V	Cr	Mn
Detection Limit	0.01	0.05	0.05	0.05	0.05	0.10	0.05	0.00	0.01	0.01	0.01	0.01

## Well ID

011302 ula	<dl	378.00	0.78	<dl	0.05	10.90	3.97	<dl	0.02	<dl	<dl	0.20
011302 ula field dup	<dl	379.00	0.76	0.09	0.06	13.00	3.94	<dl	<dl	<dl	<dl	0.20
011302 ulb	<dl	365.00	0.78	0.09	<dl	9.37	4.11	<dl	<dl	<dl	<dl	0.42
011302 ura	<dl	636.00	0.73	0.12	<dl	25.70	6.08	<dl	<dl	<dl	<dl	0.14
011302 urb	<dl	575.00	0.78	0.06	0.08	19.20	5.04	<dl	<dl	<dl	<dl	0.12
011302 mla	<dl	313.00	0.09	<dl	<dl	9.74	0.98	<dl	<dl	<dl	<dl	0.01
011302 mla field dup	<dl	316.00	<dl	<dl	<dl	9.93	0.89	<dl	<dl	<dl	<dl	0.01
011302 mlb	<dl	383.00	0.19	0.06	<dl	12.70	2.01	<dl	0.01	<dl	<dl	0.18
011302 mra	<dl	326.00	0.08	<dl	<dl	11.90	0.86	<dl	<dl	<dl	<dl	0.04
011302 mrb	<dl	493.00	0.41	0.08	<dl	17.70	2.58	<dl	0.02	<dl	<dl	0.17
011302 lla	<dl	316.00	0.65	0.20	<dl	9.58	3.85	<dl	<dl	<dl	<dl	0.14

## Surface Water

011402 source	<dl	418.00	<dl	0.26	<dl	10.50	0.52	<dl	<dl	<dl	<dl	<dl
011402 source field dup	<dl	426.00	<dl	0.37	<dl	9.88	0.35	<dl	<dl	<dl	<dl	<dl
011402 location 1	<dl	462.00	<dl	0.25	<dl	11.40	0.50	<dl	<dl	<dl	<dl	<dl
011402 location 2	<dl	429.00	<dl	0.13	<dl	12.10	0.58	<dl	<dl	<dl	<dl	<dl
011402 location 3	<dl	432.00	<dl	0.19	<dl	10.30	0.57	<dl	<dl	<dl	<dl	<dl
011402 location 4	<dl	430.00	<dl	0.16	<dl	12.60	0.74	<dl	<dl	<dl	<dl	<dl

*continued*

Element	Fe	Co	Ni	Cu	Zn	As	Sr	Y	Zr	Mo	Ag	Cd
Detection Limit	0.05	0.01	0.01	0.01	0.01	0.03	0.00	0.01	0.01	0.01	0.00	0.01

## Well ID

011302 ula	1.35	<dl	<dl	<dl	0.02	1.05	0.02	<dl	<dl	0.02	<dl	<dl
011302 ula field dup	1.43	<dl	<dl	<dl	0.02	1.05	0.02	<dl	<dl	0.02	<dl	<dl
011302 ulb	1.72	<dl	<dl	<dl	0.02	1.64	0.02	<dl	<dl	0.04	<dl	<dl
011302 ura	0.85	<dl	<dl	0.01	0.02	3.30	0.03	<dl	<dl	0.07	<dl	<dl
011302 urb	0.73	<dl	<dl	<dl	0.02	3.17	0.03	<dl	<dl	0.08	<dl	<dl
011302 mla	<dl	<dl	<dl	<dl	0.05	1.44	0.00	<dl	<dl	0.03	<dl	<dl
011302 mla field dup	<dl	<dl	<dl	0.01	0.06	1.45	0.00	<dl	<dl	0.03	<dl	<dl
011302 mlb	0.53	<dl	<dl	<dl	0.03	1.79	0.01	<dl	<dl	0.04	<dl	<dl
011302 mra	<dl	<dl	<dl	<dl	0.03	1.57	0.00	<dl	<dl	0.03	0.00	<dl
011302 mrb	0.87	<dl	<dl	<dl	0.02	0.17	0.02	<dl	<dl	<dl	<dl	<dl
011302 lla	0.23	<dl	<dl	<dl	0.02	1.35	0.02	<dl	<dl	0.03	0.00	<dl

## Surface Water

011402 source	<dl	<dl	<dl	<dl	0.03	1.86	0.00	<dl	<dl	0.03	<dl	<dl
011402 source field dup	<dl	<dl	<dl	<dl	0.03	1.81	0.00	<dl	<dl	0.03	<dl	<dl
011402 location 1	<dl	<dl	<dl	<dl	0.02	1.86	0.00	<dl	0.13	0.03	<dl	<dl
011402 location 2	<dl	<dl	<dl	0.01	0.03	1.82	0.00	<dl	<dl	0.03	<dl	<dl
011402 location 3	<dl	<dl	<dl	<dl	0.03	1.83	0.00	<dl	<dl	0.03	<dl	<dl
011402 location 4	<dl	<dl	<dl	<dl	0.05	1.84	0.00	<dl	<dl	0.03	<dl	<dl









continued

Element	Sn	Sb	Ba	La	W	Pb	Bi	B	Si
Detection Limit	0.05	0.05	0.01	0.01	0.05	0.03	0.05	0.01	0.10

Well ID

040802 ula	<dl	<dl	0.23	<dl	0.14	<dl	<dl	2.76	58.70
040802 ula field dup	<dl	<dl	0.21	<dl	0.14	<dl	<dl	2.70	57.43
040802 ulb	<dl	0.10	0.39	<dl	0.17	<dl	<dl	3.43	55.06
040802 ura	<dl	<dl	0.18	<dl	0.36	<dl	<dl	4.32	43.68
040802 urb	<dl	<dl	0.22	<dl	0.31	<dl	<dl	3.44	52.85
040802 mia	<dl	0.09	0.06	<dl	0.29	<dl	<dl	2.22	100.58
040802 mlb	<dl	0.08	0.07	<dl	0.31	<dl	<dl	2.54	87.43
040802 mra	<dl	0.09	0.12	<dl	0.31	<dl	<dl	2.52	82.40
040802 mrb	<dl	<dl	0.27	<dl	0.16	<dl	<dl	3.40	41.15
040802 lla	<dl	0.06	0.18	<dl	0.18	<dl	<dl	2.39	51.82
040803 li	<dl	0.12	0.13	<dl	0.39	<dl	<dl	3.52	45.48

Surface Water

040802 source	<dl	0.09	0.10	<dl	0.39	<dl	<dl	3.06	114.74
040802 source field dup	<dl	0.10	0.08	<dl	0.39	<dl	<dl	3.09	116.94
040802 location 1	<dl	0.10	0.06	<dl	0.38	<dl	<dl	3.08	122.68
040802 location 2	<dl	0.10	0.03	<dl	0.39	<dl	<dl	3.12	124.14
040802 location 3	<dl	0.10	0.04	<dl	0.37	<dl	<dl	3.04	121.84
040803 location 4	<dl	0.10	0.04	<dl	0.38	<dl	<dl	3.04	121.53
040802 field blank	<dl	<dl	<dl	<dl	<dl	<dl	<dl	<dl	<dl

June

Element	Be	Na	Mg	Al	P	K	Ca	Sc	Ti	V	Cr	Mn
Detection Limit	0.01	0.05	0.05	0.05	0.05	0.10	0.05	0.00	0.01	0.01	0.01	0.01

Well ID

060402 ula	<dl	328.26	0.81	<dl	<dl	15.50	4.78	<dl	0.04	<dl	<dl	0.36
060402 ula field dup	<dl	333.21	0.85	<dl	<dl	15.63	5.51	<dl	0.04	<dl	<dl	0.37
060402 ulb	<dl	291.91	0.72	0.28	<dl	13.88	4.30	<dl	0.03	<dl	<dl	0.25
060402 ura	<dl	353.67	0.38	0.35	<dl	15.03	2.89	<dl	0.03	<dl	<dl	0.09
060402 urb	<dl	324.35	0.58	0.17	<dl	14.59	3.12	<dl	0.02	<dl	<dl	0.08
060402 mia	<dl	252.39	0.05	<dl	<dl	11.74	0.67	<dl	<dl	<dl	<dl	0.01
060402 mlb	<dl	276.55	0.14	0.08	<dl	12.62	1.10	<dl	<dl	<dl	<dl	0.07
060402 mra	<dl	288.99	0.12	<dl	<dl	12.11	0.98	<dl	<dl	<dl	<dl	0.08
060402 mrb	<dl	392.08	0.40	<dl	<dl	19.49	2.47	<dl	0.02	<dl	<dl	0.16
060402 lla	<dl	259.04	0.26	0.13	<dl	11.88	1.61	<dl	<dl	<dl	<dl	0.21

Surface Water

060402 source	<dl	356.62	<dl	0.23	<dl	12.70	0.43	<dl	<dl	<dl	<dl	<dl
060402 source dup	<dl	351.60	<dl	0.22	<dl	12.55	0.29	<dl	<dl	<dl	<dl	<dl
060402 location 1	<dl	352.72	<dl	0.19	<dl	12.67	0.40	<dl	<dl	<dl	<dl	<dl
060402 location 2	<dl	347.68	<dl	0.14	<dl	12.82	0.47	<dl	<dl	<dl	<dl	<dl
060402 location 3	<dl	357.73	<dl	0.13	<dl	13.21	0.52	<dl	<dl	<dl	<dl	<dl
060402 location 4	<dl	351.62	<dl	0.14	<dl	12.88	0.51	<dl	<dl	<dl	<dl	<dl

*continued*

Element	Fe	Co	Ni	Cu	Zn	As	Sr	Y	Zr	Mo	Ag	Cd
Detection Limit	0.05	0.01	0.01	0.01	0.01	0.03	0.00	0.01	0.01	0.01	0.00	0.01

Well ID

060402 ula	2.05	<dl	<dl	<dl	0.02	1.69	0.02	<dl	<dl	0.04	<dl	<dl
060402 ula field dup	1.93	<dl	<dl	<dl	0.03	1.71	0.02	<dl	<dl	0.03	0.00	<dl
060402 ulb	2.10	<dl	<dl	<dl	0.03	2.51	0.02	<dl	<dl	0.05	0.00	<dl
060402 ura	0.79	<dl	<dl	<dl	0.02	2.59	0.01	<dl	<dl	0.05	0.00	<dl
060402 urb	0.61	<dl	<dl	<dl	0.02	2.16	0.01	<dl	<dl	0.05	<dl	<dl
060402 mla	<dl	<dl	<dl	<dl	0.07	1.43	<dl	<dl	<dl	0.03	<dl	<dl
060402 mlb	0.32	<dl	<dl	<dl	0.01	1.51	0.00	<dl	<dl	0.03	<dl	<dl
060402 mra	<dl	<dl	<dl	<dl	0.04	1.75	0.00	<dl	<dl	0.04	<dl	<dl
060402 mrb	0.52	<dl	<dl	<dl	0.03	0.57	0.01	<dl	<dl	<dl	<dl	<dl
060402 lla	0.20	<dl	<dl	<dl	0.01	1.43	0.01	<dl	<dl	0.03	<dl	<dl

Surface Water

060402 source	<dl	<dl	<dl	<dl	0.03	1.90	0.00	<dl	<dl	0.03	<dl	<dl
060402 source dup	<dl	<dl	<dl	<dl	0.03	1.91	0.00	<dl	<dl	0.03	0.00	<dl
060402 location 1	<dl	<dl	<dl	<dl	0.02	1.89	0.00	<dl	<dl	0.03	<dl	<dl
060402 location 2	<dl	<dl	<dl	<dl	0.02	1.86	<dl	<dl	<dl	0.03	0.00	<dl
060402 location 3	<dl	<dl	<dl	<dl	0.03	1.88	<dl	<dl	<dl	0.03	0.00	<dl
060402 location 4	<dl	<dl	<dl	<dl	0.03	1.87	0.00	<dl	<dl	0.03	0.00	<dl

*continued*

Element	Sn	Sb	Ba	La	W	Pb	Bi	B	Si
Detection Limit	0.05	0.05	0.01	0.01	0.05	0.03	0.05	0.01	0.10

Well ID

060402 ula	<dl	<dl	0.04	<dl	0.26	<dl	<dl	2.95	68.00
060402 ula field dup	<dl	<dl	0.04	<dl	0.23	<dl	<dl	2.97	67.86
060402 ulb	<dl	0.06	0.05	<dl	0.32	<dl	<dl	2.87	60.57
060402 ura	<dl	<dl	0.05	<dl	0.47	<dl	<dl	3.56	48.13
060402 urb	<dl	<dl	0.03	<dl	0.41	<dl	<dl	3.21	57.21
060402 mla	<dl	0.09	0.06	<dl	0.29	<dl	<dl	2.34	99.64
060402 mlb	<dl	0.07	0.05	<dl	0.33	<dl	<dl	2.56	86.06
060402 mra	<dl	0.11	0.04	<dl	0.32	<dl	<dl	2.69	85.84
060402 mrb	<dl	<dl	0.05	<dl	0.25	<dl	<dl	3.65	47.79
060402 lla	<dl	<dl	0.04	<dl	0.28	<dl	<dl	2.35	63.19

Surface Water

060402 source	<dl	0.10	0.07	<dl	0.39	<dl	<dl	3.32	115.76
060402 source dup	<dl	0.10	0.11	<dl	0.40	<dl	<dl	3.31	119.49
060402 location 1	<dl	0.10	0.02	<dl	0.40	<dl	<dl	3.26	127.34
060402 location 2	<dl	0.10	0.04	<dl	0.39	<dl	<dl	3.19	122.85
060402 location 3	<dl	0.10	0.04	<dl	0.39	<dl	<dl	3.24	118.95
060402 location 4	<dl	0.10	0.04	<dl	0.38	<dl	<dl	3.17	120.68



*continued*

Element	Sn	Sb	Ba	La	W	Pb	Bi	B	Si
Detection Limit	0.05	0.05	0.01	0.01	0.05	0.03	0.05	0.01	0.10

**Well ID**

071602 ula	<dl	0.08	0.07	<dl	0.30	<dl	<dl	2.63	88.70
071602 ula field dup	<dl	0.08	0.02	<dl	0.29	<dl	<dl	2.54	84.65
071602 ulb	<dl	0.05	0.07	<dl	0.29	<dl	<dl	2.68	70.41
071602 ura	<dl	0.05	0.24	<dl	0.39	<dl	<dl	3.51	57.19
071602 urb	<dl	0.11	0.25	<dl	0.29	<dl	<dl	2.63	84.56
071602 mia	<dl	0.09	0.24	<dl	0.28	<dl	<dl	2.44	102.44
071602 mlb	<dl	0.09	0.25	<dl	0.30	<dl	<dl	2.51	94.19
071602 mra	<dl	0.10	0.25	<dl	0.32	<dl	<dl	2.79	90.55
071602 mrb	<dl	<dl	0.23	<dl	0.27	<dl	<dl	3.59	51.18
071602 Ila	<dl	0.08	0.26	<dl	0.30	<dl	<dl	2.61	78.76

**Surface Water**

071602 source	<dl	0.10	0.10	<dl	0.39	<dl	<dl	3.41	120.07
071602 source field dup	<dl	0.10	0.02	<dl	0.39	<dl	<dl	3.39	119.72
071602 location 1	<dl	0.10	0.06	<dl	0.40	<dl	<dl	3.49	130.40
071602 location 2	<dl	0.10	0.06	<dl	0.40	<dl	<dl	3.48	128.34
071602 location 3	<dl	0.10	0.16	<dl	0.39	<dl	<dl	3.38	125.90
071602 location 4	<dl	0.11	0.12	<dl	0.40	<dl	<dl	3.47	129.78
071602 spring ss	<dl	0.09	0.07	<dl	0.33	<dl	<dl	2.83	106.18
071602 field blank	<dl	<dl	<dl	<dl	<dl	<dl	<dl	0.02	<dl

**ANIONS****August (mg/L)**

Sample Name	F	Cl	PO <sub>4</sub>	SO <sub>4</sub>	alk (mg/L)
<b>Well ID</b>					
082101 ula	19.41	202.51	<dl	13.13	360.00
082101 ula field dup	19.44	202.69	<dl	13.00	540.00
082101 ulb	17.40	199.51	<dl	<dl	220.00
082101 ura	22.04	234.89	<dl	12.64	340.00
082101 urb	21.20	224.49	<dl	14.10	245.00
082101 urb field dup	21.14	223.48	<dl	14.07	290.00
082101 mla	19.58	202.96	<dl	12.93	345.00
082101 mla field dup	19.55	202.49	<dl	12.92	315.00
082101 mlb	21.51	224.90	<dl	13.37	470.00
082101 mra	20.98	222.39	<dl	14.56	250.00
082101 mrb	22.66	171.01	<dl	7.01	310.00
082101 lla	19.47	205.01	<dl	12.77	405.00
082101 lla field dup	19.51	205.22	<dl	12.68	390.00

**October**

Sample Name	F	Cl	PO <sub>4</sub>	SO <sub>4</sub>	alk (mg/L)
<b>Well ID</b>					
100601 ula	17.99	191.87	<dl	12.79	155.00
100601 ulb	17.32	187.06	<dl	12.49	143.00
100601 ulb field dup	17.76	187.52	<dl	12.51	133.00
100601 ura	21.87	235.32	<dl	14.94	135.00
100601 ura field dup	21.91	235.74	<dl	15.07	105.00
100601 urb	20.34	220.71	<dl	14.38	125.00
100601 mla	17.98	190.83	<dl	12.58	133.00
100601 mlb	19.87	209.65	<dl	13.53	120.00
100601 mra	19.24	221.15	<dl	14.43	123.00
100601 mra field dup	19.30	220.83	<dl	14.50	123.00
100601 mrb	14.64	159.66	<dl	9.18	383.00
100601 lla	18.32	193.01	<dl	12.44	120.00

**Surface Water**

100701 source	25.32	278.36	<dl	16.05	255.00
100701 source field dup	25.40	279.14	<dl	16.11	-----
100701 location 1	31.96	284.74	<dl	17.11	248.00
100701 location 2	28.26	284.34	<dl	18.17	230.00
100701 location 3	29.46	279.11	<dl	17.80	258.00
100701 location 4	28.80	282.00	<dl	18.07	240.00



## January

Sample Name	F	Cl	PO <sub>4</sub>	SO <sub>4</sub>	alk (mg/L)
-------------	---	----	-----------------	-----------------	------------

### Groundwater

011302 ula	23.05	318.73	<dl	14.06	256.00
011302 ula field dup	23.26	324.23	<dl	14.26	258.00
011302 ulb	22.54	290.42	<dl	19.34	240.00
011302 ura	39.08	576.01	<dl	35.23	338.00
011302 urb	36.01	318.89	<dl	29.69	330.00
011302 mla	20.38	216.14	<dl	12.34	228.00
011302 mla field dup	20.49	217.53	<dl	12.32	237.00
011302 mlb	24.09	282.48	<dl	14.76	258.00
011302 mra	22.41	242.86	<dl	14.97	234.00
011302 mrb	19.73	217.30	<dl	12.50	417.00
011302 lla	20.68	254.15	<dl	13.46	217.00

### Surface Water

011402 source	26.85	305.77	<dl	16.28	324.00
011402 source field dup	27.70	319.39	<dl	17.50	326.00
011402 location 1	27.70	328.67	<dl	18.34	320.00
011402 location 2	26.92	315.02	<dl	17.99	311.00
011402 location 3	26.71	314.89	<dl	17.84	309.00
011402 location 4	26.63	321.31	<dl	17.77	307.00

## February

Sample Name	F	Cl	PO <sub>4</sub>	SO <sub>4</sub>	alk (mg/L)
-------------	---	----	-----------------	-----------------	------------

## Well ID

022302 ula	26.53	374.36	<dl	20.14	263.00
022302 ula field dup	26.44	372.44	<dl	20.15	275.00
022302 ulb	24.97	342.43	<dl	26.04	254.00
022302 ura	36.37	460.93	<dl	32.86	298.00
022302 urb	37.69	537.23	<dl	34.25	345.00
022302 mla	19.07	208.42	<dl	12.90	218.00
022302 mlb	23.67	272.70	<dl	15.95	262.00
022302 mlb field dup	23.45	266.70	<dl	15.45	253.00
022302 mra	21.61	241.53	<dl	16.16	237.00
022302 mrb	29.21	318.03	<dl	3.72	386.00
022302 lla	20.17	238.43	<dl	14.64	198.00

## Surface Water

022302 source	25.98	298.41	<dl	17.05	316.00
022302 location 1	16.30	16.08	<dl	13.80	316.00
022302 location 2	19.46	222.24	<dl	18.85	301.00
022302 location 3	25.69	295.20	<dl	18.71	298.00
022302 location 4	25.96	296.94	<dl	18.88	293.00
022302 cold creek	17.05	204.10	<dl	14.10	201.00
022302 marsh	21.54	239.60	<dl	14.95	244.00

## April

Sample Name	F	Cl	PO <sub>4</sub>	SO <sub>4</sub>	alk (mg/L)
040802 ula	27.41	277.42	<dl	21.58	262.40
040802 ula field dup	27.62	278.65	<dl	21.57	251.60
040802 ulb	36.28	301.56	<dl	32.27	257.60
040802 ura	46.13	316.72	<dl	30.62	345.60
040802 urb	36.26	298.87	<dl	23.30	312.40
040802 mia	22.10	213.05	<dl	13.87	223.20
040802 mlb	24.09	224.14	<dl	14.71	245.60
040802 mra	25.34	242.49	<dl	18.00	244.00
040802 mrb	31.67	275.69	<dl	8.50	377.20
040802 lla	24.44	223.17	<dl	14.58	215.60
040802 li	24.26	303.28	<dl	20.82	248.40

## Surface Water

040802 source	29.44	265.87	<dl	17.57	315.20
040802 source field dup	29.27	266.14	<dl	18.99	327.20
040802 location 1	29.02	263.60	<dl	19.34	318.80
040802 location 2	29.41	265.87	<dl	17.51	310.80
040802 location 3	28.62	261.18	<dl	19.11	292.80
040802 location 4	28.58	260.67	<dl	19.04	306.80

## June

Sample Name	F	Cl	PO <sub>4</sub>	SO <sub>4</sub>	alk (mg/L)
-------------	---	----	-----------------	-----------------	------------

## Well ID

060402 ula	28.46	331.18	<dl	19.60	256.80
060402 ula field dup	28.11	327.07	<dl	19.45	255.20
060402 ulb	28.70	268.44	<dl	19.27	243.60
060402 ura	34.72	324.10	<dl	19.09	307.20
060402 urb	30.03	286.76	<dl	15.86	295.20
060402 mia	21.41	235.50	<dl	13.54	239.60
060402 mlb	22.62	239.02	<dl	12.63	259.60
060402 mra	24.37	272.87	<dl	16.84	239.60
060402 mrb	30.27	333.30	<dl	7.48	357.20
060402 lla	20.30	229.06	<dl	10.94	243.20

## Surface Water

060402 source	28.22	333.57	<dl	17.12	323.20
060402 source field dup	28.45	336.24	<dl	17.19	336.00
060402 location 1	28.27	337.07	<dl	17.60	323.20
060402 location 2	22.69	170.42	<dl	15.83	302.80
060402 location 3	27.09	321.45	<dl	19.05	306.80
060402 location 4	27.87	330.03	<dl	19.01	306.80

## July

Sample Name	F	Cl	PO <sub>4</sub>	SO <sub>4</sub>	alk (mg/L)
-------------	---	----	-----------------	-----------------	------------

## Well ID

071602 ula	21.00	203.02	<dl	14.49	217.20
060402 ula field dup	20.89	203.03	<dl	14.62	219.20
071602 ulb	23.57	220.79	<dl	16.67	242.80
071602 ura	30.49	287.61	<dl	20.01	281.60
071602 urb	22.44	215.85	<dl	15.05	245.60
071602 mla	20.71	197.94	<dl	13.60	229.20
071602 mlb	23.07	212.09	<dl	15.20	238.80
071602 mra	21.66	208.66	<dl	16.48	233.20
071602 mrb	29.54	281.94	<dl	9.96	359.20
071602 lla	21.63	207.46	<dl	14.24	228.00

## Surface Water

071602 source	29.23	295.22	<dl	17.95	321.20
060402 source field dup	28.78	292.57	<dl	17.95	323.60
071602 location 1	30.00	307.32	<dl	19.49	326.00
071602 location 2	29.51	299.94	<dl	20.54	314.40
071602 location 3	29.59	299.34	<dl	20.25	300.00
071602 location 4	29.70	299.80	<dl	20.41	309.20
071602 spring ss	24.22	239.86	<dl	16.72	266.00

**FIELD METER****August**

Sample Name	pH	temp (°C)	cond (mS/cm)	DO (mg/L)
-------------	----	-----------	--------------	-----------

**Well ID**

082101 ula	7.32	30.30	1.20	-----
082101 ulb	7.35	31.40	1.10	-----
082101 ura	7.75	25.10	1.20	-----
082101 urb	7.64	28.10	1.00	-----
082101 mla	7.38	46.20	1.30	-----
082101 mlb	7.59	36.30	1.20	-----
082101 mra	7.81	42.30	1.50	-----
082101 mrb	7.19	20.20	1.20	-----
082101 lla	7.24	31.80	1.20	-----

**Surface Water**

082101 source	-----	-----	-----	-----
082101 location 1	-----	-----	-----	-----
082101 location 2	9.23	37.50	0.60	-----
082101 location 3	9.15	36.40	1.20	-----
082101 location 4	9.13	37.60	2.00	-----

**October**

Sample Name	pH	temp (°C)	cond (mS/cm)	DO (mg/L)
-------------	----	-----------	--------------	-----------

**Well ID**

100601 ula	7.55	30.80	1.20	-----
100601 ulb	7.45	26.50	1.10	-----
100601 ura	7.39	18.60	1.10	-----
100601 urb	7.52	23.20	1.10	-----
100601 mla	7.17	42.50	1.20	-----
100601 mlb	7.19	28.50	1.20	-----
100601 mra	7.56	39.30	1.50	-----
100601 mrb	7.98	11.70	2.00	-----
100601 lla	6.97	26.30	1.10	-----

**Surface Water**

100701 source	8.98	52.09	-----	-----
100701 location 1	-----	-----	-----	-----
100701 location 2	9.18	30.76	-----	-----
100701 location 3	-----	-----	-----	-----
100701 location 4	-----	-----	-----	-----

**January**

Sample Name	pH	temp (°C)	cond (mS/cm)	DO (mg/L)
-------------	----	-----------	--------------	-----------

**Well ID**

011302 ula	7.38	19.40	1.71	1.40
011302 ulb	7.43	16.50	1.65	2.30
011302 ura	7.67	8.00	2.41	0.50
011302 urb	7.53	10.40	2.33	1.70
011302 mla	7.75	31.40	1.35	2.00
011302 mlb	7.67	18.40	1.64	3.20
011302 mra	8.34	21.70	1.46	2.60
011302 mrb	7.34	4.30	1.84	2.60
011302 lla	7.79	15.40	1.28	3.30

**Surface Water**

011402 source	9.87	58.70	1.87	13.80
011402 location 1	9.68	45.60	1.78	3.70
011402 location 2	9.77	29.90	1.38	2.70
011402 location 3	9.72	30.60	1.67	7.20
011402 location 4	9.80	28.50	1.68	8.10

**February****Sample ID**

GW wells	pH	temp (°C)	cond (mS/cm)	DO (mg/L)
----------	----	-----------	--------------	-----------

022302 ula	6.97	19.20	1.79	6.90
022302 ulb	7.65	10.50	1.70	3.50
022302 ura	7.80	8.30	2.26	20.30
022302 urb	7.67	11.10	2.52	3.20
022302 mla	7.62	31.20	2.30	1.34
022302 mlb	7.61	21.80	1.52	3.40
022302 mra	8.64	25.70	1.36	4.80
022302 mrb	6.98	5.30	1.69	4.40
022302 lla	7.39	17.10	1.29	3.50

**Surface Water**

022302 source	9.41	80.80	1.72	-----
022302 location 1	9.60	48.50	1.83	12.00
022302 location 2	9.43	24.80	1.72	13.00
022302 location 3	9.60	26.20	1.50	14.60
022302 location 4	9.10	23.40	1.66	13.50
022302 cold creek	8.56	30.60	1.19	-----
022302 marsh	8.44	7.20	1.34	13.90

**April**

Sample Name	pH	temp (°C)	cond (mS/cm)	DO (mg/L)
040802 ula	6.57	19.70	1.56	2.12
040802 ulb	6.81	15.90	1.74	2.01
040802 ura	6.75	12.90	2.02	1.27
040802 urb	6.50	15.90	1.47	2.01
040802 mla	7.10	37.30	1.15	1.73
040802 mlb	7.08	23.20	1.25	1.81
040802 mra	7.52	27.60	1.42	1.11
040802 mrb	6.33	11.20	1.83	3.15
040802 lla	6.62	19.90	1.32	1.81
040802 li	7.09	22.90	1.85	4.08

**Surface Water**

040802 source	9.13	82.10	1.71	-----
040802 location 1	9.35	47.00	1.80	-----
040802 location 2	9.52	31.40	1.58	5.76
040802 location 3	9.45	33.90	1.70	5.42
040802 location 4	9.44	32.30	1.69	5.70

**June**

Sample Name	pH	temp (°C)	cond (mS/cm)	DO (mg/L)
-------------	----	-----------	--------------	-----------

**Well ID**

060402 ula	7.06	27.20	1.47	2.14
060402 ulb	6.97	22.80	1.34	3.29
060402 ura	7.41	20.40	1.63	2.68
060402 urb	7.28	22.30	1.51	2.64
060402 mla	7.47	38.50	1.22	2.65
060402 mlb	7.38	29.00	1.22	3.01
060402 mra	8.27	29.10	1.35	2.83
060402 mrb	7.17	20.10	1.68	4.15
060402 lla	7.44	25.80	1.22	2.62

**Surface Water**

060402 source	9.34	82.00	1.88	-----
060402 location 1	9.48	52.20	1.83	-----
060402 location 2	9.70	33.90	1.29	6.73
060402 location 3	9.66	33.70	1.71	6.06
060402 location 4	9.70	32.00	1.53	6.64

**July**

<b>Sample Name</b>	<b>pH</b>	<b>temp (°C)</b>	<b>cond (mS/cm)</b>	<b>DO (mg/L)</b>
--------------------	-----------	------------------	---------------------	------------------

**Well ID**

<b>071602 ula</b>	7.68	32.80	1.23	4.10
<b>071602 ulb</b>	7.42	27.60	1.36	6.80
<b>071602 ura</b>	7.95	23.00	1.55	6.20
<b>071602 urb</b>	7.97	27.80	1.16	5.70
<b>071602 mla</b>	7.76	25.00	1.26	4.10
<b>071602 mlb</b>	8.03	32.70	1.26	5.30
<b>071602 mra</b>	8.48	32.60	1.33	4.40
<b>071602 mrb</b>	7.56	23.50	1.68	4.20
<b>071602 lla</b>	7.77	31.30	1.20	4.80

**Surface Water**

<b>071602 source</b>	9.46	82.50	1.63	6.20
<b>071602 location 1</b>	9.65	52.40	1.88	6.00
<b>071602 location 2</b>	9.85	36.80	1.42	9.50
<b>071602 location 3</b>	9.84	37.80	1.76	9.30
<b>071602 location 4</b>	9.91	38.30	1.35	10.10

<b>071602 spring ss</b>	8.98	42.20	1.56	6.80
-------------------------	------	-------	------	------



**Appendix X: Ion chromatography QA/QC.****August**

<b>Sample Name</b>	<b>Fluoride</b>	<b>Chloride</b>	<b>Sulfate</b>	<b>Fluoride</b>	<b>Chloride</b>	<b>Sulfate</b>
autocal 1	1.00	15	5			
autocal 2	2.00	30	10			
autocal 3	10.00	150	50			
autocal 4	20.00	300	100			

**external standards****within range?**

1/2 alltech	10.38	18.5827	17.6	yes	yes	no, 2.25 %
2x qc spec	2.17	4.80574	13.577	yes	yes	yes

**standard readbacks****% difference from Autocal**

std 1	0.87	14.2707	5.2139	13.64	4.98	4.19
std 1	0.83	14.2829	5.2206	18.13	4.90	4.32
std 1	0.84	14.3238	5.2351	17.55	4.61	4.59
std 1	0.83	14.2418	5.2333	18.05	5.19	4.56
std 2	2.11	30.2449	9.7234	5.53	0.81	2.80
std 2	1.85	29.214	9.7343	7.64	2.65	2.69
std 2	1.92	29.469	9.748	3.87	1.79	2.55
std 2	1.86	29.2028	9.7589	7.39	2.69	2.44
std 3	10.02	151.181	50.433	0.23	0.78	0.86
std 3	10.00	151.648	50.585	0.00	1.09	1.16
std 3	10.00	151.844	50.601	0.03	1.22	1.19
std 3	9.99	152.012	50.743	0.13	1.33	1.47
std 4	19.97	300.454	99.571	0.16	0.15	0.43
std 4	19.92	301.229	99.687	0.42	0.41	0.31
std 4	20.04	301.98	99.71	0.22	0.66	0.29
std 4	20.02	302.135	100.21	0.09	0.71	0.21

**lab blanks**

blank	-0.06	0.633114	1.4662			
blank	0.00	0.539102	0			
blank	0.00	0.591145	1.4652			
blank	-0.01	0.769192	1.4729			

**spikes**

blank	-0.06	0.633114	1.4662
lab fortified blank	1.88	29.2733	9.7295
% recovery	96.81	95.68	84.10
lla	19.51	205.22	12.684
lla spike	19.78	216.607	24.188
% recovery	110.94	106.36	127.72
lla 1/2	9.94	107.136	6.8514
lla lab dup spike 1/2	10.94	128.924	17.642
% recovery	100.07	108.34	114.76

**duplicates**

ula	19.41	202.508	13.126
ula field dup	19.44	202.69	12.998
% difference	0.20%	0.09%	0.98%
urb	21.20	224.493	14.103
urb lab dup	21.14	223.48	14.075
% difference	0.29%	0.45%	0.20%
m1a	19.58	202.955	12.931
m1a field dup	19.55	202.489	12.916
% difference	0.18%	0.23%	0.11%
lla	19.47	205.008	12.768
lla field dup	19.51	205.22	12.684
% difference	0.19%	0.10%	0.66%
lla	19.47	205.008	12.768
lla lab dup	19.43	205.185	12.688
% difference	0.22%	0.09%	0.63%
m1a rerun	9.89162	103.474	6.8224
m1a lab dup 1/2	9.89	105.555	6.8224
% difference	0.00%	1.99%	0.00%

**dilution corrections**

				<b>Fluoride Amount</b>
ula 1/2	9.44	102.004	6.7235	18.88
ulb 1/2	9.82	103.24	0	
urb 1/2	21.14	225.023	13.892	42.28
m1a 1/2	19.68	203.863	12.801	39.35
lla 1/2	9.94	107.136	6.8514	19.87

**October**

<b>Sample Name</b>	<b>Fluoride</b>	<b>Chloride</b>	<b>Sulfate</b>	<b>Fluoride</b>	<b>Chloride</b>	<b>Sulfate</b>
autocal 1	0.4	6	2			
autocal 2	1	15	5			
autocal 3	2	30	10			
autocal 4	4	60	20			
<b>external standards</b>			<b>within range?</b>			
1/2 alltech	10.0348	20.0609	20.2832	yes	yes	yes
QC Spex A-1	1.03123	0	7.92028	yes	<dl	yes
<b>standard readbacks</b>			<b>% difference from autocal</b>			
std 1	0.409157	6.06131	2.10796	2.26334	1.016639	5.25614
std 1	0.423216	6.01193	2.0676	5.64032	0.198636	3.32383
std 1	0.425424	6.01943	2.06302	6.16023	0.32331	3.10213
std 1	0.455972	6.00856	2.06669	13.078	0.142565	3.27982
std 2	0.996134	14.9537	4.89805	0.38735	0.309144	2.06
std 2	1.01329	15.0013	4.93445	1.32023	0.008666	1.31965
std 2	1.00746	15.0018	4.90284	0.74323	0.011999	1.96227
std 2	1.0238	15.0266	4.98245	2.35201	0.177176	0.35162
std 3	2.00578	30.0875	10.063	0.28858	0.291242	0.62802
std 3	2.0134	30.2031	10.1108	0.66776	0.674716	1.1019
std 3	2.01337	30.2037	10.0815	0.66627	0.676703	0.81169
std 3	2.06288	30.4476	10.1227	3.09534	1.480952	1.21952
std 4	4.06463	60.3267	20.0603	1.6028	0.543022	0.30105
std 4	4.07155	60.2385	20.0717	1.77289	0.396712	0.35786
std 4	4.06463	60.3267	20.0603	1.6028	0.543022	0.30105
std 4	4.05391	60.434	20.1296	1.33873	0.720727	0.64591
<b>blanks</b>						
blank	0	0	0			
blank	0	0	0			
blank	0	0	0			
blank	0	0	0			
field blank	0	0	0			
field blank dup	0	0	0.36559			

**spikes**

blank	0	0	0
lab fortified blank	3.74697	29.4462	10.1762
% recovery	93.67425	98.154	101.762
urb	3.98639	46.415	2.89816
urb lab spike	5.914	53.5352	11.2189
% recovery	98.02013	101.0923	97.6982
source	4.88703	59.4754	3.28648
source lab spike	6.40061	60.3764	11.4445
% recovery	98.92738	102.129	98.0126
L1	4.8781	59.5717	3.38808
L lab spike	6.38831	59.999	11.5742
% recovery	98.7315	100.7105	98.8016

**duplicates**

ulb	3.46481	37.4129	2.49713
ulb field dup	3.5527	37.5043	2.50164
% difference	2.504877	0.244003	0.18044
ura	4.37466	47.0631	2.98872
ura field dup	4.38289	47.1486	3.01416
% difference	0.187952	0.181506	0.84759
urb	4.1287	44.1428	2.87587
urb lab dup	4.06537	44.1288	2.87785
% difference	1.545752	0.03172	0.06883
mra	4.29467	42.1676	2.8888
mra field dup	3.99262	41.939	2.86557
% difference	7.289476	0.543596	0.80739
source	5.06328	55.6726	3.20957
source field dup	5.08033	55.8271	3.22278
% difference	0.336172	0.277131	0.41074
source	5.06328	55.6726	3.20957
source lab dup	4.74887	55.8368	3.44053
% difference	6.408585	0.294504	6.94606
L1	5.02937	56.9487	3.42226
L1 lab dup	4.92636	55.9472	3.6006
% difference	2.069361	1.774201	5.07884

**January**

<b>Sample Name</b>	<b>Fluoride</b>	<b>Chloride</b>	<b>Sulfate</b>	<b>Fluoride</b>	<b>Chloride</b>	<b>Sulfate</b>
autocal 1	4	30	4			
autocal 2	10	75	10			
autocal 3	20	150	25			
autocal 4	40	300	50			
<b>standard readbacks</b>				<b>% difference from autocal</b>		
standard 1	3.727967	30.7017	4.11969	7.040219	2.311971	2.94812
standard 2	10.36582	76.28706	11.0143	3.592524	1.701476	9.65363
standard 3	21.12886	154.0341	23.7454	5.489395	2.653689	5.14746
standard 4	40.92133	310.1199	52.3203	2.277095	3.317357	4.53537
<b>external standards</b>				<b>within range?</b>		
1/2 alltech	9.743331	20.5155	17.9674	yes	yes	yes
1/50 alltech						
1/2 alltech	9.901363	21.98985	19.6146	yes	yes	yes
1/50 alltech						
1/2 alltech	10.07965	21.12114	18.642	yes	yes	yes
1/50 alltech						
<b>spikes</b>						
L4	26.63369	301.8411	17.774			
L4 lab spike	33.90509	304.8799	34.4958			
% recovery	1.029413	1.026396	1.02435			
lab blank	-0.33608	4.196753	0			
lab spike	21.64949	157.4722	24.4327			
% recovery	1.090876	1.035826	0.97731			
<b>blanks</b>						
lab blank			0			
lab blank	-0.33608	4.196753	0			
field blank		4.189118	0			

**duplicates**

ULA	23.05129	300.8677	14.0613
ULA Field Dup	23.2599	305.1549	14.2571
% difference	0.900885	1.414841	1.38266
urb	36.00891	523.0045	29.6853
urb lab dup	36.00471	522.9496	29.6924
% difference	0.011655	0.010497	0.02394
source	26.85086	303.753	16.2769
source field dup	27.6982	313.9705	17.5001
% difference	3.106712	3.308108	7.2431
mla	20.38146	216.1368	12.3439
mla field dup	20.48683	217.5278	12.3204
% difference	0.515677	0.641508	0.19092
mla field dup	20.48683	217.5278	12.3204
mla field dup lab dup	20.51631	218.125	12.3851
% difference	0.143809	0.274184	0.52364

**Anions analyzed (IC) by U of MT and U of WY, February, 2002 (mg/L).**

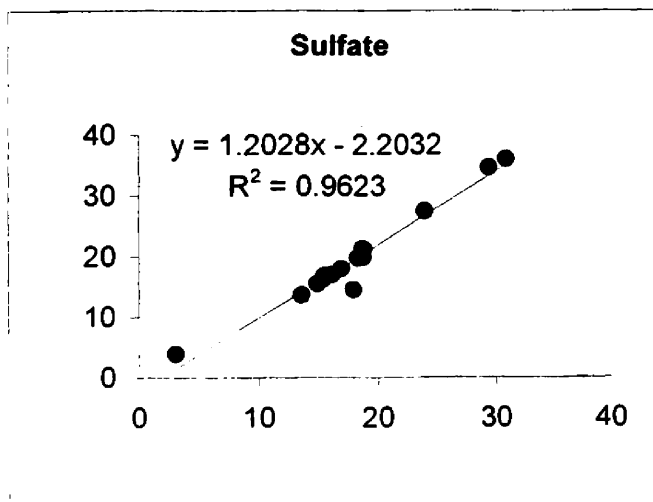
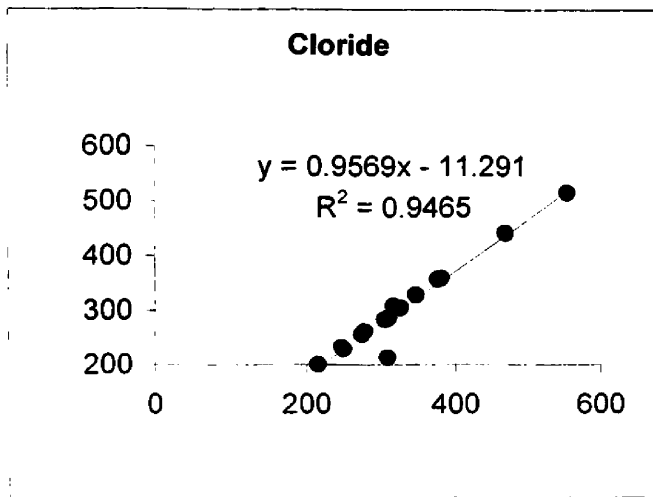
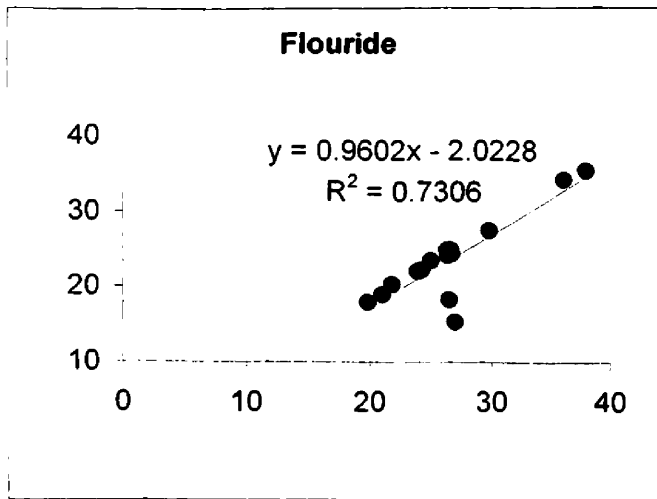
U of MT Sample Name	U of MT			U of WY		
	Fluoride	Chloride	Sulfate	Fluoride	Chloride	Sulfate
ula	26.69	381.34	18.82	24.90	359.16	21.19
ula field dup	26.44	376.96	18.74	24.82	357.33	21.20
ulb	25.07	347.47	24.08	23.43	328.54	27.40
ura	36.18	468.62	29.51	34.14	442.22	34.57
urb	38.05	554.37	31.00	35.37	515.43	36.03
m1a	19.90	215.48	13.55	17.90	199.96	13.58
m1b	24.34	278.13	15.49	22.22	261.64	16.78
m1b field dup	24.00	274.55	15.41	22.01	255.88	16.26
mra	21.88	247.15	16.20	20.28	231.73	17.00
mr1b	29.89	326.13	3.13	27.41	305.12	3.92
11a	21.11	249.44	14.89	18.93	228.75	15.41
source	26.76	310.57	16.92	24.38	286.30	17.94
location 1	27.06	317.13	17.95	15.30	308.50	14.52
location 2	26.59	308.76	18.55	18.26	213.22	19.83
location 3	26.45	305.14	18.31	24.11	283.22	19.68
location 4	26.78	308.25	18.77	24.36	284.89	19.87

**% difference**

	Fluoride	Chloride	Sulfate
	6.95	5.99	11.83
	6.33	5.35	12.33
	6.77	5.60	12.88
	5.82	5.80	15.79
	7.29	7.28	15.01
	10.61	7.47	0.19
	9.12	6.11	8.00
	8.65	7.04	5.33
	7.59	6.44	4.81
	8.65	6.66	22.37
	10.87	8.65	3.43
	9.31	8.13	5.84
	55.51	2.76	21.14
	37.13	36.61	6.68
	9.25	7.45	7.22
	9.45	7.88	5.67
<b>avg %</b>	13.08	8.45	9.91
<b>"split"</b>	6.54	4.23	4.95

*Percent error was calculated for each sample and then averaged for each set of samples. The average error was split in half to accommodate an equal standardization for the revised data set. The revised data was acceptable in this report.*

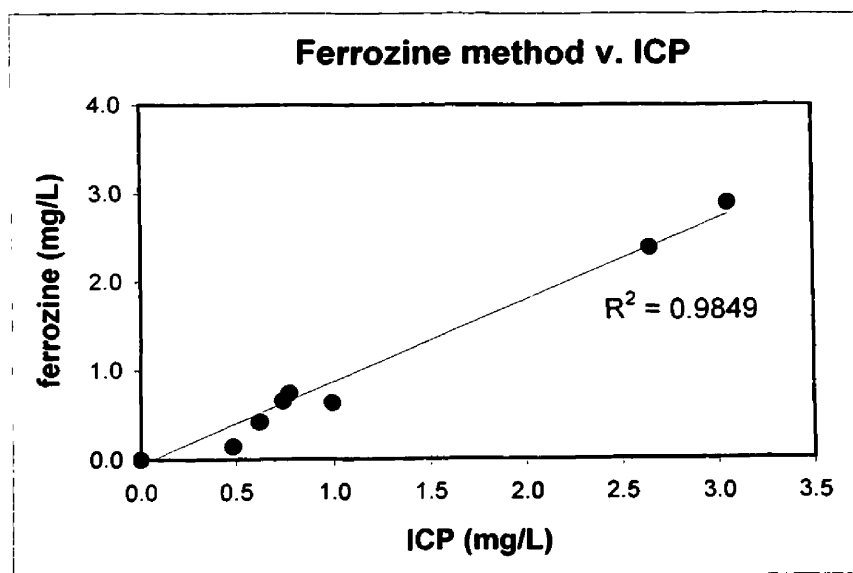
Anion analysis comparison between University of Montana and University of Wyoming.





**Iron:** Comparison between XRAL ICP200 and the ferrozine method. ICP analyses were analyzed within two weeks of collection. Ferrozine analyses were analyzed within three days of collection. The data would likely have less percent error if the ferrozine had been analyzed in the field. However, the only time during the study when the ferrozine method was done in the field was in July. July's ICP analyses were done several months after in November.

Sample ID	ICP	ferrozine (total)	% difference
ula	2.65	2.38	0.11
ulb	3.06	2.89	0.06
ura	0.74	0.65	0.12
urb	0.77	0.74	0.05
m1a	0.00	0.00	na
m1b	0.62	0.42	0.39
mra	0.00	0.00	na
mrb	1.00	0.63	0.45
l1a	0.48	0.14	1.09
source	0.00	0.00	na
Location 1	0.00	0.00	na
Location 2	0.00	0.00	na
Location 3	0.00	0.00	na
Location 4	0.00	0.00	na



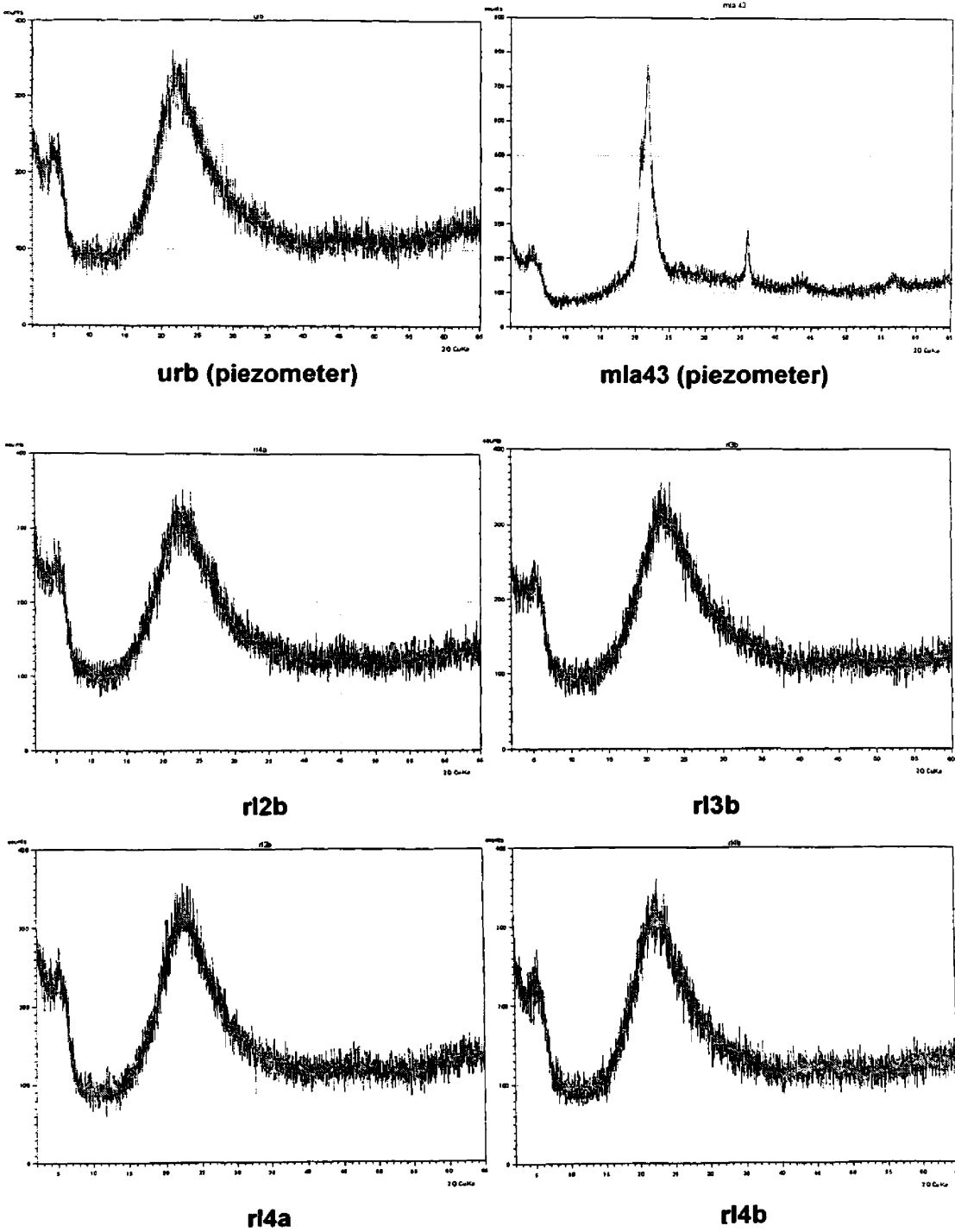
### Appendix D: Archived chemistry from the Rabbit Creek Group.

Sample ID	Date	Name and/or Description	Temp	field pH	lab pH	SiO2	Fe	Mn	As	Ca
J7518	06/06/71	HEADWATERS OF RABBIT CREEK AREA	91	9.5	9.72	213	----	1.5	98	0.35
J7519	06/06/71	HEADWATERS OF RABBIT CREEK AREA	90	9.5	9.78	266	----	----	1.669	0.37
J7520	06/06/71	HEADWATERS OF RABBIT CREEK AREA	85	9.3	9.47	236	----	----	1.367	0.65
YF362	06/18/62	TILL GEYSER	----	----	----	----	----	----	----	----
J7440	10/02/70	TILL GEYSER	78	9	9.33	333	<.02	<.02	1.67	0.66
YF230	06/06/62	SPRING BY Y-5	90	8.3	----	----	----	----	----	----
YF392	06/30/63	SPRING BY Y-5	----	----	8.44	210	0.01	0.01	----	0.4
YF541	09/08/68	SPRING BY Y-5	95	8.3	8.35	225	<.05	----	----	0.5
J7441	10/02/70	SPRING BY Y-5	93	8.2	8.77	226	<0.02	1.59	0.2	<0.01
J7629	09/30/72	SPRING BY Y-5	93	7.9	8.54	219	----	----	----	0.5
F7714	09/29/73	SPRING BY Y-5	93	7.4	8.51	213	<0.1	<0.1	----	0.8
J7951	10/09/75	SPRING BY Y-5	93	7.4	8.51	226	<0.03	0.02	----	0.78
J8127	10/07/77	SPRING BY Y-5	93	7.4	8.22	213	<.02	<.02	----	0.19
J8642	09/21/82	SPRING BY Y-5	93	7.4	8.63	346	----	----	----	0.08
F9013	09/02/86	SPRING BY Y-5	91.5	6.53	6.86	210	0.05	<.01	0.56	0.35
J7442	10/02/70	UNNAMED HIGH FLOWING WARM SPRING	72	6.9	8.75	197	<0.02	----	0.305	0.02
J7443	10/02/70	UNNAMED WARM SPRING	42	7	9.19	197	<0.02	1.78	0.3	<0.02
YM319	08/28/63	SPRING ON MARGIN OF MALLARD LAKE	72	7	----	----	----	----	----	0.05
YM322	08/28/63	UNNAMED HOT SPRING	69	7.5	----	----	----	----	----	----
T6701	03/07/00	UNNAMED CLESR POOL WITH PINK ALGAE	65	9	----	----	----	----	----	1.2
T6703	03/07/00	SUPERHEATED SPRING	96	8.6	----	----	----	----	----	1
T6705	03/07/00	VERY LARGE HOT POOL	77	9	----	----	----	----	----	1
T6709	03/07/00	VERY VIOLENT SPOUTER	93	7.7	----	----	----	----	----	1.6
T6710	03/07/00	SPRING ON WEST SIDE DEPOSITING MNO2	94	8.2	----	----	----	----	----	3.2
T6711	03/07/00	ROW OF SPRINGS TRENDING N40*W	80	8.5	----	----	----	----	----	1.5
T6715	03/07/00	ROW OF SPRINGS TRENDING N40*W	92	7.6	----	----	----	----	----	0.9
T6718	03/07/00	ROW OF SPRINGS TRENDING N40*W	71	7.5	----	----	----	----	----	1.5
YF368	06/28/63	LARGE POOL AT BEND	87	9	----	----	----	----	----	0.5
J7517	06/06/71	UNNAMED SPRING	78	9.7	9.87	283	----	----	1.73	0.35
YK369	06/28/71	SPOUTER AT S FORK OF B RABBIT CRK	92	----	8.14	----	----	----	0.7	----
YF370	06/28/63	BLUE SPG UP SIDE UP "A" RABBIT CREEK	86	----	8.76	----	----	----	----	1.4
J7521	06/06/71	UNNAMED SPRING	41	8.6	9.15	216	----	----	22	0.8
J7522	06/06/71	NW-SW TRENDING FRACTURE	91	8.8	8.98	228	----	----	1.461	0.9
J7523	06/06/71	NW-SW TRENDING FRACTURE	83	8.7	8.96	212	----	----	1.516	0.8
J7524	06/06/71	NW-SW TRENDING FRACTURE	78	8.6	8.93	211	----	----	1.524	0.73
J7525	06/06/71	NW-SW TRENDING FRACTURE	76	8.6	8.97	204	----	----	1.517	0.8
J7526	06/06/71	NW-SW TRENDING FRACTURE	46	8.5	9.03	222	----	----	1.55	0.8

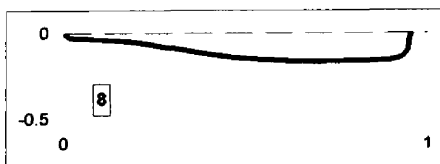
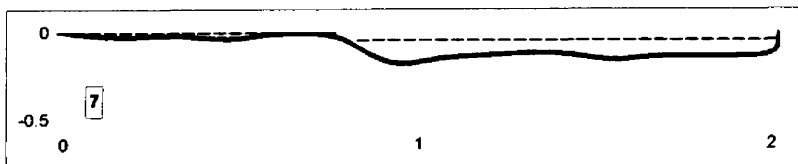
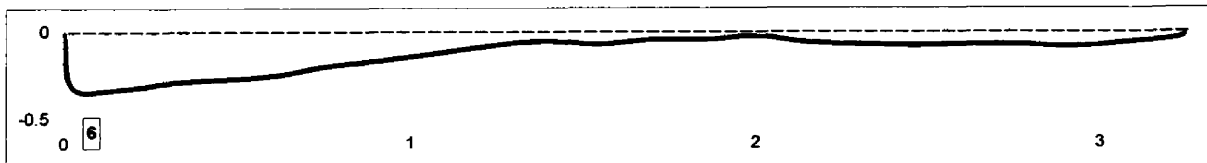
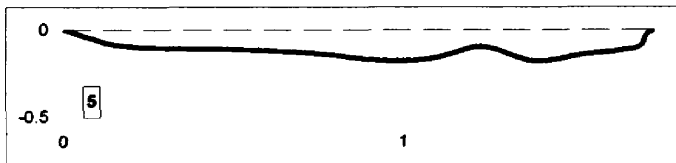
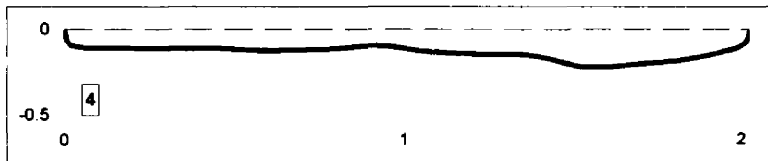
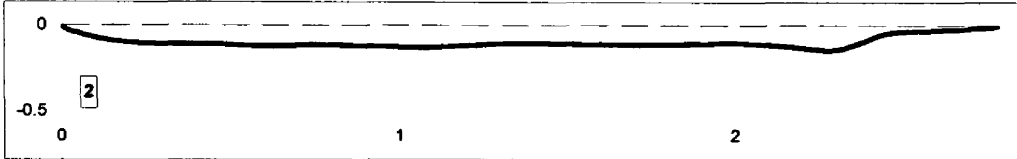
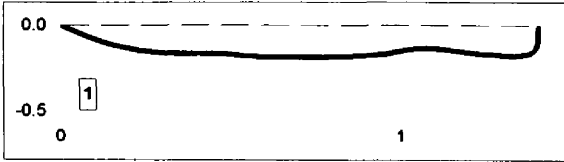
continued

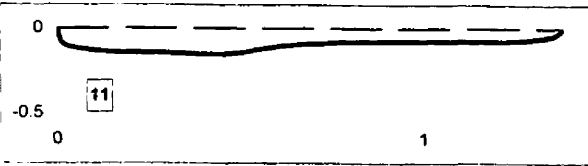
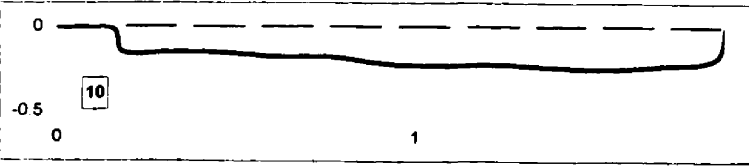
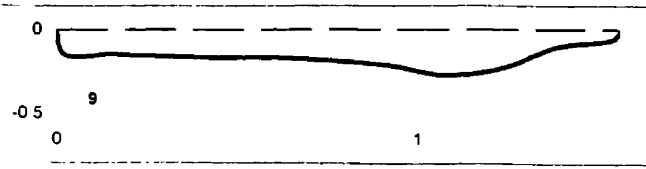
Sample ID	Mg	Na	K	Li	Rb	Cs	NH4	HCO3	CO3	SO4	Cl	F	B	H2S	O-18	deuterium
J7518	0.02	340	14	4.5	---	---	---	383	---	20	291	25	2.8	---	-16.38	-140.5
J7519	0.02	357	13.5	4.7	0.14	0.53	---	397	---	17	305	26	3	---	-16.97	-142.5
J7520	0.02	306	12	3.8	0.11	0.53	---	332	---	24	248	22	2.42	---	-16.12	-142.5
YF362	---	409	9.4	4.3	---	---	---	---	---	---	311	26.7	3.4	---	---	---
J7440	<.01	365	11.5	3.4	---	---	---	197	152	16	260	23	2.9	---	-16.75	-144.5
YF230	---	---	---	---	---	---	---	419	15	---	269	---	---	---	---	---
YF392	0.01	360	9.1	3.2	---	---	0.1	447	10	16	268	25	2.8	---	---	---
YF541	0.04	375	9.6	3.3	---	---	0.3	460	---	25	271	24	2.8	0.8	-16.92	-139.5
J7441	---	380	11.5	3.1	0.09	0.4	---	303	82	15	271	23	2.7	---	-16.79	-142.3
J7629	0.01	366	8.2	3.2	---	---	---	489	---	15	248	21.5	2.6	---	-16.62	---
F7714	0.01	345	9	3	0.08	0.44	---	470	---	15	262	21	2.9	---	-16.75	-144
J7951	<0.01	343	16	2.7	0.1	0.35	0.7	427	---	18	273	23.5	2.4	0.03	-16.7	-145.5
J8127	<.01	322	9.14	2.34	0.09	0.26	0.3	473	---	6	285	21.9	2.5	0.05	-16.9	---
J8642	<.005	348	8.05	2.95	0.15	0.44	---	454	---	21	277	27	2.7	---	-17.54	---
F9013	0.00	360	8.5	2.3	0.08	0.3	---	429.4	---	23	257.8	29.4	2.6	0.12	-16.1	-140
J7442	---	330	14.3	4.4	0.13	0.47	---	126	114	18	261	23.8	2.8	---	---	---
J7443	---	275	10.8	3.1	0.09	0.3	---	193	68	13	216	18.8	2.2	---	---	---
YM319	0.08	58	12.8	---	---	---	---	42	---	88	4	---	---	---	---	---
YM322	---	333	13.9	---	---	---	---	---	---	56	231	---	---	---	---	---
T6701	0.03	371	14.2	---	---	---	---	396	---	25	332	---	---	---	---	---
T6703	0.02	322	9.8	---	---	---	---	353	---	10	287	---	---	---	---	---
T6705	0.02	371	13.2	---	---	---	---	395	---	22	335	---	---	---	---	---
T6709	0.04	54	20.1	---	---	---	---	80	---	56	2	---	---	---	---	---
T6710	0.02	45	13.8	---	---	---	---	113	---	4	2	---	---	---	---	---
T6711	0.02	342	12.6	---	---	---	---	394	---	19	287	---	---	---	---	---
T6715	0.02	332	9.3	---	---	---	---	416	---	27	272	---	---	---	---	---
T6718	0.05	252	8.9	---	---	---	---	307	---	20	209	---	---	---	---	---
YF368	0.01	350	12.2	5.6	---	---	---	293	48	24	315	27.2	1	---	---	---
J7517	0.02	378	14	5	0.15	0.548	---	412	---	19	321	27	3.1	---	---	---
YK369	---	449	19.5	1	---	---	---	87	---	33	2	5.9	0.06	---	---	---
YF370	---	325	11.3	4.9	---	---	---	305	63	25	290	25.2	0.9	---	---	---
J7521	0.03	355	11.2	5	---	---	---	344	---	17	302	27	2.8	---	-14.97	-141
J7522	0.02	318	14.2	3.98	0.1	0.4	---	401	---	14	248	21.5	2.4	---	-17.34	-142.5
J7523	0.02	310	14	3.95	0.1	0.41	---	334	---	15	248	22	2.5	---	-16.76	-144
J7524	0.02	330	12	4.1	0.11	0.43	---	426	---	15	258	22	2.4	---	-16.21	-144
J7525	0.02	330	12	4.46	0.1	0.463	---	417	---	15	252	21.5	2.75	---	-16.31	-143
J7526	0.03	348	12	4.65	0.11	0.461	---	430	---	16	258	22	2.6	---	-15.53	-143

**Appendix E:** Representative X-ray diffraction plots of creek channel mineral deposits. X-axis is degrees 2 theta from (2-65). The y-axis is intensity.

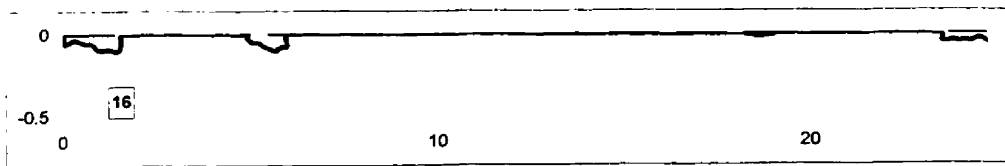
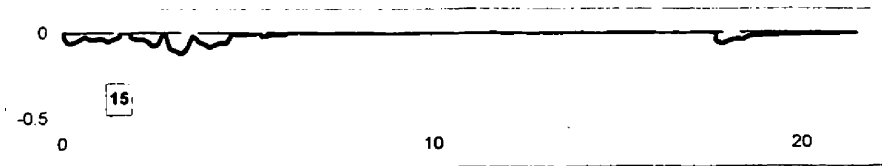
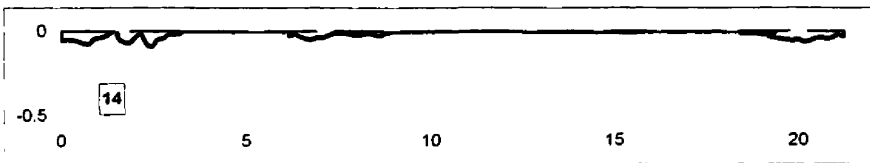
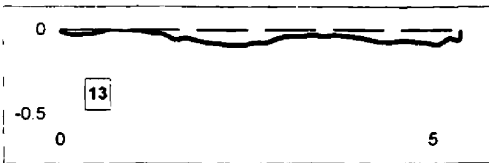
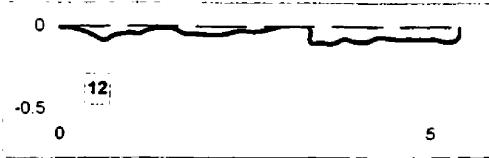


**Appendix F:** Cross sectional measurements of the creek in the study site. Cross section 1 starts at the upper staff gauge. Each cross section was taken 15 m downstream of the previous cross section. Cross section 16 is only 10 m below cross section 15 and was taken at the lower staff gauge. Depth and distance units are in meters.

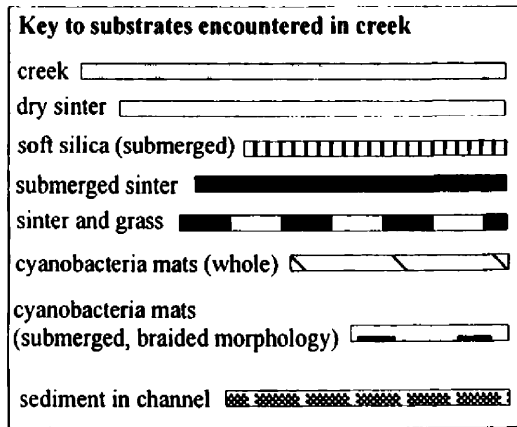




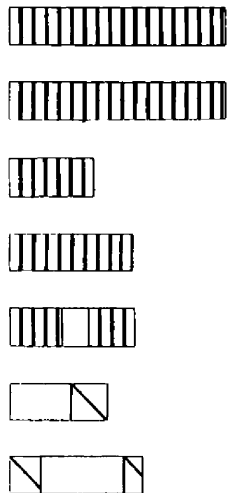
*The x-axis scale is resized in the next plots.*

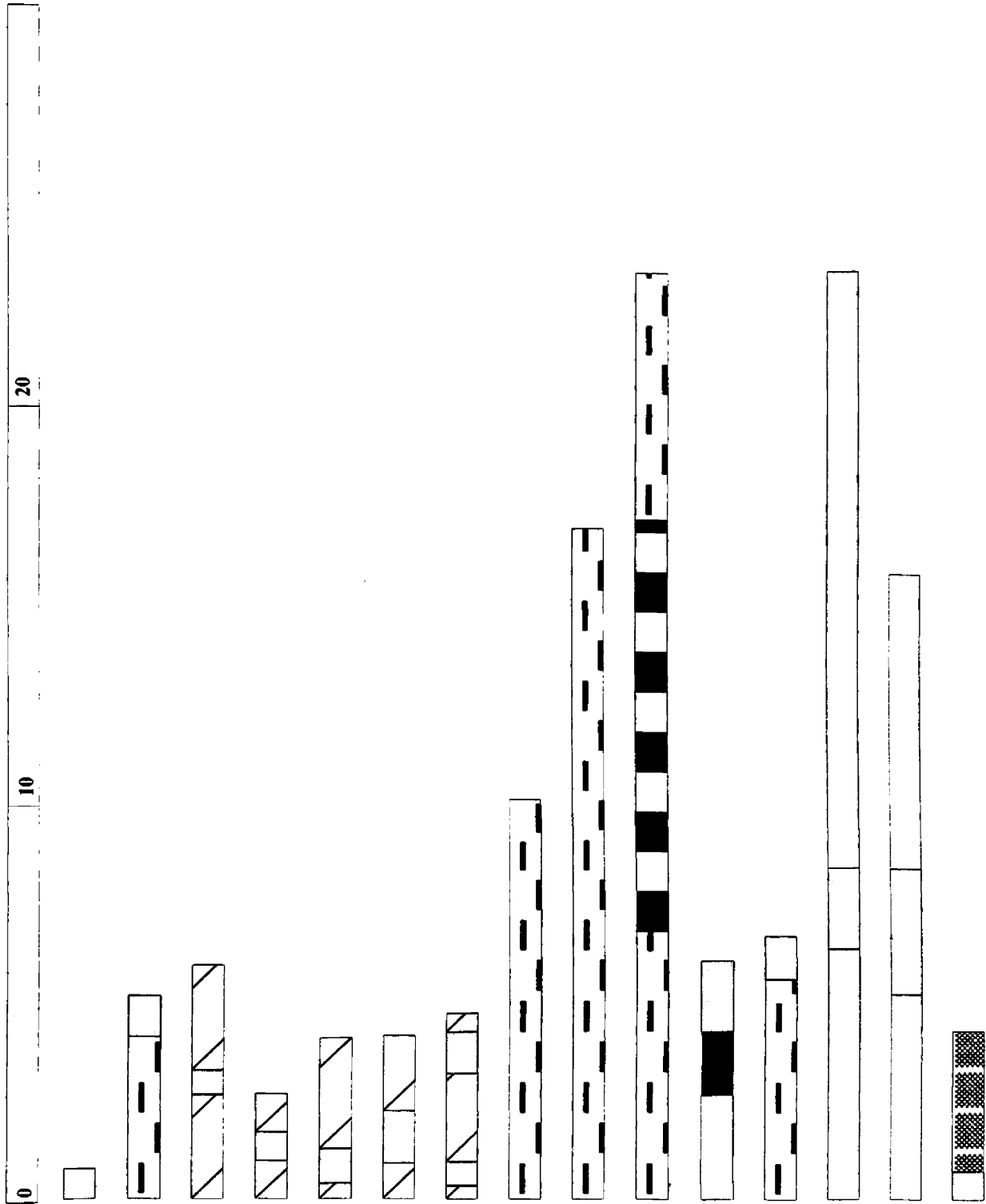


**Appendix G:** Creek mapping measured in meters from the north side of the creek to the south side of the creek. Distances across the entire channel were measured and categorized by substrate (see figure key). The first mapped section started at the beginning of the hot spring source outflow channel and each mapped section is ~30 m downstream of the previous section. The plots are not numbered. The first plot is at the start of the creek and the last plot is the most downstream plot. The extent of the creek channel measurements spanned approximately 1 km.

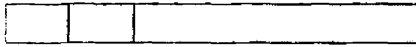


*Values are in meters where zero starts on the north side of the creek channel.*

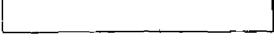
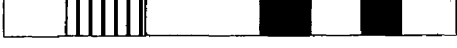
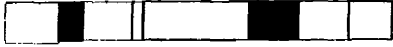
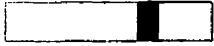
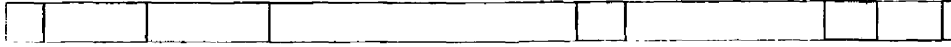


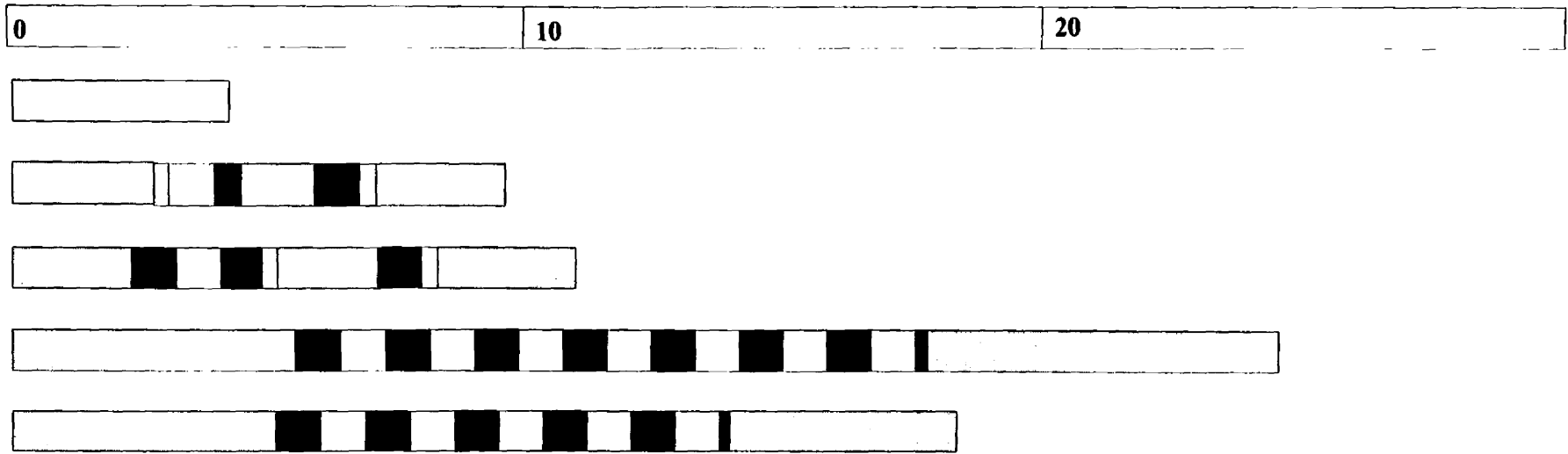






**Upper staff gauge location:** For detailed channel mapping, see the cross sectional measurements for the study site. The next channel mapping section starts below the lower staff gauge.





The last mapped channel section is just above a hot spring tributary. Below this point, the channel is similar. The Park road is approximately 200 meters downstream of this channel section.